Development of Lightweight Soft Body Armour for Ballistic Protection

A thesis submitted to the University of Manchester for the degree of
Doctor of Philosophy
In the Faculty of Engineering and Physical Sciences

by

YI ZHOU

School of Materials
September 2013

Table of Contents

LIST OF FIGURES

LIST OF TABLES

ABSTRACT

Strong and low-density fibres have been favoured materials for ballistic protection, but the choice of fibres is limited for making body armour that is both protective and lightweight. In addition to developments of improved fibres, alternative approaches are required for creating more protective and lighter body armour. This research focuses on a study of the inter-yarn friction and hybrid fabric panels for ballistic protection. Two complemetary routes have been employed to carry out the research, namely a programme of experimentation centred on ballistic shooting test and a detailed theoretical analysis based on finite element (FE) modelling. In this research, fabrics made of ultra-high-molecular-weight polyethylene (UHMWPE) were chosen for investigation due to their good mechanical properties and light weight.

For the investigation of inter-yarn friction on fabric ballistic performance, FE models were created in ABAQUS software for theoretical analysis. According to the capstan equation, yarn wrapping angle is one of the factors controlling inter-yarn friction. This being so, novel weaving techniques have been developed to manufacture woven fabrics with increased yarn wrapping angle. Ballistic shooting tests have been carried out on the structure modified woven fabrics and the results showed that the improvement of ballistic peotection on structure modified fabrics is not detectable when compared with plain woven fabric. This could be attributed to the low inter-yarn coefficient of friction of UHMWPE fibres and low increase in wrapping angle due to the high bending rigidity of UHMWPE fibres. Based on the two points, improvements have been suggested for future work.

For the development of hybrid panels, an eight-layer woven fabric FE model was created to study the response and failure model of different fabric layers in a panel upon ballistic impact. It has been established that fabrics near the impact face tend to fail by the shearing effect and those near the back face tend to fail in tension. UHMWPE woven and unidirectional (UD) fabrics were evaluated for their resistence to tensile and shearing damage. Two types of panels were designed from the fabrics and the experimental results showed that placing woven fabrics close to the impact face and UD material as the rear layers led to better ballistic performance than the panel constructed in the reverse sequence. It has also been found that the optimum ratio of woven to UD materials in the hybrid ballistic panel was 1:3. The improvement in ballistic protection of the hybrid fabric panels allows less material to be used, leading to lighter weight body armour.

DECLARATION

No portion of the work referred to in the thesis has been submitted in support of an application for another degree or qualification of this or any other university or other institute of learning.

COPYRIGHT STATEMENT

ACKNOWLEDGEMENT

I would like to thank my supervisor Dr Xiaogang Chen for his keen support, professional advices and guidance for this work.

I also appreciate the financial support (RT/COM/7/073) provided by the Ministry of Defence, UK, to cover the tuition fees and Dyneema yarns provided by DSM for this research.

I am thankful to Mr Tomas Kerr and Mr John Payne for their assistance in weaving the fabrics, and to Mr Adrian Handley and Ms Alison Harvey for their technical support in testing the mechanical properties of the fabrics.

Thanks also go to Dr Ying Wang, who helped me to improve my thought as a researcher and encouraged and inspired me during my studies, and to Dr Danmei Sun, Dr Bilal Zahid, Dr Fuyou Zhu and Dr Zhaoqun Du for their useful discussions and encouragements.

I also wish to express my appreciation to the research team members, including Dr Dan Yang, Dr Xiaozhou Gong, Ms Yanyan Chu, Ms Yanfei Yang, Miss Yue Xue, Miss Shengnan Min, Miss Nan Wang and Mr Marc Velzer, for their friendship.

Special thanks go to my dearest parents for their endless love, patience, encouragement, and huge supports during the study.

PUBLICATIONS

1. X Chen, D Sun, Y Wang, Y Zhou. 2D/3D woven fabrics for ballistic protection. Proceedings to 4th World Conference on 3D Fabrics and Their Applications. Manchester: TexEng/RWTH Aachen: 2012: -. eScholarID:171241

2. Xiaogang Chen， Yi Zhou and Garry Wells. Numerical and Experimental Investigations into Ballistic Performance of Hybrid Fabric Panels, Composite part B: Engineering, In-press.

3. Yi Zhou, Xiaogang Chen, Garry Wells, Influence of yarn gripping on the ballistic performance of woven fabrics from ultra-high molecular weight polyethylene fibre, under review.

Chapter 1 Introduction

1.1 Background

Body armour has long been used to protect soldiers in the battlefield. From the use of leather in the east to chain mail in the west, people never stopped seeking better protection for personnel. During the development of body armour, it has always been desirable to have lighter and stronger materials so that the advancement of performance could be achieved at a reduced weight. The advent of synthetic fibres speeded up the innovation of lightweight body armour. Nylon was the first synthetic fibre employed in the body armour system (M-1951). This model consisted of two parts. The first part was a nylon basket-weave flexible pad, which covered the upper chest and shoulder. The second part was Doron plates, which covered the lower chest[1]. However, it was not until the invention of aramid fibres that ushered a new area for soft body armour. Aramid fibres were first discovered by Kwolek in 1965 and commercialised by Du Pont in 1972 under the trade name of Kevlar®, later commercial products belonging to the aramid family encompassed Technora, Twaron, Nomex and Teijinconex [2]. Due to its unique molecular structure, aramid fibre gives outstanding high performance over previous synthetic fibres, which fulfils the design requirement of lightweight, flexible and covert body armour for its users. Another ballistic fibre is ultra-high-molecular-weight polyethylene (UHMWPE). This material is gaining ground in the ballistic field due to its high performance-to-weight ratio.

Modern body armour falls into two categories: hard body armour and soft body armour. Hard body armour is made of metal or ceramic plates. Soft body armour mainly consists of layers of fabrics made of high performance fibres. Soft body armour is mainly used by Law Enforcement Officers who are more likely to be subjected to low level firearm threats. For soldiers in the battlefield, soft body armour is often plated with hard body armour in order to provide enough ballistic protection. Farjo and Miclau [3] studied the tissue wounding caused by ballistic impact. It was argued that the entry of a bullet into the human body produces a cavity in the tissue and causes great damage. Even though the penetration is prevented, there could be internal injury in human muscles or organs [4]. In spite of this, body armour plays an important role in life saving. According to the data collected from a retrospective analysis on all combat casualties sustained by United States Military Forces in Mogadishu, Somalia, body armour reduced the number of fatal penetration chest injuries from 39% in the Vietnam War to 14% in the Black Sea [5]. Peleg *et al* [6] found that injury severity of wounded soldiers is about twice as severe in those who were unprotected in the battlefield. Based on a study of 118 army troops who suffered severe battlefield injuries in the Iraq war, 58 percent were wounded in either the hands, legs or eyes, only 9 percent were wounded in the abdomen or chest [7]. This means that the human torso is well protected by body armour and reduces the injuries caused by projectiles or bullets. For Police Officers and other Law Enforcement Agencies, Latourrette [8] suggested that body armour more than triples the likelihood that a police officer will survive a shooting to the torso, and he continued to suggest that equipping all the police with body armour would save at least 8.5 lives per year.

The importance of body armour makes it the central component for any military personnel's protection and brings it huge demands [9]. However, the overweight and bulky properties of modern body armour reduce its wearer's mobility and comfort during a mission. It is reported that many US marine troops refused to use new sets of body armour because they were too heavy, after complaining about not having enough protection [10]. Generally speaking, ideal soft body armour should give high ballistic performance, low weight and be comfortabe to wear, which is required to provide its wearers with sufficient ballistic protection without affecting their mobility. The present work aims to improve the ballistic performance of the existing soft body armour at a reduced weight by developing fabrics and panels with better performance.

1.2 Problems

Great efforts have been taken to produce better lightweight soft body armours, such as using high performance fibres. High performance synthetic fibres exhibit superior mechanical properties which set them apart from other man-made fibres in industrial application. For ballistic applications, materials are required not only to give high strength and tenacity, but to have low weight as well. The most widely used fibres for soft body armour manufacture are mainly aramid and UHMWPE fibre, which show higher strength based on weight and volume when compared with other types of synthetic fibre. Acomparison with other materials is shown in Figure 1-1. PBO (polyphenylenebenzobisozazole) is a type of synthetic fibre which satisfies the physical requirements for ballistic applications. Nevertheless, it has been found that its exposure to moisture may result in the loosening of fibre morphology, leading to the degradation of physical properties [11]. Moreover, PBO shows worse tensile retention properties than Kevlar when exposed to sunlight simulated radiation [12]. Another high performance fibre showing great ballistic impact potential is M5 [13]. This fibre, however, is still in the testing stage and is yet to be industrialised.

Apart from the development of more efficient fibres, alternative technologies were also investigated. One of them is combining fibres in a 0°/90° unidirectional fashion without going through the traditional weaving process. This technology is commercialised under the brand names of Dyneema SB from DSM and Spectra Shield under the Allied Signal. In addition, “shear thickening fluid” treated fabric, with the nickname “bullet proof custard”, also exhibited great potential at the Defence Conference in London on 13th Jan, 2011. BAE systems (a British defence, security and aerospace company), which created this armour, hopes that it could weigh half as much as the current flak jacket, which is around 10 kg [14].

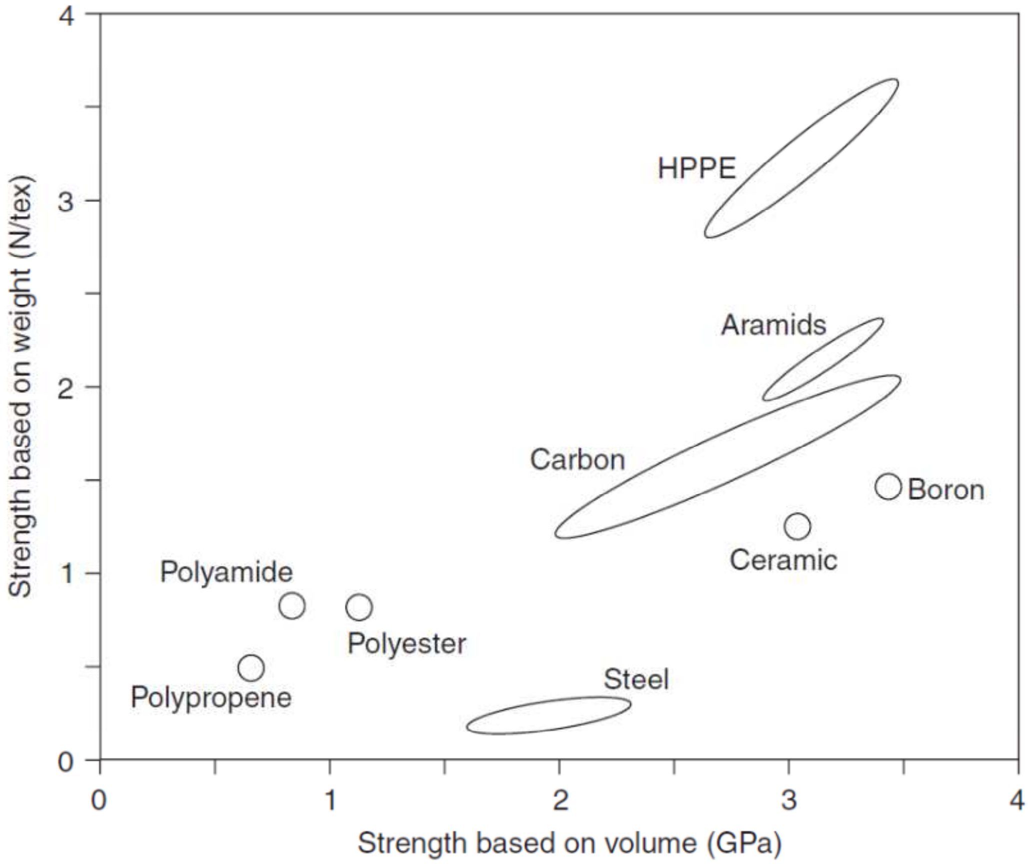

Figure 1-1 Strength based on weight VS strength based on volume [15]

As the majority of the research work focused on improving the properties of fibres and chemically treating ballistic fabrics, there is little emphasis on employing textile based technologies. In the present research, Textile technologies will be used to create UHMWPE fabrics, aiming to explore the properties of high performance fibres to be fully exhibited when used in soft body armour. In order to achieve this, two routes have been followed, modification of fabric and panel structures. These will be carried out by the development of fabric with increased inter-yarn friction and engineering design of ballistic hybrid panels. The effect of inter-yarn friction on fabric energy absorption has been studied by many researchers [16-19]. It is believed that the friction between warp and weft yarns benefits energy dissipation in woven fabrics. Increasing inter-yarn friction has the potential to improve fabric ballistic performance without adding to its weight. In this research, finite element methods will be used to study the working mechanisms and novel weaving techniques will be used to create woven fabrics with increased inter-yarn friction on power looms.

It has also been widely accepted that when an armour-grade panel is impacted, the sharp edges of the projectile shear out the first few layers, forming a plug [20-22]. For the rear layers, fibre pull-out and tensile failure are more likely to occur. The fact that different layers of fabric exhibit various responses upon ballistic impact suggests the necessity for combining more than one type of material in a panel. Mixing different materials, such as UHMWPE woven and unidirectional fabrics, in a proper sequence would hopefully serve the purpose of soft body armour weight reduction

1.3 Aim and Objectives

The aim of this research is to develop lightweight soft body armour with improved ballistic performance. Textile based technologies will be employed to create ballistic woven fabrics with increased inter-yarn friction and to engineer ballistic hybrid panels. The thesis is subdivided into two parts.

The first part analyses the influence of inter-yarn friction on woven fabric performance. The objectives in this part of the work are listed below.

1) To develop a stable Finite Element (FE) model for ballistic event investigation. This presents the establishment of fabric models with correct geometry and mechanical properties. Some of the information is obtained from the tests and some collected from published sources.

2) To investigate the mechanisms of inter-yarn friction on fabric energy absorption. The relationship between inter-yarn friction and fabric energy absorption will be built up. An exhaustive study on the influence of inter-yarn friction on stress distribution and energy dissipation will be undertaken.

3) To manufacture UHMWPE plain woven fabrics with increased yarn gripping. Novel weaving techniques are developed to explore the possibility of mass-producing gripping fabrics on power loom.

4) To undertake experiments to examine the property and performance of fabric with increased inter-yarn friction.

The second part is the investigation of the performance and engineering of hybrid panels. The objectives in this part are listed below.

1) To investigate the response and failure mode of different layers in a panel subjected to ballistic impact by using FE simulation. The information obtained provides important guidance on ballistic panel design.

2) To analyse and evaluate UHMWPE woven and UD fabrics in order to satisfy the needs of different layers in a panel.

3) To carry out ballistic non-penetration tests and FE simulation and to verify the design guidance developed.

1.4 Thesis Layout

After the introductory chapter, Chapter 2 presents a review of literature in the areas of: the energy absorption mechanisms of a fabric target upon ballistic impact, factors influencing fabric ballistic performance, current experimental techniques for ballistic performance investigation and general information on the approaches of theoretical investigation.

Chapter 3 presents the methodologies employed to carry out the research. A comprehensive description of the ballistic range and the creation of a finite element model will be given in this section.

Chapter 4 is about the theoretical study of inter-yarn friction on woven fabric. Its influence on stress distribution and fabric energy absorption will be investigated in this chapter.

Chapter 5 is about the design and manufacture of gripping fabrics. FE simulations were used to investigate the possibility of weaving tight fabrics and modifying fabric structures for inter-yarn friction increase. In addition, novel weaving techniques are developed to weave friction increased woven fabrics on power looms.

Chapter 6 presents the experimental study of friction increased woven fabrics. Both yarn pull-out tests and ballistic penetration tests were carried out to study its performance. The results were analysed and improvements on structure modified fabrics were raised.

Chapter 7 is about the theoretical investigation of the response and failure model of different layers of fabric in a panel system subject to ballistic impact. The UD and woven fabric were analysed and evaluated for their tensile and shear properties and their applications in a ballistic panel.

Chapter 8 shows the testing results of different hybrid panels from a non-penetration test. Theoretical results are also presented for comparison.

Chapter 9 ends the thesis for conclusion and recommendations for future work.

Chapter 2 Literature Review

Ballistic impact on soft body armour is an important area and has been studied for many years. A quantitative understanding of the energy absorption of fabric target has gradually been built up through both experimental and theoretical efforts. This chapter aims to provide a comprehensive literature review on this topic and to indicate how this correlates the present work on developing lightweight soft body armour.

The following aspects will be centred on fabric energy absorption, which are (1) the response of a fabric target to ballistic impact, (2) factors influencing the energy absorption capability of ballistic fabric, (3) experimental testing methods and standards for performance evaluation, (4) modelling of ballistic impact onto a fabric target.

2.1 The Response of Fabric Target to Ballistic Impact

2.1.1 The propagation of the longitudinal and the transverse wave

When a fabric sample is impacted, two wave fronts are generated, namely a transverse wave and a longitudinal wave. Energy is dissipated through the propagation of the two types of wave. The longitudinal wave travels outward along the fibre axis at the sound velocity of the material from the point of impact. This wave also causes the yarn to be stretched and have in-plane movement. The longitudinal wave travels at a velocity

$$c = \sqrt{\frac{E}{\rho}} \qquad (2.1)$$

where c is the longitudinal wave speed in m/s, E is the fibre modulus in Pa, and ρ is the yarn bulk density in g/m^3.

At the same time, the projectile tends to push the yarn forward and therefore deflect the yarn vertically, which consequently results in an out-of-plane motion of the material. The velocity of the transverse wave has been studied by Gu [23], who determined the velocity with respect to the laboratory u_{lab} is

$$u_{lab} = c(\sqrt{\varepsilon(1+\varepsilon)} - \varepsilon) \tag{2.2}$$

where ε is the strain in yarn.

The two types of wave are depicted in Figure 2-1.

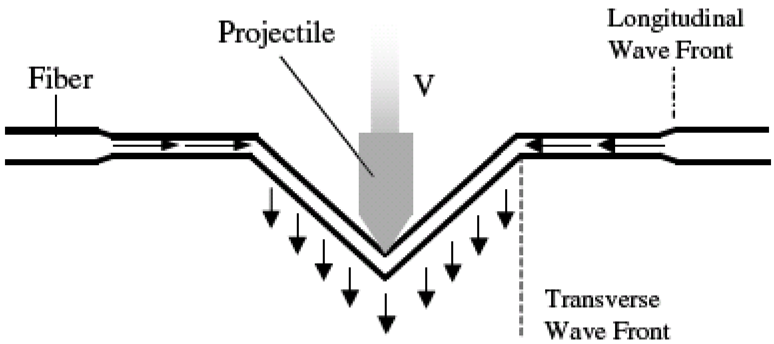

Figure 2-1 Projectile impact into a ballistic fibre [24]

2.1.2 Ballistic impact on a fabric target

When a projectile strikes a target, the response is believed to be a combination of global and local effects [25]. Global response indicates the behaviour of material away from the impact point and local response refers to the behaviour of material directly contacting the projectile, which are shown in Figure 2-2. Impact velocity is, if not the only factor, one of the most important factors to determine target response. Cantwell and Morton suggested that, on a composite target, at high impact velocity, local damage plays a major part in energy absorption [26]. While at low impact velocity, global plate deflection becomes more important [26, 27]. The velocity classification is shown in Figure 2-3, which indicates the range of high velocity and low velocity [25]. This phenomenon is also observed in Textile materials. Carr [28] found that Textile yarns also tend to have a global failure model (transmitted stress wave) at low impact velocity and a shear or plug failure mode at high impact velocity.

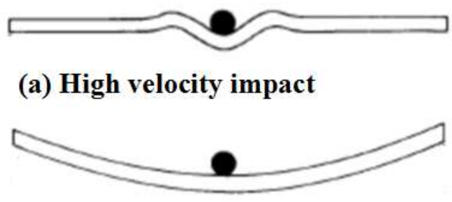

Figure 2-2 Reponse of a fabric target subjected to transverse impact

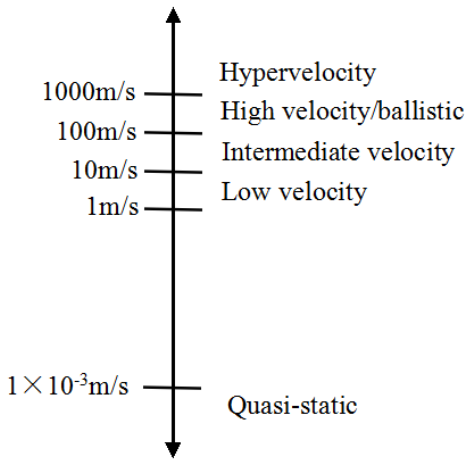

Figure 2-3 Standard classification of impact velocity [25]

2.1.2.1 Global response

At low impact velocity, as there is enough time for projectile kinetic energy to be transferred to the fabric target, larger areas get involved in energy absorption than at high impact velocity cases. The existence of yarn crossovers significantly influences the propagation of longitudinal waves. It has been observed that reflection of longitudinal waves takes place on at yarn crossovers and the strain distribution in the woven fabric is therefore influenced by the crossover density [24] .The longitudinal wave speed in plain woven fabric is suggested to be slower than that in a single yarn by a factor of $\sqrt{2}$. Roylance also pointed out that wave reflection is associated with fibre modulus and coefficient of friction [29]. Freeston built a numerical model to study the influence of wave reflections on strain distribution and concluded that the propagation of longitudinal waves is very little impeded by the effect of crossovers [30]. However, the out-of-plane motion of fabric due to the transverse deflection forms a tent-like deformation in the vicinity of the impact point. The two waves sweep across the fabric and transfer the projectile energy to fabric strain energy and kinetic energy, which are two of the principal energy absorption mechanisms. The energy stored increases with time until the projectile is stopped or the fabric is penetrated. Another energy absorption mechanism is friction. This includes energy dissipated by friction between warp and weft yarns, projectile and fabric target and between adjacent fabric layers. Although they are considered to contribute very little to overall energy absorption, frictional effects greatly influence the strain and kinetic energy absorbed by fabric [18].

2.1.2.2 Local response

At high impact velocity, as the projectile engaging time with the fabric target becomes short, the influence of global response on energy absorption diminishes. Fabric local reaction or failure mode has a major effect on ballistic performance. One of the major fabric failure modes is yarn or fibre rupture. This occurs when the yarn or fibre strain exceeds their failure strain. Different fibre rupture is characterised by different broken ends. For para-aramid fibres, it has been observed that fibre failed by fibrillation. Shear failure was noticeable on the UHMWPE fibre broken ends. There is an increased degree of melt damage as the impact velocity increases [28]. However, yarn/fibre rupture mode is also dependant on the head shape of the projectile. Tan *et al* found that yarns are more likely to be severed by flat-head projectile, causing shear damage. For round-head projectile, this is less noticeable in fabric [31]. As a mechanism for energy dissipation, the energy absorbed due to yarn/fibre rupture is based on fibre properties. This will be discussed in more detail in later chapters.

Another fabric failure mode is yarn pull-out. When the impact velocity is low or yarn-yarn friction is low or the fabric target is loosely gripped, principal yarns will be pulled out rather than damaged. Bazhenov [16] found that yarn pullout is related to the energy absorption of a ballistic fabric. Starrat [32] used a series of photographic and velocity measurement technologies and concluded that yarn pullout contributes a significant amount of energy absorption in non-penetration cases. Kirkwood and his colleagues [33, 34] present a semi-empirical model to quantify the energy dissipated yarn in pullout. They believed that the two main mechanisms associated are yarn de-crimping and yarn translation. And the pullout force is highly dependent on yarn-yarn friction.

Shim *et al* [35]observed that the hole created by the projectile is smaller than its diameter, leading to the assumption that there is hole expansion during ballistic impact. In this failure mode, the projectile tends to push the yarns aside, penetrating the fabric through a wedge-through effect. Lim *et al* [36] tested double-ply fabrics and found that the misalignment of yarns caused by wedge-through effect is more noticeable in back layer.

2.2 Factors Influencing Fabric Ballistic Performance

Literature regarding the influencing factors on fabric ballistic performance have been mentioned in a number of works [37-39]. The energy absorption behaviour of ballistic fabric is an inter-play of many mechanisms. It is difficult to isolate and discuss any one of them. For example, if fabric ballistic performance is solely dependent on fibre tensile strength, nylon would be a better material than Kevlar [40]. The fact is, Kevlar proves to be the most popular high-performance fibre in making soft body armour. This section will give a detailed description of those factors

2.2.1 Fibre properties

Roylance and Wang [41] established that approximately half of the total energy absorption is stored in the form of strain energy. By comparing the ballistic resistance of dry Spectra fabrics with their corresponding laminates, Lee *et al* [42] correlated the number of broken yarns to the energy absorbed. He also found that fibre straining is the primary mechanism of energy absorption. In the fabric target, the accumulation of strain energy is determined by the area getting strained. Strained area is directly associated with the velocity of sound in the material [43], which is also considered to be the velocity of the longitudinal wave. According to equation 2.1, this velocity is a function of material modulus and density. By using a numerical model, Roylance and Wang [41] established that higher modulus fibre gives higher wave velocity, which leads to a rapid energy absorption rate. As the modulus is decreased, the wave velocity is decreased and the strain is more concentrated in the vicinity of the impact zone, which is shown in Figure 2-4 [41]. This is reinforced by Field and Sun's experimental work [44]. They used a high speed photographic approach to observe the behaviour of fibres and woven fabrics upon transverse impact. They found that fabric with high modulus can spread load onto other fibres and layers more quickly, which is beneficial in ballistic applications.

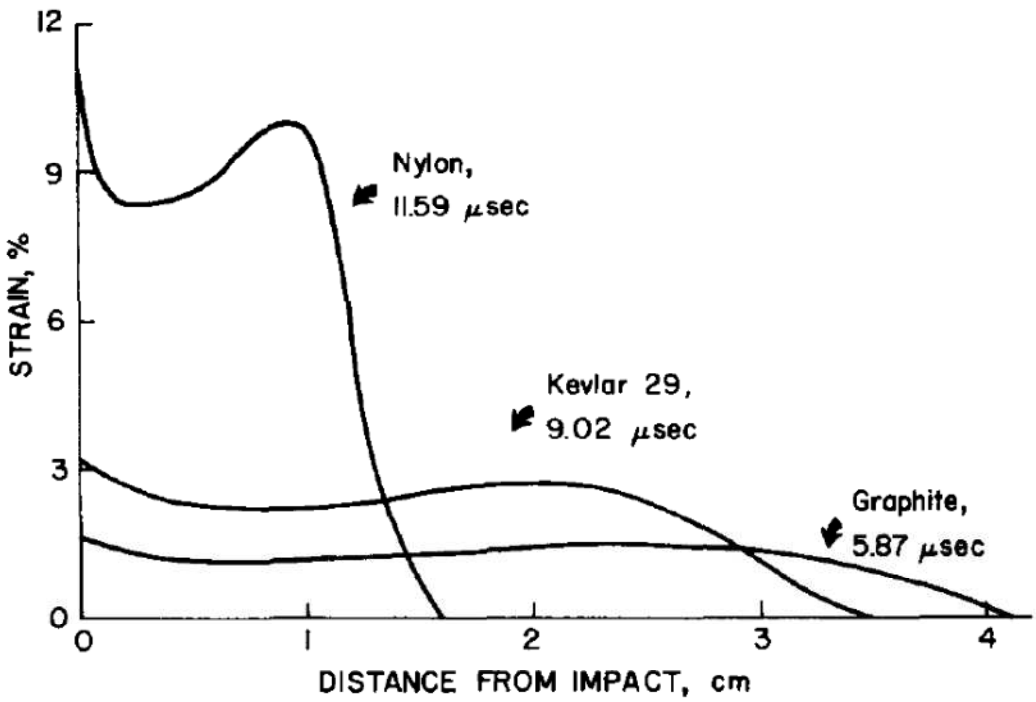

Figure 2-4 Strain profile along orthogonal yarns passing through the impact point [41]

Nevertheless, Roylance [45] analysed the strain energy-fibre modulus relationship and reported that a fibre of high modulus was usually obtained at the sacrifice of elongation at break. He suggested that high modulus (graphite) leads to a high rate of energy absorption, but the panel would fail at an early stage and therefore not be able to extract energy as effectively as the low modulus fabrics, such as Kevlar or Nylon. This feature greatly decreases the total energy absorbed by the fabric panel, which is shown in Figure 2-5 [41].

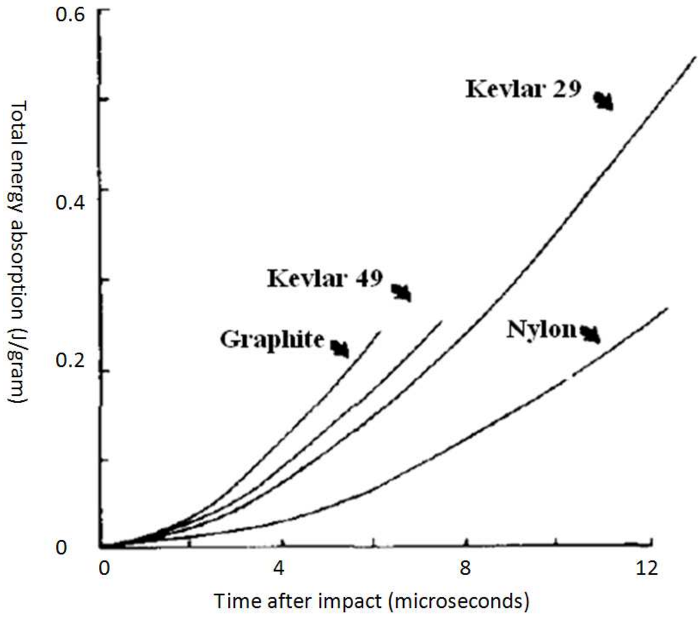

Figure 2-5 Comparison of total energy absorption for different fabric panels [41]

As a result, it is difficult to take into account just one or two factors when select high performance fibres for ballistic applications. Through research work, Cunniff [46] has determined that fibre ballistic property is a function of a number of parameters, including material density and the velocity of sound in a fibre. The fibre property is to be denoted by U^* (having units of m^3/s^3):

$$U^* = \frac{\sigma\varepsilon}{2\rho}\sqrt{\frac{E}{\rho}} \tag{2.3}$$

where σ is the fibre ultimate tensile strength in N/m^2, ε is rupture strain.

Roylance *et al* [24] suggested that at dynamic rates, the static molecular failure mechanism of low-tenacity fibres does not have enough time to take place, which considerably reduces the amount of energy absorbed. For high-tenacity fibres, however, the slow molecular mechanisms are not used, and the energy absorption is essentially not reduced much. As the strain rate of the materials under ballistic impact is often greater than 10^2/s [47], high-tenacity fibres are more likely to offer protection against a fragmentation threat than low-tenacity fibres. Ballistic fibres give different response to dynamic and static stress, reflecting the rate-dependence of their molecular properties. In many research works, the study of ballistic fibre properties at high strain rate is carried out using a split Hopkinson tension bar (SHPB). The SHPB is a device for material testing at strain rate in the range between 200 and 5,000 s^{-1}. Wang and Xia [48, 49] studied the effect of strain rate from 10^{-4} s^{-1} and 10^3 s^{-1} on Kevlar® 49 aramid fibre bundles. They found that tensile modulus, strength and failure strain increase with increasing strain rate at a constant temperature. The modulus decreases and failure strain increases with the increase in temperature at a fixed strain rate. Lim and his colleagues [50] adopted a non-contact laser technique to measure axial small strain of Kevlar® 129 fibres in a SHPB. They observed that the fibre failure strain and modulus are dependent on gauge length. Kinari *et al* [51] developed a tensile testing device based on one-dimensional elastic-stress-wave theory. This apparatus is able to perform tensile tests at different strain rates and the results showed agreement with those obtained from SHPB.

2.2.2 Yarn structure

The effect of yarn structures on ballistic protection mainly depends on the utilisation efficiency of individual fibres. Cunniff [52] found that the efficiency is lost in going from a fibre to a yarn, from a yarn to a fabric and from a single fabric to a multi-layer fabric. This is because each individual fibre shares different loads when it comes into contact with bullet, and therefore fibres tend to break successively instead of together. In order to achieve even load sharing, finer fibres are used in ballistic applications due to the higher fibre to fibre cohesion. In addition, yarn used in ballistic fabric usually has a low twist or even no twist. Too high a yarn twist angle will lead to yarn slippage and the projectiles are more likely to penetrate the fabric through the yarn spacing. Rao and Farris [53] found that the optimum twist angle which is able to maximise the yarn strength while giving the minimum yarn slippage is around 7°. Other yarn features such as the fibre array have an influence on yarn mechanical properties as well.

2.2.3 Fabric structure

2.2.3.1 Woven fabrics

The most commonly used fabric structure in the soft body armour area is woven fabric. Woven fabrics stop projectiles by forming a network of fibre or yarns. This network enables the fibre or yarns to be stretched, transmitting projectile kinetic energy to the fabric. Among various weave patterns, plain fabric is the most common pattern due to its high interlacing yarn density and dimensional stability [54]. Cunniff [52] also pointed out that loosely woven fabric or fabric with an unbalanced pattern result in inferior performance. 3-D fabrics have also been studied for their applicability in ballistic protection. Angle interlock fabrics were investigated by Yang [55] for use in female body armour and orthogonal fabric was modelled and tested by Shi *et al* [56].

Weave density of fabric, which is known as "cover factor", is a function of the number of warp picks and weft ends in a unit of length of fabric and indicates the percentage of area covered by the fabric. High cover factor will increase the available dissipation of strain energy capability by getting more fibres and yarns engaged with a projectile. Shockey [57] studied Zylon fabrics with various weave densities and observed that the increase in energy absorption is almost in proportion to the increase in weave density. It has been suggested that the cover factor should be in the range of 0.6 to 0.95 [58] for ballistic applications. When cover factors are greater than 0.9, yarn properties degrade in the process of weaving and when the cover factor fall below 0.65, the fabric will become too loose. The 'wedge through' effect is more likely to occur on loosely woven fabrics, which is depicted in Figure 2-6.

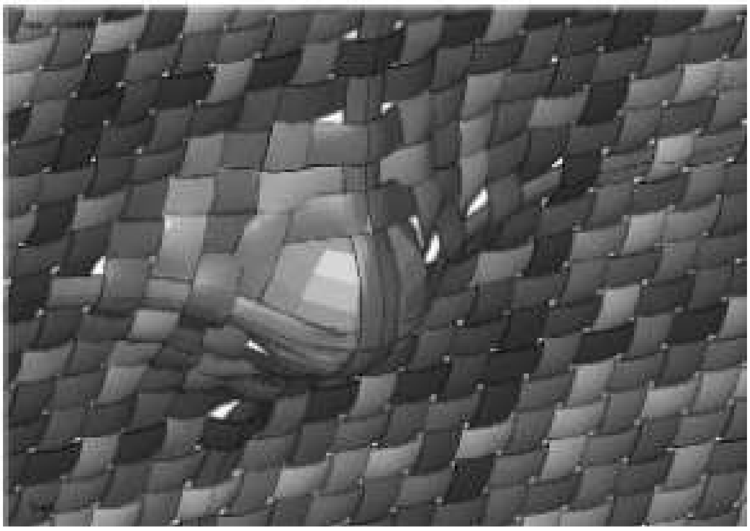

Figure 2-6 “wedge through” effect [37]

Yarn crimp is a distinct feature in woven fabric and it is not observed in unidirectional structures or felt. Yarn crimp is the undulation of the yarns caused by yarn interlacing. When a projectile strikes a fabric, the initial stage of fabric deformation gives rise to the straightening of crimped yarns. The de-crimping process reduces the modulus of the fabric at the first stage of tensile stretching [59], during which little resistance is presented to the projectile and almost no energy absorption occurs. The fabric does not function as protection until the yarns finish de-crimping and begin to stretch. According to Tan [60], this leads the fabric to cause excessive blunt trauma to the human body. Chitrangad [58] found that the warp yarns tend to have more crimp than the weft yarns, thus the weft yarn would break before warp yarns. In order to make a balanced crimp degree, he attempted to weave plain fabric and basket weaves with two different yarns, the weft yarns of which have a greater elongation rate than warp yarn. In comparing the hybridised fabrics with fabrics comprised entirely of one type of yarn, he noticed that the V_{50} from the hybridised fabric was higher (the definition of V_{50} will be presented in section 2.3.2.2). Clearly, the effect of yarn crimp on impact resistance should not be ignored when studying the performance of soft body armour.

Roylance *et al* [24] suggested that fabric which is able to distribute the energy more equitably could give better ballistic performance. One of the possible approaches to achieve that was considered to be making tri-axial fabrics. In tri-axial fabrics, three sets of parallel threads intersect at 60 degree angles. It was believed that a tri-axial fabric exhibits better performance due to the hexagonal shape of a tri-axial fabric upon impact when compared to the pyramidal shape of a biaxial fabric. Their responses to impact are shown in Figure 2-7. This gives rise to spreading of energy more evenly around the impact zone. Hearle and his colleagues [61] compared their ballistic performances by finding the number of layers required to stop the bullet. They discovered that the total areal density of the biaxial fabric (2400g/m^2) is much less than that needed in the case of tri-axial fabric (3094g/m^2). One possible explanation is that the more open structure of a tri-axial fabric would confer a reduced ballistic protection. A tri-axial fabric of much closer weave was tested and the results showed a lower V_{50} than the biaxial fabric.

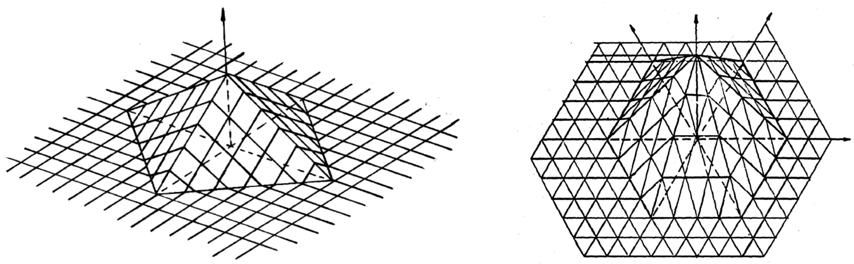

(a) Bi-axial fabric upon impact [23] **(b) Tri-axial fabric upon impact [24]**

Figure 2-7 Schematic diagrams of fabrics upon ballistic impact

2.2.3.2 Unidirectional fabrics

The unidirectional (UD) construction was first used in soft body armour for the chest and helmet by air crewman in the Second World War [62], and was reintroduced by Allied Signal with the UHMWPE fibre, Spectra in the mid-1980s. The unidirectional technology is based on the idea of combining the cross-plied filaments with an elastomeric matrix in a laminated system. Figure 2-8 shows a four-plied unidirectional system laminated by two films. Other companies such as DSM and Park Technologies also provide similar fabrics for personnel protection.

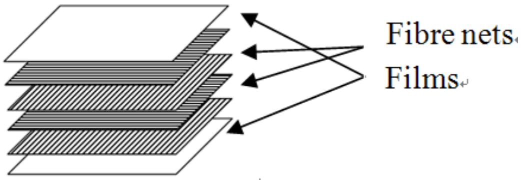

Figure 2-8 Unidirectional structure

Unlike woven fabrics, the crimp is removed and the yarn profile in unidirectional fabric is straight. As a result, the unidirectional structure does not exhibit the initial de-crimping phenomenon and the high modulus of the fibre is retained in the fabric. The fibres will react quicker with laminate stiffness coupled with fibre stiffness and spread energy to a greater extent. The woven structure, however, is more compliant. This would prolong the duration of fibre stretching and leads to more blunt trauma underneath the impact zone [63].

The superior performance of UD structure over woven structure has been realised in many publications. According to Scott [63], around 30% improvement in either weight or performance has been observed in both flexible armour and hard composites. Lee *et al* [21] found that the ballistic limit for angle plied laminates gives a higher value than woven fabric based composites as the density of the panels increases. It has also been established that a 100% UD fabric panel absorbs 12.5% to16.5% more energy than a 100% woven fabric panel [64].

2.2.3.3 Felts and knitted structures

The response of felt to ballistic impact is significantly different from that of woven fabric and UD fabric. Its energy absorption mechanisms are yet to be fully understood. The use of felts in ballistic protection is found to be limited. It has been observed that this type of structure is effective in capturing low speed fragments by having some of the fibres pre-aligned along the projectile trajectory [63]. Nevertheless, the current threat regarding ballistic impact is for small projectiles at high velocity. Hearle [65] found that needle felt Nylon (18.5Kg.cm/g) gives inferior energy absorption than woven Nylon (29.2 Kg.cm/g).

In addition, a deeper and narrower back face signature is formed for the felt panel, which is more likely to cause greater trauma than the other two structures. Thomas [66] discovered that incorporating felts between the ballistic fabrics may benefit reducing the trauma to the wearers. This finding, however, needs to be further validated. Another problem regarding the use of felt is its tendency to absorb moisture. It is believed that this could be solved by sealing it in a water impermeable bag. Therefore, due to the drawbacks mentioned above, felt is not regarded as suitable material for ballistic application.

Hearle [65] also examined the mechanical properties of warp knitted Nylon. He discovered that although the dynamic modulus of knitted fabric (4.4 g.wt/Tex) is far lower than that of woven fabric (66 g.wt/Tex), they exhibit similar energy to breaking when subjected to tensile loading. The energy absorption of knitted fabric (28.5 Kg.cm/g) also give a similar value to that of woven fabric (29.2 Kg.cm/g) upon high velocity ballistic impact. In spite of that, knitted fabric is not considered suitable to be used for soft body armour. Its low modulus would delay the fabric response to impact and transmit more force to the backing material, which may cause deep and narrow trauma as well.

2.2.4 Panel systems

There is no shortage of work regarding the ballistic performance of multiplied textiles. Shockey *et al* [67] observed that the energy absorption is always in proportion to the number of plies. Lim *et al* [36] investigated the reinforcement effect of backing layers on the ballistic performance with different projectiles. The comparison showed that the spaced armour system gives better performance than the layered system except for flat-nosed projectiles. They also concluded that the benefit of reinforcement is largely highly dependent on the impact velocity and projectile nose shape. This is supported by Porwal and Phoenix' s theoretical work. Porwal and Phoenix [68] developed an analytical model to study the response of materials in a double-plied armour system. They observed that the V_{50} degrades progressively as the spacing of the layers increase when compared to the system without spacing (the definition of V_{50} will be presented in section 2.3.2.2).

However, there are some findings which differ from the results mentioned above. Cunniff [69] observed that fabric body armour responds to ballistic impact in a decoupled fashion through the thickness of the armour panel. He [52] also assumed that if the adjacent layers are not in contact with each other in a spaced system during ballistic impact, the energy absorption would be exactly equivalent to the sum of the single-ply energy absorption. Based on his assumption, he believed that the spaced system exhibits higher ballistic performance than the layered system. Novotny *et al* [70] used an explicit finite element code, TEXIM, to study this problem and found that the influence of layer spacing is closely related to the number of layers in a panel. Their results indicate that the ballistic performance is insensitive to the layer spacing up to 10 plies thick. In the range of 20 to50 plies, the thicker the panel, the greater the effect of inter-layer spacing will be. Nevertheless, there is yet to be any experimental support for the superior performance of the spaced system.

Cunniff [52] also suggested that the subsequent plies of fabric may constrain the transverse deflection the front plies, which is considered to affect the performance of a panel. As a result, he believed that placing low modulus materials on the impact face and high modulus on the subsequent plies may avoid this phenomenon and improve the performance of ballistic panel. In addition, Nader and Dagher [71] used non aggressive barbed needles to place fibre through the thickness in a panel, preventing the projectile from spreading the individual yarns and the adjacent layers from delamination. Chitrangad [58] found that the weft yarns are stretched to break before the warp yarns in a ballistic event. By using a fabric with the weft yarns having a higher elongation to break than the weft yarns may enable the warp and weft yarns to break at the same time, which improves the performance of a fabric or panel.

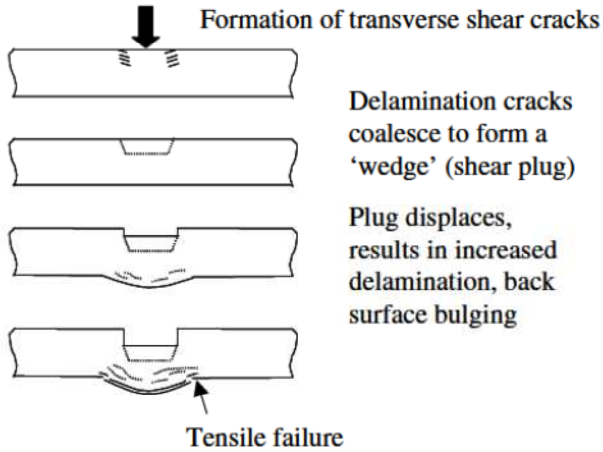

Figure 2-9 Impact upon compliant panel [37]

When a composite panel is under impact, the projectile tends to exhibit through-the-thickness shear failure in the front layers, forming a plug; for back layers, the fibre damage mode resembles tensile failure [21, 37], which is shown in Figure 2-9. Similar phenomena were found to be true on the dry fabric panel as well by Chen *et al* [72]. The fact that different layers of fabric exhibit various responses upon ballistic impact suggests the necessity for combining more than one type of material in a panel. Mixing different materials in a proper sequence would hopefully make the best use of their corresponding properties and consequently enable the ballistic panel to be more energy absorbing.

One notable step to achieve design of hybrid panels is the combination of UDfibre-reinforced laminates with woven fabrics. Hybrid panels formed by UD fabrics and woven fabrics show better performance than single-phase panels. Non-penetration ballistic impact tests carried out by Thomas [73] showed that single-phased aramid filament layer-up panels give a deeper back face signature than hybrid panels. Karahan *et al* [74] showed that around 13.9% less energy was transmitted to the backing materials through a hybrid panel than through a single-phased UD fabric panel. Price and Young [75] found that hybrid multi-plied fabric assemblies tended to exhibit a higher V_{50} than single-phased woven or UD assemblies (the definition of V_{50} will be presented in section

2.3.2.2).

2.2.5 Friction

Frictional mechanisms include frictional dissipation due to yarn slippage， the interaction of the projectile and fabric or the interaction between adjacent layers. It is believed that the magnitude of frictional energy is influenced by many factors, such as the yarn-yarn coefficient of friction and boundary conditions [76]. Duan *et al* [18] investigated the role friction played in a ballistic event through finite element analysis. They found that although energy dissipated by friction accounts for a small amount of the total energy, projectile-fabric friction resists yarn slippage and enables more yarns to engage with the projectile, which greatly increases the kinetic energy and strain energy associated with the fabric target. The fact that impact load could be distributed along the periphery of the projectile fabric contact zone also delays yarn failure. Yarn-yarn friction, however, restricts yarn movement and leads yarns to fail at an early stage.

Lee *et al* [42] studied the response of armour-grade fibre-reinforced composites and dry woven fabric upon ballistic impact and suggested that dry woven fabric is more likely to have successive fracture of individual yarns and yarn slippage. On the contrary, failure of fibre-reinforced composite mainly consists of fibre fracture due to the constraint of the matrix. The reduced yarn-yarn mobility enables the composite to have more energy absorbed than dry fabric. This is supported by Bazhenov' work. Bazhenov [16] tested dry laminates and wet (water treated) laminates. The experimental results indicate that water reduces yarn-yarn and fabric-projectile friction, which causes wet laminates to have narrower yarn pull-out zone and absorb less energy than dry laminates. Zeng *et al* [19] built a numerical model to study the yarn-yarn coefficient of friction. Their model showed that the increase in yarn-yarn friction for values of μ from 0 to 0.1 doubles the ballistic limit of ballistic fabric. Further increase yields little difference in ballistic limit. Nevertheless, the results obtained from their computational model are contrary to Briscoe *et a* 's work. Briscoe [17] chemically-treated the Kevlar 29 woven fabrics to achieve different levels of yarn-yarn friction. The soxhlet-extracted fabric (μ=0.25±0.03) gives better ballistic performance than as-received fabric (μ=0.22±0.03) and polydimethylsiloxane (PDMS) treated fabric (μ=0.18±0.03), which is shown in Figure 2-10. As a result, it is possible that further increase in yarn-yarn frictional coefficient after 0.1 may further improve the energy absorption of ballistic fabric.

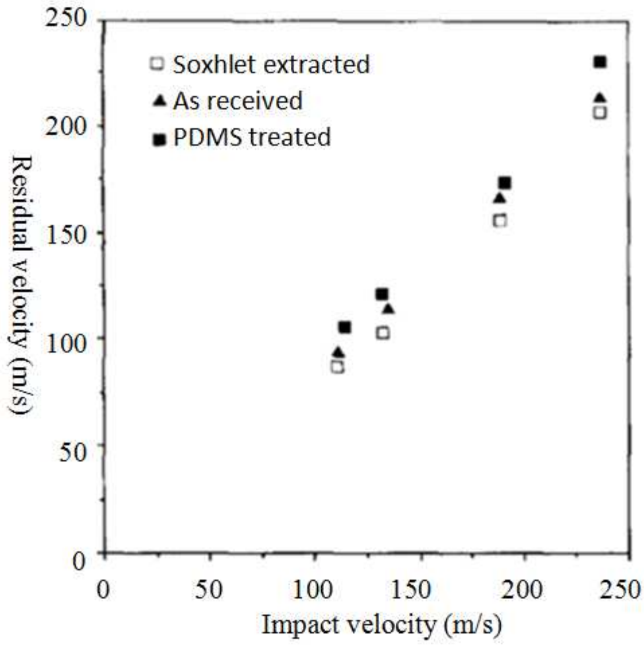

Figure 2-10 Residual velocity as a function of impact velocity for Kevlar 49 weaves [17]

The approaches developed so far to increase yarn-yarn friction have mainly been based on chemical treatment. One of the most popular methods is shear thickening fluid impregnation [77-79]. Shear thickening is defined as the increase of viscosity with increase in shear rate [80]. The most widely used shear thickening fluid in ballistic applications is the silica colloidal water suspension (SWS). Yarn pull-out tests showed that the highest force required to pull out a yarn is almost 650 N for 40 wt% particle impregnated fabric, which is 150 N greater than that of neat fabric [77]. It is also considered that the pull-out force was very sensitive to pull-out speed for treated fabrics [78]. The increase of speed from 100 mm/m to 1400 mm/m causes the highest pull-out force to increase from 6 N to almost 12 N, which means the yarn-yarn friction could be further increased at higher pull-out speeds in ballistic events. Both of the aforementioned studies show the possibilities for improved ballistic performance of impregnated fabric. Young *et al* [79] suggested that, although the weight reduction is not noticeable for the two types of panel of equivalent performance, treated panels offer considerably less thickness and more material flexibility.

For ballistic fibres, a low coefficient of friction with processing equipment is desired to reduce fibre damage. This gives rise to conflicting situations as a high yarn-yarn friction is required in ballistic applications. Chitrangad and Rodriguez-Parada [81] developed a finish with certain fluorinated compounds containing polar nitrogen groups to achieve a higher yarn-yarn friction while not increasing yarn-equipment friction. Louis [82] found that a deposition of 0.15 to 0.2 microns thick polypyrrole film on Kevlar fabrics increases the flechette resistance by about 19%. Apart from chemical-related methods, researchers also attempted to change yarn and fabric structures to increase yarn-yarn friction. Hogenboom and Bruinink [83] combined filaments of high strength and low frictional coefficient and filaments of low strength and high friction by core spinning. The combined yarns are considered to take advantage of hybridization and be useful for bulletproof materials.

2.2.6 Projectile geometry

Projectile geometry influences its ability to penetrate the fabric layers, significantly affecting the energy absorption of ballistic panels. Tan *et al* [31] investigated the energy absorption of Twaron CT 716 woven fabric impacted by four different projectiles, which are shown in Figure 2.11. The results are revealed in Figure 2.12. They established that sharper projectile shapes, such as ogival and conical, result in less energy absorption than flat and hemispherical projectiles. The highest ballistic deceleration is found to be the hemispherical projectile (159m/s), which is almost three times higher than the conical projectile (59m/s). This is because projectiles with a sharp nose are more likely to slip through the fabric between adjacent yarns due to their streamlined nose profiles. The flat nose projectile, however, possesses an angled edge and therefore is more likely to cut and shear the fabric surface during impact. The hemispherical head projectile is found to penetrate the fabric mainly by yarn stretching. As a result, the energy absorbed in accordance with the hemispherical head is more pronounced than the other types. Lim *et al* [36] investigated the reinforcement effect of the back layer in a two-ply fabric system using the four types of projectiles. It appears that all the projectiles exhibit doubled energy absorption in a two-ply system compared with a single-ply system except for flat nose projectile. This is because the cutting effect of flat nose projectiles allows easy penetration of the panel, which diminishes the reinforcement effect of the second layer. The cutting effect is also observed by Prosser *et al* [40] *and* Shockey *et al* [84]. They reported that the projectiles with a sharp face are more likely to cut the fabric to failure and more easily penetrate the target than blunt faced projectiles.

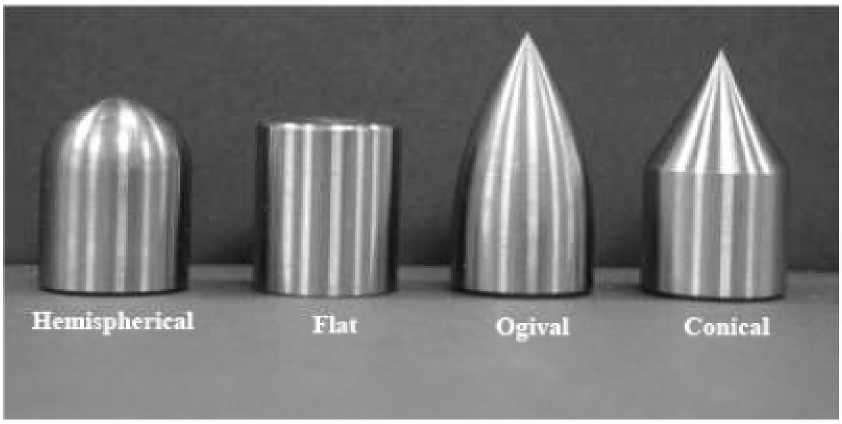

Figure 2-11 Different projectile used in Tan *et al*'s work [31]

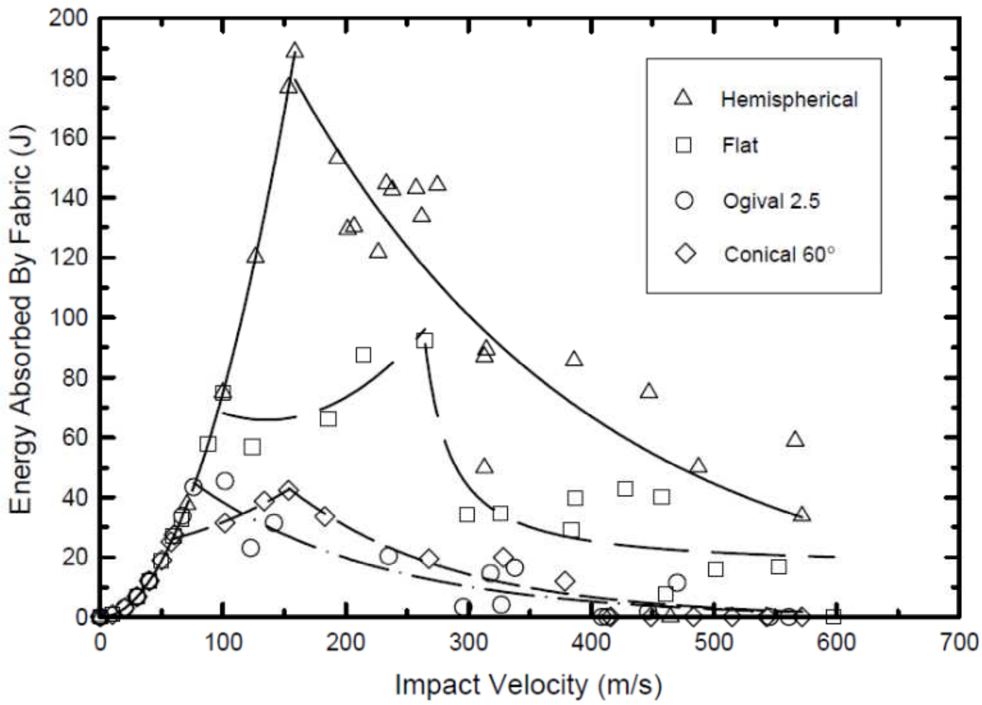

Figure 2-12 Energy absorbed by fabric impacted by different projectiles [31]

In order to investigate the energy absorption with respect to the projectile nose angle, Talebi [85] established a realistic finite element model of Twaron fabric and simulated the projectiles with nose angles ranging from 30° to 180 °. The testing results validated the findings of Tan. It is believed that decreasing the nose angle to less than 60° will not necessarily result in more damage to the fabric for a given length of the bullet. This is because sharpening the projectile head will cause the loss of its total weight, which consequently reduces the kinetic energy of the bullet and its efficiency. Moreover, projectiles with a sharp nose are more likely to break when they come into contact with the target at high velocity.

2.2.7 Projectile striking obliquity

Projectile striking obliquity is the yaw angle at which the projectile impacts the fabric target. The yaw angle is defined as the angle between the warp yarn direction and the longest dimension of the projectile impact end [38]. Cunniff [86] found that at high areal density, the V_{50} velocity is closely associated with the projectile impact obliquity (the definition of V_{50} will be presented in section 2.3.2.2). It is considered that around 50% more yarns will be damaged at a 45 degree angle than at a 0 degree angle [38]. This phenomenon is thought to be due to the fact that oblique impact allows more orthogonal yarns to assist in the energy absorption [87]. Shockey *et al* [88] suggested that a projectile may rotate during penetration in a multiply fabric system, decreasing the hole size and reducing the number of broken yarns. One thing worth noting is that the influence of striking obliquity is greatly dependent on the projectile dimensions. If the length of the projectile is equal to the diameter of the head, the yaw angle is less likely to affect the energy absorption of ballistic fabrics.

2.2.8 Boundary conditions

In penetration tests, as the fabric or panel samples need to be gripped by a clamp, the boundary condition plays an important role in fabric energy absorption. Cunniff [52] used a chisel-nosed fragment simulator to test a single-ply Kevlar woven fabric on an aluminum plate with different apertures. He found that the ballistic performance is strongly dependant on the aperture size at impact velocity near the ballistic limit of the fabric. It was believed that a small holder aperture constrains both transverse and longitudinal deflection. As the impact velocity increases, the effect of aperture decreases. Slippage of the fabric between sample holders was observed, but Cunniff paid less attention to the relationship between the fabric performance and the clamping pressure. Lee *et al* [42] investigated the energy absorption capability of compliant Spectra laminate over a range of clamping pressures in a quasi static drop-weight test. They found that the energy absorption at a clamping force of 2 kN was about 4.5 times higher than that at a force of 254 kN. When the clamping force exceeds 254 kN, the energy absorption is found to be independent of the clamping force, indicating that no slippage took place during impact. Chitrangad [89] noticed that tensioned fabrics give better ballistic performance than un-tensioned fabrics.

Shockey *et al* [57] presented that fabric samples gripped on two edges absorbed more energy than samples gripped on four edges. In order to further investigate the effect of boundary conditions on fabric energy absorption, they performed a series of quasi-static penetration tests on four-edge-clamped fabrics and two-edge-clamped fabrics. The load-stroke (penetrator displacement) curves for the two boundary conditions are shown in Figure 2-13. It is apparent from this figure that, although the peak load of four-edge-gripped fabric is 65% higher, the curve plunges abruptly to zero after the peak load, indicating immediate perforation on impact. The load for two-edge-gripped samples, however, does not drop to zero, indicating continuous deformation after peak load force. This phenomenon enables the two-edge-clamped fabric to absorb more than twice the energy than the four-edge-clamped fabric. It is believed that it is the yarn pull-out that contributes to the delayed penetration of two-edge-clamped fabric.

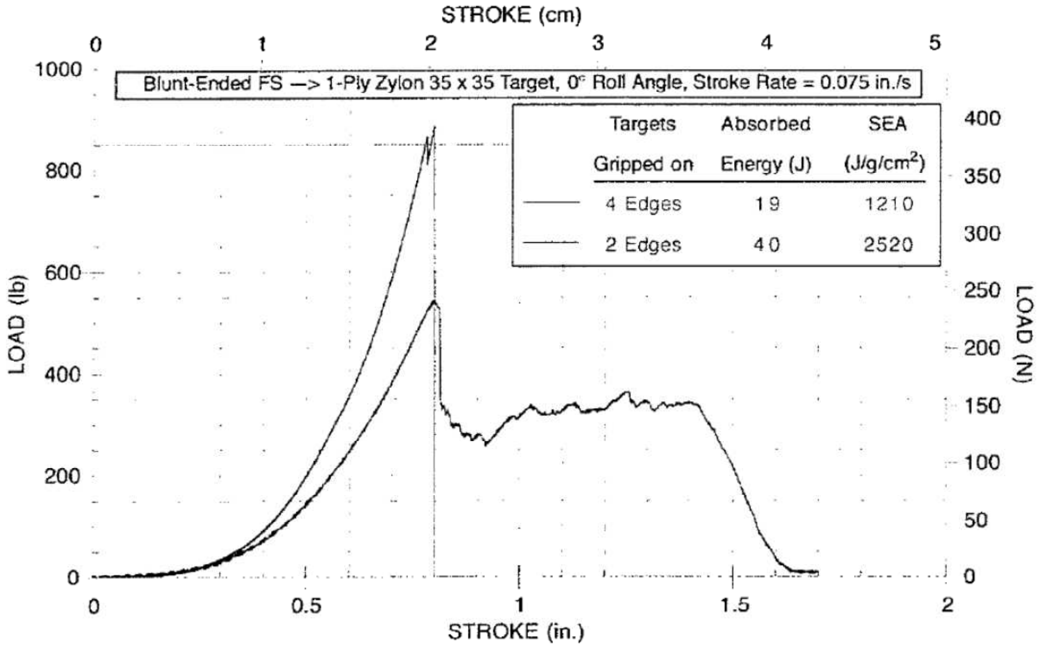

Figure 2-13 Load as a function of penetrator displacement for fabric with two edge clamped and fabric with four edge clamped [57]

Similar results were found by Zeng and his colleagues. Zeng *et al* [90] carried out ballistic tests on fabrics with three types of boundary conditions: four-edge-clamped, two-edge-clamped and four-edge-clamped with yarns running 45° to the edges and the built up computational simulation to study the effects of yarn orientations and clamping directions on energy absorption. The results suggested that for a high velocity regime, such as at an impact velocity of 450m/s, the amount of energy absorbed by the fabric on three different boundary conditions is almost equal, which is shown in Figure 2-14.

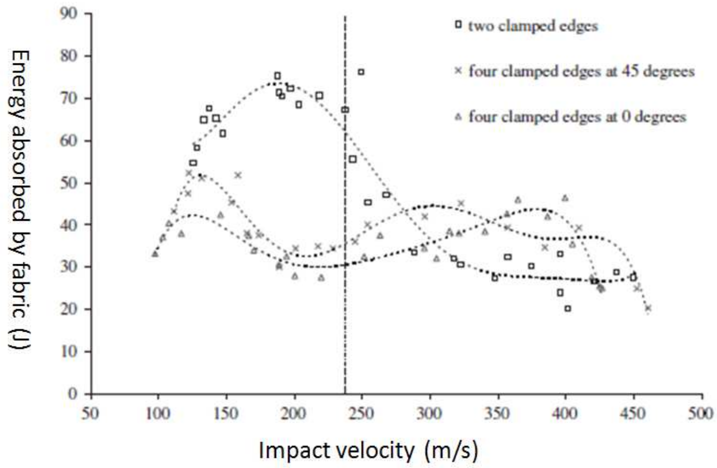

2-14 Energy absorption of fabric targets with different boundary conditions [90]

Under a low impact velocity regime (lower than 250m/s), fabrics clamped along only two edges give superior energy absorption characteristics to those of the other two conditions for the low velocity regime. It is quite interesting to note that clamping the four edges at 45° improve the ballistic resistance slightly. The prime reason for this phenomenon is that the rotation of the fabric contributes to an increase of strain energy in the whole fabric. When compared to fabric with a clamped angle of 0°, the length of the primary yarns increases and yarns originally remote from the impact point become shorter. As a result, longer principal yarns are able to distribute more projectile kinetic energy and shorter secondary yarns are more easily stretched, and therefore more of the fabric gets involved in the deformation zone.

2.3 Experimental Investigation of Ballistic Impact

Experimental work is based on data obtained from ballistic tests. This is an integral part of soft body armour design and manufacture. From a research point of view, results from experimental tests and observation not only directly indicate the performance and usability of materials in ballistic applications, but provide empirical data to test the validity of the theories put forward in this field as well. This section will list the methods and approaches adopted to study fabric response and evaluate its performance upon ballistic impact.

2.3.1 Photographic and monitoring techniques

Photographic and monitoring techniques are mainly about the observation of ballistic events using a high speed camera or other monitoring techniques. Susich *et al* [91] performed a microscopic study on nylon soft body armour and observed various types of failure mechanism on the penetrated sample. Evaluating the damaged fibres by using light microscopy, polarised light microscopy and scanning electron microscopy, Prosser *et al* [40] suggested that heat, depending on how, when and where it is generated, can degrade fibre performance in a sense. Wilde *et al* [92] observed the high-speed missile impact event using high-speed photography. One of their achievements is that fabric deformation was determined to be pyramidal before penetration and more conical after penetration. They also concluded from their observation that the primary yarns could account for 50% to 100% of the projectile energy loss. Field and Sun [44] used an image convertor camera to shorten the photography to microsecond intervals, which enabled them to observe the impact event at velocities up to 1000m/s. The significance of this study, as suggested by Roylance [41], is that the fibres which exhibit the best performance are those which combine a high modulus and large strains before failure.

Schmidt *et al* [93] used a pair of high-speed cameras for record dynamic deformation, showing shape and strain details of a fabric upon ballistic impact. The information obtained is used to validate the FE model in LSDYNA and to quantify the transverse deflection. Nurick [94] used light rays emitted from a silicon photovoltaic diode to monitor the deflection of the target. The resolution of this measurement is considered to be highly dependent on the distance between adjacent rays. Ramesh and Kelkar [95] developed a laser line velocity sensor system to measure the displacement of the projectile prior to impact, to hence determine its impact on velocity and acceleration . Starratt *et al* [32] enhanced this system and used it in the ballistic impact test. The system is schematically illustrated in Figure 2-15. A sheetlayer of light is emitted from diode layer 1 and diverted through a series of lenses (2, 3, 4, 5). The resultant layer light is a sheet of light with uniform width, thickness and intensity. The sheet is then focused and received by a silicon PIN photo detector (7). When the projectile is outside the sheet, the oscilloscope shows maximum voltage (before A in Figure 2-15 and Figure 2-16. As it moves from A to B, the light sheet is blocked out and the voltage drops. From B to C, the intensity of the sheet keeps at minimum value. As the projectile begins to leave the light sheet, the intensity increases with a corresponding rise in the voltage (from C to E). The application of this system enables them to determine the projectile velocity, acceleration, impact force and energy loss, which gives a direct understanding of the response of the fabric target.

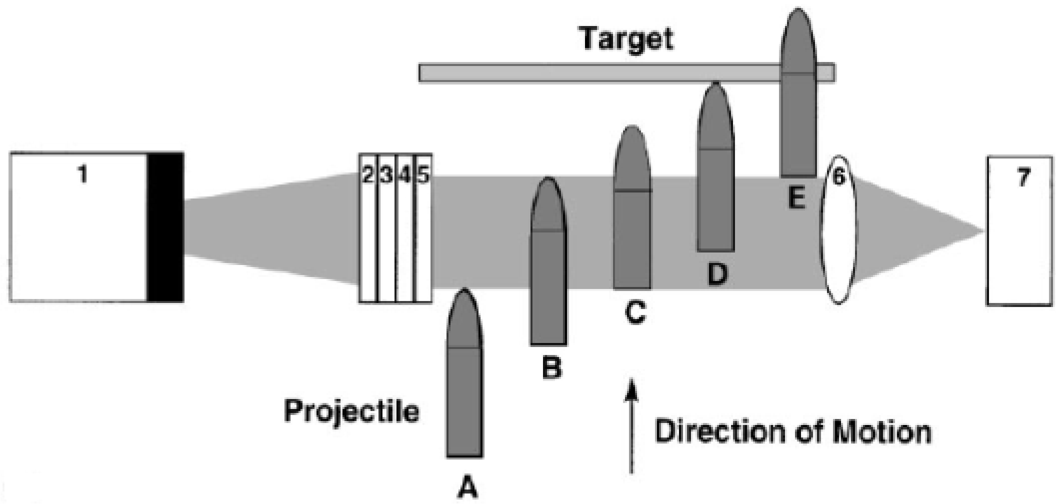

Figure 2-15 Schematic diagrams of enhanced layer velocity sensor [32]

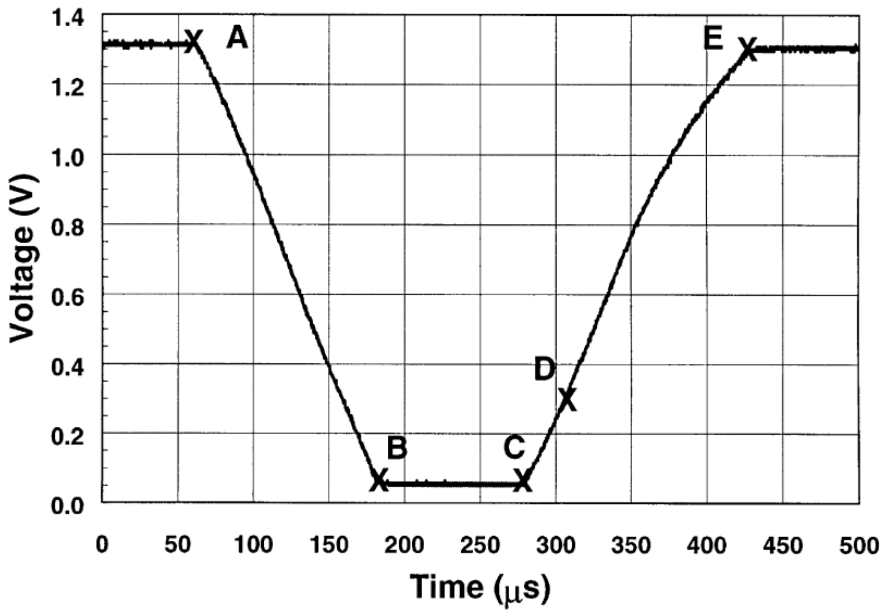

Figure 2-16 Time history of voltage curve for a ballistic impact [32]

2.3.2 Ballistic performance evaluation

Many techniques have been used to measure the velocity of a projectile. The most widely used systems are instantaneous, discrete techniques such as sensors or chronographs. The impact or residual velocity of a projectile is calculated from the distance between two sensors divided by the time taken by the projectile flying between the sensors. Sensors currently employed in the ballistic range include light emitting diodes, laser beams, thin wires or infrared beam.

2.3.2.1 Energy absorption based on impact and residual velocity

The most direct way to evaluate the ballistic performance of a fabric is to calculate its energy absorption. The following equation has been used by many researchers:

$$\Delta E = \frac{1}{2} m (v_s^2 - v_r^2) \qquad (2.4)$$

where ΔE is the kinetic energy loss of projectile in J, m is the mass of the projectile in kg, v_s and v_r are striking and residual velocities of the projectile in m/s respectively. This includes works by Shockey *et al* [84], Kocer [96], Shim *et al* [35, 97]，Prosser *et al* [98]，Wilde *et al* [99], Cunniff [52], Lim *et al* [36], Tan *et al* [31] and Lee *et al* [21].

2.3.2.2 V_{50}

The V_{50} is defined as the average of an equal number of highest partial penetration velocities and lowest complete penetration velocities, which occur within a specified velocity spread. A minimum of two partial and two complete penetration velocities are used to complete the V_{50}. Four, six and ten rounds are frequently used [100]. Cunniff [69] normalised the fabric energy absorption through dividing (v_s^2- v_r^2) by v_s^2, which is plotted as a function of v_s- V_{50}. He found that the energy absorbed is in proportion to the striking velocity and areal density of the armour system. Abiru *et al* [101] tested the V_{50} of various UHMWPE woven fabrics with a Fragment Simulated Projectile (FSP). The data were used to study the structure effect on the ballistic performance of woven fabric. Price and Young [102] designed body armour systems comprising different types of fabric and used V_{50} as a benchmark for ballistic performance. Figucia [103] developed a new Ballistic Performance Indicator (BPI) and compared the data with actual V_{50} values for five Kevlar materials. He found that satin weave gives superior ballistic performance over other structures due to its higher lateral mobility.

2.3.2.3 Ballistic performance evaluation based on back face signature (BFS)

The non-penetration test for armour performance evaluation is based on the measurement of the back face signature depression produced on the backing clay. One of the widely used standards is that of the US National Institute of Justice (NIJ). Since its first introduction in 2000, it has been applied by many countries around the world. In this standard, the performance requirement and test method for human body protection against ballistic impact are listed. The ballistic armour is classified into seven levels. Type I, II A, II and III A provide increasing levels of protection from handgun threats. Types III and IV armour, which protect against high-powered rifle rounds, are for use only in tactical situations. The standard is shown in Table 2.1[104]. The backing material in use is Plastilina$^{@}$1 (clay), the velocity of a projectile is determined by two chronographs, as shown in Figure 2.17. 48 rounds will be fired to complete the test. No penetration is allowed. 16 measurements at normal obliquity will be recorded and no depth of back face signature is allowed to be greater than 44 mm.

Table 2-1 NIJ standard 0101.04 P-BFS performance test summary[104]

Armor type	Test round	Test bullet	Bullet weight	Reference velocity (± 30 ft/s)	Hits per armor part at 0° angle of incidence	BFS depth maximum	Hits per armor part at 30° angle of incidence	Shots per panel	Shots per sample	Shots per threat	Total shots required
I	1	.22 caliber LR LRN	2.6 g 40 gr	329 m/s (1080 ft/s)	4	44 mm (1.73 in)	2	6	12	24	48
	2	.380 ACP FMJ RN	6.2 g 95 gr	322 m/s (1055 ft/s)	4	44 mm (1.73 in)	2	6	12	24	
IIA	1	9 mm FMJ RN	8.0 g 124 gr	341 m/s (1120 ft/s)	4	44 mm (1.73 in)	2	6	12	24	48
	2	40 S&W FMJ	11.7 g 180 gr	322 m/s (1055 ft/s)	4	44 mm (1.73 in)	2	6	12	24	
II	1	9 mm FMJ RN	8.0 g 124 gr	367 m/s (1205 ft/s)	4	44 mm (1.73 in)	2	6	12	24	48
	2	357 Mag JSP	10.2 g 158 gr	436 m/s (1430 ft/s)	4	44 mm (1.73 in)	2	6	12	24	
IIIA	1	9 mm FMJ RN	8.2 g 124 gr	436 m/s (1430 ft/s)	4	44 mm (1.73 in)	2	6	12	24	48
	2	44 Mag JHP	15.6 g 240 gr	436 m/s (1430 ft/s)	4	44 mm (1.73 in)	2	6	12	24	
III	1	7.62 mm NATO FMJ	9.6 g 148 gr	838 m/s (2780 ft/s)	6	44 mm (1.73 in)	0	6	12	12	12
IV	1	.30 caliber M2 AP	10.8 g 166 gr	869 m/s (2880 ft/s)	1	44 mm (1.73 in)	0	1	2	2	2
Special	*	*	*	*	*	44 mm (1.73 in)	*	*	*	*	*

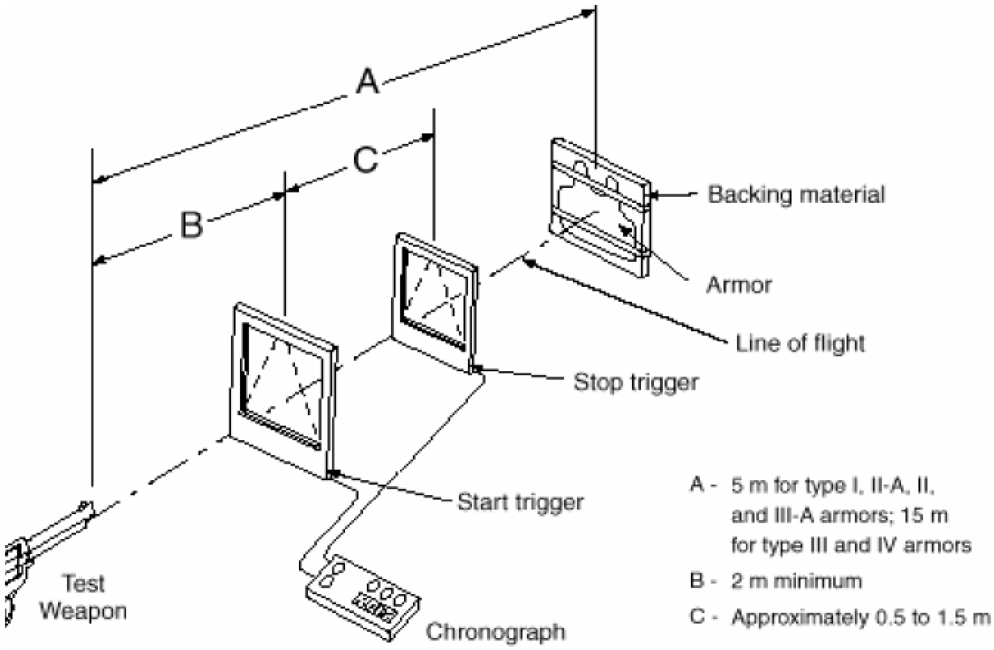

Figure 2-17 Ballistic test setup for NIJ test [104]

The Home Office Scientific Development Branch (HOSDB) ballistic armour standard is a method for evaluating the ballistic protection of body armour systems for British Police. The body armour system is required to provide sufficient protection of the human body against projectile penetration and blunt trauma. The body armour is placed against a 420mm×350mm×100mm box filled with Roma Plastilina® No.1. The threat is divided into eight levels according to different ammunition and impact velocity. Details could be referenced from the HOSDB Body Armour Standard for UK Police (2007) Part 2: Ballistic Resistance[105], which is shown in Table 2-2. Shots 1, 2, 3 and 6 will be at 90 degrees and shots 4 and 5 will be at 60 degrees. The criteria and set up are shown in Figure 2.18.

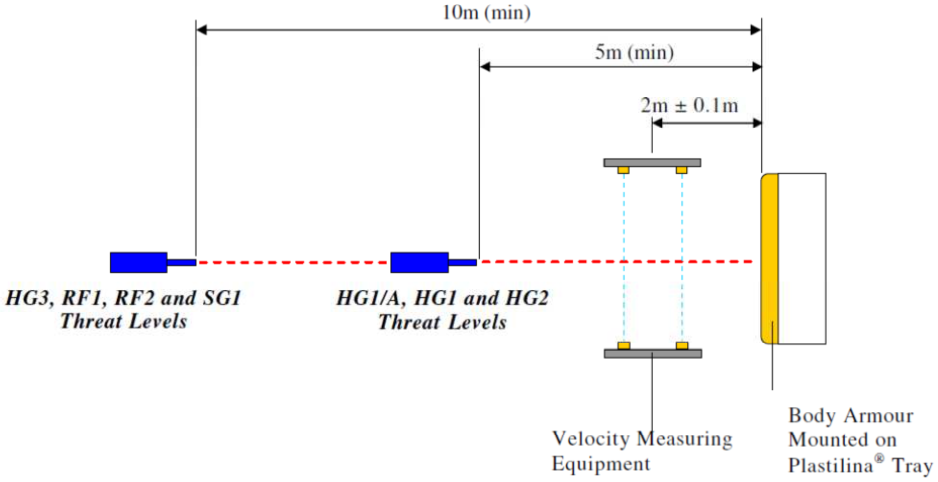

Figure 2-18 Test apparatus for HOSDB ballistic testing [105]

Table 2-2 HOSDB Ballistic Performance Levels

Performance level	Calibre	Ammunition Description	Bullet Mass	Min Range (m)	BFS(mm)	Velocity (m/s)
HG1/A (Low hand gun)	9mm	9mm FMJ Dynamit Nobel DM11A1B2	8.0g (124 grain)	5	44	365 ± 10
	0.357” Magnum	Soft Point Flat Nose Remington R357M3	10.2g (158 grain)	5	44	390 ± 10
HG1 (Low hand gun)	9mm Calibre	9mm FMJ Dynamit Nobel DM11A1B2	8.0g (124 grain)	5	25	365 ± 10
	0.357” Magnum	Soft Point Flat Nose Remington R357M3	10.2g (158 grain)	5	35	390 ± 10
HG2 (High hand gun)	9mm Calibre	9mm FMJ Dynamit Nobel DM11A1B2	8.0g (124 grain)	5	25	365 ± 10
	0.357” Magnum	Soft Point Flat Nose Remington R357M3	10.2g (158 grain)	5	25	390 ± 10
HG3 (Protection against specific 5.56mm ammunition up to 228mm barrel length)	Carbine 5.56x45 NATO 1 in 7” Twist	Federal Tactical Bonded 5.56mm (.223) LE223T3 Law Enforcement Ammunition	4.01g (62 grain)	10	25	750 ± 15

Table 2-2 Continued: HOSDB Ballistic Performance Levels

Performance level	Calibre	Ammunition Description	Bullet Mass	Min Range (m)	BFS(mm)	Velocity (m/s)
RF1 (Rifle)	Rifle 7.62mm Calibre 1 in 12” Twist	BAE Systems Royal Ordnance Defence Radway Green NATO Ball L2 A2	9.3g (144 grain)	10	25	830 ± 15
RF2 (Rifle)	Rifle 7.62mm Calibre 1 in 12” Twist	BAE Systems Royal Ordnance Defence Radway Green Nato Ball L40A1 7.62 X 51mm High Power (HP)	9.7g	10	25	850 ± 15
SG3 (Shotgun)	Shotgun 12 Gauge True Cylinder	Winchester 1 oz. Rifled Lead Slug 12RS15 or 12RSE	28.4g (437 grain)	10	25	435 ± 25

Other standards such as the NATO standardisation agreement, STANAG 2920 and International standard, ISO/FDIS 14876 protective clothing- body armour also cover methods to classify and to test body armours of different protective levels. There is a large volume of published work investigating the performance of a panel through the back face signature [78, 106-108]. However, approaches of this kind are limited to the measurement of the depth and diameter of the back face signature. Karahan [64] used Maple 10 software to determine the volume of the back face signature. Combined with the data obtained from the quasi-static weight-dropping test, the energy for unit volume of clay was calculated. The value is employed in the ballistic non-penetration test to calculate the energy absorbed by the backing clay. Knowing the projectile impact energy, the energy absorbed by the fabric panel is then able to be obtained. One major drawback of this approach is that the author paid less attention to differentiate the material response from quasi-static impact loading and high-velocity impact loading. As has been mentioned in the previous section, local damage dominates energy absorption when the fabric target is subjected to high-speed impact. It is not appropriate to apply the data obtained from quasi-static test to calculate the energy absorbed by the backing clay in a ballistic test. In addition, the volume of the back face signature is formed by turning the curve 360 degrees around the central line in his research. It has been found in many other people's work that back face signature is irregularly shaped, and therefore the validity of this approach should be questioned.

2.4 Theoretical Investigation of Ballistic Impact

Modelling ballistic impact is an integral part of the research work and has been the subject of much interest. Generally speaking, the investigation of ballistic impact on fabric body armour is based on three aspects: experimental, analytical and numerical studies. Experimental studies, which have been exhaustively discussed in the previous section, seek to evaluate fabric target performance through some parameters, such as V_{50} and back face signature. Although experimental work is essential for ensuring the utility and effectiveness of the body armour system, they are both time and money consuming. With the development of computer power and the understanding of the mechanisms of ballistic impact, ballistic simulations, both analytical and numerical, have made the research work increasingly cost-effective and flexible. This section aims to provide an elemental overview of the literature in this area.

2.4.1 Analytical models

Analytical models are based on the general continuum mechanics equations. As the impact events become more complex and more influencing factors need to be taken into consideration, the equations used become increasingly complicated. The development of an analytical model requires thorough understanding of the physical phenomena taking place during ballistic impact. Analytical models enable the investigation to be carried out with less time than numerical models. However, this is believed to be achieved at the expense of complete accuracy.

Smith *et al* [43] used an analytical model to study the response of a single-yarn to transverse impact and correlate the velocity of transverse wave front with the longitudinal wave velocity and yarn strain. The surveys of analytical models of ballistic impact upon woven fabric have been noted in a number of publications [109, 110]. Gu [23] pointed out that these models only take into consideration the breakage of the principal yarns, the energy absorbed on the secondary yarns and fabric kinetic energy have not been paid enough attention. He built an analytical model taking into account the tetrahedron deformation of fabric. The fabric strain and kinetic energy in that area were considered. Porwal and Phoenix [68, 111] developed an analytical model to study the "system effects" in a two-layered fabric panel. The "system effects" include the contact between the adjacent layers and the stacking order of different materials. Chen *et al* [72] further perfected the analytical model by incorporating shear failure criteria into the model, which reveals different damage mode for fabrics near the impact face and fabrics near the back face.

2.4.2 Numerical models

Numerical models are based on finite element or finite difference code. As this method provides a more correct representation of the fabric (some numerical models enable fabric to be simulated at yarn level), a more precise simulation of ballistic impact can be achieved. Among the main numerical works undertaken so far, four classes can be identified: the pin-jointed model, the 3D continuum finite element model, the unit-cell based model and the membrane/shell element based model.

2.4.2.1 Pin-jointed models

This type of finite element mode uses orthogonal pin-jointed bars to represent fabric samples. Roylance and Wang [112] used a network of interconnected fibre elements to simulate ballistic impact and suggested that the pin-jointed model leads to a good agreement with the transverse deformation observed under high speed camera. Shim *et al* [35, 97] incorporated a three-element linear viscoelastic model into the model to capture the strain rate sensitivity of Twaron fibres. Prediction of the residual velocity and energy absorption in the model show good agreement with experimental data. Based on this work, Tan *et al* [60] incorporated yarn crimp into the fabric model using two methods. The first method is to include the initial low modulus region [59] of woven fabric subjected to tensile stretching in the viscoelastic model. The second method is to reshape the yarn path into a zigzag manner. The latter model is found to give a closer agreement with experimental results than the former one. This is because the fabric model with a zigzag yarn path is able to reproduce the whole impact event, whereas the model with a straight yarn path begins to deviate during the process. Billon and Robinson [113] compared the validity of a pin-jointed model and the analytical model and found that both models are useful in predicting the ballistic performance of fabric armour. While the pin-jointed model is capable of presenting the fabric response to ballistic impact, the discrete nature of the fabric forming yarns is oversimplified. As a result, factors such as fabric structure, yarn-yarn and layer-layer contact are not taken into consideration.

2.4.2.2 Three-dimensional continuum element models

Three-dimensional continuum element model model is formed by 3D continuum element, which enables the simulation to take account of the discrete nature of woven fabrics. For the modelling of flexible fabrics, the most commonly used commercial finite element packages are ABAQUS by the ABAQUS Inc, DYNA3D by Methods Development Group at Lawrence Livermore National Laboratory and LS-DYNA by the Livermore Software Technology Corporation. In recent years, there has been an increasing amount of published work in this area. Shockey *et al* [57, 67, 84, 88] modelledplain woven fabric with solid elements and found that the model became unstable as the number of elements increases. Gu [114] incorporated Weibull constitutive equations into LS-DYNA and considered the effect of strain rate on fabric energy absorption. Zhang *et al* [115] studied the influence of frame size, frame type and clamping pressure on panel energy absorption in the finite element model. The key problem of their model is that the sine-wave shape of the yarn path has been simplified as a rectangular wave, which affects the yarn-yarn movement. Duan *et al* [18, 116, 117] and Rao *et al* [118] also used the FE model to investigate the effect of boundary conditions and friction on the performance of a single-layer woven fabric. However, they made no attempt to differentiate the material properties in various directions. Their conclusions might have been far more persuasive if the transverse modulus and shear modulus were studied in detail in the models. Talebi *et al* [85] employed FE methods to analyse the influence of nose angle of the projectile ranging from 30° to 180° through fabric energy absorption, size of the hole and stress distribution. Jin *et al* [119] made an exhaustive investigation on the ballistic performance of angle-interlock fabrics. The theoretical data are validated and shows a good agreement with experimental results.

By using three-dimensional finite element models, the dynamic response of fabric upon ballistic impact could be predicted in a more accurate manner. Yarn-yarn, layer-layer contact and friction related properties could be taken into consideration. Nevertheless, this method is found to be computer effort consuming, especially when it is used to simulate a panel system containing 20 to 40 layers of fabric.

2.4.2.3 Unit-cell based model

The unit-cell based model is dependent on the recreation of the membrane response of fabric in a cell element. It aims to study the yarn and fabric properties at a meso-scale. In this approach, a fabric model is formed by the repeating cells of yarn crossovers. The main issue regarding this type of model is that a clear and realistic representation of yarn behaviour when subjected to impact load is required, such as yarn pull-out.

Shahkarami and Vaziri [120] simulated the woven fabric in three steps: (1) development of the biaxial behaviour of the unit-cell; (2) development of the in-plane shear response of the unit-cell; (3) development of the out-of-plane shear response. The resultant model is incorporated into a material subroutine, which can be readily used with dynamic-explicit finite element softwares.

The biaxial response of fabric was first studied by Kawabata et al [121]. In their analytical model, the yarn crossover is simplified to a pair of rods, and the relationship between compression force and the movement of contact point was established. Figure 2-19 shows the unit structure of a crossover in a fabric. Based on the analytical model, Shahkarami and Vaziri [120] adopted a two-variable Newton-Raphson iterative scheme to numerically determine the displacement of the contact point. The out-of-plane shear modulus is set to be zero as there is little resistance against shear force at the crossover point. For the in-plane shear modulus, it is believed that this parameter is not a mechanism influencing fabric ballistic performance. Grujicic *et al* [122] used the same model for fabric biaxial behaviour and for shear properties, they applied an in-plane and an out-of-plane shear stress to the unit cell model and found that the two parameters are related to yarn-yarn friction.

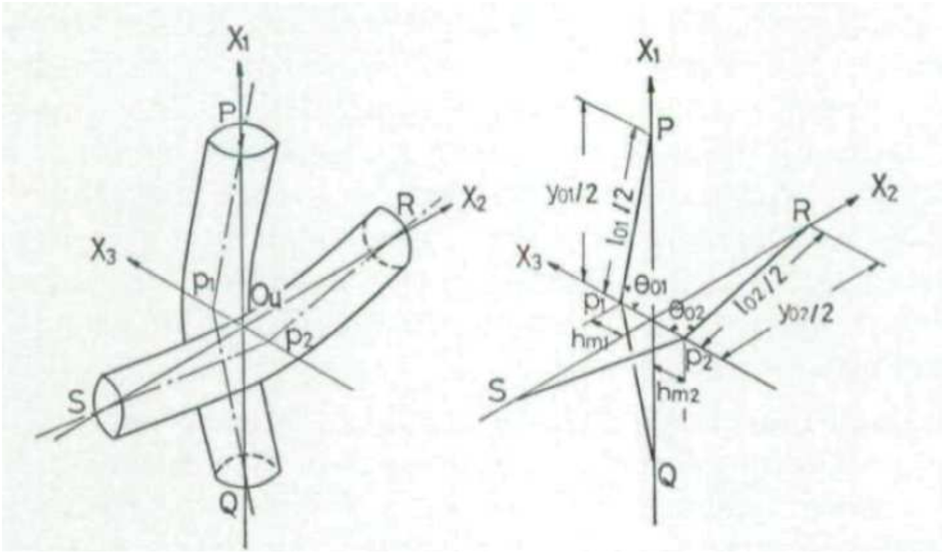

Figure 2-19 Unit structure of a crossover [121]

2.5 Summary

In this chapter, literature related to this research has been reviewed for the need to develop an in-depth understanding of the research background. Four aspects have been covered, namely energy absorption mechanisms of fabrics upon ballistic impact, factors influencing fabric performance, experimental testing methods and standards, and the modelling of ballistic impact on soft body armour. While the objective of the research is to develop lightweight soft body armour, previous work provides guidance for improving the performance of ballistic fabrics at a reduced weight.

One of the approaches to improve the performance of ballistic fabric is to develop materials with a high modulus combined with sufficient energy absorption at break when a panel is subjected to high strain rate impact. While weight is an essential requirement in designing soft body armour, material density is an important factor which needs to be considered. For ballistic applications, the options of fibres are limited. These days, the most widely used fibres for soft body armour manufacture are mainly aramid and UHMWPE fibre, which show higher strength based on weight and volume when compared with other types of synthetic fibres[15]. Other high-performance fibres which meet the requirements are considered not suitable to be used in soft body armour, which has been discussed in Chapter 1. Fibre materials used for ballistic application are fundamental. On top of that, it is also very important to investigate how to imprve the ballistic performance through engineering fabrics by using appropriate structures.

According to the literature, inter-yarn friction is one of the factors determining the performance of woven fabrics. Although there is no shortage of literature on the working mechanisms of yarn-yarn friction [16-19], little attention has been paid to the relationship between friction and strain distribution. This research will examine the influence of yarn-yarn friction on fabric stress distribution by using FE methods. In addition, as the majority of the approaches employed to increase yarn-yarn friction are based on chemical treatment technologies, there is little work focused on employing textile-based technologies. In the present research, novel weaving techniques will be used to create real woven fabrics with increased inter-yarn friction on power looms, aiming to explore the possibility of improving the ballistic performance of soft body armours.

While the literature also shows that different layers of fabric in a panel tend to exhibit different failure mechanisms [21, 72], it is possible to mix different materials in a proper sequence which would hopefully make the best use of their corresponding properties and consequently enable the ballistic panel to be more energy absorbent. Detailed planning and methodologies for undertaking this research will be discussed in the next chapter.

Chapter 3 Methodology and Preliminary Work

As has been mentioned in Chapter 1 and 2， the problem presented in this research is to develop lightweight soft body armour with improved ballistic performance, which encompasses the investigation of fabric with increased inter-yarn friction and the engineering of hybrid panels. In order to conduct the research work and achieve the listed objectives listed in Section 1.3, research methodology has been planned and described in steps. Two complementary approaches were employed to complete the research, namely an experimental investigation based on ballistic penetration and a theoretical investigation based on finite element (FE) analysis. A comprehensive description of the ballistic range and the creation of FE models will be presented in this chapter.

3.1 Methodology

The ballistic shooting test enablesto have a direct understanding of how soft body armour dissipates and absorbs projectile energy. In this research, fabric performance was determined by two evaluation methodologies: penetration and non-penetration tests. The former method is based on working out the projectile kinetic energy loss absorbed by fabric when it completely penetrates a fabric or panel target, which has been described in Section 2.3.2.1. For the latter method, the projectile does not penetrate the fabric panel and remains in it. Although enough fabric layers are stacked to stop a projectile, the energy absorbed by the fabric panel is difficult to determine. This is because the impact may transmit great force through a panel target, leading a certain amount of energy to be absorbed by the backing material and forming a back face signature. As a result, the depth of back face signature is employed as an indicator of the ballistic performance.

The second approach used to conduct this research is finite element analysis on UHMWPE plain woven and UD fabric. A reliable FE model serves two purposes, i.e., obtaining data which are not available in experimental tests and providing guidance for panel design. The employment of finite element analysis also allowssimulations which are difficult to achieve in practice. These lead an in-depth understanding of the energy absorption mechanism and to reduce the cost of developing novel fabrics for ballistic protection.

3.2 Ballistic Range

The ballistic range in use is capable of carrying out both penetration and non-penetration ballistic tests. Penetration tests are carried out on single layer fabrics and panels with small numbers of fabrics to measure the fabric or fabric panels' ability to absorb energy from the impacting projectile, which are shown in Figure 3-1 and Figure 3-2. In this set-up, the projectile is a 1 gram, cylindrical projectile whose length and diameter both measure 5.5 mm. The velocity of the projectile propelled by a powder cartridge is in the range from 400 m/s to 500 m/s. The ballistic range is equipped with a high speed camera, which is able to show the ballistic impact upon fabric targets. The fabric sample is fixed on a clamp with an aperture diameter of 15 cm. The ballistic performance of the fabric is measured by the energy loss of the projectile. The projectile kinetic energy loss is determined by equation 2.4

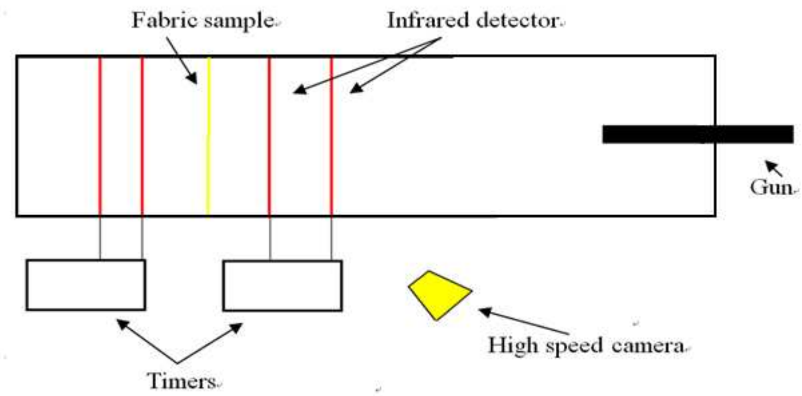

Figure 3-1 Schematic diagram of the ballistic range

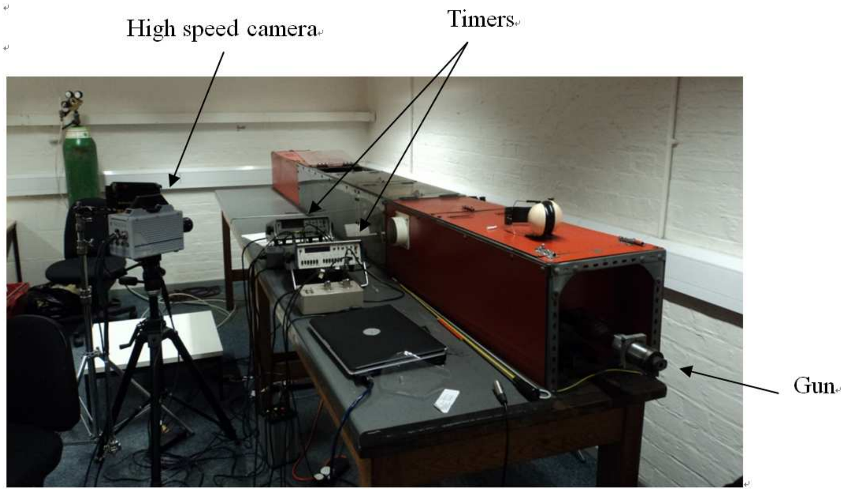

Figure 3-2 Ballistic range

For non-penetration tests, fabric panels, which are made from sufficient numbers of layers to stop the projectile, are mounted unclamped against a clay block simulating human muscle. The clay in use is Roma Plastilina® No.1. In most cases, the panels are not fully perforated, and the ballistic performance of the panels is assessed by the number of fabric layers fractured and the depth of the back face signature. The shape and volume of the back face signature can be taken to study the residual energy carried by the projectile when it is checked.

3.3 Creation of Finite Element Models

3.3.1 A brief introduction to ABAQUS

As has been mentioned in the previous chapter, ABAQUS is a commercial finite element package developed by ABAQUS Inc. Its extensive element library coupled with powerful sketching tools enables the modelling of any geometry. The equally extensive built-in material models make possible the simulation of most engineering models. ABAQUS also offers the option of the use of user-defined material models, which is quite flexible for the testing of new theories through numerical method. There are many ABAQUS products. In this research, ABAQUS/explicit was employed for simulation due to its suitability to process brief, transient dynamic simulations such as impact or blast problems [123].

In ABAQUS, a complete finite element analysis is usually composed of three stages: pre-processing, simulation and post-processing. In the pre-processing stage, an input file is created through ABAQUS/CAE, an interactive environment allowing the description of physical problems and the importing of model details into the processor. Simulation is the stage in which the problem is analysed and processed. Depending on the power of a computer, it may take from minutes to weeks to complete an analysis. The results are stored in an output file and evaluated using the Visualisation Module of ABAQUS/CAE in the post-processing stage.

The description of a physical problem encompasses several components, including creating the model geometry, identifying the element section and the material properties, setting loads and boundary conditions, defining the analysis type and the output request. In ABAQUS, a model part could be either sketched in the ABAQUS/CAE environment or imported from external software. The part is formed by many interconnected elements, which represent the basic geometry of the model structure. In the next stage, the material section is specified for the elements, aiming to define the coordinates of nodes and their material properties. As the physical properties of material data are difficult to measure, the accuracy of the ABAQUS model is limited when it comes to the simulation of those materials. Loads are applied to the model to specify the initial conditions, and boundary conditions are used to constrain the model or to allow the model to move by a prescribed amount. The analysis type could be either defined as static or dynamic, among which dynamic analysis is of more interest for cases like ballistic impact. The final step of model creation is to set the output request. By limiting the output results, both computer running time and disk space can be saved.

3.3.2 Creation of geometrical model

3.3.2.1 Projectile model

In the event of high velocity impact, a projectile of a more rigid material is collided with a panel of fabric which is flexible. The projectile model is of a cylindrical shape with the diameter and height both being 5.5 mm, and the mass of the projectile 1 gram, which is the same as the projectile used for practical ballistic tests. The projectile is shown in Figure 3-3. The density of the projectile model is set to be 7.8g/cm^3. As there is little deformation on a projectile in real test, model property is defined as rigid body.

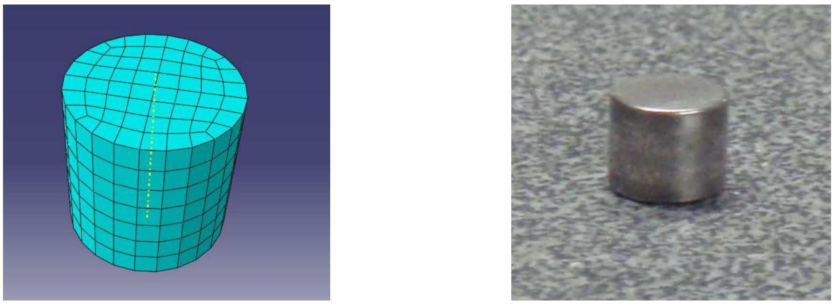

(a) Projectile model **(b) Real projectile**

Figure 3-3 Projectile simulation

3.3.2.2 Geometric model of a single yarn

Yarn cross-section

Circular cross-section model

The modelling of yarn geometry has been a subject of interest for a long time. Scientists have developed numerous models to study the behaviour of yarn and fabric. Peirce [124] made an early attempt to describe the yarn cross-section as circular, which is shown in Figure 3-4. This model, however, ignored yarn bending rigidity and suggested that fabric gives little resistance when subjected to internal stresses. In addition, Peirce's yarn model might be applicable for staple yarns with high twist. For filament yarns with low twist, such as the Dyneema yarns used in this work, the circular model is not suitable. He later considered the yarn geometry under compression. The ellipse was proposed to be the shape of the yarn cross-section.

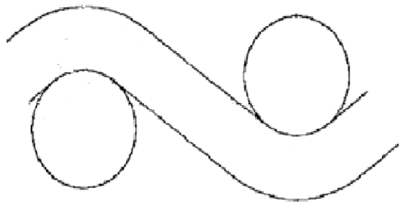

Figure 3-4 Circular cross-section model [124]

Racetrack cross-section model

Kemp [125] described the yarn cross-section as a racetrack. This model is formed by a rectangle with four circular arcs attached on the four corners, which is shown in Figure 3-5. The racetrack model facilitates the modelling of yarn flattening and the calculation of the yarn path. However, the accuracy of this model is questionable as it does not represent the true shape of the yarn cross-section. As a result, the racetrack model is less suitable in simulating yarns with few number of twist in this research. The geometry of the racetrack can be presented as below.

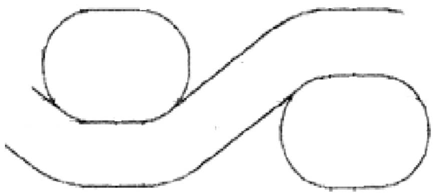

Figure 3-5 Racetrack cross-section model [125]

Lenticular cross-section model

Shanahan and Hearle [126] proposed a lenticular model which gives a more precise representation of yarn cross-section. This model is formed by two arcs and is thought to be able to best embody the mechanical behaviour of fabric forming yarns [126], which is shown in Figure 3-6. For ballistic impact simulation on woven fabrics, many works have used this model for yarn modelling due to its good fit to true yarn geometry.

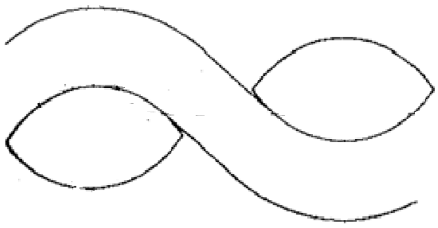

Figure 3-6 Lenticular cross-section model [126]

Simulation of yarn cross-section in UHMWPE plain woven fabric

Optical microscopy observation

Optical microscopy was used to obtain the cross-sectional image of Dyneema yarn. The fabric was gripped by a clip and was cast in resin to restrict its movement. The mould was then polished on a grinding machine to have a smooth flat surface for observation. As can be seen in Figure 3-7, the shape of the yarn cross-section is close to the shape of a len. As a result, the lenticular model will be used for FE simulation

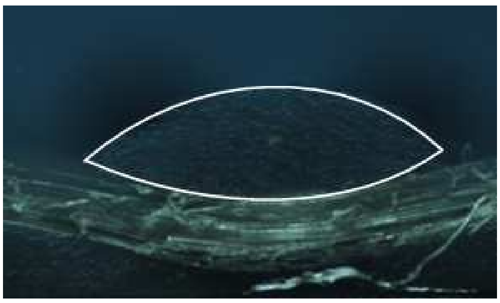

Figure 3-7 Optical microscopy observation for the cross-section of fabric forming yarn

Yarn cross-section height

As the fabric forming yarn is a bundle of filaments, it is difficult to measure the height and the yarn cross section with conventional approaches. As a result, the value is taken from real yarns when all the filaments are intensely packed together. The Kawabata Evaluation

System (KES) was used to measure the fabric thickness under compression, from which the value of yarn thickness was obtained. KES was developed by Professor Kawabata and is widely used for the testing of fabric mechanical properties. For the compression test, an area of $2cm^2$ is measured with a KES-FB3 compression tester and fabric compressibility is obtained from an increase in vertical pressure. The relationship between compression stress and strain is recorded and is shown in Figure 3-8. The thickness of the fabric decreases with the increases of pressure up to a value of 50 P.gf/cm^2. It is considered that the filaments are closely packed under the ultimate compression force and half of the thickness will be taken as the height of the yarn cross section. The value is determined to be around 0.380 mm and therefore the height of the yarn cross section is 0.19 mm, which is shown in Appendix Table 1.

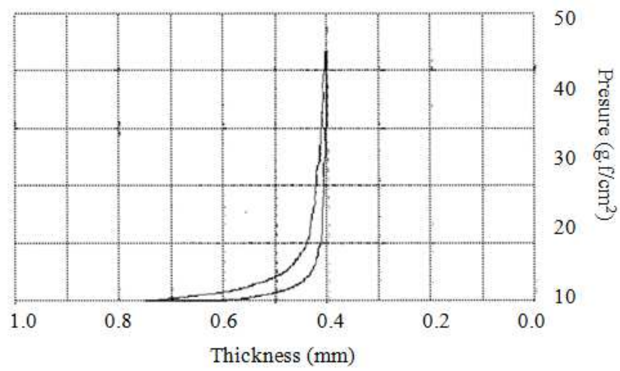

Figure 3-8 Pressure as a function of fabric thickness

Yarn cross section width

The weave density of real fabric is 6.75 threads /cm in both the weft and warp directions. As neighbouring yarns are not closely packed in the woven fabric, it is not appropriate to determine the yarn cross section width through weave density. As it can be seen in Figure 3-9, yarn spacing is noticeable and could not be neglected. Due to the effect of yarn interlacing, the width varies in different locations. For finite element models, the yarn cross-section width was determined to be 1.35 mm.

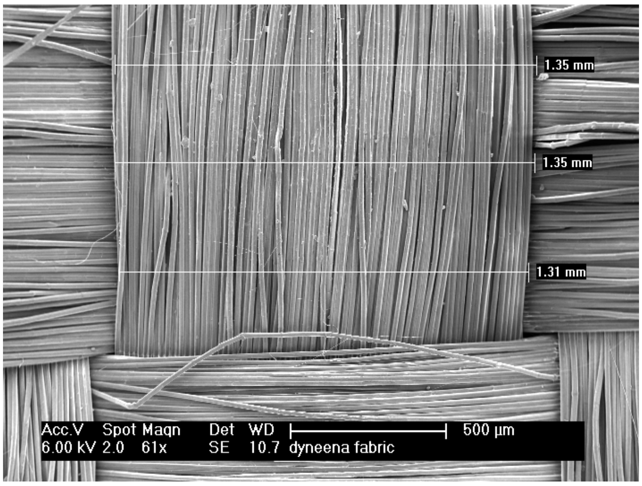

Figure 3-9 SEM observation for the woven fabric

Yarn path

The yarn path can be considered as lenticular arcs which share the same centre of a circle with the cross-section of its orthogonal yarns. In addition, as is proposed by Hearle *et al* [127], the model must possess constant curvature over all along the yarn path.

3.3.2.3 Definition of contact

For ballistic event simulation, the general contact algorithm is used to define yarn-yarn interaction and the contact pair algorithm is used to define projectile-fabric interaction. As the interaction property is determined by the coefficient of friction in ABAQUS, tests were carried out to obtain these values.

Coefficient of projectile-fabric friction

The coefficient of friction between a steel projectile and fabric surface was determined by using the KES-FB4 surface tester. In this instrument, a finger-simulating sensor rubs against the surface of the fabric sample, detecting the resistance of friction between the interfaces. The frictional property of UHMWPE woven fabric was revealed in Appendix Table 2. The coefficient of friction was determined to be around 0.174, the value of which is used in ABAQUS to define the coefficient of friction between a projectile and a fabric model.

Coefficient of inter-yarn friction

The coefficient of inter-yarn friction is determined from a yarn frictional test. The method is suggested by Standard ASTM D3412 [128] and details will be presented later in Chapter 5. The value for UHMWPE yarn was determined to be 0.119.

3.3.2.4 Mesh scheme

The projectile and yarn in the model are both meshed with eight node hexahedron elements. It has been found that the time needed to run the job is greater and job storage requirement is higher when the element density is higher. According to previous work [116-118, 129] associated with using finite element software, the seed number along the yarn cross-section upper and lower arcs was set to be 6 and that along the yarn profile was set to be 12 per wavelength, which is shown in Figure 3-10.

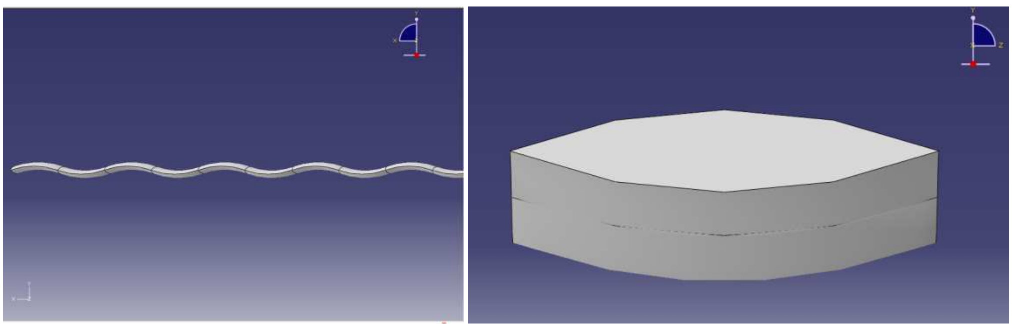

(a) Lateral view **(b) Front view**

Figure 3-10 Yarn model

3.3.2.5 Boundary Conditions

The woven fabric model is 15 cm in diameter, which equals the aperture diameter of the clamp. As the model is symmetrical about the the X-axis and the Z-axis through the centre point, only a quarter of the section is required to be simulated. By doing this, only a quarter as many elements and a quarter the number of degrees of freedom are used, which significantly reduces the run time and storage requirement for analysis. The simulation was based on the following assumptions:

- the impact point is in the centre of the fabric target;
- the centre point is an interlacing point of a warp and a weft yarn; and
- the bullet hits the fabric at 90°.

For the fabric and bullet boundary on the YZ and the YX plane, the translational freedom perpendicular to the symmetrical plane and the rotational freedom in the symmetrical plane, are constrained and the value of freedom is set to be zero. It has been found that the quarter model is able to reflect the nature of the real ballistic event as accurately as a full-sized model.

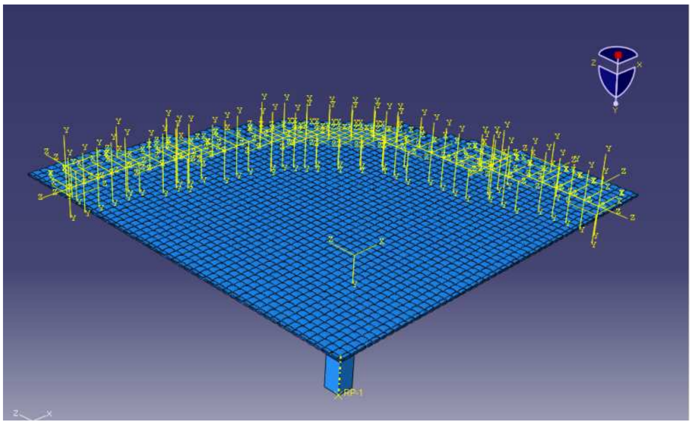

Figure 3-11 Quarter model for projectile and UHMWPE woven fabric

3.3.2.6 Mechanical properties of yarn model

Yarn density

Due to the existence of fibre-spacing in a yarn, it is inappropriate to set the yarn density to be the value of the fibre density (970 kg/m^3). As the yarn is formed by a bundle of fibres, it is assumed that the yarn will have a tightest volume ratio of 0.91[118]. Yarn density was based on from the density of UHMWPE fibre, leading to a value of ρ_{yarn}= 882 kg/m^3.

Transversely isotropic material

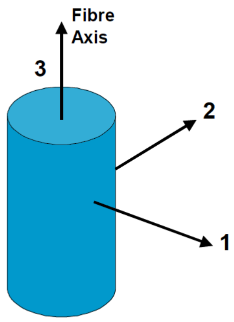

Figure 3-12 Transverse isotropy; axis 1 and 2 are equivalent

"Transverse isotropy" is a special kind of anisotropic material in which there are three mutually perpendicular principal directions, with two of these being equivalent, which is shown in Figure 3-12. This type of material model is mainly used for fibres, especially those which have been uniaxially drawn during the spinning process, such as melt-spun synthetics. In a transversely isotropic material,

$$E_{ij} = \begin{bmatrix} E_{11} & E_{12} & E_{13} & 0 & 0 & 0 \\ & E_{22} & E_{23} & 0 & 0 & 0 \\ & & E_{33} & 0 & 0 & 0 \\ & & & E_{44} & 0 & 0 \\ & & & & E_{55} & 0 \\ & & & & & E_{66} \end{bmatrix}$$

$E_L = E_{33}$

$E_T = E_{22} = E_{11}$

$\nu_{23} = \nu_{13}$

$G = E_{44} = E_{55}$

$$E_{66} = G_{12} = \frac{2E_T}{(1+\nu_{21})}$$

$E_{12} = -\nu_{21} E_T$

$E_{13} = E_{23} = -\nu_{31} E_T$

As a result, only five constants are needed and the matrix could be written as follows:

$$
E_{ij} = \begin{bmatrix} E_T & -E_T\nu_{21} & -E_T\nu_{31} & 0 & 0 & 0 \\ & E_T & -E_T\nu_{31} & 0 & 0 & 0 \\ & & E_L & 0 & 0 & 0 \\ & & & G & 0 & 0 \\ & & & & G & 0 \\ & & & & & \dfrac{2E_T}{(1+\nu_{21})} \end{bmatrix}
$$

Longitudinal modulus E_L

The longitudinal modulus of the material was obtained from the DSM Dyneema high-strength, high-modulus polyethylene fibre fact sheet [130]. As can be seen in Table 3-1, the tensile modulus is within the range from 109 GPa to 132 GPa, an average value of 120 GPa was taken for Finite Element model simulation.

Table 3-1 Tensile properties of Dyneema yarns [130]

Fibre type	Tensile strength			Tensile modulus			Elongation to break %
	N/tex	g/den	Gpa	N/tex	g/den	Gpa	
Dyneema®SK78 Dyneema®SK75	3.4-4.0	38-45	3.3-3.9	112-137	1267-1522	109-132	3-4
Dyneema®SK65 Dyneema®SK62 Dyneema®SK60	2.5-3.4	28-38	2.4-3.3	67-102	759-1158	65-100	
Dyneema®SK25	2.2	25	2.2	54	608	52	

Transverse modulus E_T

Sherburn [131] characterised yarn transverse modulus as a function of the volume fraction and the transverse strain. Lin *et al* [132] used this theory to calculate the transverse modulus of Chomarat yarns in plain weave and sateen weave, which are 75 MPa and 15 MPa respectively. Nevertheless, for simulations of ballistic impact on woven fabrics, the model was found to be unstable if E_T is too low. In order to investigate the influence of E_T on fabric performance, three E_T values were tested in the finite element model. Figure 3-13 shows the Contour plots of stress distribution for ballistic impact onto woven fabric models with different transverse moduli. As can be seen, the elements are more likely to exhibit excessive distortion when E_T equals 0.075 GPa, which considerably affect the stability of the finite element simulation. For higher values of E_T, this phenomenon is less noticeable and elements subjected to damage are less distorted. In order to keep the stability of the finite element model, the yarn's transverse modulus was considered to be equal to the fibre's transverse modulus, which was taken from another high-molecular weight polyethylene fibre [133]. The value was determined to be 1.21 GPa.

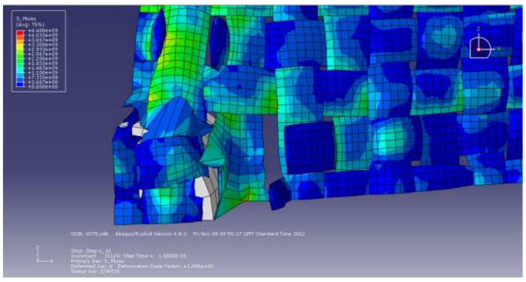

(a) E_T= 0.075GPa

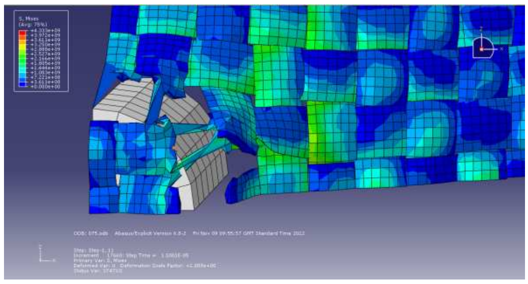

(b) E_T= 0.75GPa

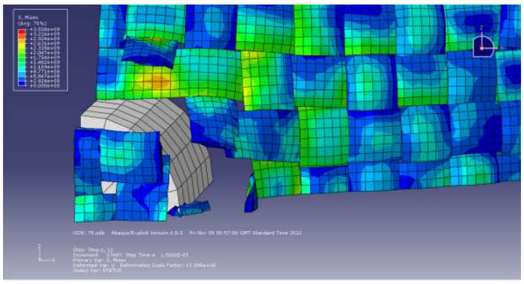

(c) E_T= 7.5GPa

Figure 3-13 FE fabric models with different E_T upon ballistic impact

Poisson's ratio ν_{21} and shear modulus

A Poisson's ratio of 0.2 for both ν_{23} and ν_{21} was chosen for the yarn model [134]. For transverse shear modulus G_{12}, the value was taken from the equation,

$$G_{12} = \frac{2E_T}{(1+\nu_{21})} \tag{3.1}$$

where E_T is the yarn transverse modulus and ν_{21} is Poisson's ratio along directions 1 and 2. G_{12} was determined to be 0.504. For transverse-longitudinal shear properties G_{23} *and* G_{13}, there is limited literature published in this field. Finlayson [135] set up a shear test apparatus and made measurements of a series of fibres. He found that the shear strength was in proportion to the amount of materials tested and was less than the tensile strength. As it is difficult to measure directly, yarn shear modulus along directions 2 and 3, a value of 3.28 GPa is taken for G_{23} and G_{13} according to Grujicic *et al*'s model [129].

3.3.2.7 Failure criteria

In ABAQUS, yarn failure is defined as strain controlled in the finite element model. Both tensile and shear criteria are used to define element failure. An element fails when either of these reaches a failure level in the FE model. The tensile failure strain is obtained from the DSM fact sheet [130], which is 0.04. According to the literature [136, 137], the shear modulus and shear strength of polyethylene fibre are determined to be 1 GPa and 0.02 GPa respectively, the shear failure strain is therefore calculated to be 0.02.

3.3.3 FE simulation of UHMWPE UD fabric

The model for UHMWPE UD fabric was also simulated by using 3D solid continuous elements. The model was partitioned into four layers to simulate the four layers of oriented fibre nets in real fabric. Each layer has a yarn tensile modulus of E_{11} along one direction. The UD fabric model is 0.8g/cm^3 in bulk density and 0.18 mm in thickness. The coefficient of friction between a projectile and the UD fabric model was determined to be 0.415 from the Kawabata Evaluation System. Other material parameters are similar to those used in the woven fabric model.

3.3.4 Model validation

Validation of the plain woven and UD fabric models was performed using experimental data. The impact velocity of the projectile propelled by a powder cartridge is in the range from 400 m/s to 500 m/s, giving rise to different data points. The residual velocities of the projectile were extracted from experimental tests and FE simulation, and compared. The accuracy of FE predictions is indicated by the value of the gradient of the regression line, which indicates how well the FE results match the experimental results. If the value of gradient is 1, then the FE model perfectly matches the real fabric. The gradient of the regression line is 0.9406 and 0.9781 in Figure 3-14 and Figure 3-15 respectively, which shows a good agreement between the FE models and real fabrics.

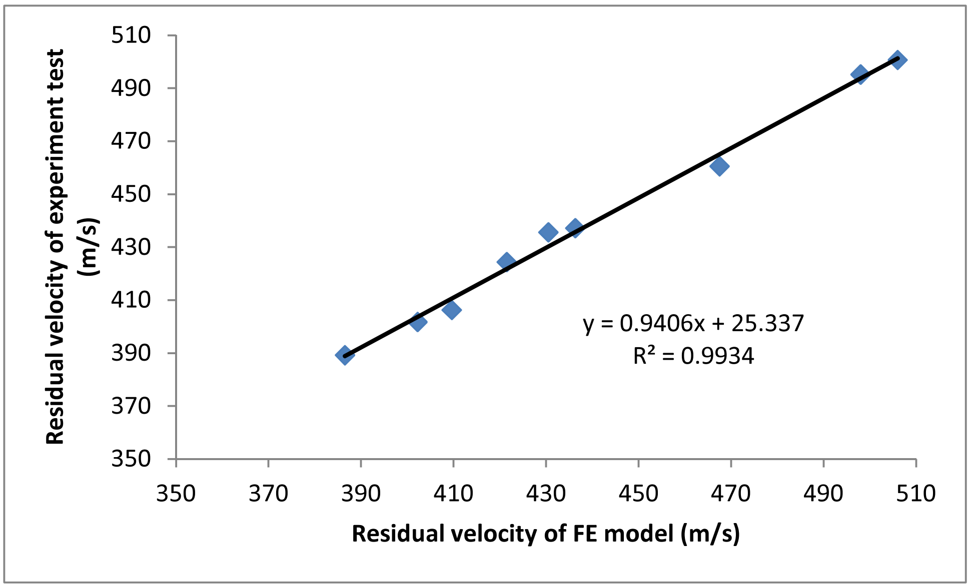

Figure 3-14 Comparison of FE and experimental residual velocities for the woven fabric

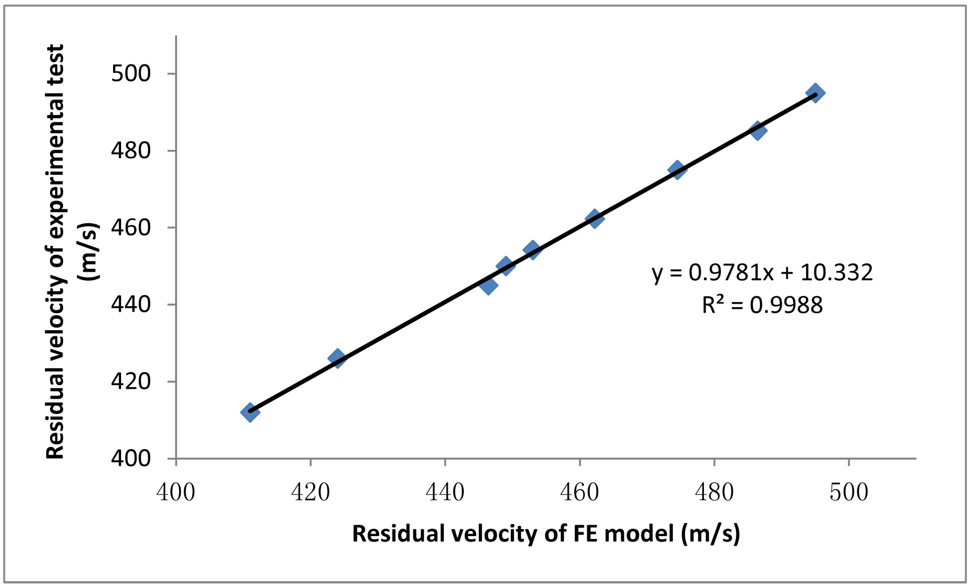

Figure 3-15 Comparison of FE and experimental residual velocities for the UD fabric

3.3.5 Ballistic impact event on UHMWPE woven and UD fabric model

Figures 3-16 and 3-17 show the contour plot of the woven and UD fabric models upon ballistic impact. The coloured area indicates the stress distribution in the fabrics. Take the woven fabric model for example, at 3μs, the stress is mainly concentrated in the primary yarns. As the projectile continues to push forward, the yarn interaction at the crossovers enables the primary yarns to deflect secondary yarns out, forming transverse deformation. From 6μs onwards, the transverse deformation becomes increasingly noticeable, causing more stress to be distributed into the secondary yarns. The stress distribution and transverse deflection could also be observed in the UD fabric model. One thing worth noting is that the velocity of the longitudinal wave on the UD fabric model (9397.6m/s) is around $\sqrt{2}$ times higher than that on the woven fabric model (6405m/s). This may be explained by the fact that the existence of crossovers in the woven structure impedes the propagation of the longitudinal wave. Its velocity is considered to be reduced by a factor of $\sqrt{2}$ [24].

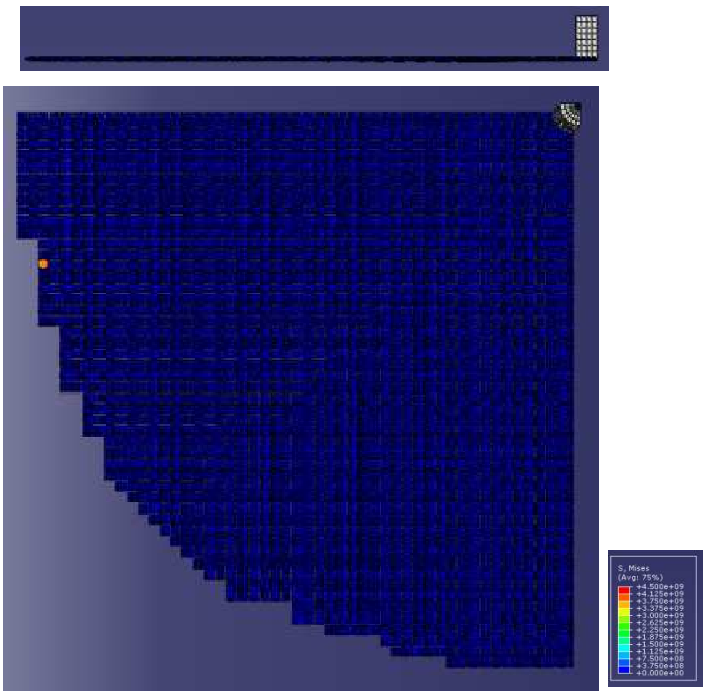

0µs

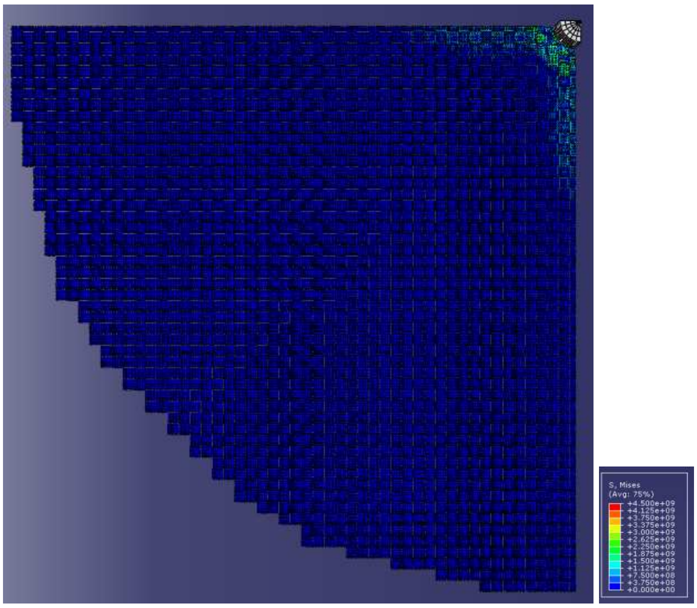
S, Mises
(Avg: 75%)
+4.500e+09
+4.125e+09
+3.750e+09
+3.375e+09
+3.000e+09
+2.625e+09
+2.250e+09
+1.875e+09
+1.500e+09
+1.125e+09
+7.500e+08
+3.750e+08
+0.000e+00

3µs

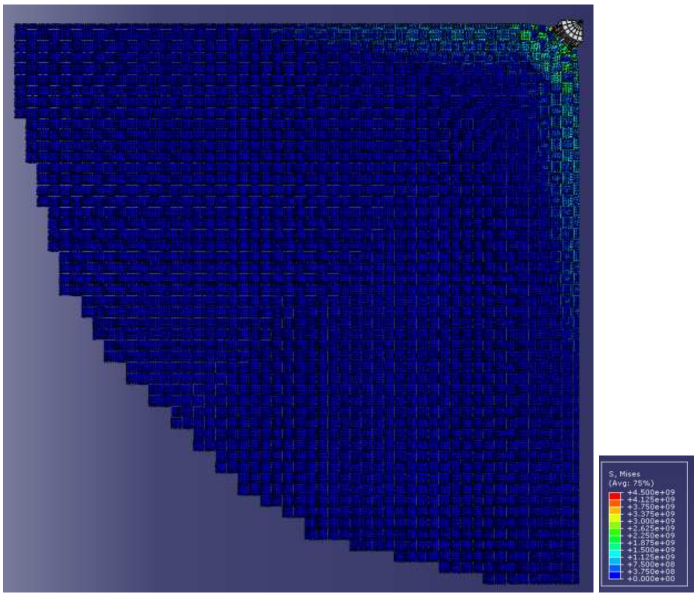

6µs

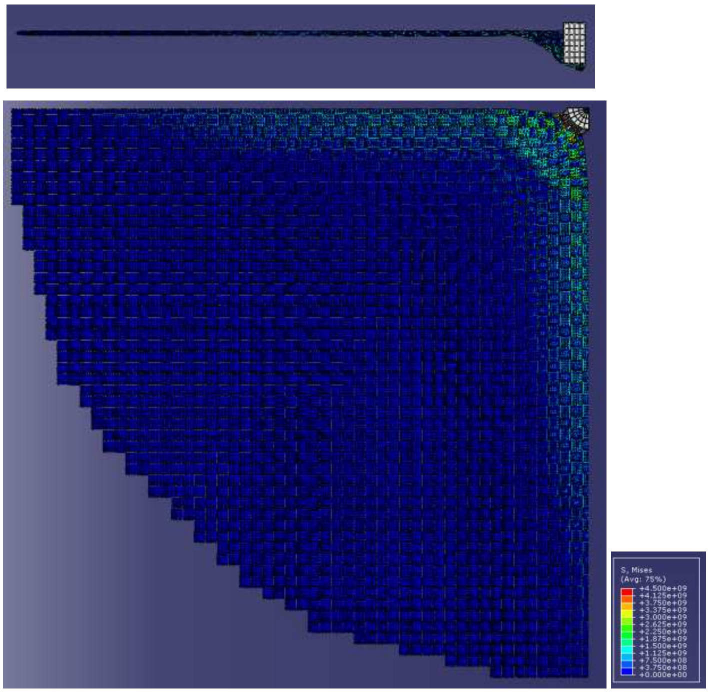

9µs

Figure 3-16 Contour plot of the woven fabric model during ballistic impact

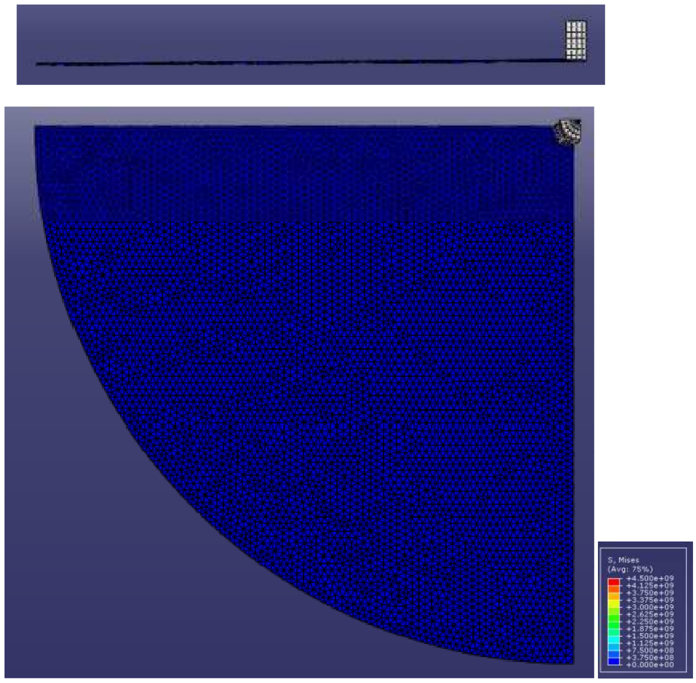

S, Mises
(Avg: 75%)
+4.500e+09
+4.125e+09
+3.750e+09
+3.375e+09
+3.000e+09
+2.625e+09
+2.250e+09
+1.875e+09
+1.500e+09
+1.125e+09
+7.500e+08
+3.750e+08
+0.000e+00

0μs

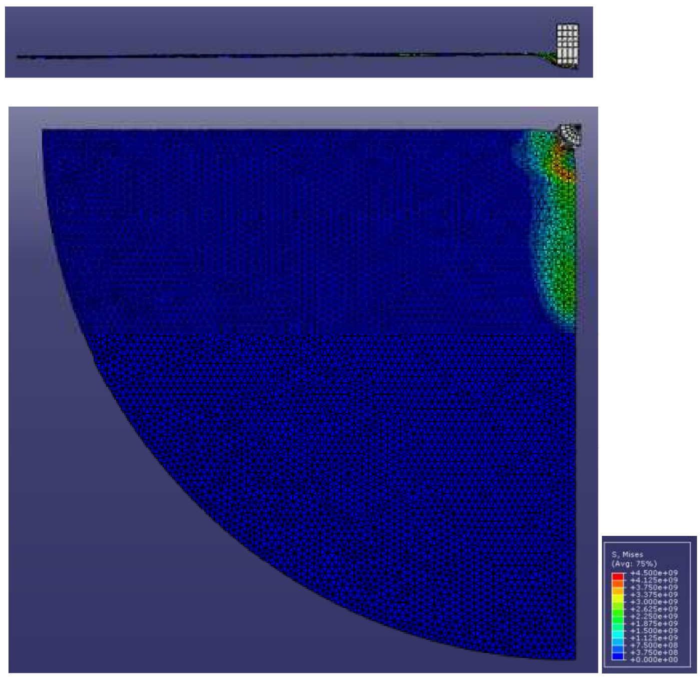

S, Mises
(Avg: 75%)
+4.500e+09
+4.125e+09
+3.750e+09
+3.375e+09
+3.000e+09
+2.625e+09
+2.250e+09
+1.875e+09
+1.500e+09
+1.125e+09
+7.500e+08
+3.750e+08
+0.000e+00

3μs

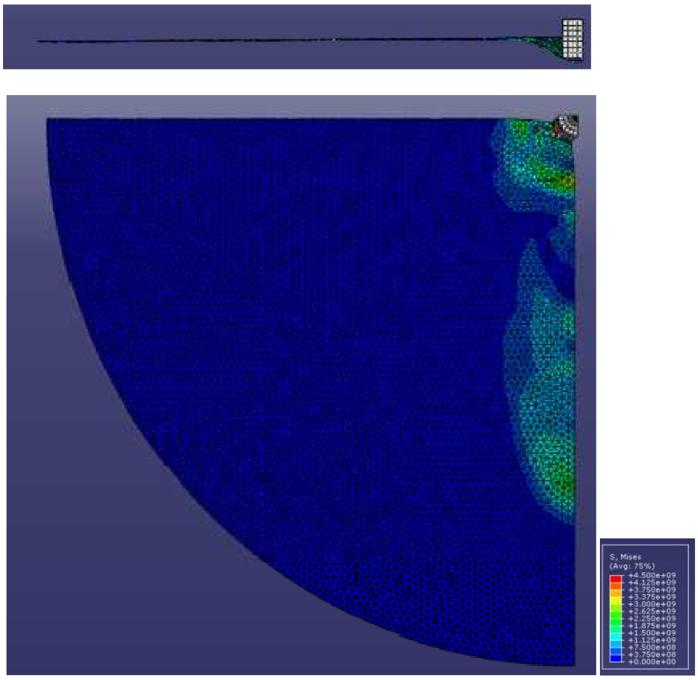

6μs

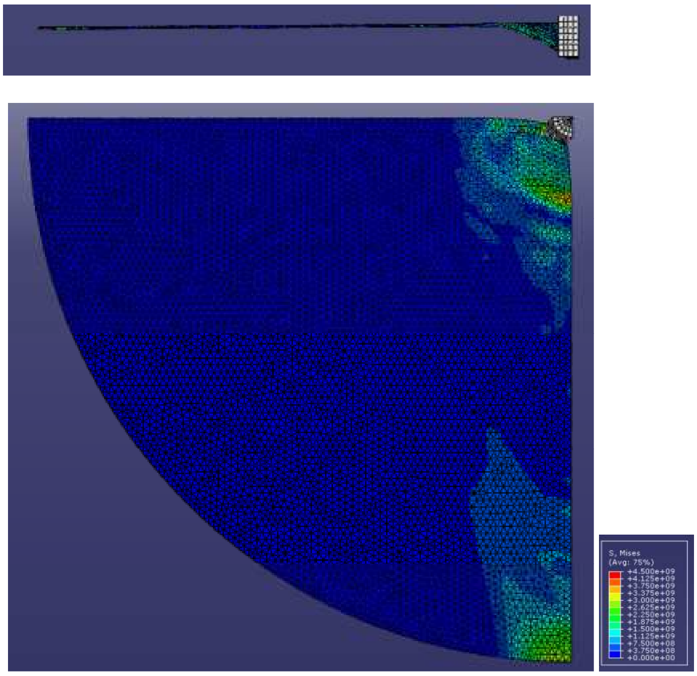

9μs

Figure 3-17 Contour plot of the UD fabric model during ballistic impact

Figure 3-18 reveals the time history of projectile kinetic energy loss during the impact events on the woven and UD fabric models at the impact velocity of 500 m/s. As the energy dissipated by air friction is not taken into consideration, the projectile kinetic energy loss is regarded as being equal to fabric energy absorption. Ascan be seen in Figure 3-18 (a), the energy absorbed by the fabric increases sharply within the first 0.8 µs. The curve continues to rise but more gently and finally levels off after 9 µs, at 2.9 J. This is because within the first 0.8 µs, energy transference occurs so quickly that fabric out of the contact zone does not react to the deformation at all. This results in the sharp increase of the curve [18]. After this, the fabric begins to respond to the bullet impact and the principal yarns are stretched. Bullet kinetic energy is transferred to fabric strain energy, fabric kinetic energy and frictional dissipation energy. At the 9 µs point, the projectile penetrates the fabric. Asimilar trend could be observed in Figure 3-18 (b).

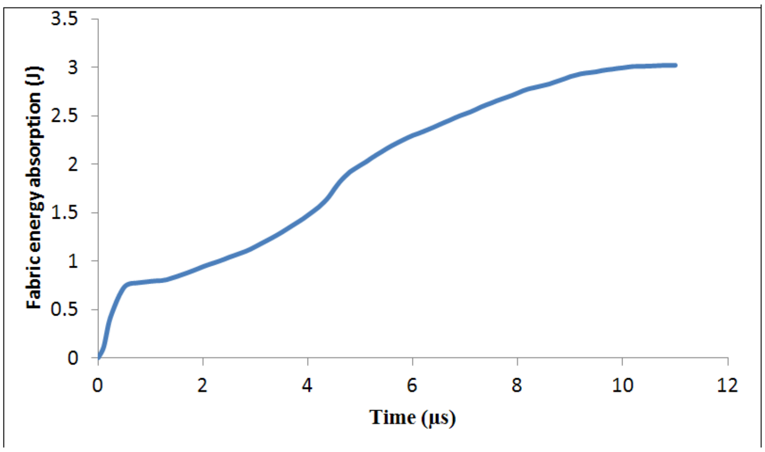

(a) The woven fabric model

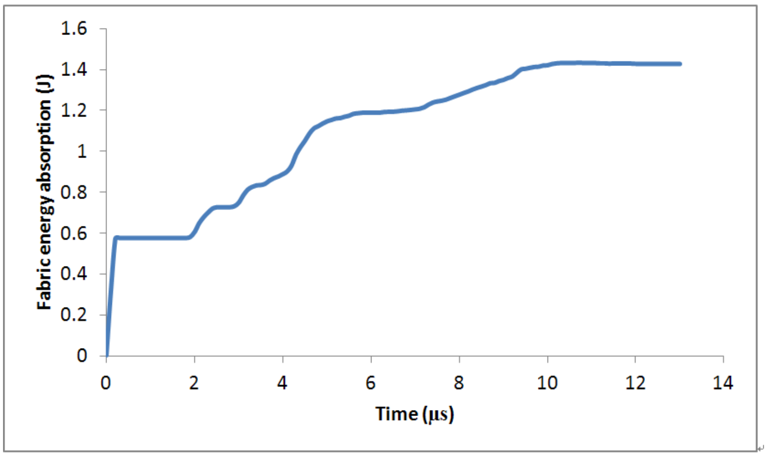

(b) The UD fabric model

Figure 3-18 Time history of fabric energy absorption at the impact velocity of 500 m/s

Figure 3-19 (a) shows energy transformation for the woven and UD fabric models. Three types of energy are investigated: fabric kinetic energy, strain energy and energy dissipated by the frictional effect. For the woven fabric model, it has been found that the dominating energy absorption mechanism—fabric kinetic energy—accounts for most of the fabric energy absorption, at 53.3%, which is almost double that of fabric strain energy and quadruple that of friction dissipation energy (this includes bullet-fabric friction dissipation energy and yarn-yarn friction dissipation energy). For the UD fabric, up to 38.58% of the energy is transformed into fabric strain energy, which is 40% more than that of the woven fabric. However, less energy is absorbed due to frictional dissipation. This is because there is no yarn or fibre interaction in the UD fabric, and the only frictional dissipation mechanism is based on projectile-fabric interaction.

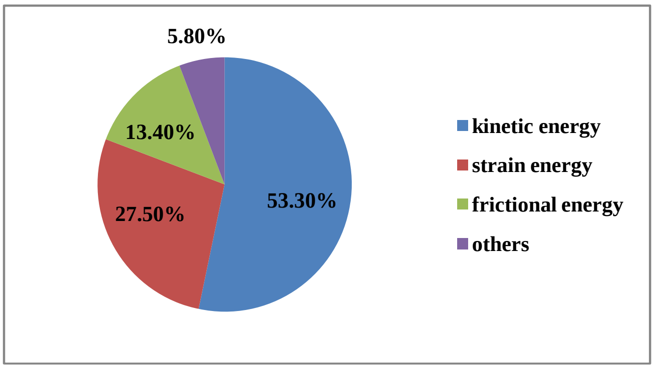

(a) The woven fabric model

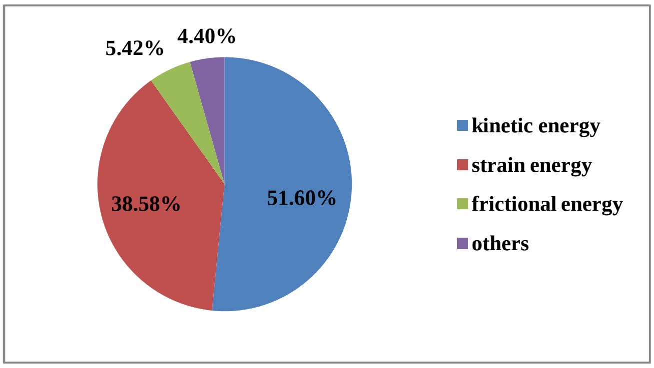

(b) The UD fabric model

Figure 3-19 Energy transformation for the two types of model

3.3.6 Study of the factors influencing ballistic performance of the woven fabric model

3.3.6.1 The effect of impact velocity

Figure 3-20 reveals the fabric ballistic performance at various impact velocities ranging from 0 m/s to 600 m/s for the woven fabric model. At the velocity region below the fabric ballistic limit (around 180 m/s), energy absorption is identical to the impact energy. Beyond the ballistic limit, energy absorption continues to grow until a peak value is reached. Further increases of impact velocity lead to a decrease of energy absorption. This is probably because the fabric target responds globally at low impact velocities, allowing energy to be dissipated away from the impact point. As the impact velocity increases, energy dissipation becomes more localised around the impact point, leading less energy to be absorbed. The results are comparable to Tan *et al* [31] and Cunniff's [52] work.

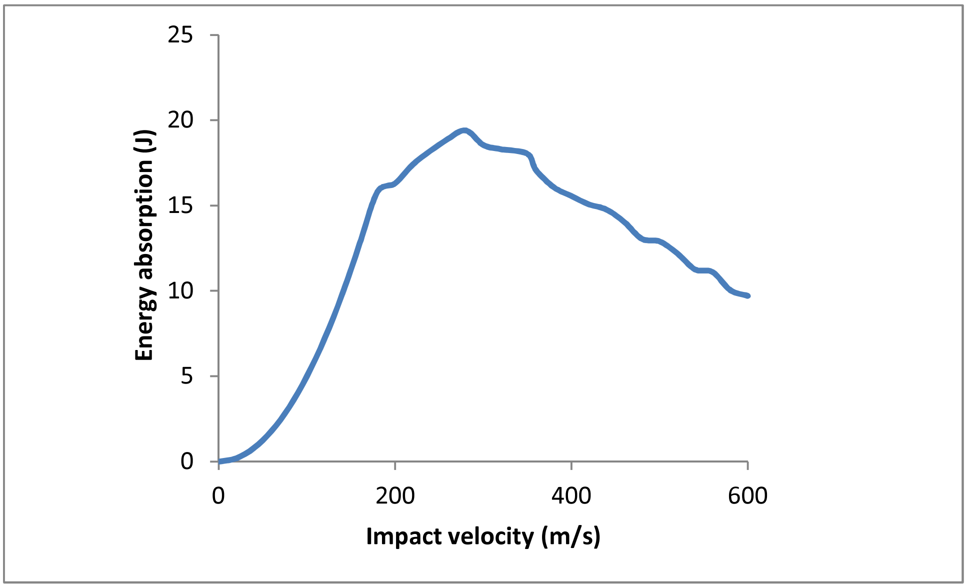

Figure 3-20 Energy absorption as a function of impact velocity for the woven fabric model

3.3.6.2 Effect of Far-field Boundary Conditions

The far-field boundary condition is considered to be indispensible when analysing the effect of impact velocity on fabric energy absorption. As has been discussed in the previous chapter, the constraint of the fabric boundary plays an important role in yarn lateral movement. In order to study its influence on energy absorption, woven fabric models with a constrained boundary and an unconstrained boundary were compared. Figure 3-21 shows the energy absorption for the two cases. As can be seen, the two cases display identical trends beyond 460 m/s. A considerable increase of energy absorption begins to occur for the case with the boundary unconstrained, below the impact velocity of 460 m/s. For the fabric model with a constrained boundary, the increase is comparatively steady. This phenomenon could be explained by the yarn's lateral displacement under different conditions. For the former case, yarns are more likely to be pulled out by the bullet and this therefore delays fabric damage, which allows more transverse deflection and more fabric strain energy storage. For the latter case, as the fabric edges are constrained, there is no yarn lateral displacement during the whole impact process, which speeds up the strain accumulation in the impact zone and results in yarn failure. In the region of high impact velocity, energy dissipation and fabric penetration occur so quickly that yarns far away from the impact zone are not even affected by the longitudinal wave. In other words, the fabric damage is localised at the impact zone and the far-field boundary does not take any effect.

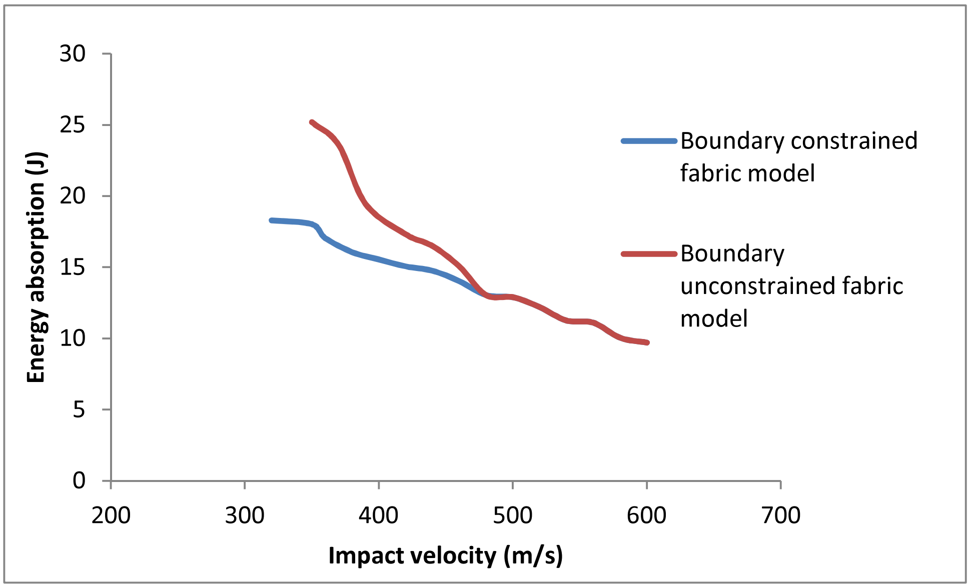

Figure 3-21 Comparison of specific energy absorption for boundary constrained and unconstrained model

3.3.6.3 Effect of woven fabric structures

In this section, the influence of fabric structure on ballistic performance will be studied. Four other types of structures, 2/1 S twill fabric model, 3/1 S twill fabric model, 5-end satin with M=3 (3 satin weave steps) warp wise fabric model and 7-end satin with M=4 warp wise fabric, will be put into comparison with the plain fabric and the UD fabric. Due to the fact that twill weave and satin weaves are not symmetrical about the x and z axis, a full-sized model is employed for simulations. In addition, in order to compare the performance of different fabrics at the same areal density, energy absorption is normalised by "specific energy absorption". Due to the limitation of computer power, the yarn mesh scheme is modified to support the simulation of multi-layered fabrics. Details of this computer cost reduction approach will be described in Chapter 7.

Figure 3-22 shows the specific energy absorption for different structures. Among the six types of structures, plain weave is found to exhibit the best ballistic protection. This is followed by 2/1 S twill and 3/1 S twill fabrics. 7-end M=4 satin weave gives the worst performance. UD fabric, however, shows worse performance than the majority of the woven fabrics and is only better than 7-end M=4 satin weave.

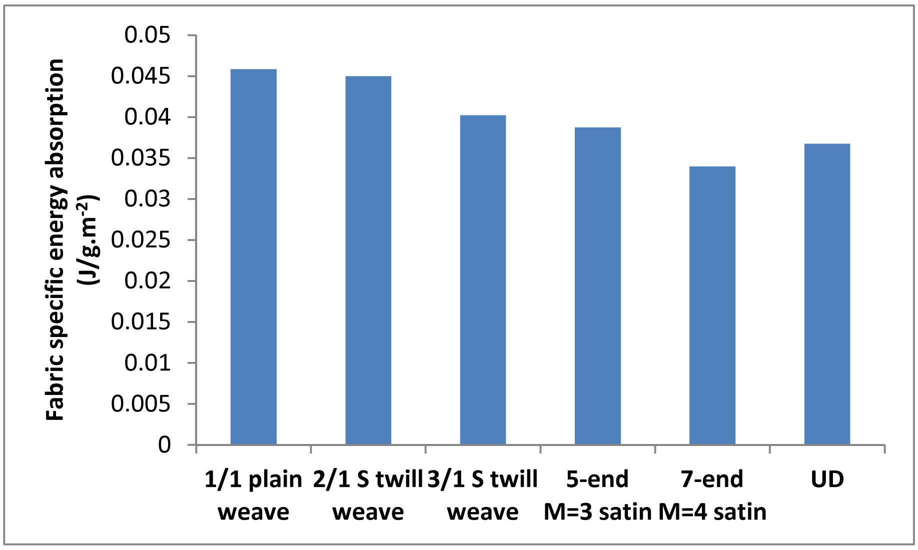

Figure 3-22 Energy absorption for single-layer fabrics

Figure 3-23 reveals the change of fabric energy absorption with the increase of the number of layers in a panel. For the woven fabrics, 1/1 plain woven fabric shows the highest energy absorption. The superiority of plain weave over other fabrics found in the FE model has been supported by previous research [54] [52]. This helps to explain the fact that plain weave is one of the most widely used structures for soft body armour. What is interesting in the results is that the value gives an upward-concaved increase for the woven fabric models and a downward-concaved increase for the UD fabric model, leading the UD fabric to give a comparatively poorer performance in the lower areal density region and a better performance in the high areal density region.

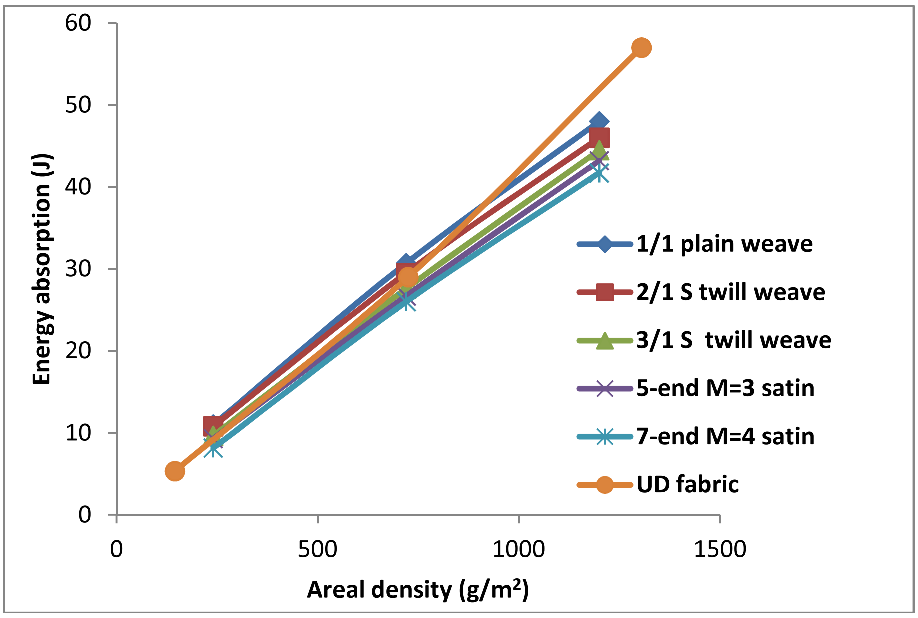

Figure 3- 23 Energy absorption for multi-plied fabrics

In order to further explore the effect of structure on woven fabric performance, strain distribution was investigated. Strain distribution indicates a fabric's capability to dissipate and absorb projectile kinetic energy. As strain energy is a direct function of strain for the material, it is employed to reflect fabric strain upon ballistic impact. Figure 3-25 compares the amount of strain energy stored in the secondary yarns with that in the whole fabric. It has been found that around 31.4% of the strain energy in plain woven fabric is accumulated in the secondary yarns. This is followed by 2/1 S twill weave (25.3%) and 3/1 twill weave (23.5%). 7-end M=4 satin weave gives the lowest value (16%). A strong relationship between the length of float and the strain distribution is built based on the results. Fabrics with longer float, such as satin weaves, have a smaller number of crossovers between the weft and warp yarns. This impedes the transmission of energy from the primary yarns to the secondary yarns, which consequently leads to poor performance. For fabrics with shorter floats, such as plain weave and twill weave, more crossovers facilitate the energy dissipation between the primary yarns and secondary yarns, which results in better performance.

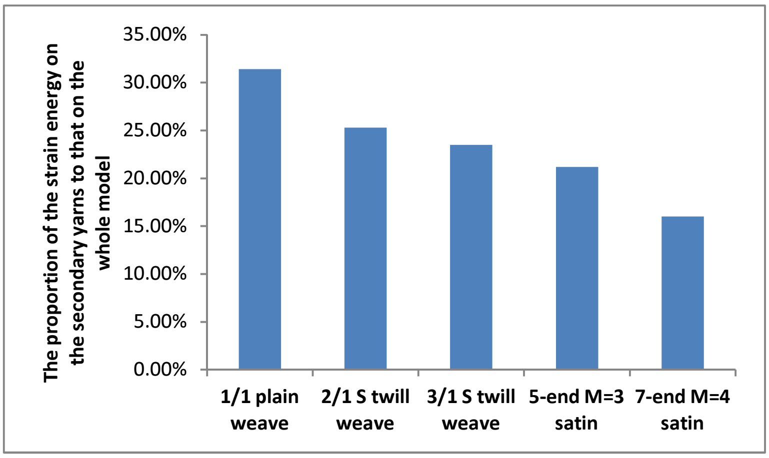

Figure 3-24 The proportion of the strain energy on the secondary yarns to that on the whole model

3.3.6.4 Effect of weave density on plain woven fabric

Weave density is one of the important factors that determine the ballistic performance of plain woven fabrics. Since the woven fabric model is validated by experimental data, it is possible to further study the performance of UHMWPE fabric with other weave densities. The shape of fabric-forming yarn was modified to set up different fabric models. The weave density was determined to range from 4 threads/cm to 9 threads/cm. In order to obtain accurate results, the geometry and energy absorption capability of fabric-forming yarns of different models must be kept consistent with the original.

Creation of FE models with different weave density

Yarn geometry is mainly dependant on yarn cross-section and yarn path. As has been mentioned in previous sections, the shape of the yarn cross-section is determined to be lenticular, formed by two arcs. Modification of weave density leads to a change in the width and height of the shape. For the original model, which has a weave density of 6.75 threads/cm, it is termed as 6.75-thds fabric. As the height and width of the yarn model was tested to be 0.19 mm and 1.35 mm respectively, it is not difficult to calculate the area of the cross-section.

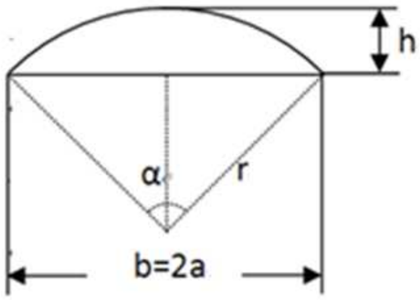

Figure 3-25 Top half of the lenticular yarn cross section

$$r = \frac{a^2 + h^2}{2h} \tag{3.2}$$

$$\alpha = 4\arctan(\frac{h}{a}) \tag{3.3}$$

$$S = \frac{\alpha r^2}{2} - a\sqrt{r^2 - a^2} \tag{3.4}$$

where *a* is half of the cross-section width, *h* is half of the cross-section height, *α* is the radius angle and *r* is the radius of the arc. The radian of yarn path is set to be equal to that of the yarn cross-section, so that the weft and warps yarn can be perfectly in contact with each other.

The yarn cross-section area for the 6.75-thds yarn model is 0.347 mm^2. For fabric models with different weave density, it is considered that the area of the yarn cross-section and the yarn spacing will not change. The cross-section of width, which varies with weave density, is not difficult to work out. According to Equations 3.2, 3.3 and 3.4, the height of the yarn cross-section can be obtained. Table 3-4 reveals the width and height for fabric with different weave densities.

Table 3-2 Woven fabric models with different areal density

Weave density (threads/cm)	Cross-section width (mm)	Cross-section height (mm)	Areal density (g/m^2)	Crimp	Abbreviation
4	2.37	0.108	139	0.48%	4-thds
5	1.87	0.138	178	0.73%	5-thds
6	1.54	0.167	215	1.03%	6-thds
6.75	1.35	0.19	240	1.29%	6.75-thds
8	1.12	0.23	286	1.80%	8-thds
9	0.98	0.258	329	2.31%	9-thds

The energy absorption capability of a single yarn

For the FE model, it is of importance that the modification of yarn cross-section does not influence the yarn energy absorption capability. In order to verify this, a half-yarn model is employed to simulate single-yarns subjected to transverse impact and the projectile energy losses are examined. Figure 3-27 reveals the time history of the projectile energy when striking a single yarn. As can be seen, the projectile residual energies are in the vicinity of 60.8J. There is not much difference between the energy absorption of different yarn models.

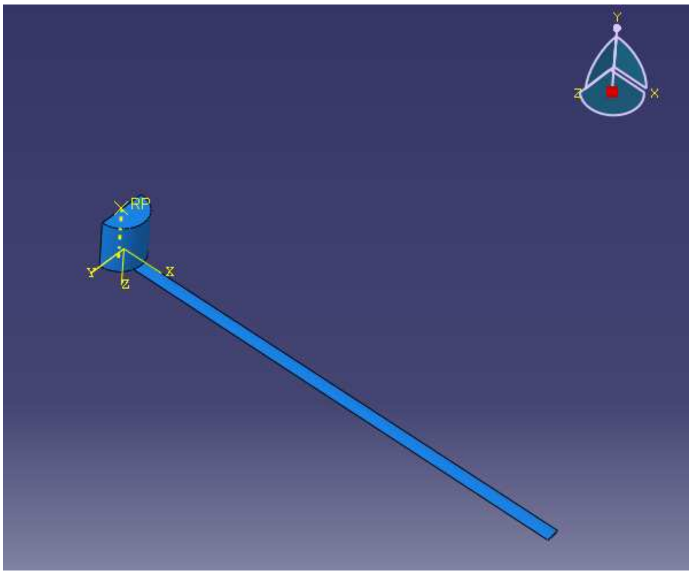

Figure 3-26 Yarn subjected to transverse impact

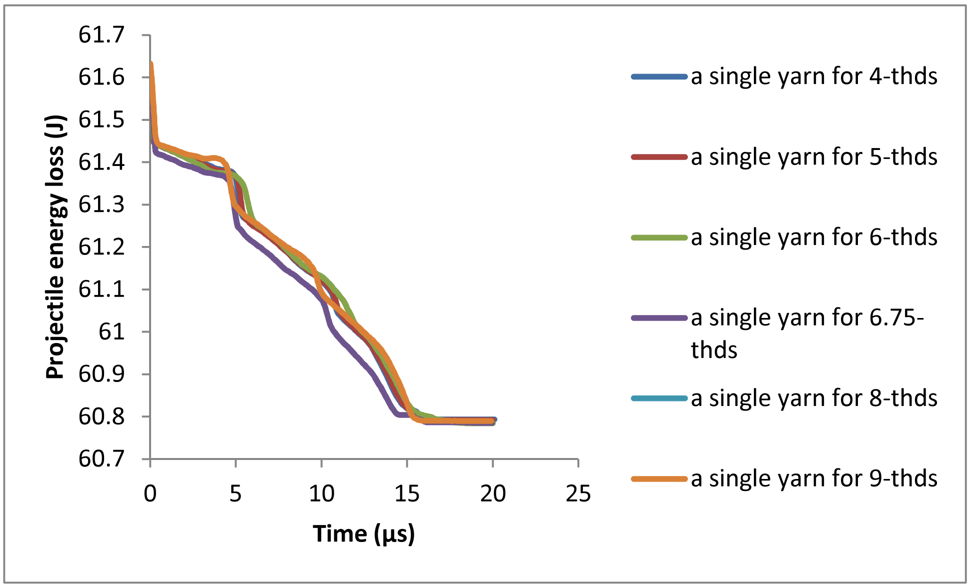

Figure 3-27 Time history of projectile energy loss of different yarns

The ballistic performance of fabric models with different weave density

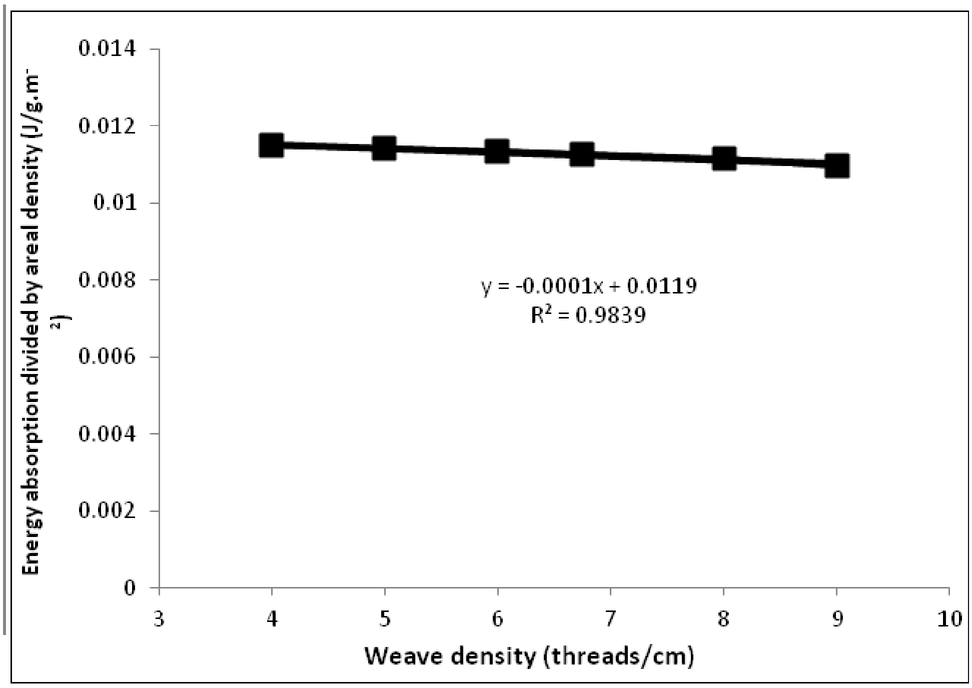

Figure 3-28 Specific energy absorption as a function of thread density

For fabrics with different weave densities, energy absorption is tightly associated with fabric areal density. In order to better compare fabric ballistic performance, specific fabric energy absorption was obtained by dividing normal energy absorption by areal density. Figure 3-28 reveals that the specific energy absorption decreases slightly as the weave density is increased. However, as the number of layers increases in a panel, the difference becomes more remarkable. Low-weave-density fabrics, such as 4-thds, give a sharply linear increasing trend with the increase of fabric layers. High-weave-density fabrics, such as 8-thds, exhibit a logarithmic increasing trend, which results in an inferior energy absorption in high areal density regions. Due to the limit of computer power, simulation of multi-ply fabric upon impact could not be achieved if the full size model is to be used. For this reason, the mesh scheme was modified to reduce the computing cost without affecting the energy absorption capability of the fabric. The method will be described in detail in Chapter 7.

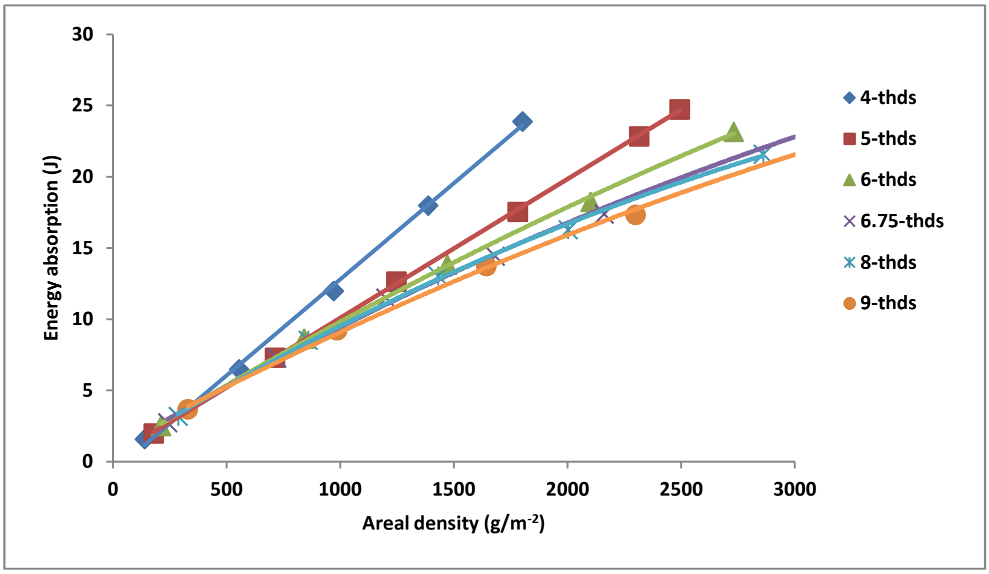

Figure 3-29 Energy absorption as a function of panel areal density

This raises the question why does fabric weave density have comparatively little influence on energy absorption in low areal density regions and greater influence in high areal density regions. As the areal density of 4-thds is almost half that of 8-thds, the two types of fabric model were selected to investigate the effect of fabric tightness on ballistic performance. A comparison of one-layer of 8-thds and two layers of 4-thds reveals their different responses upon impact. It has been observed in Figure 3-30 that the width of transverse deflection for two layers of 4-thds (13.5 mm) is slightly larger than that of one-layer of 8-thds (12.2 mm), which leads to a slightly higher specific energy absorption for the former case, which is shown in Figure 3-31. This is probably because that fabric with higher weave density gives yarns higher crimp (here, crimp could also be regarded as wrapping angle), which reduces the fabric tensile modulus [59] and a decrease both of the longitudinal and transverse velocity. For this reason, energy absorption is influenced. Due to the size of the current model, the longitudinal wave reaches the boundary within a short time period. It is the transverse deflection that determines the fabric energy absorption.

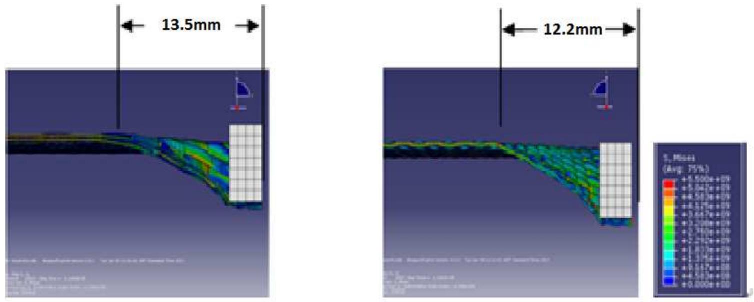

(a) Two-layer of 4-thds (b) One-layer of 8-thds

Figure 3-30 Transverse deformation at break

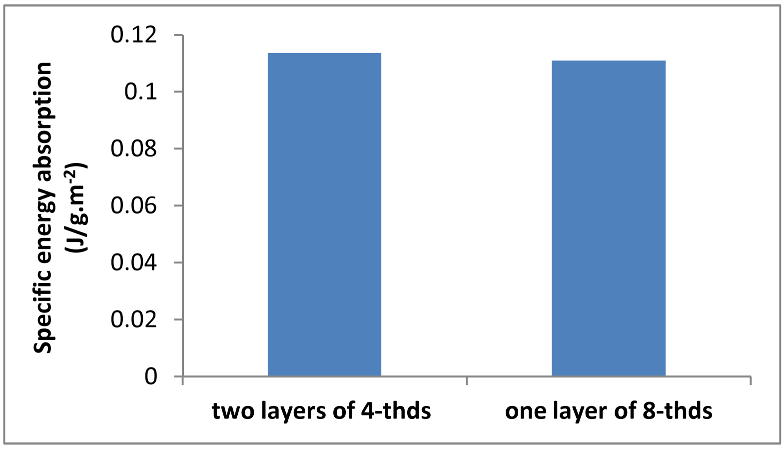

Figure 3-31 Specific energy absorption for two-layers of 4-thds and one-layer of 8-thds

As the panel areal density increases, the influence of yarn crimp on fabric energy absorption becomes more pronounced. As can be seen in Figure 3-32, the difference of the transverse reflection width between the two cases (3.2mm) is greatly increased when compared with that in Figure 3-30 (1.3mm), and the specific energy absorption for eight layers of 4-thds is 0.0023J/g.m^{-2} higher than that for four layers of 8-thds, which is shown in Figure 3-34. This could be explained by two reasons. First, the longer engagement time with the projectile forms a wider transverse deflection of the 4-thds panel, which enables a larger area of fabric to get involved in energy dissipation. Secondly, as a panel is formed by individual fabric layers rather than a whole body, the increase in the number of layers makes the difference even greater and more noticeable.

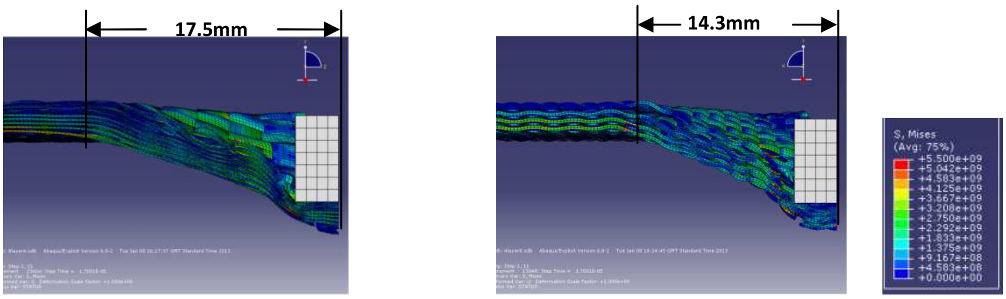

(a) Eight-layers of 4-thds **(b) Four-layer of 8-thds**

Figure 3-32 Transverse deformation at break (at 17 μs)

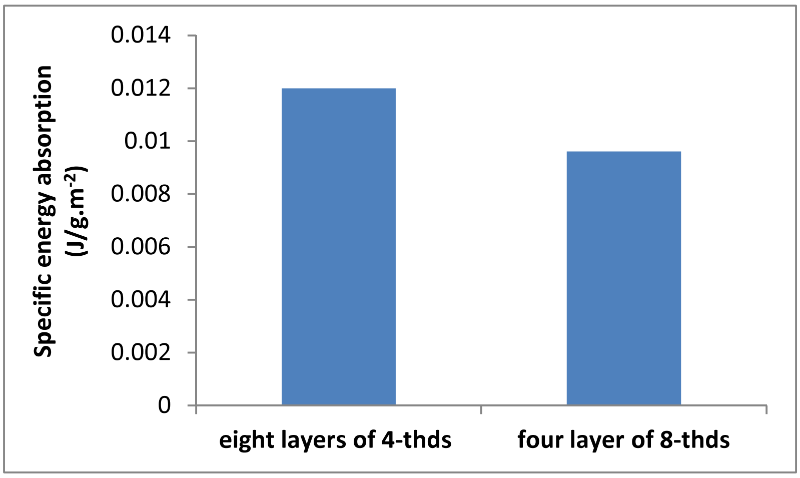

Figure 3-33 Specific energy absorption for eight layers of 4-thds and four layers of 8-thds

3.3.6.5 Impact position

As the woven fabric is formed by yarn interlacing, the gap between adjacent yarns becomes the weak point in the fabric. This makes the fabric ballistic performance varies from part to part, resulting in a decreased reliability and usability for woven fabrics. In this section, finite element methods will be employed to investigate the influence of impact position on fabric performance. As can be seen in Figure 3-34, three cases were studied. In case A, the interlacing of weft and warp yarns cross the centre of the projectile. In Figure case B, the projectile centre point is located on the warp yarn and in-between two adjacent weft yarns. In Figure case C, the centre point is located in the hole of the interwoven warp and weft yarns. The three cases represent three conditions where the projectile covers a different number of yarns, which plays an important role in the amount of material involved in energy dissipation.

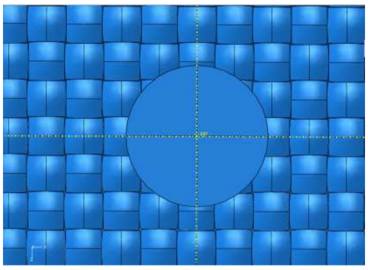

(a) Case A: projectile centre point located on the cross point of weft and warp yarns

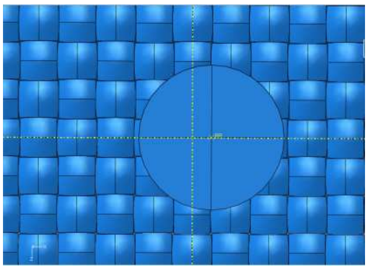

(b) Case B: projectile centre point located on the weft yarn and in between two adjacent warp yarns

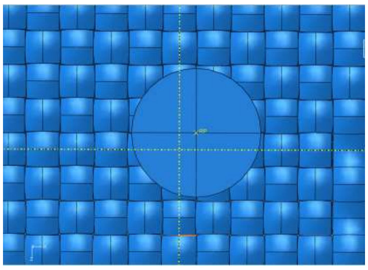

(c) Case C: projectile centre point located in the hole of the interwoven warp and weft yarns

Figure 3-34 Projectile impact point at different locations

Figure 3-35 compares fabric energy absorption for different impact positions. Of the three cases, the fabric absorbs the most energy in case C. And in case A, where weft and warp yarn cross the centre point of projectile, the fabric exhibits its worst performance. This is because more yarns are engaged and are broken by the projectile in case C. The number of yarns damaged by the projectile for the three cases could be seen in Figure 3-36. As a result, more energy is absorbed when the projectile covers four weft and warp yarns.

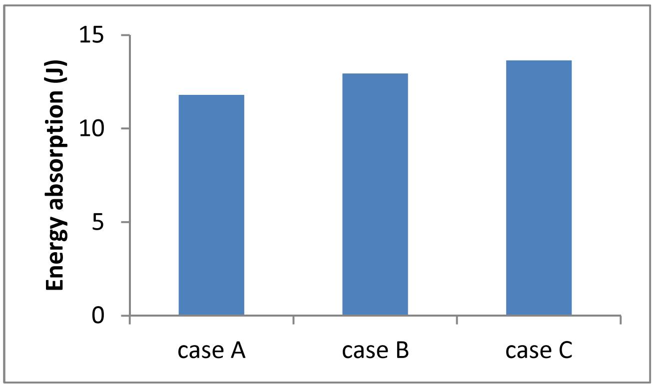

Figure 3-35 Energy absorption for different impact positions

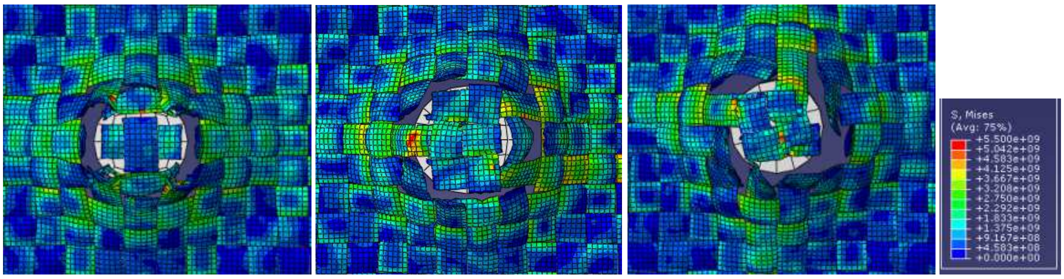

(a) Case A **(b) Case B** **(c) Case C**

Figure 3-36 Model Contour plots of stress distribution for different impact points

3.4 Summary

This chapter presents the experimental and theoretical methodologies employed to achieve the aims and objective in this research. Both the ballistic range and the creation of finite element models have been comprehensively described. The models were validated and showed good agreement with the experimental results. It has also been revealed from the models that the majority of projectile kinetic energy is transmitted to fabric strain and kinetic energy on both the woven and UD fabrics. A higher proportion of energy is dissipated by frictional effects in the woven fabric model due to the movement between warp and weft yarns.

Factors such as impact velocity, fabric boundary conditions, fabric structure, weave density and impact positions have been analysed for their influence on woven fabric energy absorption using FE models. It has been found that energy absorption decreases with the increase of impact velocity. Fabric boundary conditions play a more important role at low impact velocity than at high impact velocity. In addition, plain woven fabric shows superior ballistic performance over other types of fabric due to its ability to enable more energy transmission between the primary yarns and the secondary yarns. For a plain structure, it has been established that fabrics with lower weave density absorb more energy than those with higher weave density. This is considered to be related to yarn undulation, which influences the propagation of the transverse wave during a ballistic event. FE simulation also reveals that the impact position determines the number of yarns loaded by a projectile, which results in uneven ballistic performance in woven fabrics.

Chapter 4 Study of the Influence of Inter-yarn Friction on Fabric Ballistic Performance

As has been mentioned in previous chapters, one of the aims of this research is to investigate the influence of inter-yarn friction on the ballistic performance of woven fabrics. In order to achieve this aim, theoretical studies will be undertaken in this chapter. The finite element model created in Chapter 3 was used to predict fabric performance at different levels of inter-yarn friction and to develop a comprehensive understanding of exactly how inter-yarn friction has an effect on fabric stress distribution and energy dissipation.

4.1 Effect of Friction on Woven Fabric Energy Absorption

Figure 4-1 shows the predicted fabric energy absorption as a function of yarn-yarn coefficient of friction in the FE model. The curve increases from μ=0, reaches a peak at μ=0.4 and decreases from that point onwards. The energy absorption for μ=0.4 was almost 1J higher than that for μ=0. Further increase in the coefficient led to a decrease in fabric energy absorption. The results display a similar trend to that of Zeng *et al.*'s [19] though the coefficient of friction giving the highest ballistic performance was found in that study to be at the lower value of 0.1. It is noteworthy that fabric penetration time gives a similar trend to the case of energy absorption. For example, the penetration moment for the case of μ=0 is around 7.5 microseconds, while it takes around 10 microseconds to perforate the fabric for the case of μ=0.4, which is shown in Figure 4-2. The penetration time decreases as the inter-yarn frictional coefficient further increases.

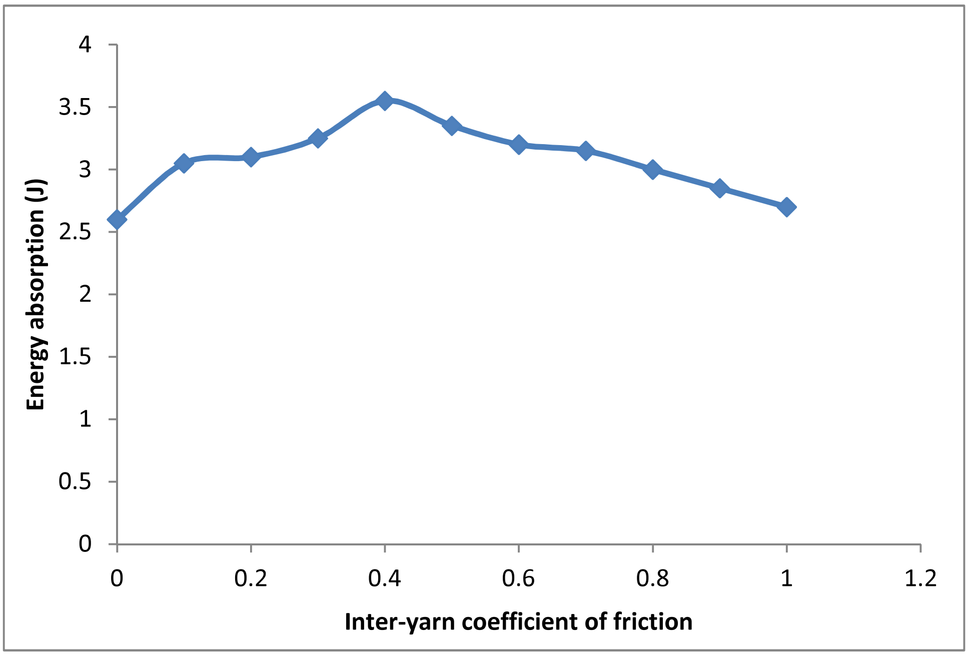

Figure 4-1 Fabric energy absorption as a function of coefficient of inter-yarn friction

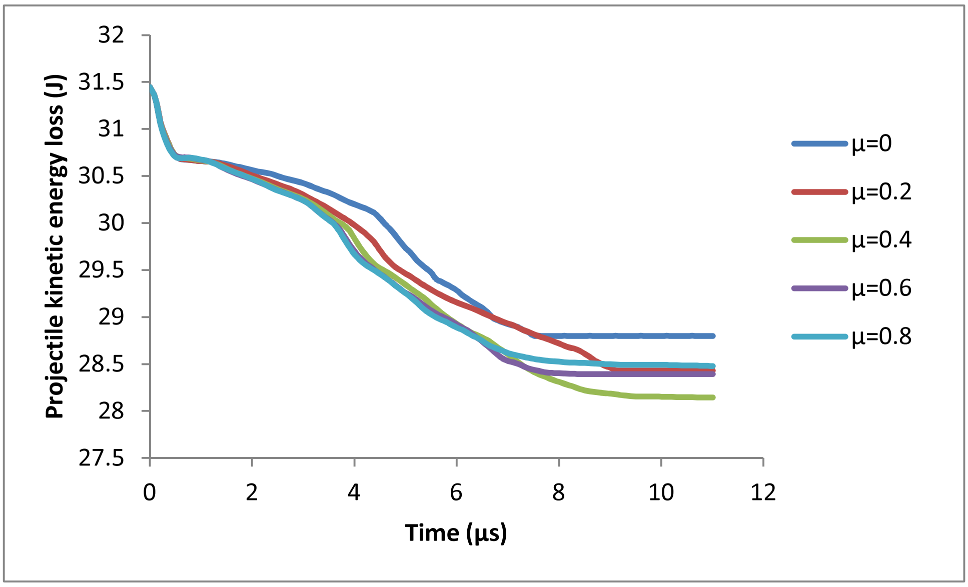

Figure 4-2 Time history of projectile kinetic energy loss for fabrics with different inter-yarn friction

This could be explained as follows: due to the lack of yarn-yarn friction, slippage occurs between the principal yarns and the secondary yarns. This leads the principal yarns to sustain most of the impact load, which is shown in Figure 4-3 (a). As a result, the strain is more quickly accumulated and therefore early failure occurs of the primary yarns. For the case of μ=0.4, the coupling caused by yarn-yarn friction prevents yarn slippage and enables the strain to be distributed to the secondary yarns, which is shown in 4-3 (b). This elongates the fabric engagement time with the projectile and delays yarn failure. The results corroborate the findings of Briscoe and Motamedi [17], whose observation from a high speed camera shows that fabric with low inter-yarn friction tend to fail earlier than those with high friction. If the frictional force is too high, yarn mobility will be over-constrained. This leads the primary yarns to be damaged at an early stage, which is reinforced by the work of Zeng *et al.* [19] and Duan *et al.* [18]. In addition, this finding could also be supported by experimental data. A good example is the comparison of unidirectional fabric and woven fabric. As the fibres are stuck together by binding materials in unidirectional fabric, it is reasonable to regard the frictional force as infinite in this type of structure. The results from ballistic test show that single-layer woven fabric absorbs around 12.7% more energy than the single-layer unidirectional fabric on the same areal density basis, which will be presented in detail in Chapter 7.

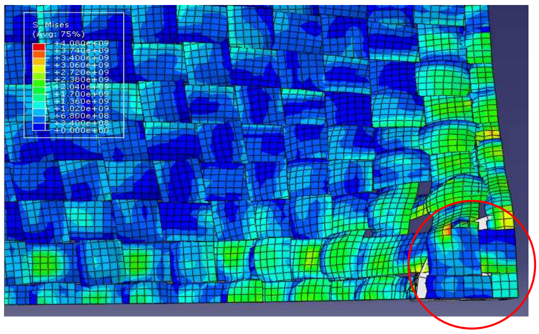

(a) μ=0

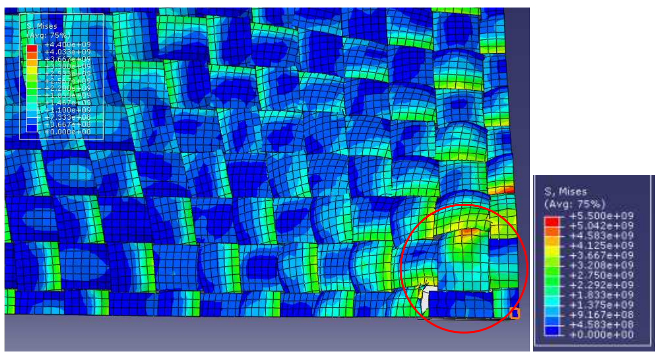

(b) μ=0.4

Figure 4-3 Single-layer fabric model upon ballistic impact at 6 μs

4.2 Effect of Inter-Yarn Friction on Stress Distribution

In order to investigate the influence of inter-yarn friction on the fabric energy absorption mechanism, three cases, μ=0, μ=0.4 and μ=0.8, will be selected to represent different magnitudes of friction. As materials are subjected to different stresses in the x, y and z directions, Von Mises Stress is taken as an indicator of fabric stress distribution upon ballistic impact. Von Mises Stress σ' is a combination of the three primary stresses σ_x, σ_y, σ_z and the shear stress τ_{xy}, τ_{yz}, τ_{xz}. The von Mises Stress can be expressed as

$$\sigma' = \frac{1}{\sqrt{2}}\left[(\sigma_x - \sigma_y)^2 + (\sigma_y - \sigma_z)^2 + (\sigma_z - \sigma_x)^2 + 6(\tau_{xy}^2 + \tau_{yz}^2 + \tau_{zx}^2)\right]^{\frac{1}{2}} \tag{4.1}$$

4.2.1 Contour plot of woven fabric upon ballistic impact

Figure 4-4, Figure 4-5 and Figure 4-6 reveal Contour plots of stress distribution for the cases of μ=0, μ=0.4 and μ=0.8. It can be seen that stress distribution is noticeably affected by inter-yarn friction. For the case of μ=0, the coloured area along the primary yarns gives a longer but narrow shape. The increase of inter-yarn friction leads to a decrease of the length and an increase of the width for the coloured area. In addition, larger areas in the vicinity of the impact point are affected by the effect of friction. This indicates that although inter-yarn friction impedes the stress propagation along the primary yarns, it enables more secondary yarns to get involved in energy dissipation. In order to quantify the stress distribution, a primary yarn and a secondary yarn will be selected for investigation.

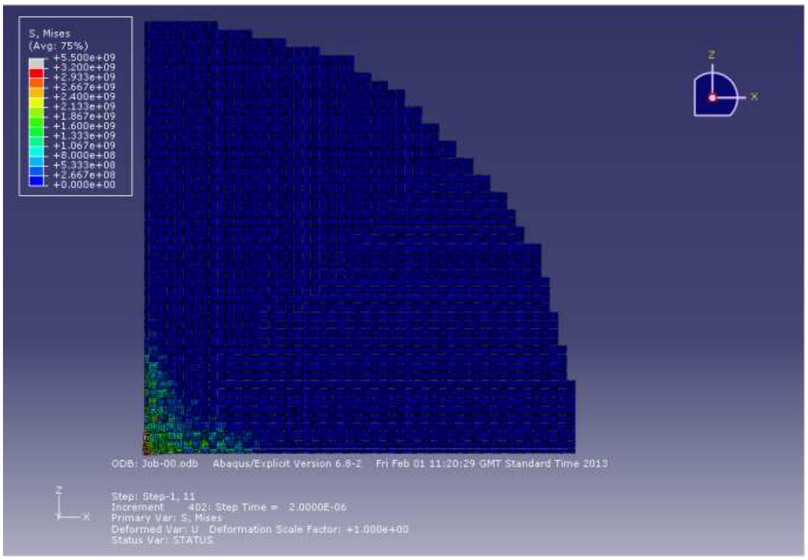
S, Mises
(Avg: 75%)
+5.500e+09
+3.200e+09
+2.933e+09
+2.667e+09
+2.400e+09
+2.133e+09
+1.867e+09
+1.600e+09
+1.333e+09
+1.067e+09
+8.000e+08
+5.333e+08
+2.667e+08
+0.000e+00
ODB: Job-00.odb Abaqus/Explicit Version 6.8-2 Fri Feb 01 11:20:29 GMT Standard Time 2013
Step: Step-1, 11
Increment 402: Step Time = 2.0000E-06
Primary Var: S, Mises
Deformed Var: U Deformation Scale Factor: +1.000e+00
Status Var: STATUS

μ=0

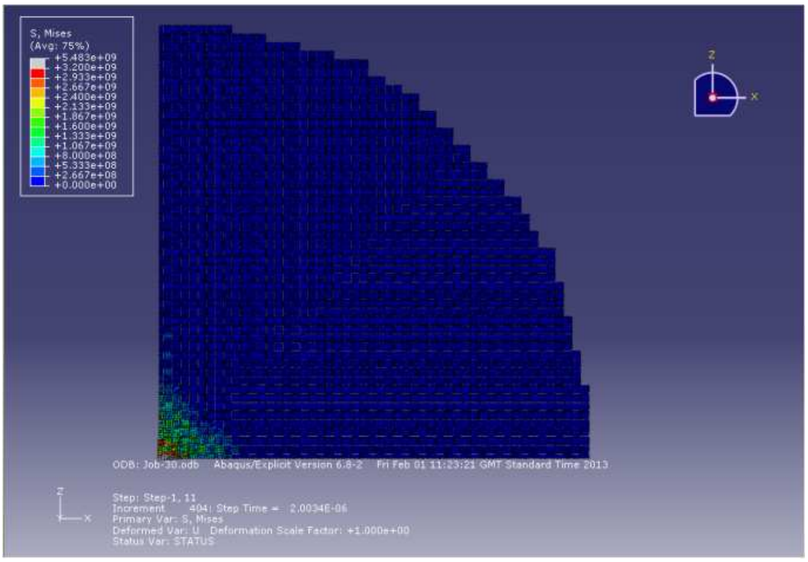
S, Mises
(Avg: 75%)
+5.483e+09
+3.200e+09
+2.933e+09
+2.667e+09
+2.400e+09
+2.133e+09
+1.867e+09
+1.600e+09
+1.333e+09
+1.067e+09
+8.000e+08
+5.333e+08
+2.667e+08
+0.000e+00
ODB: Job-30.odb Abaqus/Explicit Version 6.8-2 Fri Feb 01 11:23:21 GMT Standard Time 2013
Step: Step-1, 11
Increment 404: Step Time = 2.0034E-06
Primary Var: S, Mises
Deformed Var: U Deformation Scale Factor: +1.000e+00
Status Var: STATUS

μ=0.4

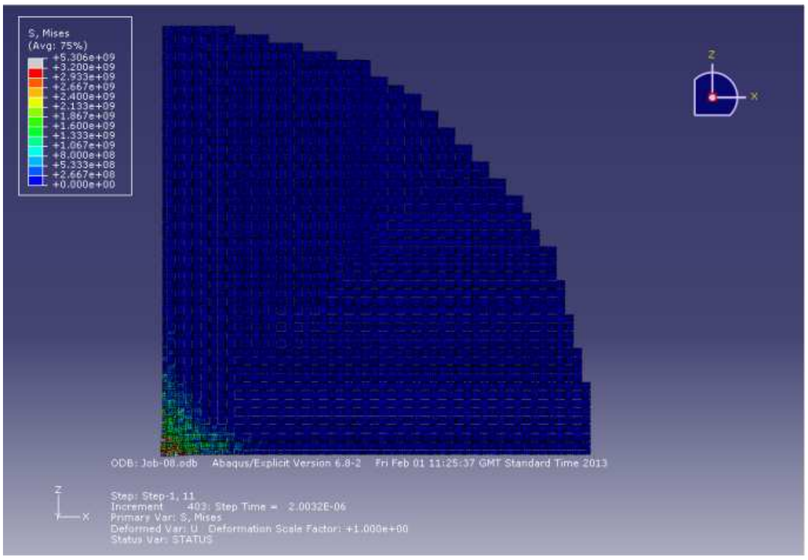

μ=0.8

Figure 4-4 Contour plots of stress distribution for fabrics at 2 μs after impact

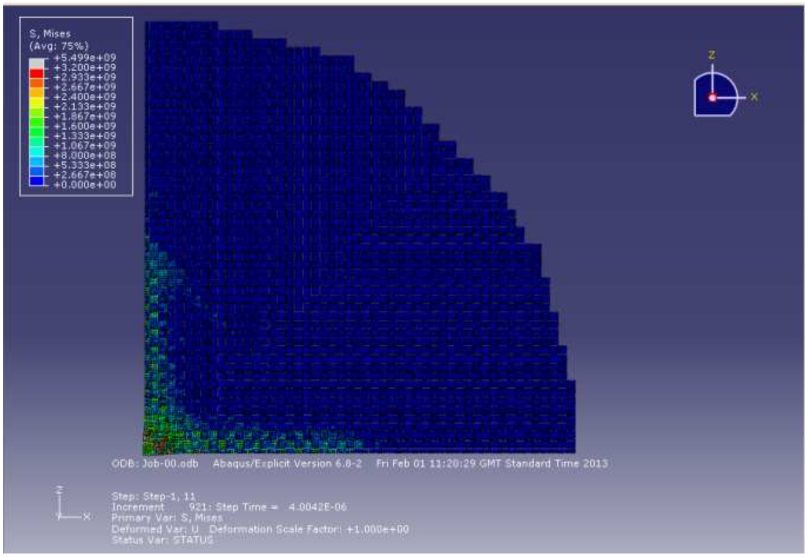

μ=0

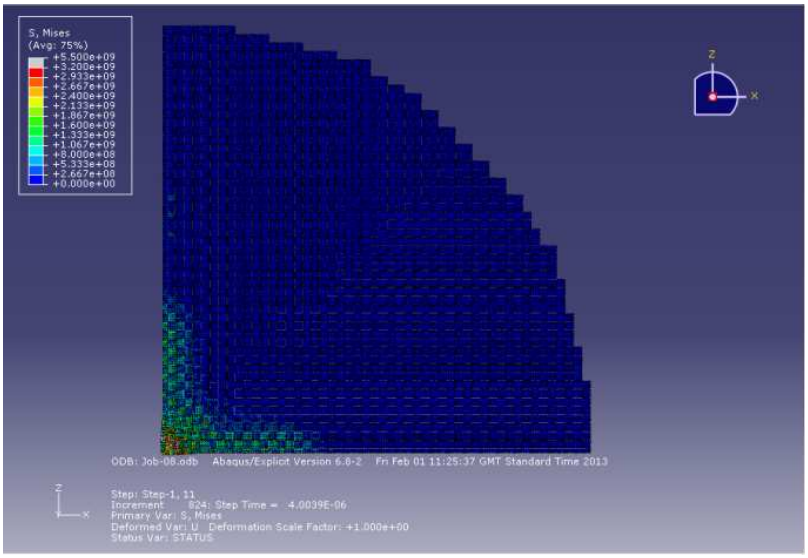

μ=0.4

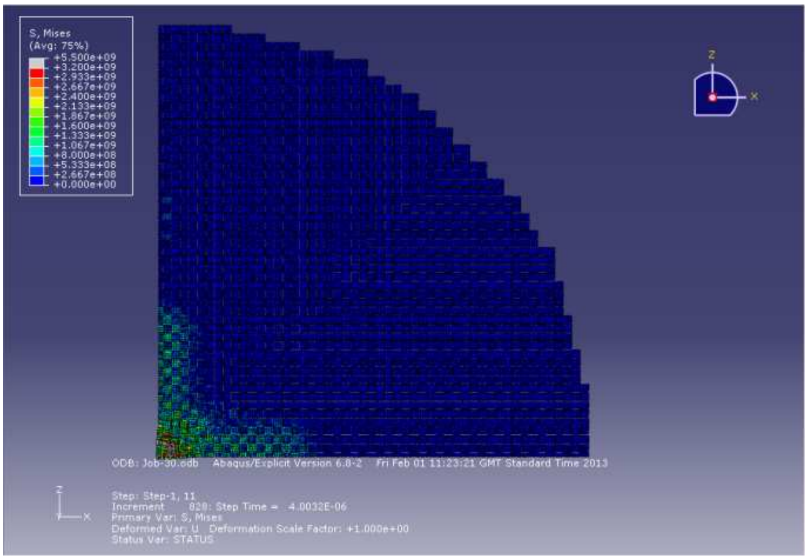

μ=0.8

Figure 4-5 Contour plots of stress distribution for fabrics at 4 μs after impact

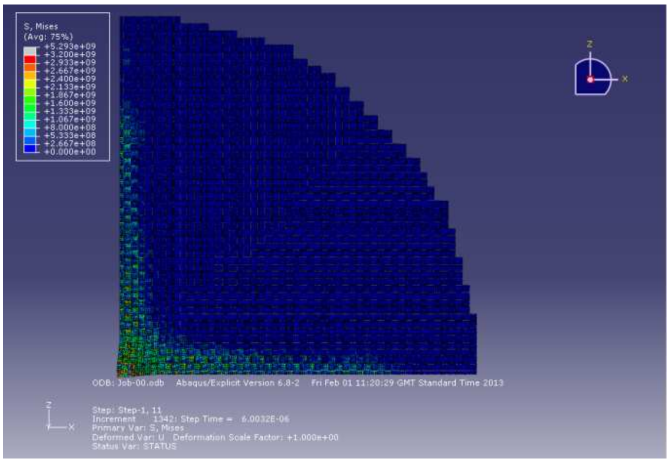

μ=0

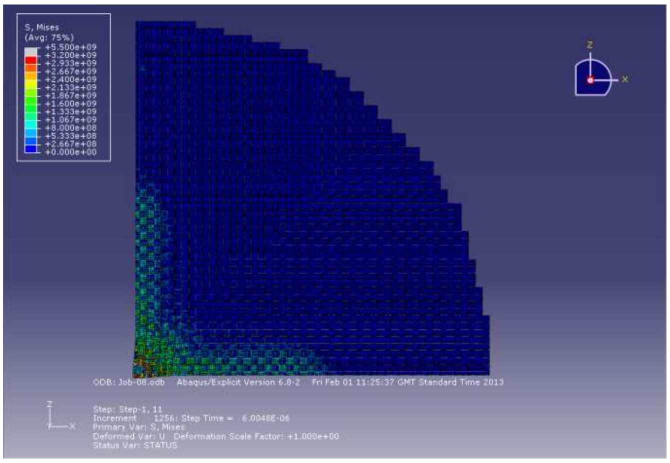

μ=0.4

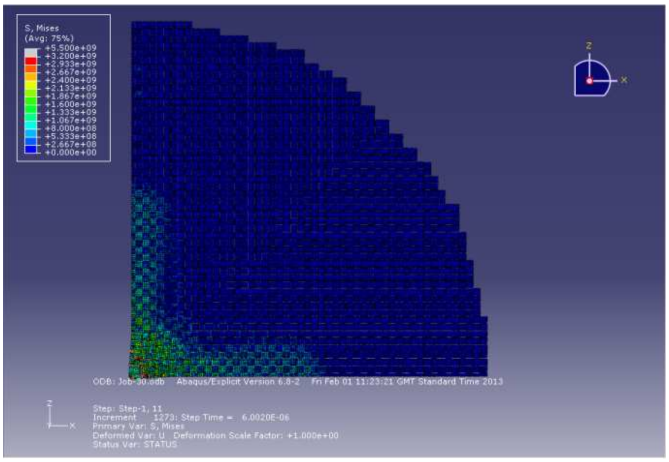

μ=0.8

Figure 4-6 Contour plots of stress distribution for fabrics at 6 μs after impact

4.2.2 Stress distribution on the primary yarn

In order to investigate the stress distribution on a primary yarn, a selection of elements was recorded for their von Misis stress as a fucntion of time history. The elements are shown in Figure 4-7.

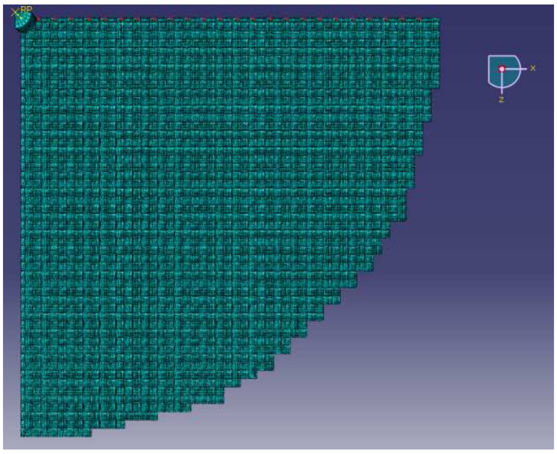

Figure 4-7 Element selection on the primary yarn

Figure 4-8 reveals the stress distribution on the selected primary yarn at 2 μs, 4 μs and 6 μs. The cases of μ=0, μ=0.4 and μ=0.8 are selected to represent fabrics with different inter-yarn friction. The figures bring out a number of features of general interest. The longitudinal wave velocity, which determines the capability of a fabric to dissipate energy, is found not to be influenced by inter-yarn friction. The stress distribution, however, exhibits a significant difference. For fabric with high inter-yarn friction, such as μ=0.8, the area in the vicinity of the impact point exhibits higher stress than the other two cases, which could possibly be associated with yarn mobility. The reduced yarn mobility may restrict the propagation of the stress wave and lead to a concentration of stress at the impact point. This consequently causes breakage at an early stage. The results are shown in Figure 4-2. For the case of μ=0, although the increased yarn mobility enables the stress to be distributed far away from the impact point, yarn slippage causes more load to be sustained on the primary yarns and also leads to early failure.

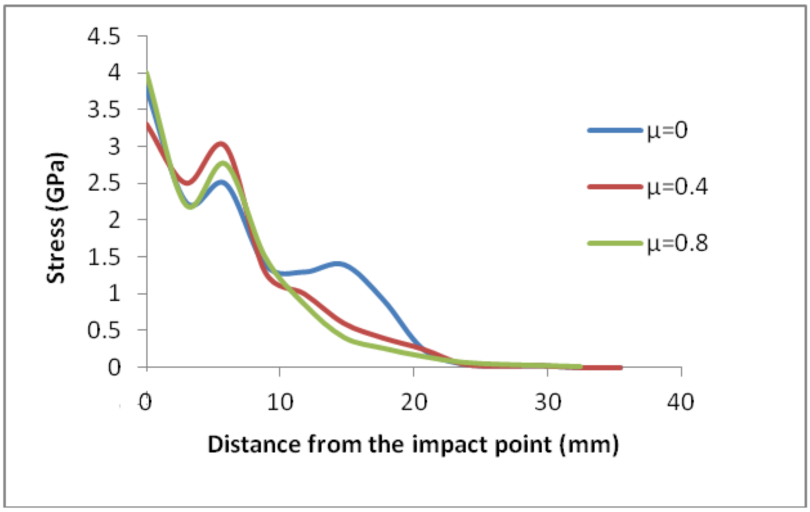

(a) 2μs

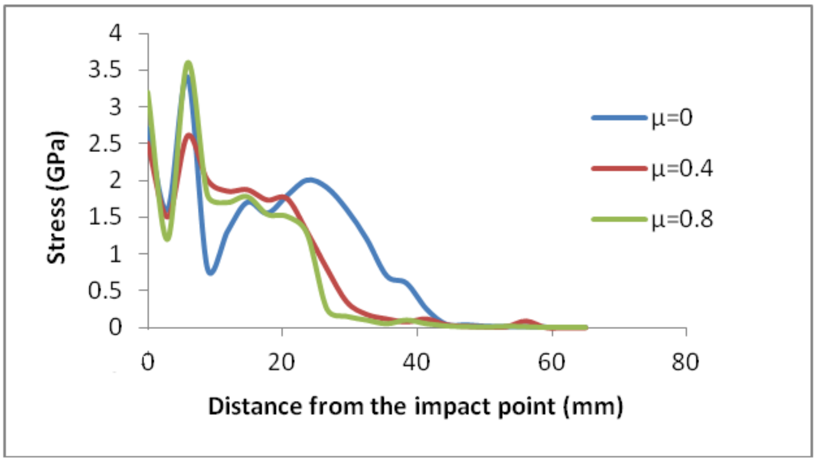

(b) 4μs

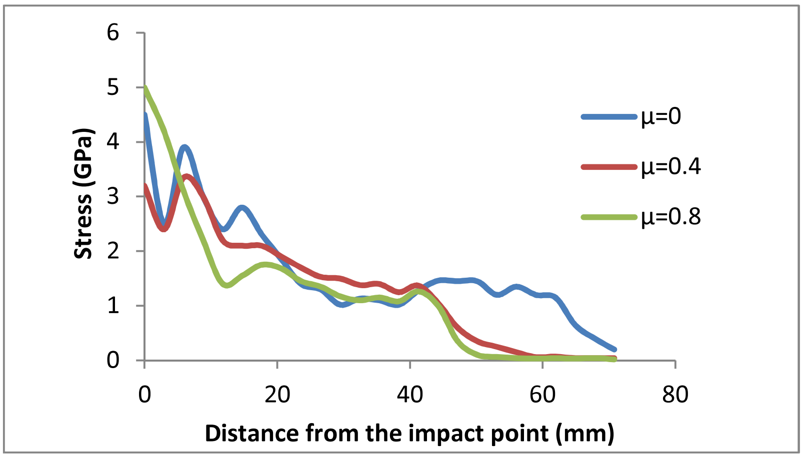

(c) 6μs

Figure 4-8 Stress distribution on the primary yarn for fabrics with different inter-yarn coefficients of friction

4.2.3 Stress distribution on the secondary yarn

In order to explore the stress distribution in the secondary yarns, a secondary yarns is selected for investigation, which is shown in Figure 4-9. As can be seen in Figure 4-10, although inter-yarn friction enables the secondary yarn to have more stress deposited on the area near the primary yarn, the areas affected for the three cases are almost identical as time elapses. It is believed that inter-yarn friction increases the binding force between orthogonal yarns and therefore enhances their interplay. This being so, when a yarn is displaced, its orthogonal yarns are more likely to move due to the existence of binding force.

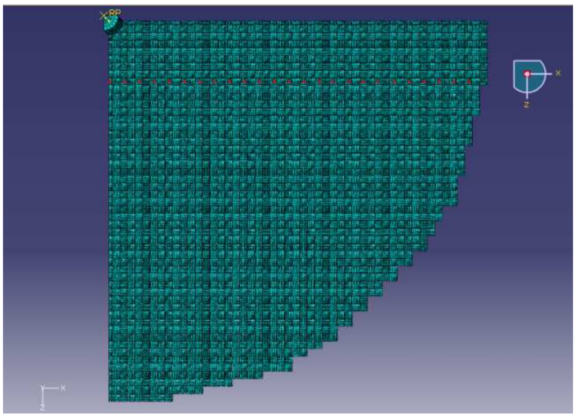

Figure 4-9 Element selection on one secondary yarn

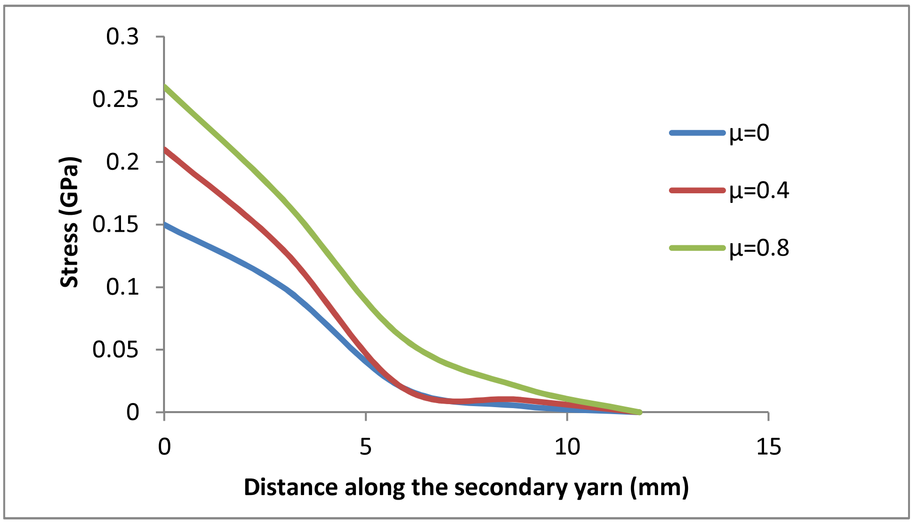

(a) 2 μs

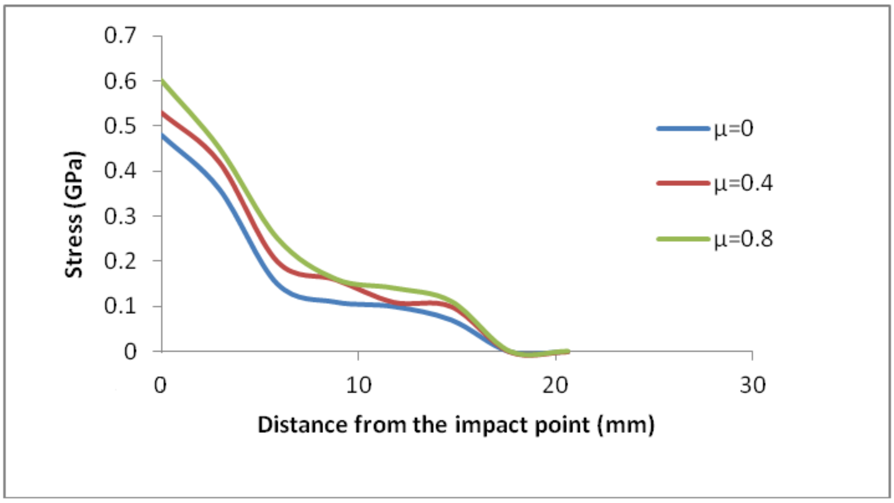

(b) 4 μs

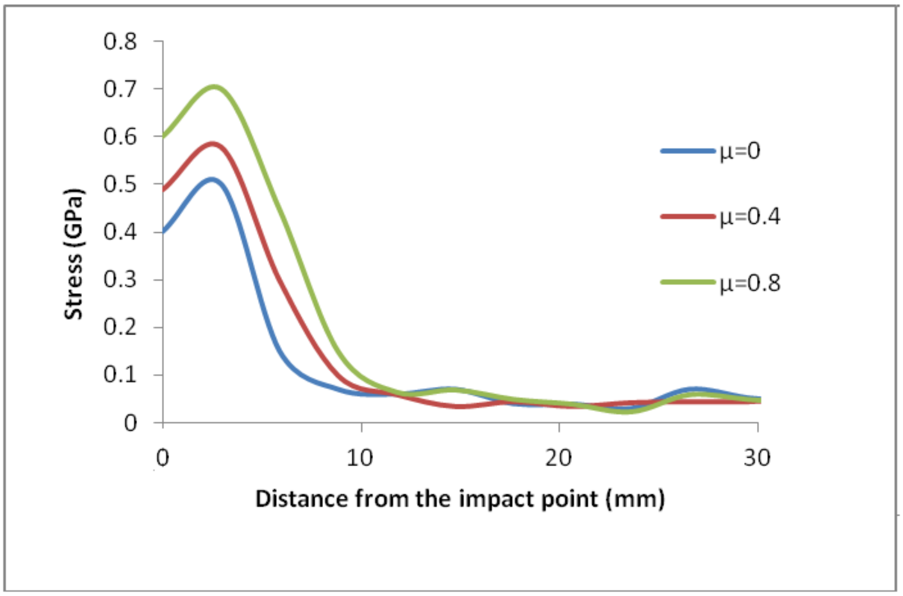

(c) 6 μs

Figure 4-10 Stress distribution on the secondary yarn for fabrics with different inter-yarn coefficients of friction

4.3 The Influence of Inter-Yarn Friction on Strain Energy Dissipation

Figure 4-11 shows the strain energy absorption on all the primary yarns for the cases of μ=0, μ=0.4 and μ=0.8. As can be seen, for the case of μ=0, the strain energy accumulated on the primary yarns more quickly than the other two cases, indicating the fact that more load is engaged by the primary yarns in this situation. The longer engaging time enables the case of μ=0.4 to have more strain energy absorbed at break than for the cases of μ=0 and μ=0.8. For the case of μ=0.8, the over-constraint of yarn movement not only impedes the propagation of the stress wave along the primary yarns, but results in the concentration of stress in the vicinity of the impact point as well, causing the least amount of strain energy to be stored in the primary yarns.

In Figure 4-12, the strain energy on the secondary yarns exhibits the highest value for the case of μ=0.4. This reinforces the analysis that the coupling effect due to yarn-yarn friction enables more stress to be distributed in the secondary yarns. For the case of μ=0, as there is little coupling between the primary and secondary yarns, the interplay between them is reduced, leading less strain energy to be distributed in the secondary yarns. Similar findings were established by Duan *et al* [18]. But they considered that it is the projectile-fabric friction that plays a vital important role in distributing stress on more yarns rather than yarn-yarn friction.

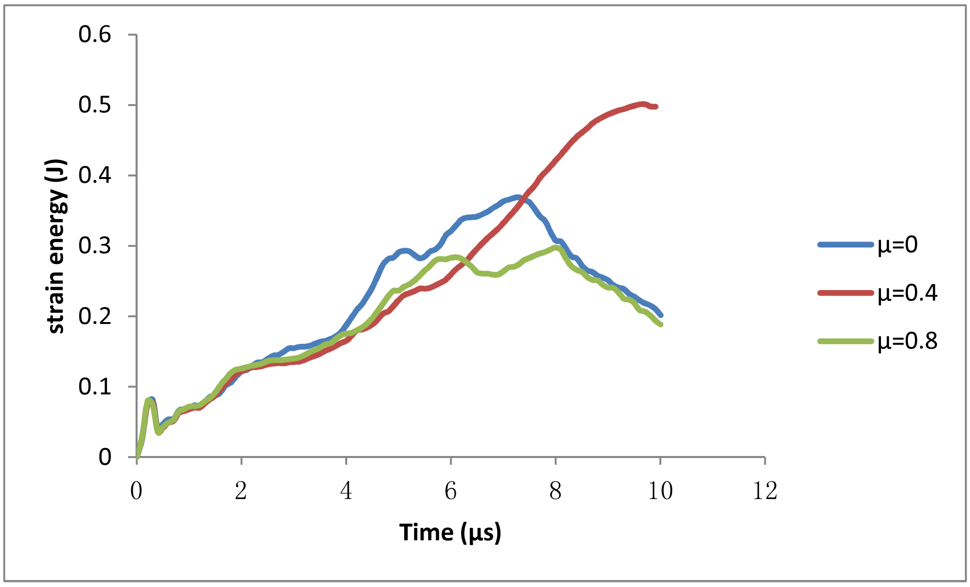

Figure 4-11 Time history of strain energy on the primary yarns

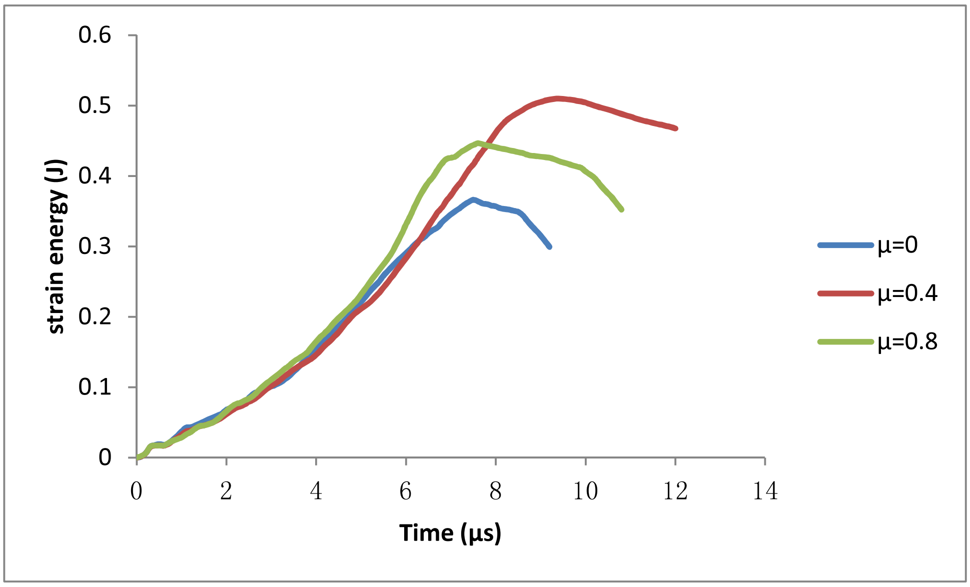

Figure 4-12 Time history of strain energy on the secondary yarns

4.4 The Influence of Inter-Yarn Friction on the Energy Dissipated by Friction

Energy dissipated by friction is one of the major energy absorption mechanisms and is directly determined by the magnitude of inter-yarn friction. As can be seen in Figure 4-13, the frictional energy for the case of μ=0 is far lower than for the other two cases. For example, at around 8 μs, the energy dissipated by the effect of friction reaches 0.044 J for the case of μ=0, while the value for the case of μ=0.4 is 0.53, which is more than ten times higher. It is apparent that only the interaction between a projectile and the fabric model serves to dissipate energy, the amount of which could be neglected. What is noteworthy is that, contrary to expectation, energy dissipation due to friction is higher for the case of μ=0.4 than μ=0.8. This could be attributed to the over-constraint of high inter-yarn friction, which hinders yarn movement and reduces the interplay between weft and warp yarns.

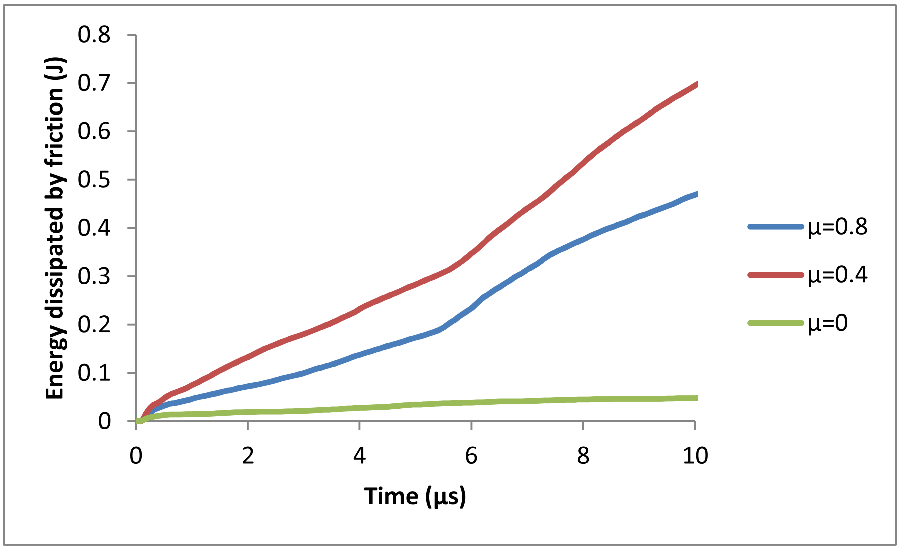

Figure 4-13 Time history of energy dissipated by friction

4.5 Summary

One of the objectives in this research is to investigate the influence of inter-yarn friction on fabric ballistic performance. In this chapter, the FE model has proved an effective way to investigate the ballistic performance of woven fabric at different magnitudes of inter-yarn friction. It has been found that woven fabric exhibits the highest energy absorption when the coefficient of friction reaches 0.4. By virtue of the analysis of stress distribution and energy transmission, it has been established that low-friction fabrics tend to have less energy dissipated through frictional effects and have fewer secondary yarns influenced. Stress is mainly concentrated on the primary yarns, leading to early failure of the fabrics. Fabrics with higher inter-yarn friction tend to have stress concentrated in the vicinity of the impact point, which also leads the fabric to fail at an early stage. The longer engaging time of fabrics with moderate inter-yarn friction enables it to have more strain energy absorbed. In addition, more energy is dissipated by the frictional effect on fabrics with moderate inter-yarn friction.

As the coefficient of inter-yarn friction for UHMWPE is determined to be around 0.14 from yarn frictional testing, there is a potential for ballistic performance improvement for

UHMWPE plain woven fabrics. This finding is of considerable interest and importance for bulletproof vest design. If by some innovative weaving techniques one can increase inter-yarn friction, an improvement in soft body armour system is to be expected.

Chapter 5 Fabric Design and Manufacture

As an extension of previous work, the present chapter gives a comprehensive description of the design and manufacture of woven fabrics with increased inter-yarn friction. Wrapping angle theory is introduced as guidance for weaving gripping fabrics. It is believed that increasing the yarns's wrapping angle has the effect of increasing the yarn pull-out force. One of the approaches is to weave tight fabrics. This method, however, has problems and FE models were employed to study the issues related to the ballistic performance of tightly woven fabrics. In chapter 3, an alternative is to modify the structure of plain woven fabric to increase the wrapping angle. FE simulation is employed to study the performance of structured modified fabrics. Three types of weave, leno, weft cramming and double weft insertion and cramming were selected to incorporate into plain woven fabric. A procedure for making UHMWPE plain woven fabric and structure modified fabrics is also presented in this chapter.

5.1 Design for Fabrics with Increased Inter-Yarn Friction

A valuable contribution to the research as discussed before is the approach of increasing the inter-yarn friction in a woven fabric. To date, development of the aforementioned body armour system is primarily based on chemical treatment, such as with shear thickening fluids [77-79]. These techniques are not only costly, but also time and labour consuming. In addition, mass-production of such types of fabric could not be guaranteed. In this section, wrapping angle theory will be introduced to increase inter-yarn friction in woven fabric. Different approaches will be suggested and the results based on finite element simulation will be presented. Manufacture and testing of those fabrics will be detailed in the following chapters.

5.1.1 Wrapping angle theory

When a yarn is pulled over a cylindrical surface (Figure 5-1), the pulling tension T is greater than the tension T_0. The increment is determined by the coefficient of friction between the yarn and cylindrical surface and the angle of contact. Their relation could be described by the capstan equation:

$$T = T_0 e^{\mu\theta} \tag{5.1}$$

where T is the pulling tension, T_0 is the tension on the free end, e is 2.718, μ is the coefficient of friction between a yarn and a cylindrical surface, and θ is the angle of contact.

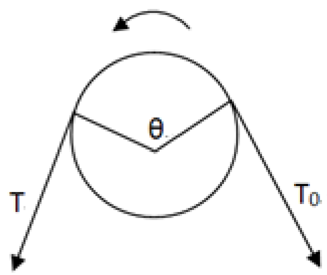

Figure 5-1 Schematic of capstan equation

As the plain woven structure is formed by yarn interlacing, it is reasonable to simplify it to yarns pulling over a series of cylindrical surfaces, which is shown in Figure 5-2. This being so, apart from modifying the inter-yarn coefficient of friction, which most of the chemical treatment based technique aim at, it is also possible to increase the pulling tension T by enlarging the interface between the warp and weft yarns, which is also termed as wrapping angle in this work. It must be noted that modifying the yarn wrapping angle does not essentially change the frictional force between the yarns, it is the pulling out force that is increased. As yarns are more tightly gripped under this condition, the word "gripping" is employed to describe the amount of force required to pull out a yarn from the fabric.

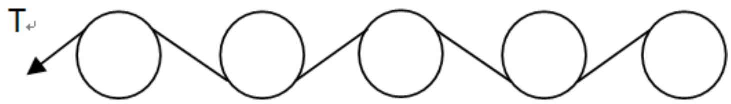

Figure 5-2 Simplification of woven fabric structure

The simplest way of increasing the yarn wrapping angle is to weave tight fabrics. Sebastian [138] established a numerical model to identify the factors influencing yarn pull-out and found that the frictional force between the pull-out yarn and each crossover yarn is in propotional to the number of crossovers involved. The higher the weave density, the higher the yarn pull-out force will be. Nevertheless, the ballistic performance of tightly-woven fabrics has been a controversial topic. Shockey [57] pointed out that the increase in yarn density is almost in proportion to the increase in energy absorption. Abiru and Lizuka [101] suggested that when the fibres are severely undulated, the original high tenacity turns to a lower one, which reduces fabric energy absorption during the impact event. In Chapter 3, ABAQUS was employed to investigate the influence of weave density on fabric energy absorption. The results reveal that fabrics with high weave density tend to severely undulate the path of the warp and weft yarns, influencing the propagation of transverse wave and energy dissipation.

5.1.2 Structure modified fabrics

Apart from increasing fabric weave density, it is also possible to modify the structure of plain woven fabric in a designated area to achieve an increase in yarn gripping. The advantage of this approach is that the yarn profile of the majority of the fabric is unaffected, retaining the ballistic performance of the original fabric. In this research, woven fabric is modified by applying three insertions, namely leno structure, weft cramming structure and double weft insertion and cramming structure.

5.1.2.1 Leno insertion

Leno weaves, which are also called cross weaves, are open fabrics with warp and weft threads crossing with two adjacent warp yarns crossing over each other and wrapping around a weft yarn [139]. Fabrics made with leno weaves are mainly intended for fashion requirements. Leno structures are used by designers to decorate fabrics in combination with other patterns. Apart from that, leno weaves are also widely used in products such as mosquito netting and bags for laundry. Figure 5-3 shows a schematic of the geometry of leno structure. As can be seen, the weft yarns are gripped by the loops formed by the two leno yarns, which gives higher resistance to slippage of yarns.

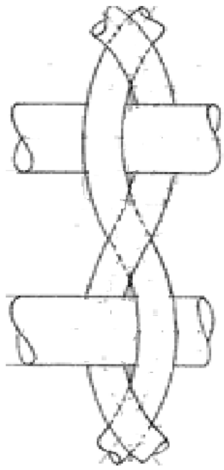

Figure 5-3 Geometry of leno structure [139]

Ahmed [139] did a comprehensive investigation of the geometry and mechanical properties of leno weave. He found that the force required to pull a weft yarn out from a leno weave is much higher than that from a corresponding plain weave, indicating that weft yarns are more tightly gripped in leno weave than in plain weave. This is probably because leno weave gives a larger contact area, creating a higher frictional force between weft and warp yarns. In spite of the increased yarn gripping in leno structure, it is not suitable to be directly used for ballistic applications. Due to its open structure, a projectile may easily slip through the fabric in-between the adjacent yarns. This hinders the ballistic fibres to exhibit their superior properties and severely reduces fabric energy absorption.

Current weaving techniques enable leno weaves to be combined with plain fabric. Due to the insertion of leno structure, weft yarn gripping is increased. While the majority of the fabric is formed by plain weave, its ballistic performance would not be reduced. The leno weave is termed as half-cross or complete-cross according to whether the warp ends embrace a half or a complete cross (Figure 5-4 a). Half-cross leno is classified into upper-shed leno (Figure 5-4 b) and lower shed leno (Figure 5-4 c). In the upper shed leno, the leno ends bind over the weft picks and below the standard ends. In the lower shed leno, the leno ends pass below weft picks and over the standard ends. In this research, upper leno is used for insertion. The structured modified fabric is shown in Figure 5-5.

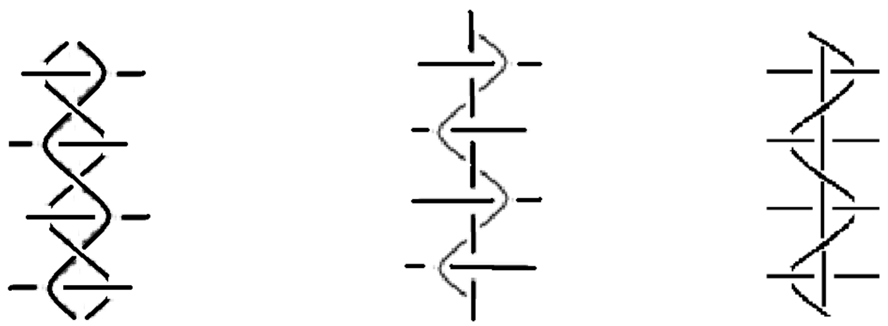

(a) Complete cross leno **(b) Upper shed leno** **(c) Lower shed leno**

Figure 5-4 Schematic diagrams for different leno structures

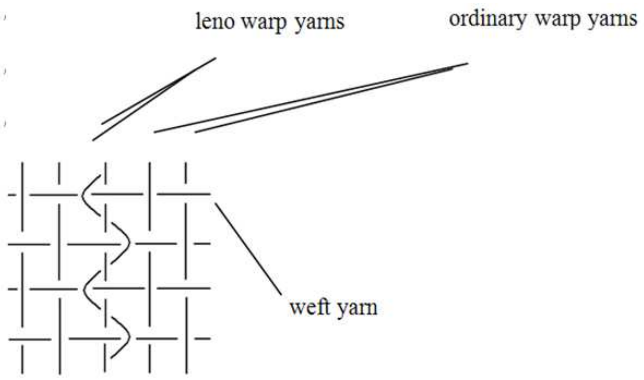

Figure 5-5 Schematic diagram of plain woven fabric with leno insertion

5.1.2.2 Weft cramming

As high-density-weaves tend to yield inferior ballistic performance, it is possible to create a zone in which weft yarns are crammed densely. This type of weave is shown in Figure 5-6. Weft cramming is performed by periodically stopping the take-up process, but keeping all other actions as usual during weaving. It is supposed that the cramming zone increases warp yarn gripping without affecting the performance of the fabric when the impact event occurs on the plain weave.

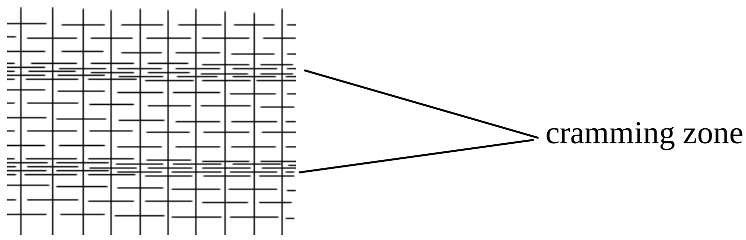

Figure 5-6 Plain weave with weft cramming insertion

5.1.2.3 Double weft insertion and cramming

Another approach to increase the wrapping angle is to insert two weft yarns and to do the cramming at the same time. As the two weft yarns are combined into one, the warp yarn wrapping angle is believed to increase, which is shown in Figure 5-7.

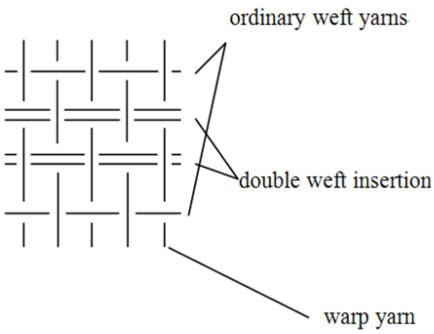

Figure 5-7 Schematic diagram of plain woven fabric with double weft insertion

5.1.2.4 Simulation of structure modified fabrics upon ballistic impact

In order to predict the ballistic performance of structure modified fabrics, FE models are employed to simulate the impact events. Plain woven fabric with leno insertion is selected to be modeled in ABAQUS. As the essence of the application of leno insertion is to increase the frictional force over a small area, the simulation is achieved by increasing the coefficient of friction between the designated warp yarns and all the weft yarns. In this regard, "surface to surface contact" is used to define the interaction, which is shown in Figure 5-8.

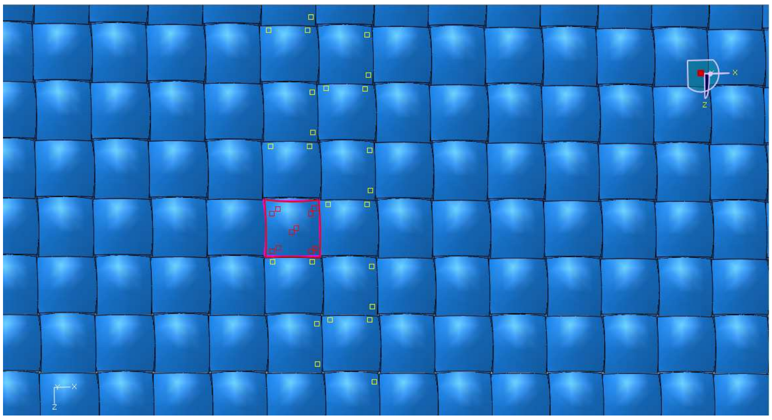

Figure 5-8 Surface to surface contact between two warp yarns and all the weft yarns

Effect of leno interval and coefficient of friction

For the frictional models, leno insertion of different intervals and the coefficient of friction was simulated. The abbreviations are listed in Table 5-1 and the FE results are presented in Figure 5-9. As it can be seen, energy absorption curve for all the models give an increasing trend before μ=0.5. At around μ=0.55 andμ=0.8, the curves for PWL01 and PWL02 reach at their peak respectively. The energy absorptions for other cases increasesas the coefficient of friction increases. This is probably because, the shorter the interval distance, the more likely the over-constraint of weft yarns may occur, which leads to lower energy absorption. As the interval increases, the influence of yarn gripping decreases. This being so, in order to reach an energy absorption peak, fabrics like PWL05 or PWL06 required higher inter-yarn friction between weft yarns and leno warp yarns. In order to comprehensively study the energy absorption capability of the structure of plain woven fabric with leno insertions, PWL03 at a frictional coefficient of 1 was selected for analysis.

Table 5-1 Abbreviations for plain woven fabric with leno insertion

PW	Plain woven fabric
PWL01	Plain woven fabric with leno insertion at the interval of 1cm
PWL02	Plain woven fabric with leno insertion at the interval of 2cm
PWL03	Plain woven fabric with leno insertion at the interval of 3cm
PWL04	Plain woven fabric with leno insertion at the interval of 4cm
PWL05	Plain woven fabric with leno insertion at the interval of 5cm
PWL06	Plain woven fabric with leno insertion at the interval of 6cm

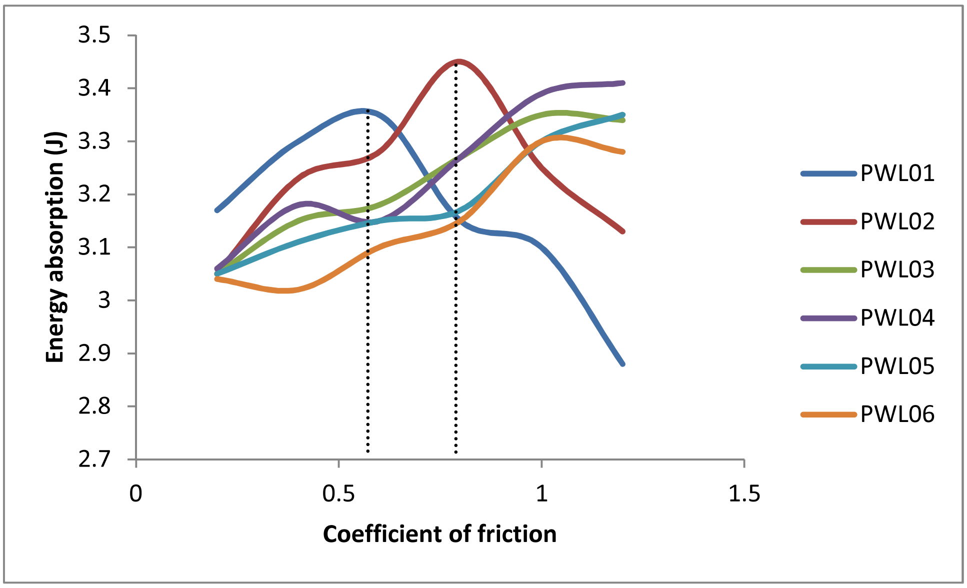

Figure 5-9 Comparison of energy absorption for different woven fabric with leno insertions

Results and discussions

Figure 5-10 reveals the energy absorption of the FE model at different impact velocities. The energy absorption gives a decreasing trend with the increase in impact velocity both of the PW and the PWL03 models. The PWL03 exhibits higher energy absorption than the PW, and the differences decrease with the increase of the impact velocity.

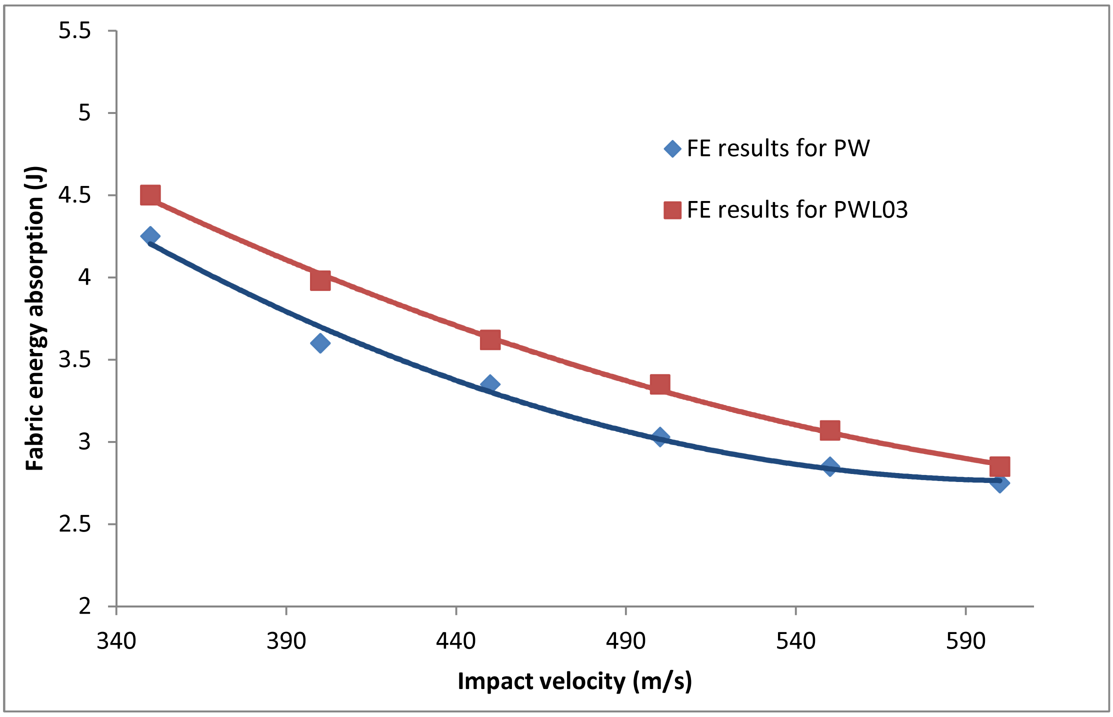

Figure 5-10 Fabric energy absorption as a function of impact velocity for different FE models

It is of interest to investigate how the leno insertions influence fabric energy dissipation during ballistic impact. Figure 5-11 compares the contour plots of stress distribution of PW and PWL03 fabric models upon ballistic impact. It could be seen that the change of coefficient of friction on the PWL03 model enables more stress to be distributed to the secondary yarns in the vicinity of the leno weave. On the PW model, the strain and kinetic energy stored on the weft primary yarns is slightly higher than that on the PWL03 model, which is shown in 5-12 (a). This is probably due to the constraint effect of leno warp yarns on the primary weft yarns. The energy in the primary weft yarns, however, gives similar values for the two models, which is shown in Figure 5-12 (b).

In terms of the secondary yarns, Figure 5-13 reveals that the PWL03 model gives higher energy absorption than the plain woven fabric model. This is in agreement with the results obtained from the model presented in Chapter 4, in which similar findings have been established. This is believed to be how inter-yarn friction essentially affects fabric performance. In addition, the increase in coefficient of friction between leno yarns and weft yarns also enable more energy to be dissipated through the friction effect, making the fabric more energy absorbing. For simulation of impact on multi-layer fabrics, it can be seen in Figure 5.15 that PWL03 shows better ballistic performance than PW as the number of layers increased, indicating the benefit on yarn gripping of leno structure.

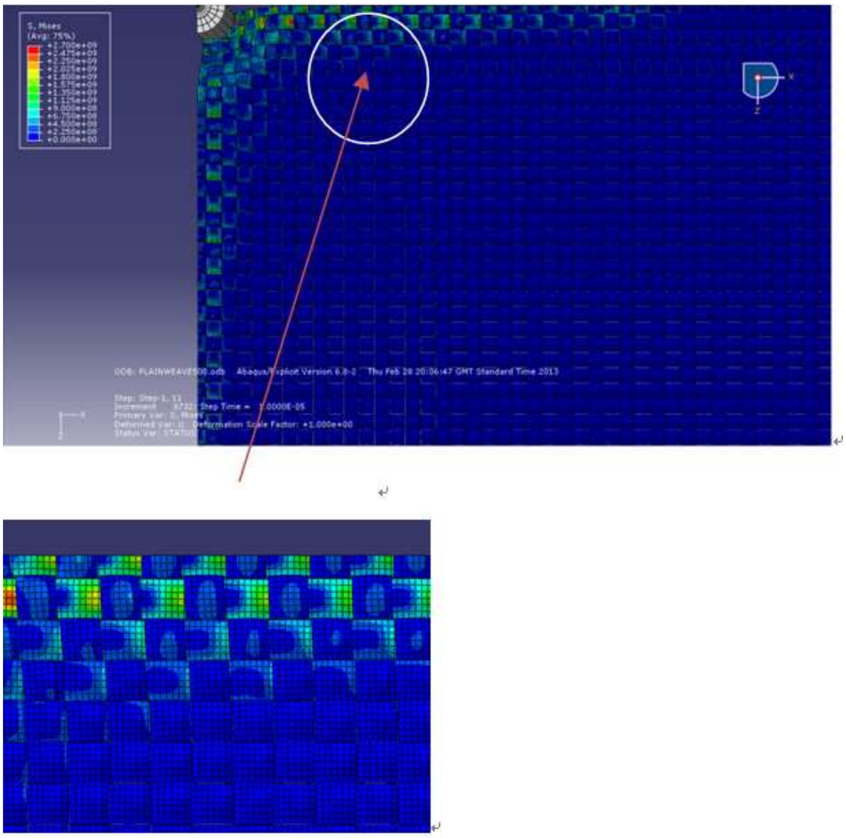

(a) PW model

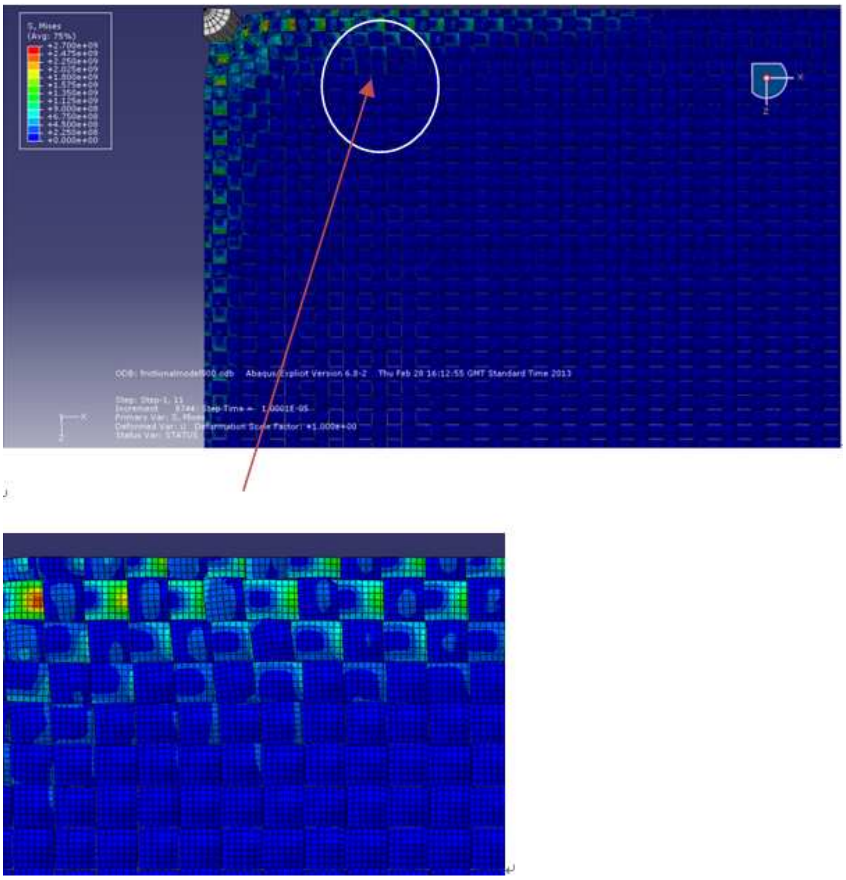

(b) PWL03 model

Figure 5-11 Contour plots of stress distribution of different fabric models upon ballistic impact

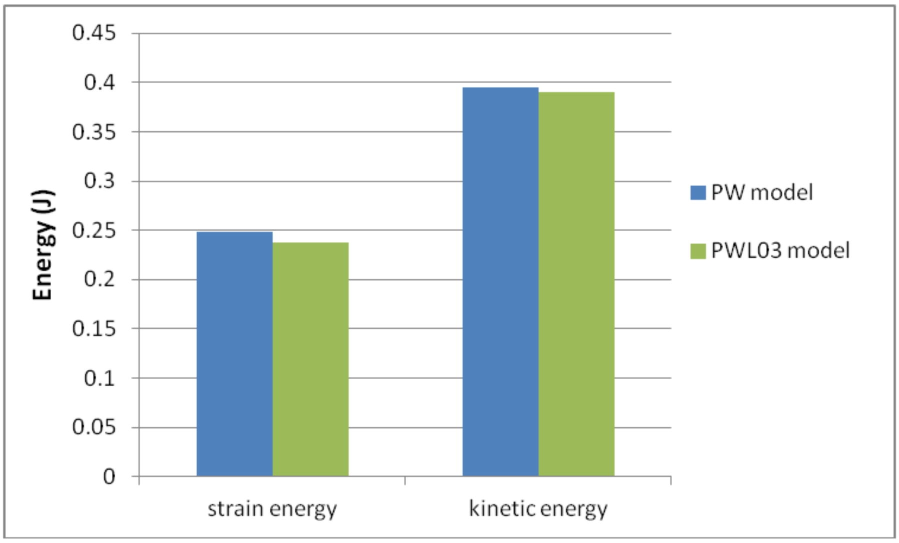

(a) Weft primary yarns

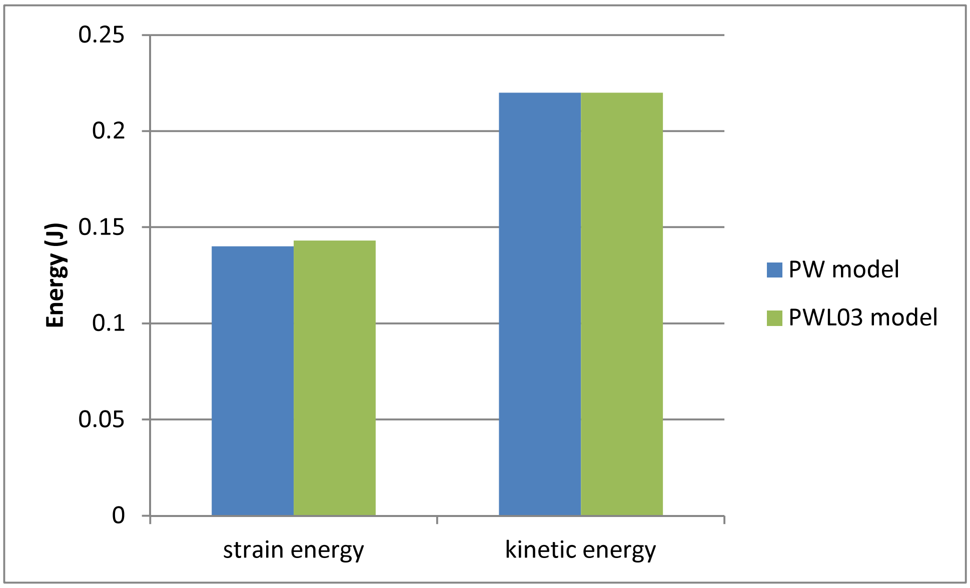

(b) Warp primary yarns

Figure 5-12 Comparison of strain energy and kinetic energy on primary yarns

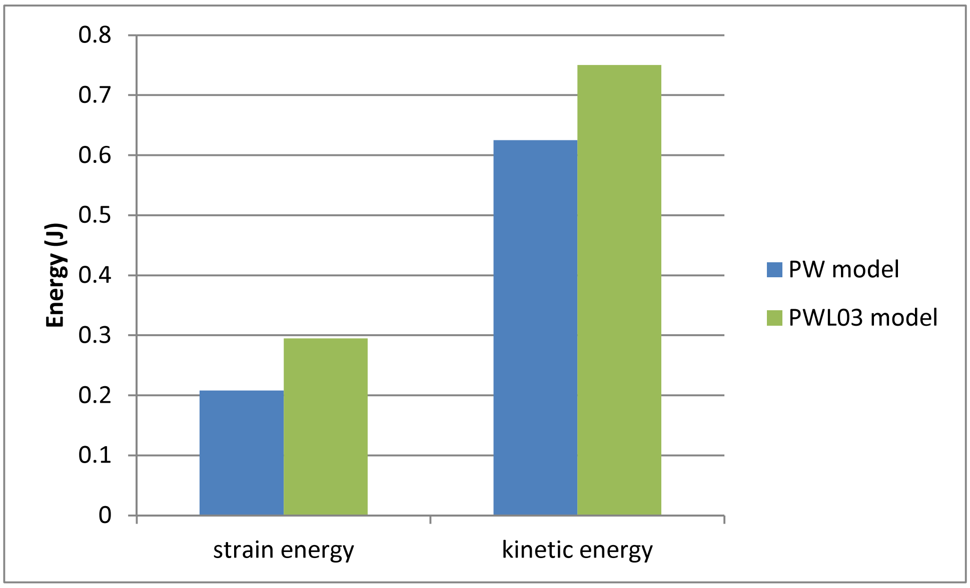

Figure 5-13 Comparison of strain energy and kinetic energy on secondary yarns

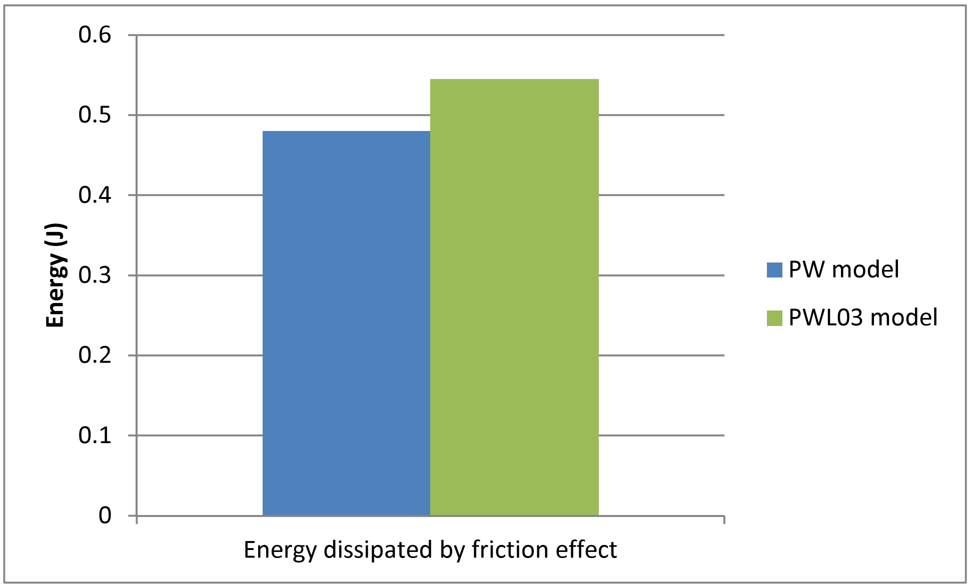

Figure 5-14 Comparison of energy dissipated by frictional effect

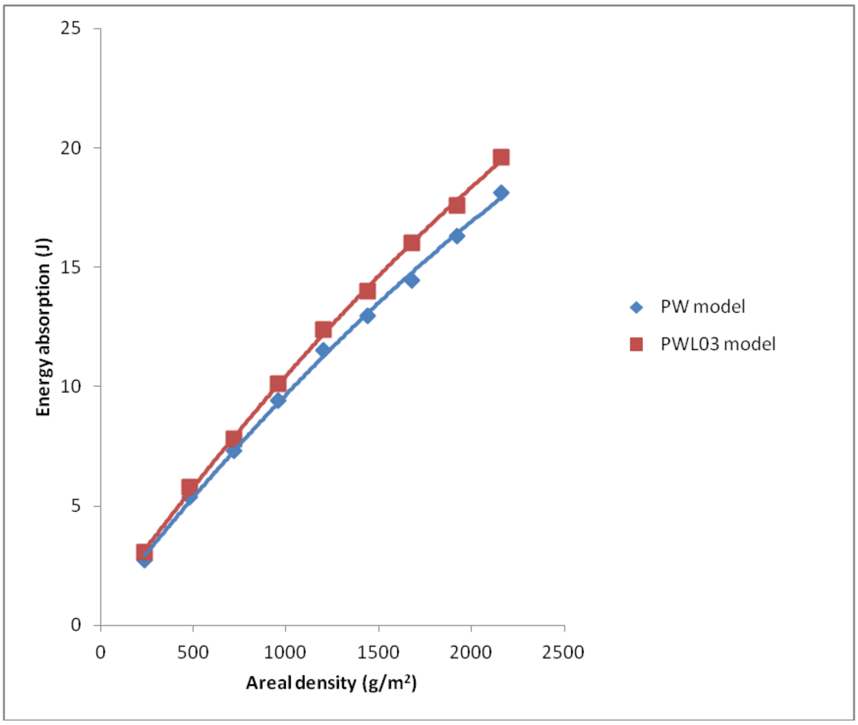

Figure 5-15 Energy absorption of fabric panels as a function of areal density

The performance of leno lines

Cork and Foster [140] found that narrow fabric panels in a two-edges gripped configuration give better ballistic performance than wide fabric panels. However, the lines between the adjacent fabrics prove to be a weakness for this type of panel in ballistic applications. This could also be a problem for structure modified fabrics, as the insertion lines may lead to poor ballistic performance when struck by a projectile. As the leno structure in the current model is presented by increasing the coefficient of inter-yarn friction, it is insufficient to use this model to investigate the aforementioned problem. This being so, a geometric model was created, aiming to simulate the geometric structure of leno weave. The model is shown in Figure 5-16.

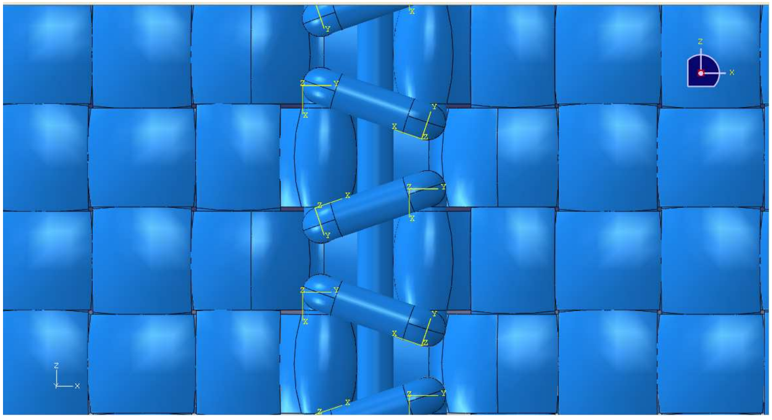

(a) Front face

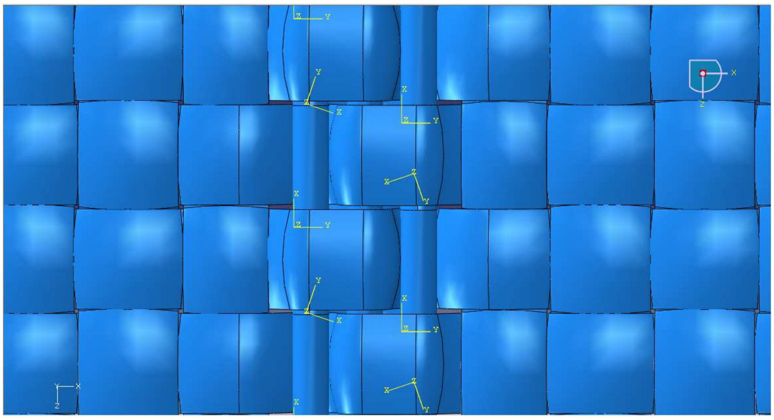

(b) Back face

Figure 5-16 Geometric model for fabric with leno insertion

As the leno structure is not symmetrical about the Z axis, a quarter-model is not sufficient to show its geometry; a half-model was utilised. In Figure 5-17, the results reveal that the frictional model gives similar values for energy absorption at different impact points whereas the geometric model shows a difference, which is around 2J. This is because the leno structure of the frictional model is essentially a plain structure. For the geometric model, due to the crimp of the leno ends and the weft yarns, the impact energy could not be dissipated effectively on both primary and secondary yarns Figure 5-18 compares the Contour plots of stress distribution of the two types of model upon ballistic impact. It can be seen that the area influenced by the stress for the frictional model is detectably larger than that for the geometric model, indicating the weakness of leno structure when subjected to ballistic impact.

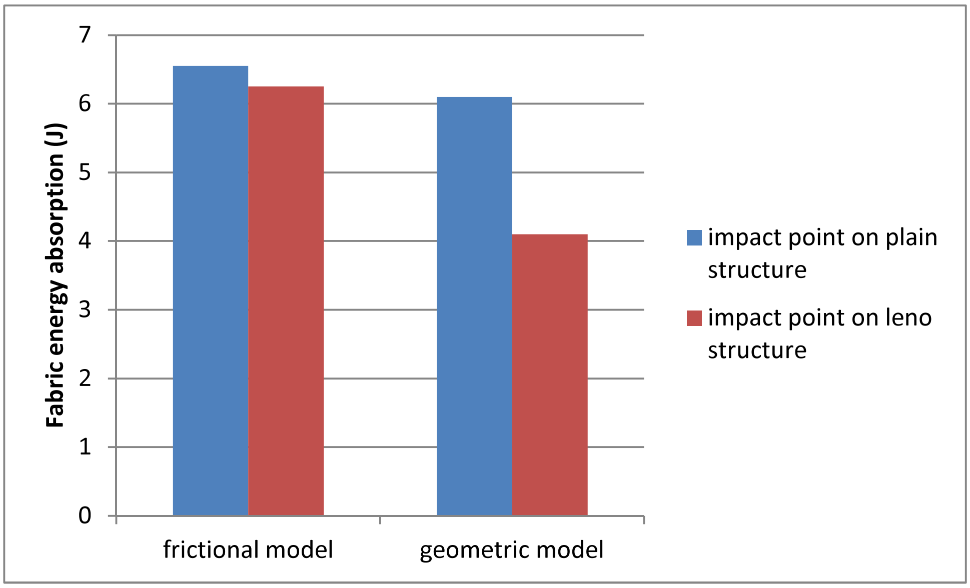

Figure 5-17 Comparison of the energy absorption between frictional and geometric models at different impact point

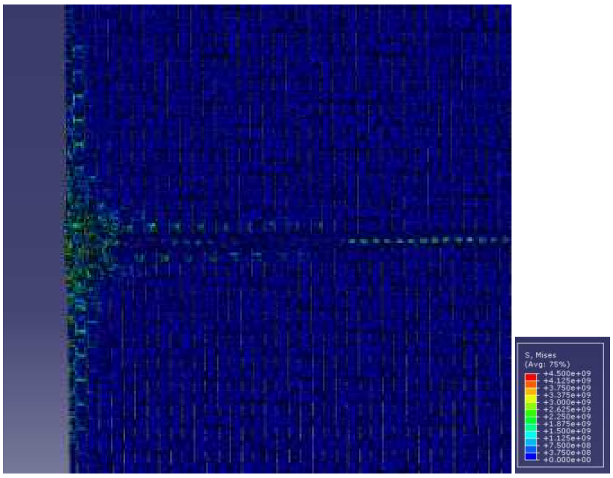

(a) PWL03 geometric model

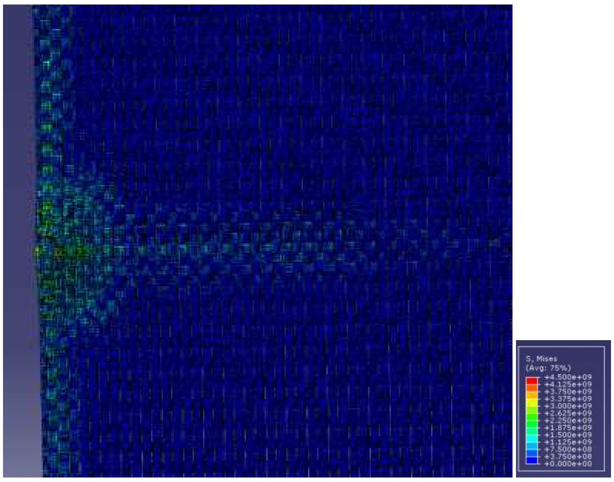

(b) PWL03 frictional model at

Figure 5-18 Contour plots of stress distribution of different models at 8 μs

In conclusion, FE simulation reveals that the insertion of leno structure leads to an increase of energy absorption in woven fabric for both single- and multi-plied cases. When impacted on leno lines, the response of the geometric model and the frictional model shows a greater difference. The weakness of the leno lines is a problem worthy of further investigation. Due to the improvement predicted in simulation, this method will be used to manufacture fabrics with increased yarn wrapping angle.

5.2 Fabric Specifications

In order to develop ballistic woven fabrics with increased yarn gripping, three types of insertions are incorporated with plain woven structure in the hope of modifying the yarn wrapping angle. This section presents the specifications of UHMWPE plain woven and structure modified fabrics

5.2.1 Plain woven fabric

The UHMWPE fibre in use was Dyneema SK75 and was provided by DSM. The yarn has a linear density of 174 Tex and a twist of around 10 turns per metre. Although 0 degree twisted yarn is desired in ballistic fabrics, fabrication of filament yarns would result in fibrillation during weaving. A small amount of yarn twisting helps to hold the filament together and prevents yarns from being jammed on power looms. In order to study the system effect of woven fabrics and compare the ballistic performance of UHMWPE woven fabrics with that of the conventional Kevlar woven fabrics, the fabrics were designed in such a way that they have the same tightness.

As warp and weft tightness E is given by:

$$E = Pd = PC\sqrt{T} \qquad (5.2)$$

where P is thread density in threads/cm, d is yarn diameter in cm, T is the yarn linear density in Tex, and C is the conversion factor between yarn diameter and yarn linear density. If the conversion factors for both yarns are considered to be identical, the yarn density of Dyneema fabric, $P_{Dyneema}$, could be worked out by:

$$P_{Dyneema} = \frac{P_{Kevlar}\sqrt{T_{Kevlar}}}{\sqrt{T_{Dyneema}}} \qquad (5.3)$$

As the linear density of Kevlar yarn is 158 Tex and the pick density of the Kevlar fabric was set to be 7.5 threads/cm, the pick density of the Dyneema fabric was required to be 7.14 threads /cm. Due to the limitation of the power loom, the yarn density of UHMWPE fabric is set to be 6.75 picks/cm. A combination of weave diagram, harnesses plan, lifting plain and reed plan is shown in Figure 5-19.

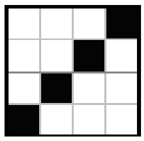

Harnesses plan

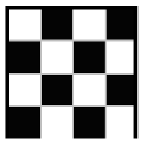

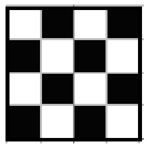

Weave structure **Lifting plan**

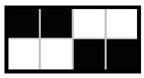

Reed plan

Figure 5-19 Weave diagram, harnesses plan, lifting plan and reed plan for UHMWPE plain woven fabric

5.2.2 Specification of structure modified fabrics

As has been mentioned in the previous chapter, three types of structure will be applied on plain woven fabric. In order to manufacture fabrics with a different level of yarn gripping, the intervals are set to be different. The details are presented in Table 5-2.

Table 5-2 Fabric specifications

Fabric structure	**Distance of the intervals (cm)**	**Abbreviation**
Plain weave	N/A	PW
Plain weave with leno insertions	2	PWL02
Plain weave with leno insertions	3	PWL03
Plain weave with leno insertions and double weft insertions	3	PWL03DW
Plain weave with leno insertions and weft cramming	2	PWL02WC

5.3 Fabric Manufacture

Fabric manufacture consists of two steps: warp preparation and weaving. Technically, warping is transferring yarn from a single-end package forming a parallel sheet of warp yarns wound onto a beam ready for weaving. Weaving is to interlace warp yarns and weft yarn orthogonally to each other.

5.3.1 Warping

The machine in use was MS/1800-8 Hergeth Hollingsworth Sample Warper. The Sample Warper mainly consists of three parts: the creel, the warping machine and the beaming machine, each part serves a different function. The role of the creel is to guide the yarn end to the warping machine, the warping machine is just what its name implies: it forms the yarn into a warp shape and a beaming machine enables the warps to be wound onto the weaver's beam. The machine specifications are listed below.

Machine height: Basic warping length: 8 metres, height: 4.6 metres
Total weight 4 tons

Warping velocity: 360 metres per minute

Warp density: 6.9 ends per cm

Distance from creel towarping machine: min 1.5 metres

Distance from beaming machine towarping machine: 1 metre

A yarn cone is fixed in the creel and the yarn end is passed through a thread guide. The catch bar and thread guide serve to support the yarn ends and apply a certain amount of tension to it, so that the yarn end can be straightened when being still. On the warping machine, a lease will be formed automatically to prevent yarn fibrillation. Before taking the warp off the warping machine, the warp is fixed by two clamps to keep it straight. Four binds are drawn in to replace the four lease rods so that the warp does not get disoriented. Before binding the warp onto the weaver's beam, the yarn ends must be drawn through an expanding zigzag comb which is used to control the width of the beam and keep the warp parallel.

5.3.2 Weaving

The power loom in use is a Northrop L16 shaft negative dobby weaving machine. Basically, there are five main mechanisms that are essential for continuous weaving: warp let-off, shedding, filling insertion, beat-up and fabric take-up. Each mechanism is controlled by different parts of the loom.

Figure 5-20 Northrop L16 machine

5.3.2.1 Weaving of plain woven fabric

After the drawing-in process, the warp yarns are split into several bundles and tied onto the fabric beam. A certain amount of tension is applied to the warp so that the warp ends are kept straight. The weft yarns are stored in a wood-made shuttle and are ready to be used. The weaving of plain woven fabric is performed on the loom.

5.3.2.2 Weaving of plain woven fabric with leno insertions

Leno yarns are drawn from special bobbins and their movement is controlled by leno healds. The leno heald is made up of one doup-needle and two legs, which is shown in Figure 5-21. There is a magnet at the bottom of the leg, which serves to catch up the steel needle. The two legs are controlled by two individual frames. The reed-plan for leno insertion fabric is different from that of plain weave, that is, a specific dent should be saved for the leno warp pair. For instance, if lenos are inserted every two cm (every 14 yarns), one in every eight dents needs to be reserved.

Figure 5-21 Doup-heald

As can be seen in Figure 5-22 (a), the two leno yarns, standard end and leno end, run together between the two lifting legs L_1 and L_2. The standard end passes through the eye of the doup-needle (D) and under the ease E, which has the function of equalising the warp tension. The leno end is drawn into an ordinary heald S, but above the doup-needle. In order to reduce the warp tension, two leno yarns are drawn through the same dent.

In Figure 5-22 (b), when the doup-needle is raised by leg L_1, its right-hand shank is disconnected with the magnet on the bottom of L_2 which is now in the down position. A cross shed is formed and the leno end is on the right side of the standard end. After the insertion of weft yarn, the doup-needle is carried upwards by L_2 and its left shank is disconnected with L_1. The position change pushes the standard end on the right hand side of the leno end to form a cross shed which is ready for insertion. Thus the repetitive crossing of one warp end over another is maintained continuously. In this method of weaving, leno structure is formed.

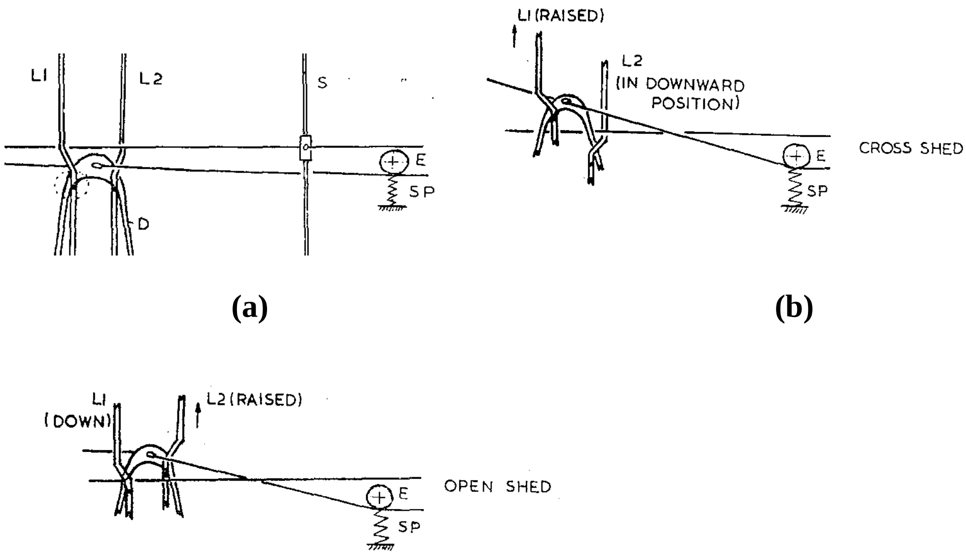

(a) (b)

(c)

Figure 5-22 Leno heald movements [139]

5.3.3 Fabric samples

The resultant fabrics are shown in Figure 5-23. One issue of concern is that the weft cramming zone depicted in Figure 5-6 is not noticeable in the real fabric. Due to the low yarn-yarn friction of Dyneema fabric, yarn sllipage may occur during the weaving process. As a result, crammed yarns tend to be squeezed forward in the fabric forming zone by the ordinary yarns. The cramming zone could not actually be formed in real fabric, only leading to the increase of weave density in the fabric.

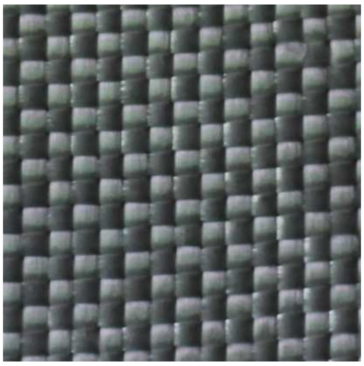

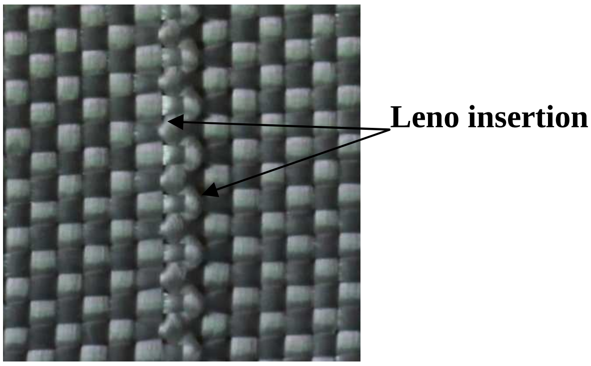

(a) Plain woven fabric **(b) Plain woven fabric with leno insertion**

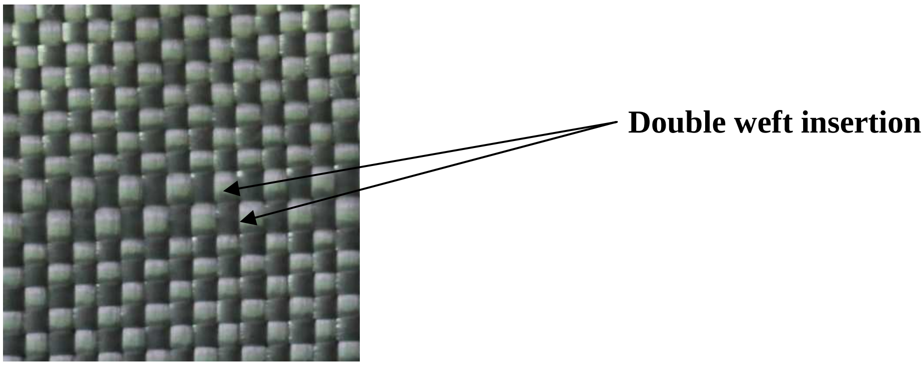

(c) Plain woven fabric with double weft insertion

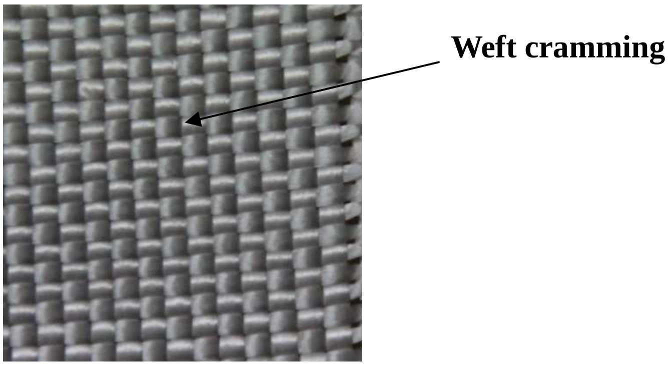

(d) Plain woven fabric with weft cramming

Figure 5-23 Plain woven fabric and structure modified fabrics

5.3.4 Optimisation in manufacturing UHMWPE woven fabrics

A problem of yarn filamentation occurs during the UHMWPE manipulation at the weaving stage. The low-twisted warp yarns tend to mingle with each other during shedding, which cause the filaments forming the yarns to be dispersed and consequently give rise to machine stoppages or fault during fabric weaving.

It is considered that this is caused by static electricity on the fibre surface. In order to address this problem, it is necessary to have a basic understanding of the mechanism of static electricity. When two materials are rubbed together, the electrons associated with the surface atoms come into very close proximity with each other. The surface electrons can be moved from one material to another. The material which gives the electrons become positive and the material which receives electrons become negative. Hence, a static electricity force is generated and results in attraction between the two materials. The effect of static electricity is particularly noticeable on high-performance fibres like UHMWPE. As a result, elimination of static electricity could be achieved by neutralising the static charges by bringing electrons back to the positive surface or removing excess electrons from the negative side.

One of the approaches is to apply some humidity to Dyneema yarns. In that case, the static charge is removed. Figure 5-24 shows that a humidifier was put behind the weaving machine facing the warp beam. During the weaving process, a certain amount of humidity is created by the humidifier and applied to the warp yarns. The alternative is to use yarns with a high level of twist. Twisting gives filaments a certain degree of cohesion so that yarns are less likely to be dispersed. Nevertheless, as has been mentioned before, twisted yarns are not desirable for ballistic fabrics, as they lead to poor ballistic performance. In addition, paper sheets were rolled with the warp sheet in the warp beam, avoiding the contact between the adjacent warp layers. This eliminates the possibility of warp jam during the take-off process. The combination of all these measures aims to minimise yarn filamentation and to optimise the weaving process.

Figure 5-24 Paper sheets used to separate warp layers and the humidifier

5.4 Summary

In this chapter, the design and manufacture of plain fabric and structure modified fabric have been discussed in detail. According to the capstan equation, increasing the yarn wrapping angle may lead to an increase in inter-yarn friction. Two approaches were suggested, namely increasing the weaving density and modifying the woven fabric structure. The practicability of the two approaches was investigated by using FE simulation and it has been determined that the latter one proved to give an improvement in the fabric energy absorption capability. The increase of yarn gripping in woven fabric has been achieved by the insertion of three structures: warp leno structure, double weft insertion and weft cramming. The necessary arrangement to eliminate the problem of fibrillation during the weaving process has also been described. The techniques applied in weaving explore the possibility of mass-producing friction-increased fabrics at a comparatively low cost when compared with chemical treatment based techniques. In addition, the successful fabrication of UHMWPE plain woven and structure modified fabrics has been presented. The problem of filamentation during the weaving process has been solved by taking appropriate measures.

Chapter 6 Experimental Study on Fabrics with Increased Inter-Yarn Friction

Development of gripping fabrics is one of the objectives of the research and has been mentioned in the previous chapter. This chapter presents the evaluation of the increase in yarn gripping for structure modified fabrics in both weft and warp directions by using the yarn pull-out test. In order to develop a good understanding of their impact resistance, a ballistic penetration test was carried out. The results were discussed and factors influencing fabric performance were also analysed.

6.1 Yarn Pull-Out Test

The yarn pull-out test aims to characterise the increase in yarn gripping for structure modified woven fabrics. The force required to pull a yarn out from the fabric is used as a measure of the ease of yarn slippage and a parameter for defining inter-yarn friction.

6.1.1. Method and sample preparation

An Instron 4411 with a 1 kN load cell was used for the experiments. Before testing, transverse yarns were removed from the top edge of the fabric, forming yarn tails. A single yarn was selected and loaded using upper jaw to perform the pull-out test, which is shown in Figure 6-1 (b). The lower edge was clamped by a rectangle plastic piece, which is shown in Figure 6-1 (c). The specimen on the machine is extended at a constant rate (250 mm/min) and the measuring mechanism moved a negligible distance with increasing load. Yarns were pulled out in both the weft and warp directions. In the weft direction, three different samples: PW, PWL02 and PWL03 were tested to investigate the influence of leno insertion. In the warp direction, PW, PWL02WC and PWL03DW are tested to study the influence of weft cramming and double weft insertion and cramming.

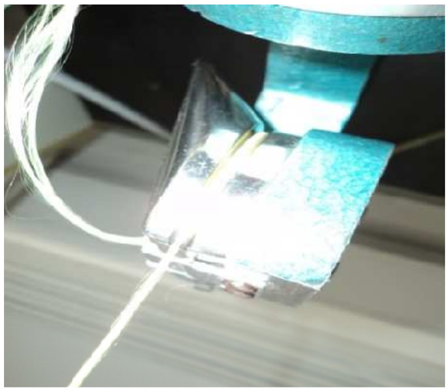

(a) Instron 4411 **(b) Upper jaw**

(c) Lower clamp

Figure 6-1 Yarn tensile testing machine

One problem which needed to be solved was that, due to the shape of the bottom clamp, all the yarns were gripped on the lower edge of a fabric sample. The pull-out force recorded by the load cell was not caused by inter-yarn friction, but by the clamping force of the lower fixture. Given this situation, two methods, method A and method B, were designed. In method A, fabric samples were placed upside down and all the yarn tails were clamped by the plastic grip. The pulled-out yarn was gripped by a jaw and was drawn from the fabric zone, which is shown in Figure 6-2. In this case, the plastic jaw only served to hold the fabric and did not give any additional force to the pulled-out yarn. In method B, the lower part of fabric sample was cut in such a shape that only the right and left corners were gripped by the clamp. This is shown in Figure 6-3 that the remaining part of the fabric zone was not affected. Both method A and method B are employed to study for their reliability. The results are revealed in the next section.

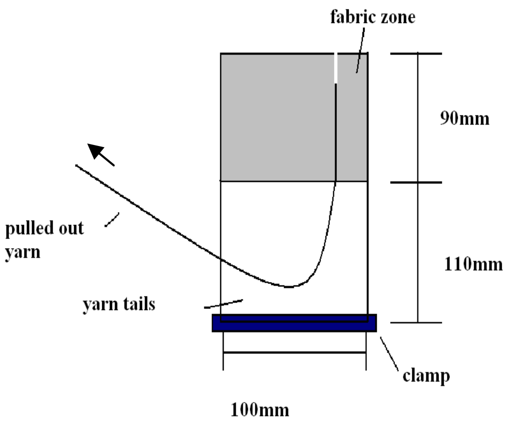

(a) Schematic diagram of method A (b) Method A on Instron

Figure 6-2 Method A of yarn pull-out test

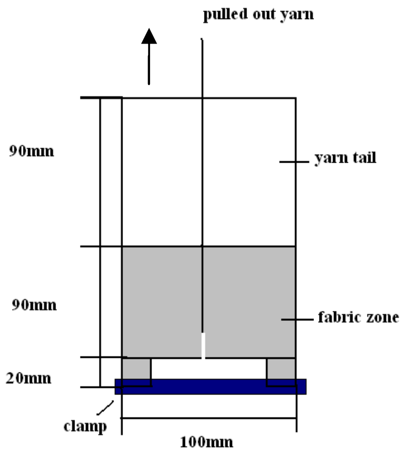

(a) Schematic diagram of method B (b) Method B on Instron

Figure 6-3 Method B of yarn pull-out test

6.1.2 Results and Discussions

Figure 6-4 shows the load-displacement curves for the two methods. Each method was repeated 8 times and the peak load forces on the curve were put into comparison. The results were revealed in the Appendix, Table 3. As has been shown in both Figures 6-4 and 6-5, the peak load force for method A is much higher than that for method B. This is probably because that the pull-out force applied is not in parallel with the fabric plane in method A, which consequently leads to fabric deviation. This is shown in Figure 6-2 (b). Fabric deviation hinders yarns from being pulled out and increases the randomness of the result (here the randomness of the result is determined by the value of 95% confidence interval, which is shown in Figure 6-5). As the pull-out force is in parallel with the fabric plane, the peak load force is only determined by the inter-yarn frictional force. The values are comparatively lower and exhibit less randomness than those from method A. For the reasons mentioned above, method B was employed to perform the yarn pull-out test.

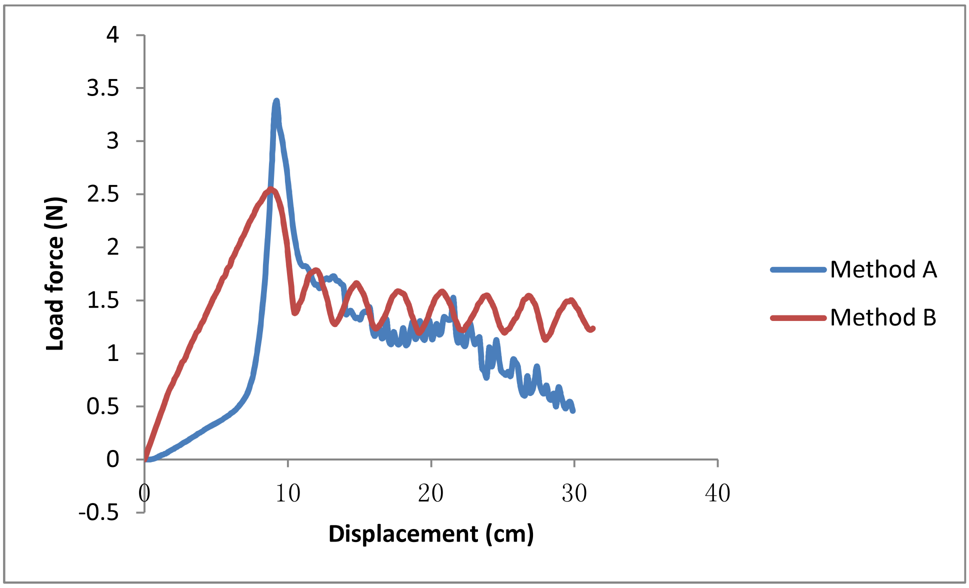

Figure 6-4 Load-displacement for method A and method B

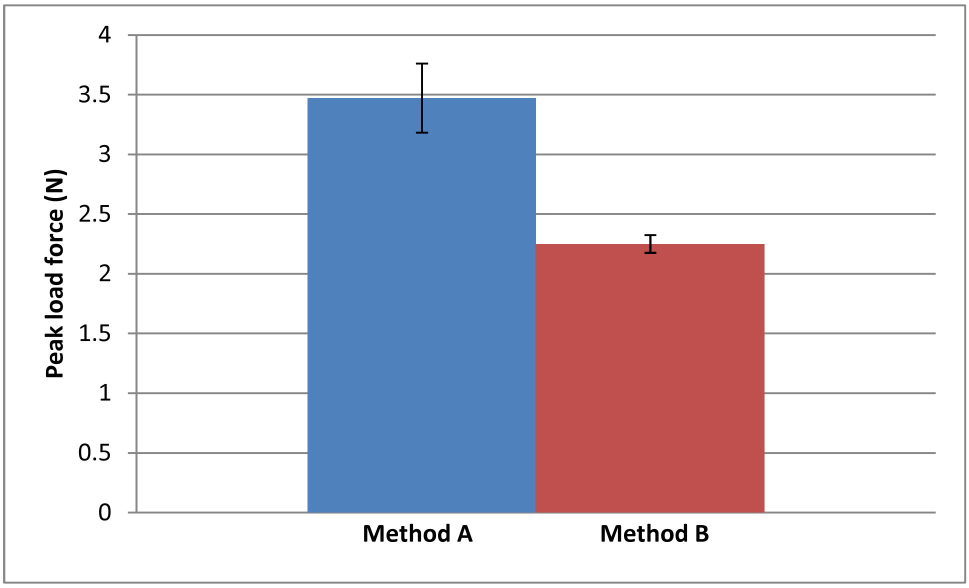

Figure 6-5 Comparison of peak load point between method A and method B

When a yarn is being pulled out from a fabric, it causes the fabric to bend towards the direction of the pull-out force. Then yarn un-crimping takes place, forming a number of frictional points on the crossovers along the pulled-out yarn. As the frictional points build up, the pull-out force increases as well. When the yarn is fully un-crimped, the peak load point is reached. Then, slippage occurs and the yarn is translated over the first frictional point, which leads to the sudden drop of the pull-out force. Then, the load begins to build up to overcome the second frictional point and so on, in a cycle. This explains the occurrence of maxima and minima on the load-displacement curve shown in Figure 6-6.

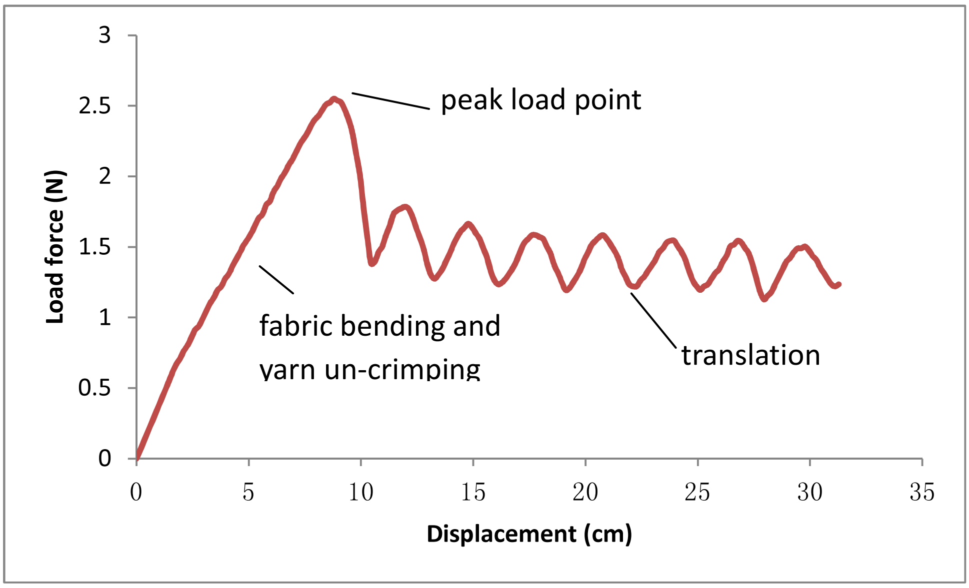

Figure 6-6 Load-displacement curve for yarn-pull out test

Figure 6-7 exhibits the comparison of peak load force in the weft direction, aiming to study the yarn gripping effect of leno insertion. It has been established that the insertion of leno weave enables the weft yarns to have increased pull-out force. The decrease in leno structure interval has the effect of increasing the yarn gripping. The results are shown in the Appendix, Table 4. The mean value for plain weave is 2.24N, which is 0.29N and 0.75N lower than PWL03 and PWL02 respectively. A glance at the load-displacement curve from Figure 6-8 reveals that the initial modulus of the curves for the gripping fabrics is higher than that of the plain woven fabric. The results show good agreement with Ahmed [139], who argued that leno weave gives higher inertia on the weft yarns.

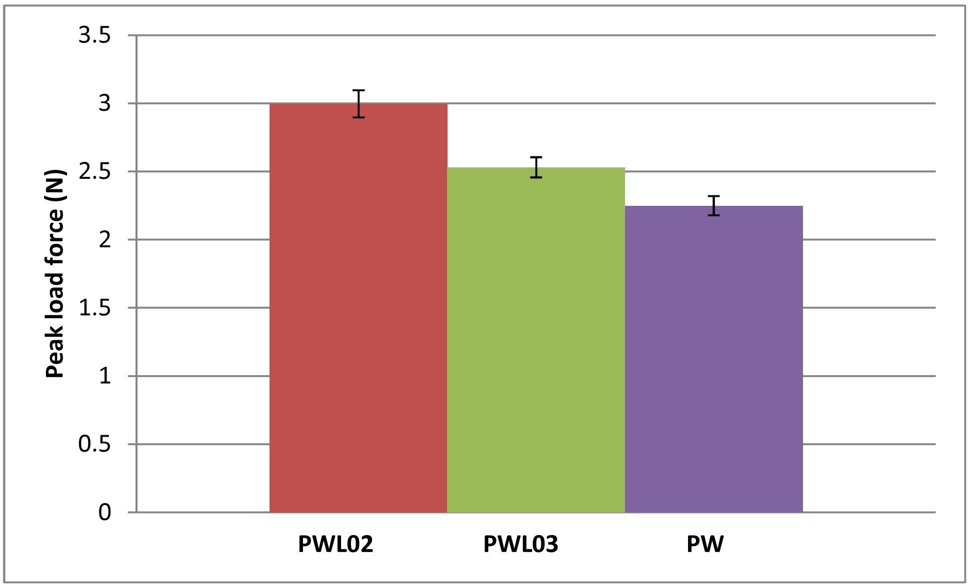

Figure 6-7 Comparison of peak load force for different fabrics in the weft direction

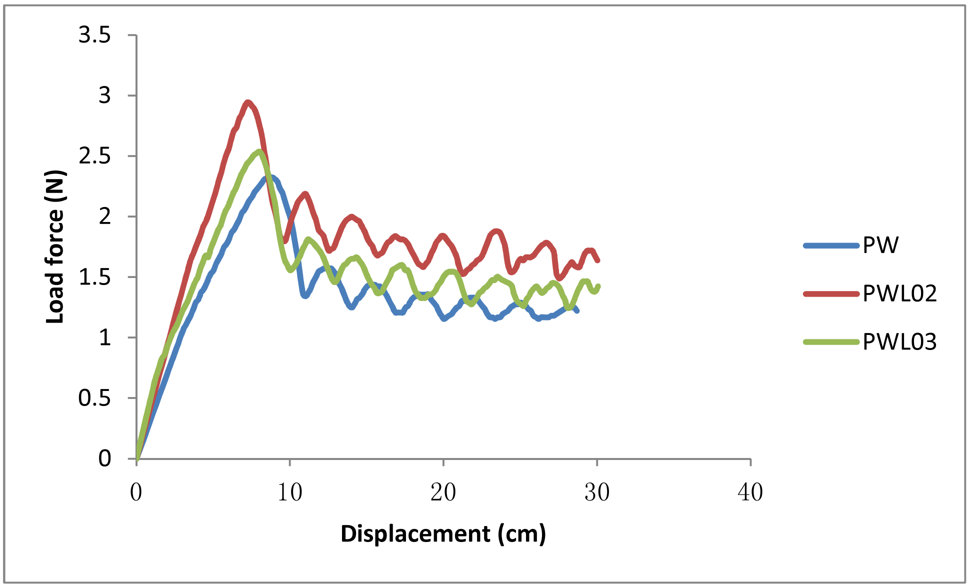

Figure 6-8 Load-displacement curves for pull-out for difference fabrics in the weft direction

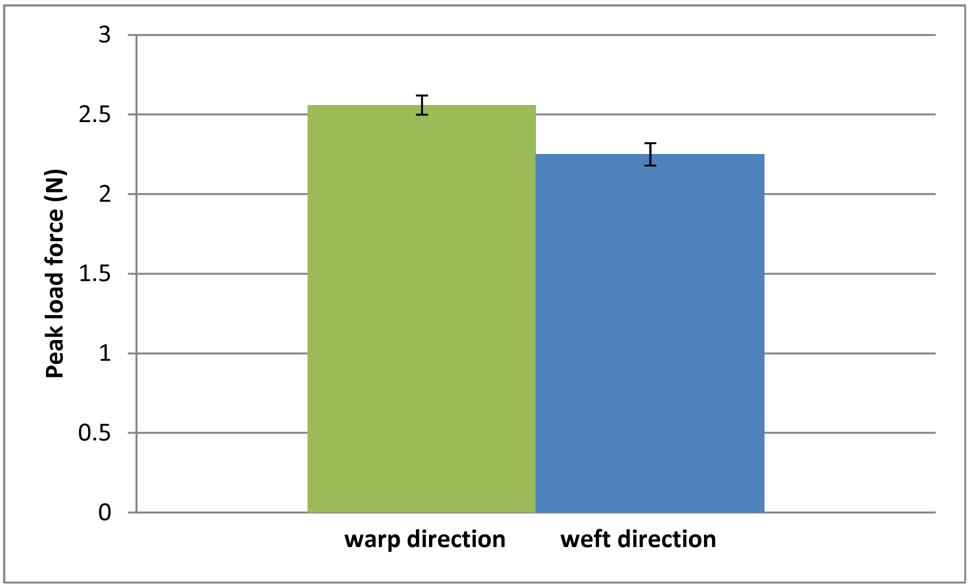

Figure 6-9 Comparison of peak pull-out force for the weft and warp directions

For the warp direction, the peak load force to pull out a warp yarn from plain weave fabric is around 0.31 N higher than that from the weft yarn. This is because during the weaving process, the warp yarns are at a higher tension than the weft yarns, and therefore the warp yarns give higher crimp than the weft yarns. For weft cramming and double weft insertion and cramming, Figure 6-10 shows that that they give a similar increase in yarn gripping of the weft yarns. The increase in yarn inertia is also found in the warp direction, which is shown in Figure 6-11. The results are shown in the Appendix, Table 5.

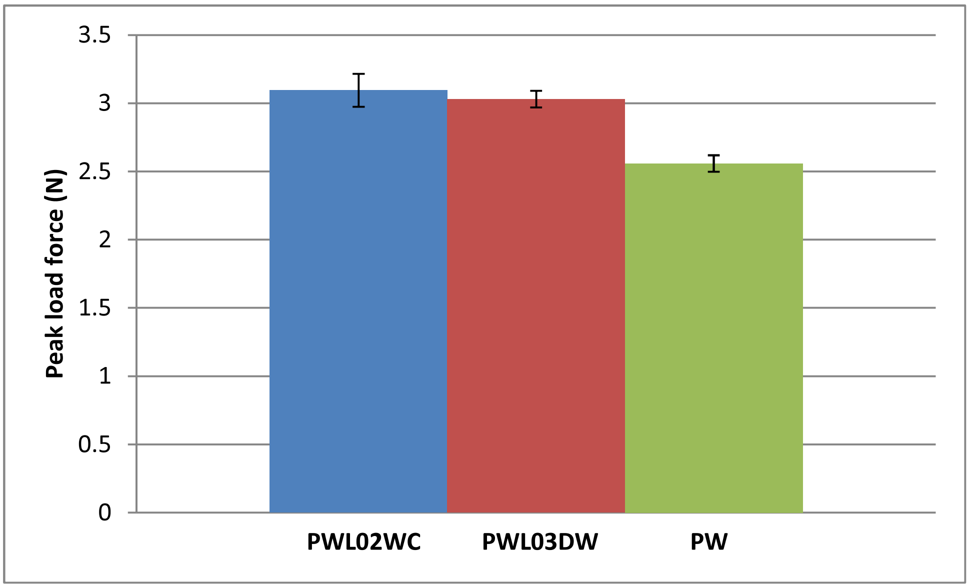

Figure 6-10 Comparison of peak pull-out force for different fabrics in the warp direction

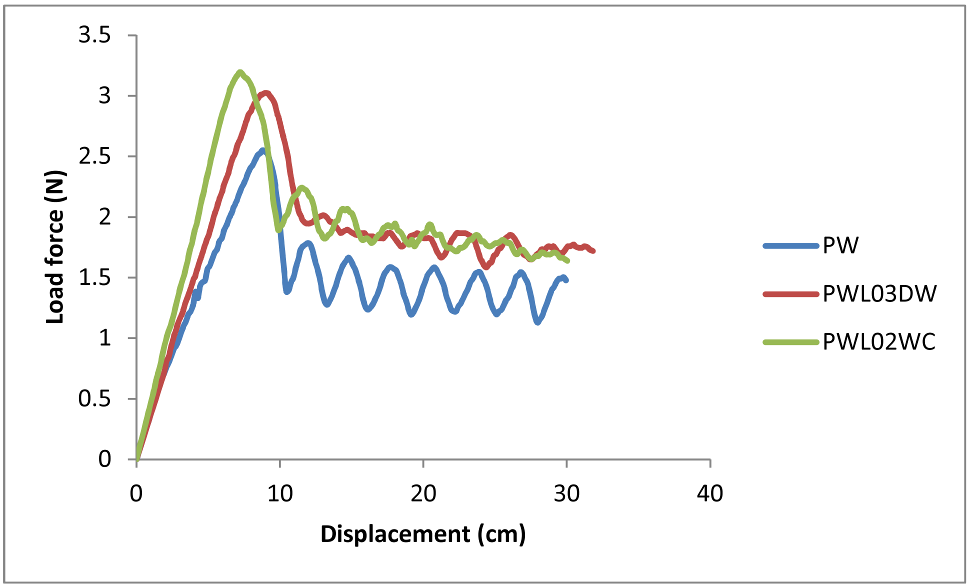

Figure 6-11 Load-displacement curves for pull-out from different fabrics in the warp direction

6.2 Ballistic Penetration Test on Structure Modified Fabrics

Since it has been established that the insertion of leno structure, weft cramming and double weft structure increases the yarn pull-out force, it is interesting to investigate the ballistic performance of gripping fabrics. In this section, ballistic penetration testing was carried out to study the influence of the structured insertions on the fabric energy absorption capability.

6.2.1 The ballistic results

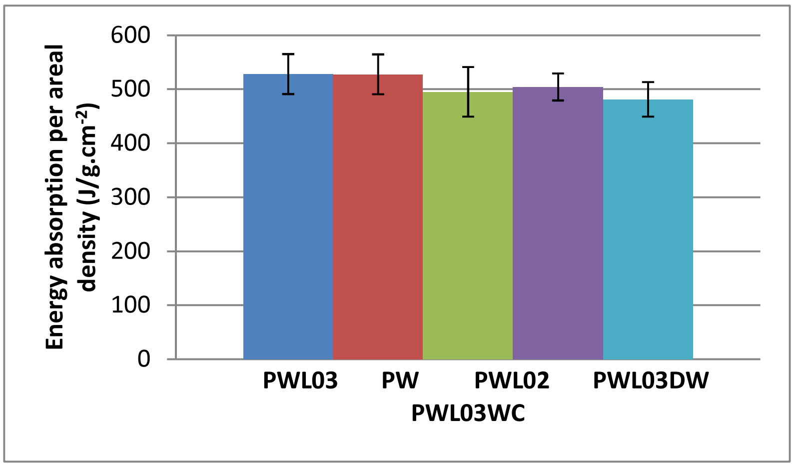

Figure 6-12 Normalized results for different Dyneema woven fabrics

The raw data for different woven fabrics is shown in the Appendix, Table 6 to Table 10. The results were extracted from the raw data and were normalised to eliminate the effect of fabric areal density on energy absorption, which is shown in Figure 6-12. Contrary to expectation, there was no significant difference in ballistic performance. The energy absorption for all the fabrics was found to be in the vicinity of 500J/g.cm^{-2}. Although the PWL03 and PW fabrics give slightly higher values than other cases, the error bars overlap with each other, indicating that the improvement in the ballistic performance of structure modified fabrics is not obvious.

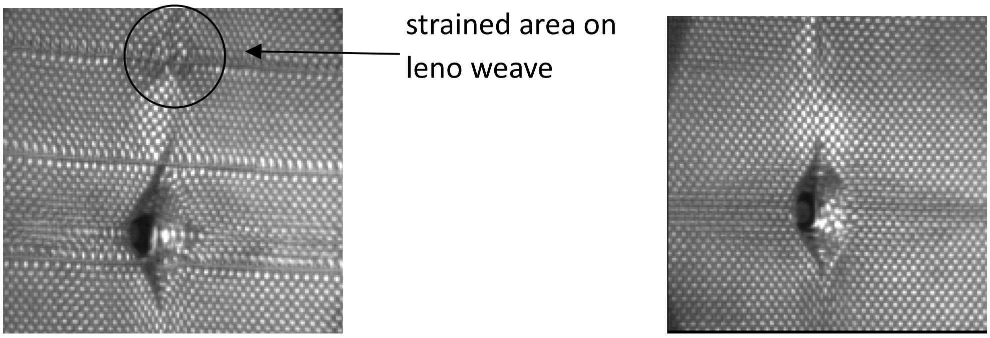

(a) PWL02 **(b) PW**

Figure 6-13 High speed photograph of woven fabric undergoing ballistic impact

Figure 6-13 shows the images captured by a high speed photograph for PWL02 and PW. The pyramidal transverse deflection and the trace of yarn pull-out are noticeable in Figure 6-13 b, which is typical of plain structure. In Figure 6-13 a, a strained area can be seen in the vicinity of the leno structure. This indicates that, although the energy absorption capability of gripping fabric is not remarkably increased, the insertion of leno weave changes the fabric strain distribution upon impact.

6.2.2 Discussion

The results of similar work on Kevlar fabrics, however, showed that the best gripping fabric gives an energy absorption of 650 J/g.cm^{-2}, while the value for plain woven fabric is around 500 J/g.cm^{-2} [141, 142]. This could be explained by the fact that the increase in yarn gripping in Dyneema fabrics is not high enough to give a noticeable influence on the ballistic performance. A comparison of yarn pull-out force has been made between Dyneema and Kevlar fabrics to investigate the effect of leno structure. The results are revealed in Figure 6-14. It has been found that for plain weave, the yarn pull-out force for

Kevlar fabric is more than 1N higher than for Dyneema fabric. The insertion of leno weave, gives an increase of 1.63 N in the peak load force for Kevlar PWL02, the value of which is more than double that of Dyneema PWL02.

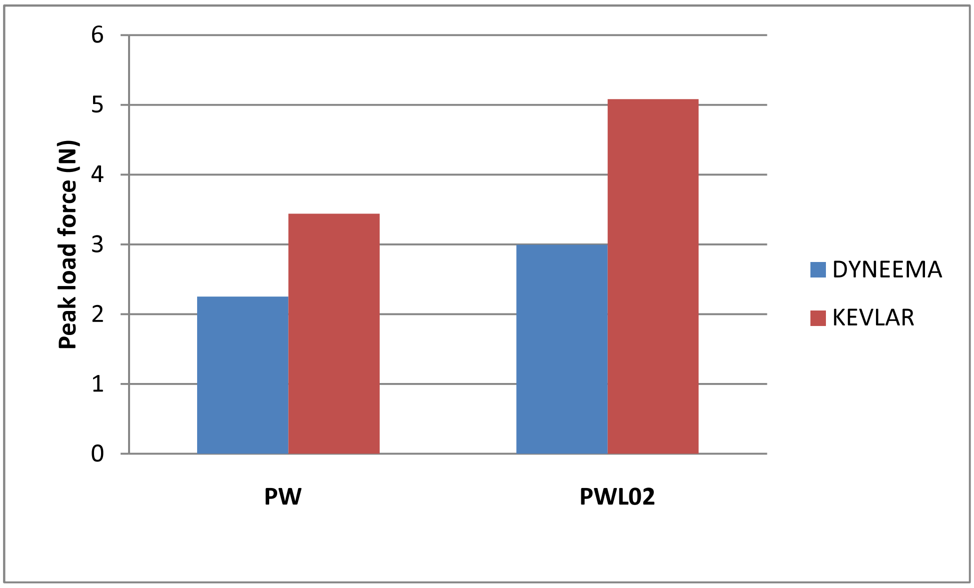

Figure 6-14 Comparison of peak yarn pull-out load force for Dyneema and Kevlar fabrics

6.2.2.1 Effect of the coefficient of inter-yarn friction

According to the capstan equation 5.1, the pulling tension T is determined by the coefficient of friction and the yarn wrapping angle. The low increase in yarn gripping on the Dyneema structure modified fabric could be attributed to the low coefficient of inter-yarn friction. In order to study inter-yarn friction, frictional tests were carried out on both Dyneema and Kevlar yarns.

This approach is suggested by Standard ASTM D3412 [128]. An Instron number 4411 tensile testing machine was used in the experiment. In the test, a yarn was pulled over two cylinders of a radius of 2cm with one end gripped by a terminal and the other end fixed by an initial load to keep it taut. The two cylinders are fixed horizontally on a rig so that the contact angle between yarn and cylinder, θ, is 90°. A Schematic diagram of the set-up is shown in Figure 6-15. As the the output tension T, input tension T_0 and wrapping angle θ are known, according to the capstan equation, the coefficient of friction between the yarn and the cylindrical surface could be obtained.

As it was considered that the test carried out at the yarn angle of 90° may reflect the movement between the weft and warp yarns in a woven fabric, the cylinders were wrapped with yarns in the circular direction. By doing this, it is not difficult to measure the coefficient of inter-yarn friction. Table 6-1 and Table 6-2 show the friction test conditions and the specifications of the yarn sample. According to Standard ASTM D3412, the free hanging weight to provide an input tension should be 10±0.5 mN/Tex. As a result, the weight employed for Kevlar and Dyneema yarn samples were 161g and 177g respectively. Due to the limited option, a weight of 50 g was chosen for test.

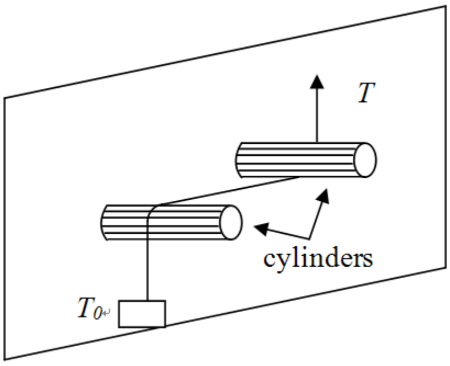

Figure 6-15 schematic diagram of capstan method

Table 6-1 Frictional test conditions

Material	Kevlar®49, Dyneema®SK75
Initial load force	161g, 177g
Temperature	21.8°
Sliding speed	500 mm/m
Humidity	50%
Yarn angle	90°

Table 6-2 Yarn properties

	Kevlar	Dyneema
Linear density (Tex)	158	174
Tensile strength (N/Tex)	55.6	59.76

Results and discussion

Figure 6-16 shows the load-displacement curve for the materials undergoing yarn frictional testing. The curve gives a sharp increase at the beginning and levels off as the test carries on. According to the capstan equation, it is not difficult to work out the coefficient of friction between a yarn sample and the cylindrical surface. Average values for Dyneema-Dyneema, Dyneema-Kevlar and Kevlar-Kevlar are given in Table 6-3. Detailed results are shown in the Appendix, Table 11. As can be seen, the Dyneema-Dyneema coefficient of friction is 0.119, which is one third lower than that of Kevlar yarns. According to the information on-line [143], the coefficient of friction between UHMWPE fibre is from 0.1 to 0.2, which reinforces the experimental results obtained from the frictional test. Briscoe and Motamedi [17] used a hanging-yarn configuration to measure the coefficient of friction between Kevlar fibres, μ was found to be 0.22±0.03, which is slightly higher than the value obtained from the capstan method. This could be attributed to different testing methods and conditions. It has also been found that a coefficient of friction between Dyneema and Kevlar yarns is higher than that between Dyneema yarns.

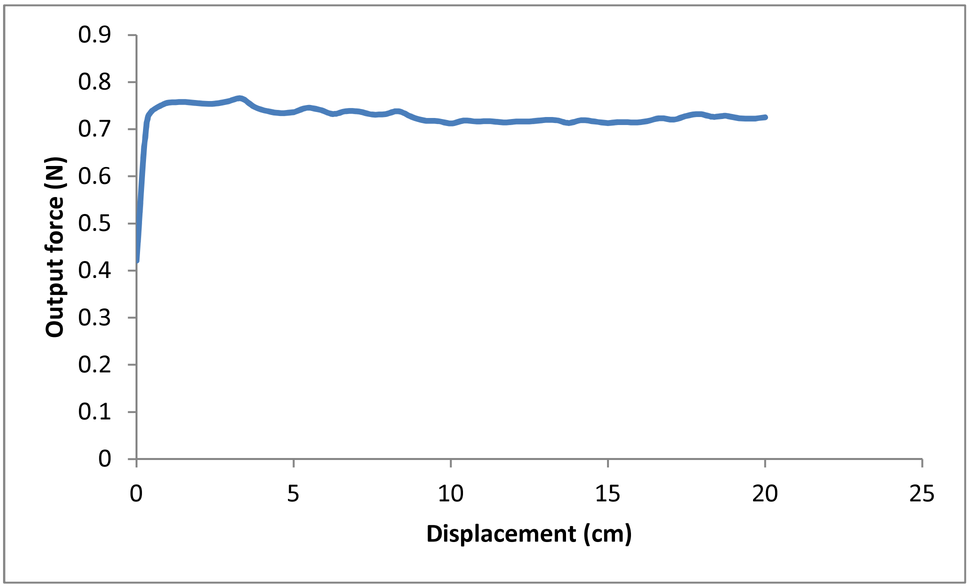

Figure 6-16 Load-displacement curve in the capstan method

Table 6-3 Coefficient of friction between Dyneema and Kevlar yarn

	Coefficient of friction
Dyneema-Dyneema	0.119
Kevlar-Kevlar	0.192
Kevlar-Dyneema	0.142
Dyneema-Kevlar	0.136

PS: Kevlar-Dyneema indicates that Kevlar yarn is pulled over cylinders wrapped by Dyneema, and vice versa

From the data obtained from the frictional test, it was concluded that the coefficient of inter-yarn friction for Dyneema yarn is lower than that for Kevlar yarn, which leads to the insufficient gripping effect of the insertions on Dyneema woven fabrics. One of the alternatives to solve this problem is to use Kevlar yarns to fabricate leno or other insertions on Dyneema woven fabric. Although the value is higher for the case of Kevlar-Dyneema and Dyneema-Kevlar, the increase of the coefficient is limited, raising the question as to whether Kevlar leno yarns are really able to provide more sufficient yarn gripping than Dyneema leno yarns. As a result, it is suggested to use materials giving a higher inter-yarn friction with Dyneema yarns to form insertions so that sufficient gripping could be achieved.

6.2.2.2 The influence of yarn wrapping angle

According to the capstan equation, another factor that influences yarn gripping is the yarn wrapping angle θ. Take the leno structure for example, the wrapping angle of weft yarns over leno yarns is determined by the flexural rigidity of the weft yarns and the force applied by the leno yarns. Flexural rigidity is defined as the couple required to bend a fibre to unit radius of curvature and was obtained by Morton and Hearle [144]:

$$Flexural\ Rigidity = \frac{1}{4\pi} . \frac{\eta E_s T^2}{\rho} \tag{6.1}$$

where η is the shape factor, which has a value of 1 for fibres having a solid circular cross-section, fibre with differently-shaped cross-sections will have a different value of η; E_s is the specific modulus in N/tex; and T is the linear density in tex and ρ is the bulk density in kg/m^3.

SEM observation revealed that the diameters of Dyneema fibre and Kevlar fibre are 17.5 μm and 13.5 μm respectively, then T could be obtained using:

$$T = A\rho \tag{6.2}$$

where A is fibre cross-section in m^2. The fibre linear density could be obtained.

The ratio between the FR (Flexural Rigidity) of Kevlar fibre and Dyneema fibre can therefore be worked out by:

$$\frac{FR_{Dyneema}}{FR_{Kevlar}} = \frac{E_{sDyneema} A_{Dyneema}^2 \rho_{Dyneema}}{E_{sKevlar} A_{Kevlar}^2 \rho_{Kevlar}} \tag{6.3}$$

It is established from Equation (6.3) that the flexural rigidity of the Dyneema fibre is around 2.22 times higher than that of the Kevlar fibre, indicating that the Kevlar yarn is more flexible and softer than the Dyneema yarn. This enables it to be bent more easily and to form a larger wrapping angle with the orthogonal leno warp yarns in a fabric.

The Kawabata Evaluation System enables the measurement of bending rigidity of a yarn or fabric sample through an experimental method. It aims to measure the bending moment as a fabric or yarn sample is bent through a curvature ranging from -2.5 cm^{-1} to 2.5 cm^{-1}. The test is conducted at a constant rate of 0.5 cm^{-1}/s. The sample is fixed vertically in the tester to diminish the influence of gravity on the results. The results obtained from the test are revealed in the Appendix, Table 12. It can be seen that the bending rigidity of the Dyneema yarn is much higher than that of the Kevlar yarn. Normalised by yarn linear density, the value for Dyneema is around 7.41×10^{-4} ($g.cm^2/yarn.Tex^{-1}$), which is 37.9% higher than for Kevlar (5.37×10^{-4} $g.cm^2/yarn.Tex^{-1}$). The experimental results seem to collaborate the theoretical prediction.

As it has been mentioned previously, the wrapping angle is also controlled by the force of the leno yarns applied on the weft yarns. Since it is difficult to change the yarn properties to reduce its flexural rigidity, it is considered that the improvement could be made by increasing the tension of leno yarns during the weaving process, which appears to increase the contact force between leno yarns and weft yarns, which enlarges the yarn wrapping angle.

6.2.2.3 The influence of projectile roll angle

Projectile roll angle is the angle between the fabric plane and the longest dimension of the projectile's impact end [38]. Shockey *et al* [88] suggested that a fragment presents more of an interface area with the fabric target at a 45° roll angle than at a 0° roll angle.

However, this may cause yarn slippage rather than yarn fracture during the impact event. In Figure 6-17, it has been observed from the high speed photograph that the projectile may tumble when flying, which leads to a different roll angle when impacting the fabric target. As a result, head-on impact (90° roll angle) enables a projectile to have a larger contact area with the target than edge-on impact (roll angle less than 90°) In order to investigate this issue, an FE model was built to simulate a projectile with different roll angles. The schematic diagrams are shown in Figure 6-18

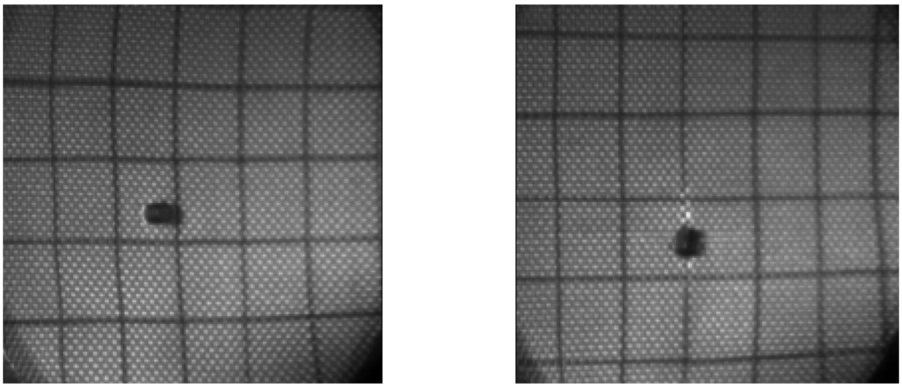

(a) 90° roll angle **(b) Roll angle less than 90°**

Figure 6-17 Woven fabric impacted by a projectile at different roll angles

(a) 90° roll angle **(b) Roll angle less than 90°**

Figure 6-18 Schematic diagrams of a projectile with different roll angles

A half-model is employed to investigate the roll angle effect on fabric energy absorption at the impact velocity of 500 m/s. Figure 6-19 shows that projectile energy loss decreases with the increase in roll angle, reaching a minimum at 45° and then increases to a peak of 6.2 J. In Figure 6-20, although the number of yarns broken by a projectile is found to be the same, the stressed area for the case of 45° is much smaller than the cases of 0° and 90°. This is probably due to the fact that a 0° or a 90° impact present greater a cross-sectional area to a fabric than a 45° impact. For this reason, it is more likely for the ballistic fabric to catch a projectile and to dissipate energy at high or low roll angle.

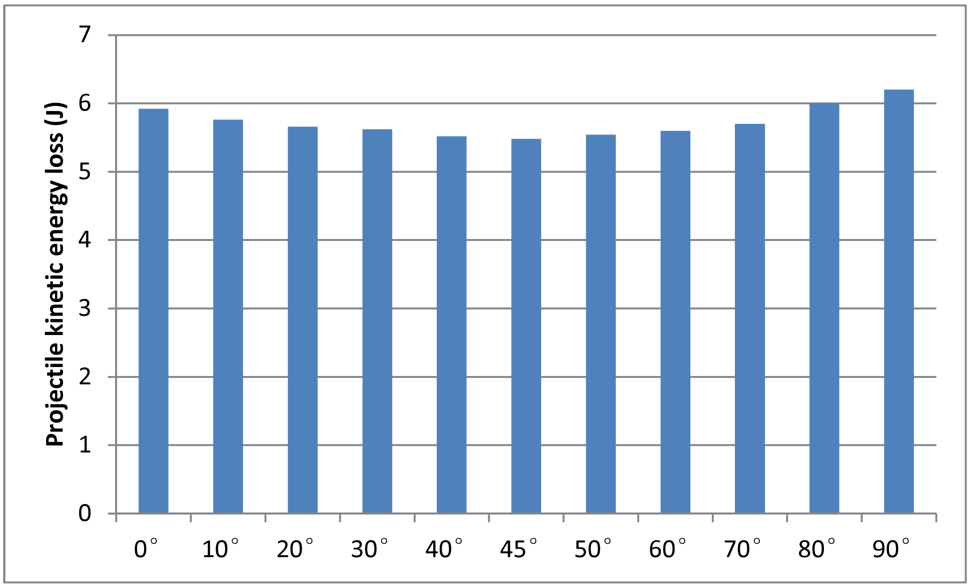

Figure 6-19 Projectile kinetic energy loss at different roll angles in simulation

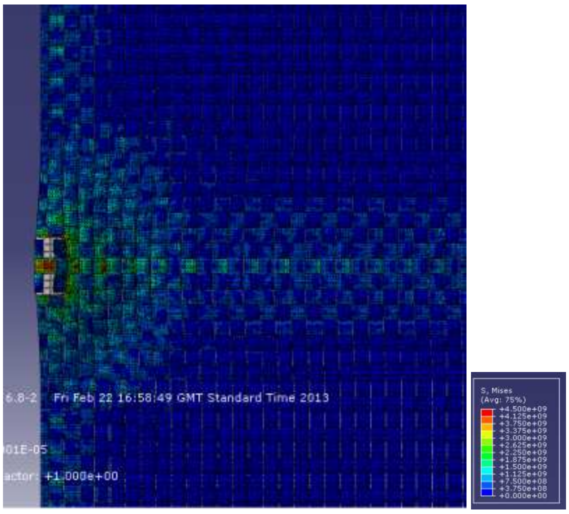

(a) 0°

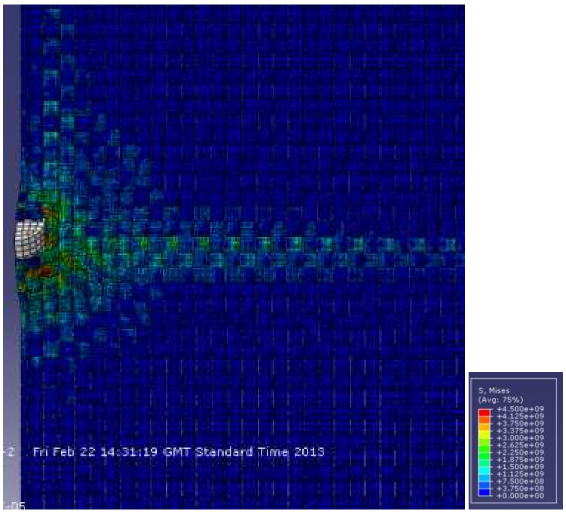

(b) 45°

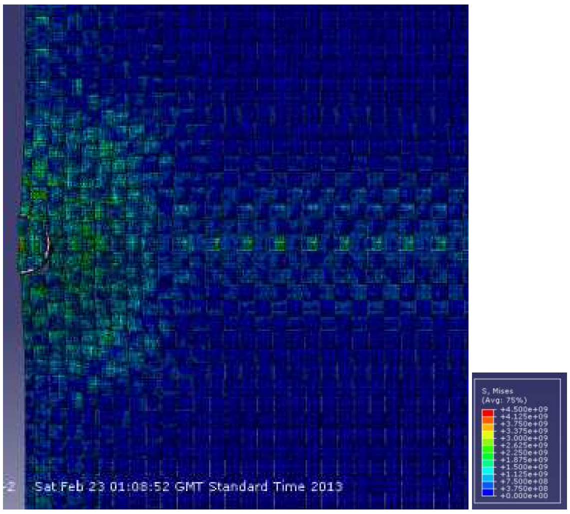

(c) 90°

Figure 6-20 Fabric upon ballistic impact at different roll angles at 8 μs

As it is difficult to predict projectile roll angle in the ballistic range and different projectile roll angles result in random data for the ballistic impact test, the limited influence of gripping structures on the performance becomes less detectable. One of the approaches to solve this problem is to use a spherical projectile to eliminate the effect of roll angle. Table 13 in the Appendix, shows the ballistic results of using a 5.5 mm-diameter spherical projectile. The employing of a spherical projectile gives a coefficient of variance of 8.58%, which is almost half that of the cylindrical projectile (13.56%). This means there is improved data consistency by using a spherical projectile. Other factors, such as different impact velocity, also influence the analysis and comparison of fabric energy absorption. It is suggested that if the projectile impact velocity could be kept constant by some means, it is possible to further reduce data randomness.

6.3 Summary

In this chapter, the yarn pull-out test has been performed on structure modified fabrics to evaluate the magnitude of yarn gripping. It has been found that the three types of insertion applied to woven fabric, warp leno insertion, weft cramming and double weft insertion and cramming, give an increase in yarn pull-out force. The ballistic performance of structure modified fabrics, however, does not show noticeable improvement when compared to that of plain woven fabric. Similar work on Kevlar fabrics shows that the insertions enable Kevlar woven fabrics to have a remarkable improvement in energy absorption capacity. Through the yarn pull-out test, it is suggested that the less obvious energy absorption improvement on Dyneema fabrics could be due to its lower yarn pull-out force when compared to Kevlar fabrics.

According to the capstan equation, the output force is determined by the interface coefficient of friction and wrapping angle. Yarn frictional tests show that the Dyneema fibre surface gives a smoother property than the Kevlar fibre surface, which leads to lower inter-yarn friction in Dyneema woven fabric. Yarn wrapping angle is considered to be associated with bending rigidity. As the softer the weft yarns are, the easier it is for them to have a large curvature when gripping by insertions such as leno structure. Data obtained from the Kawabata bending tester reveal that the bending rigidity of Dyneema yarn is higher than that of Kevlar yarn. Combined with the two factors mentioned above, it is understandable that the insertions in Dyneema fabric give lower yarn gripping than in Kevlar fabric. One of the solutions to this problem is to increase the tension of leno yarns, forming larger yarn wrapping angles.

Apart from yarn properties, projectile striking roll angle is considered to be another factor that influences the ballistic performance improvement of Dyneema fabrics. FE simulation shows that low or high roll angle tends to present more of a cross-sectional area to a fabric, leading stress to be dissipated over a larger area. A moderate roll angle causes a projectile to slip through the fabric and the stress is then concentrated on a small area. As a result, the variation of projectile roll angle increases the randomness of ballistic results, which consequently makes the energy absorption increase less.

Chapter 7 Response of Fabric Layers in a Ballistic Panel

It has been mentioned in the literature review part that different layers of fabric in a panel respond differently to ballistic impact. It is generally believed that fabrics near the impact face tend to be sheared to failure and those near the back face tend to be subjected to tensile failure. For this reason, it is suggested that using shear damage resistant materials near the impact face and tensile damage resistant materials near the back face may improve the performance of a ballistic panel. This chapter aims to further explore the response of a ballistic panel upon impact in order to provide information and develop guidance for soft body armour design. The present chapter is divided into two parts. In the first part, FE models will be created to analyse the response and failure mode of different layers in a panel upon ballistic impact. In the second part, two types of fabric, UHMWPE woven and unidirectional fabrics, will be characterised in terms of their properties for panel design. The experimental and FE evaluation for different designs will be presented in the next chapter.

7.1 Computer Costs Reduction

As the main objective of this chapter is to investigate the failure mode of fabric layers in a ballistic panel upon impact, a multi-plied fabric system is required to be created in ABAQUS for FE analysis. The major cause of concern is that the enlargement of the FE model would increase the computer costs. Due to the limit of CPU power, it is only possible to simulate four layers of fabric if the original quater model is to be used, which is not satisfactory for multi-ply fabric system analysis. For this reason, two approaches, model size reduction and mesh modification, will be investigated in this section to reduce computer costs. It is important that the modified woven fabric model gives a satisfactory accuracy. The accuracy is mainly obtained from the comparison of fabric energy absorption between the FE model and experimental testing.

7.1.1 Model size reduction

In the present study, models of four different radiuses, 7.5 cm, 5.5 cm, 3.5 cm and 1.5 cm are put into comparison. The results are revealed in Figure 7-1. It can be seen that, the increasing trends for 7.5 cm and 5.5 cm model are almost linear, as the model size reduces, the trend becomes more logarithmic. This is probably because small sized models tend to have less fabric area to get involved in energy dissipation, which leads to decreased energy absorption when compared to large sized models. The reduction of energy absorption becomes more pronounced in a multi-plied fabric system than in a single-ply system. In addition, the reflection of the stress wave between the fabric boundaries is more frequent in small sized models. This being so, the strain in the vicinity of the impact point is quickly increased and the model tends to break at an early stage. As a result, although reducing the model size decease the computer costs, the fabric performance has been greatly changed and is not appropriate to be used for multi-ply fabric system analysis.

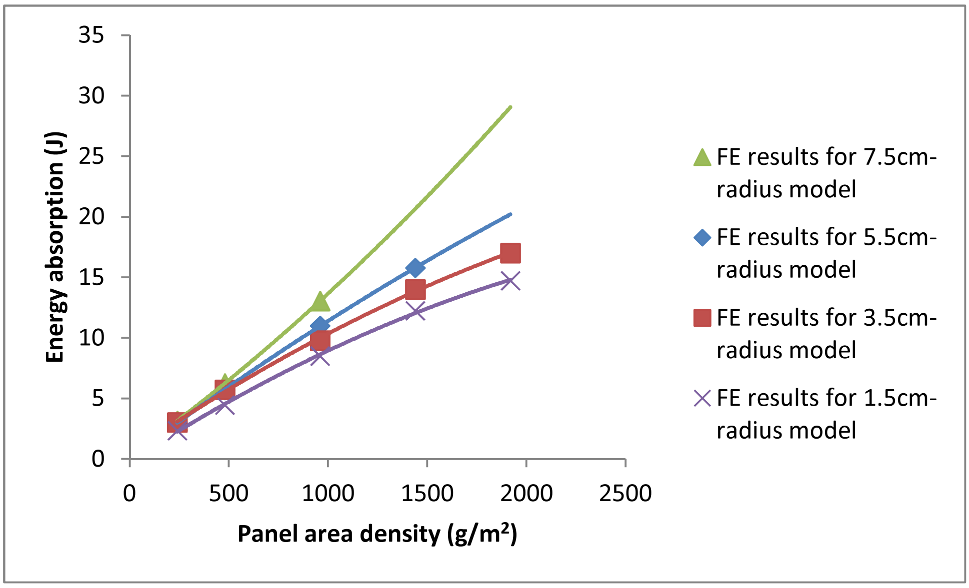

Figure 7-1 Energy absorption as a function of panel areal density for models of different sizes

7.1.2 Meshing scheme modification

Since reducing fabric size would seriously affect fabric energy absorption, especially in multi-ply fabric system, FE simulation accuracy is greatly reduced using this approach. An alternative method is to coarsen the meshing scheme on the fabric-forming yarns so that fewer elements and degrees of freedom are taken into consideration in the calculation. As it is the primary yarns that absorb the majority of the energy [24] and being subjected to failure, the meshing scheme on them is kept unchanged. In the present case, the mesh coarsening is carried out on the secondary yarns in the hope of minimizing its influence on energy dissipation and transmission. The mesh coarsened yarn model is shown in Figure 7-2. In the original model, the arcs forming the yarn cross-section and yarn path were designed to have six elements, which is termed as a 6×6 model, and so forth for 4×4, 3×3 and 3×2 models. 3×2 is the coarsest mesh scheme that is possible on the current yarn model. In Figure 7.3, it can be seen that 4×4, 3×3 and 3×2 models give similar energy absorption capacity as the original 6×6 model, which indicates that the modification of the meshing scheme on the secondary yarns does not significantly change the fabric performance like the reduction of model size. In order to save computer CPU power, a 3×2 model was employed.

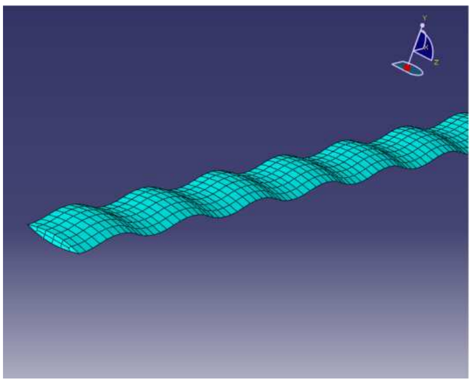

(a) 6×6

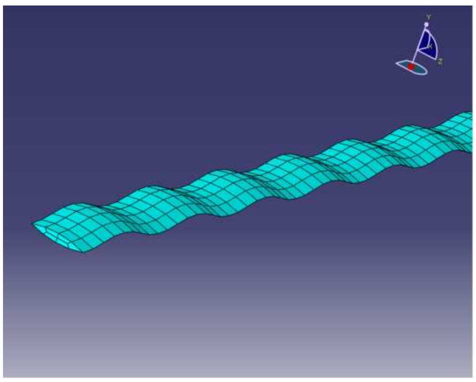

(b) 4×4

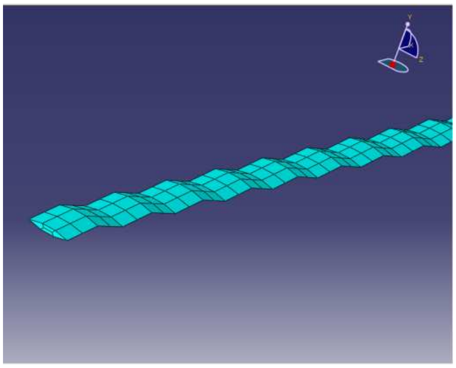

(c) 3×3

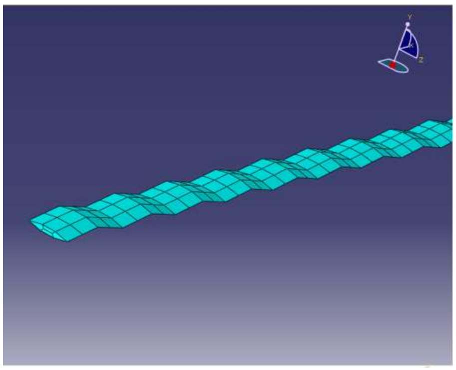

(d) 3×2

Figure 7-2 Illustration of yarn models with different mesh scheme

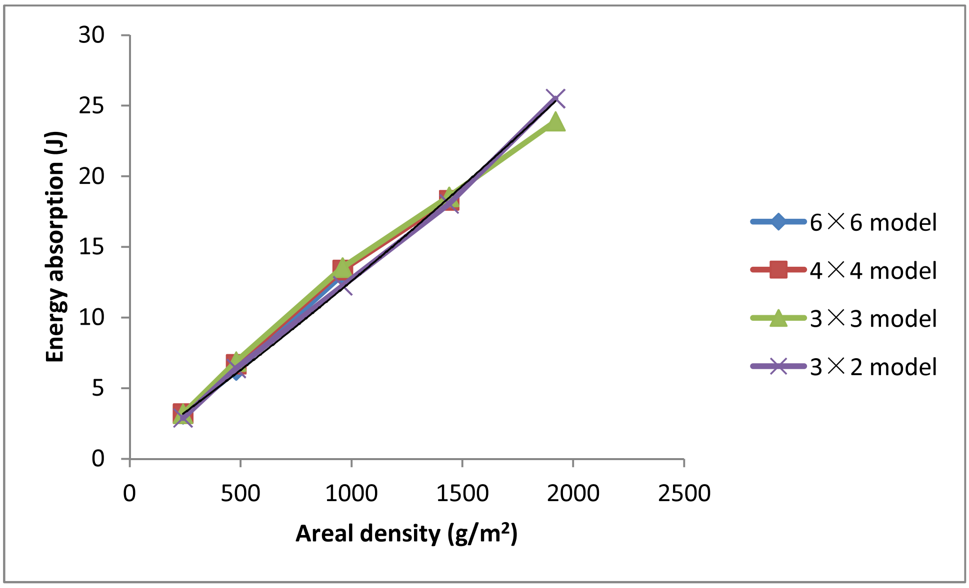

Figure 7-3 Energy absorption as a function of panel areal density for models with different mesh schemes on the secondary yarns

7.2 The Response of Different Layers in A Panel

Since the mesh simplified model has been proven to be able to reduce the computer costs without affecting the energy absorption capability of the fabric, it will be employed for investigation in this research. This section is divided into two parts. The first part aims to study the deformation of different layers. The second part presents a detailed exploration of the failure mode of the different layers. An FE model of an eight-layer woven fabric system was created to undertake this research. The performance of the first layer, second layer, fourth layer and eighth layer fabrics were extracted from the model and put into comparison so that a good understanding of the response of a panel to ballistic impact could be developed.

7.2.1 Deformation of fabrics of different number of layer

In Figure 7-4, it has been determined that fabrics near the impact face tend to fail earlier than those near the back face. For instance, the first and second layers break within the first five microseconds, the eighth layer engages with the projectile for about 30 microseconds. As a result, the longer engaging time enables rear layers of fabric to have wider transverse deflection and to have a larger area of fabric get stressed at break, which increases its energy absorption. The Contour plots of stress distribution are shown in Figure 7-5 and Figure 7-6. It can be seen in Figure 7-7 and Figure 7-8 that far more strain energy and kinetic energy is stored in rear layers of fabrics. Also, Figure 7-9 shows that energy is more locally concentrated on the primary yarns for front layers of fabric. For rear layers of fabrics energy is more equally distributed over the whole fabric. Take the eighth layer for example, only 33.8% of the total energy absorbed is accumulated on the primary yarns.

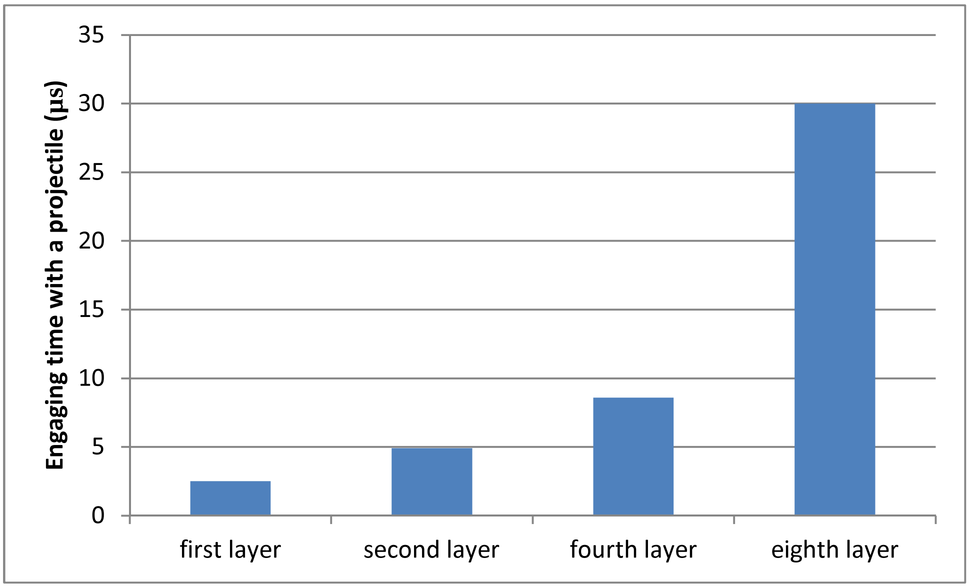

Figure 7-4 Engagement time of different layers of fabric with a projectile

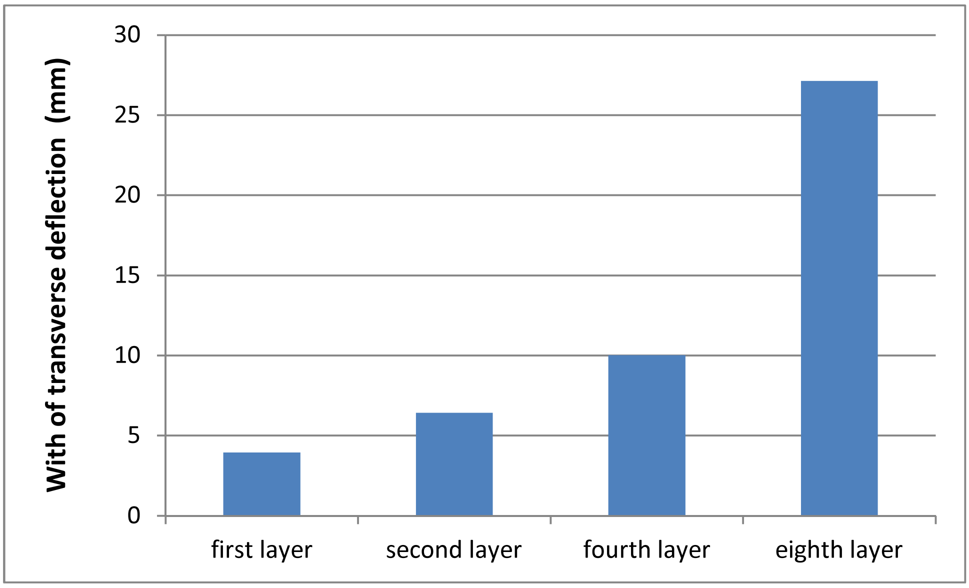

Figure 7-5 Width of the transverse deflection of different layers at break

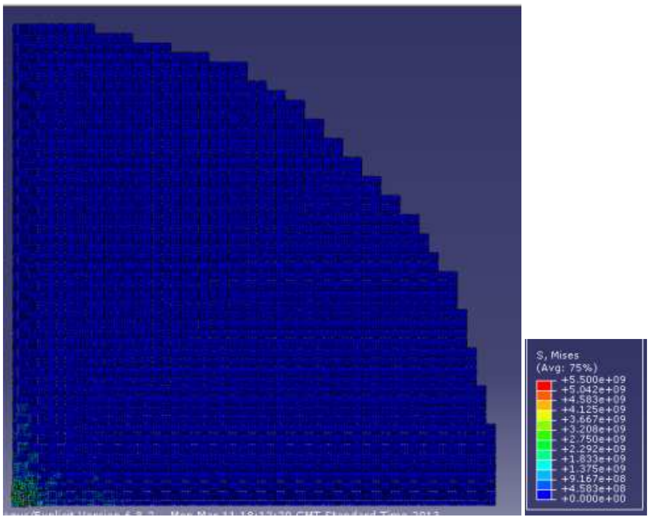

(a) The first layer

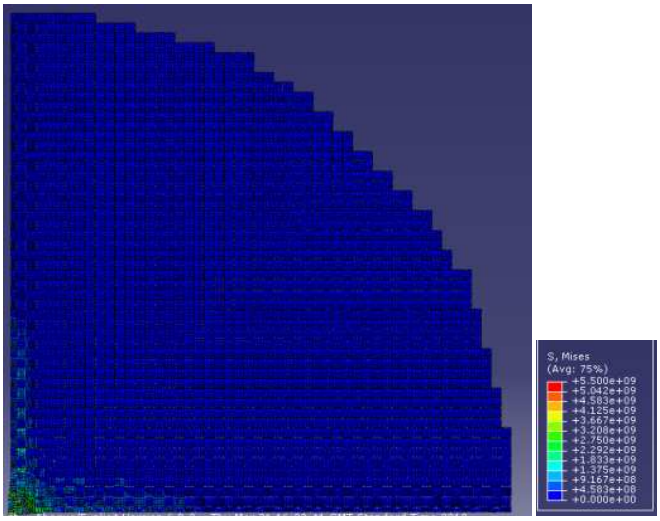

(b) The second layer

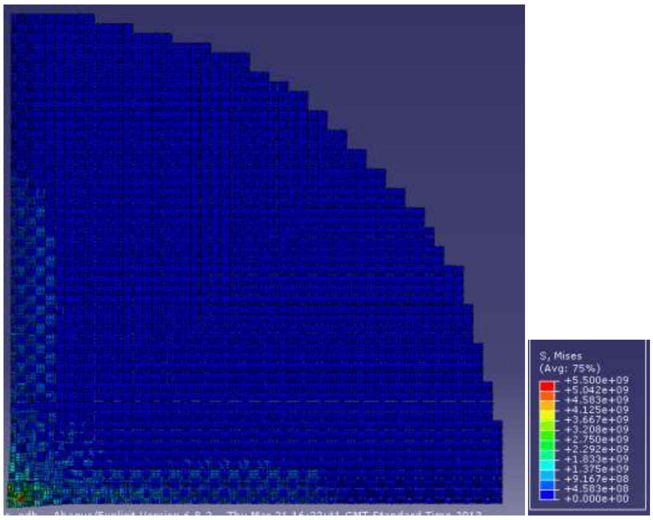

(c) The fourth layer

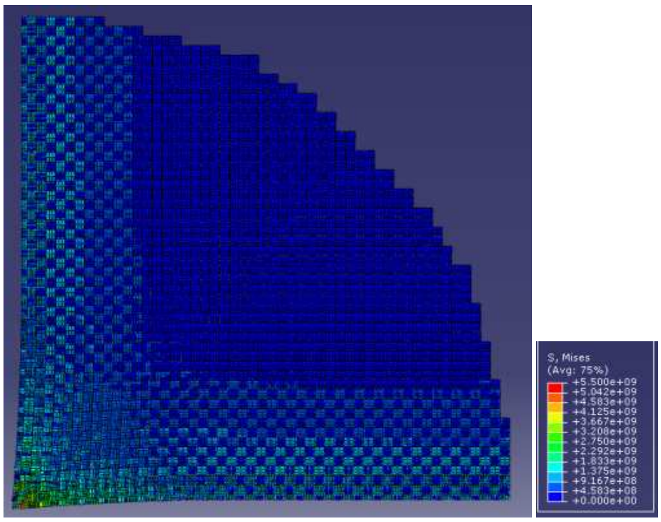

(d) The eighth layer

Figure 7-6 Contour plots of stress distribution for different fabrics at break

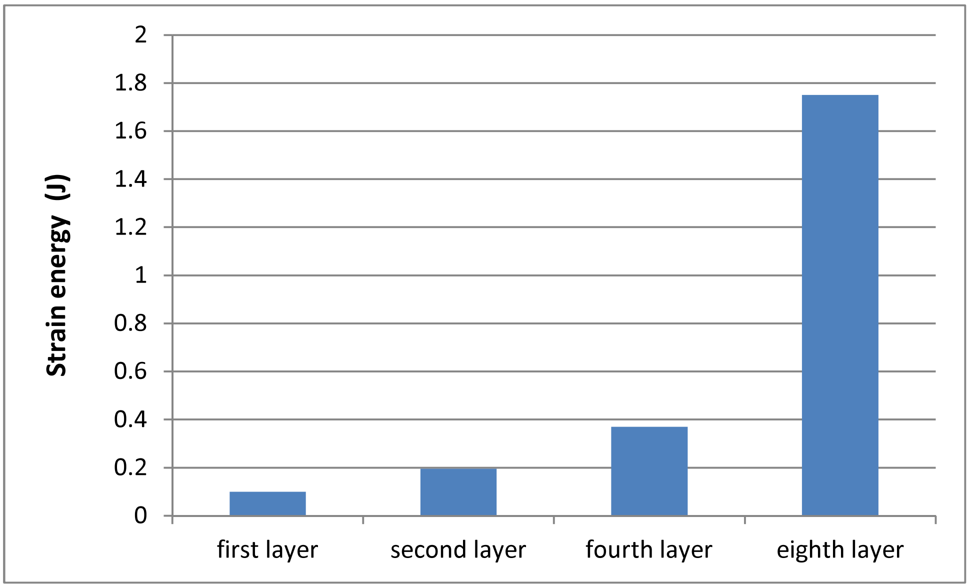

Figure 7-7 Strain energy of each layer at break

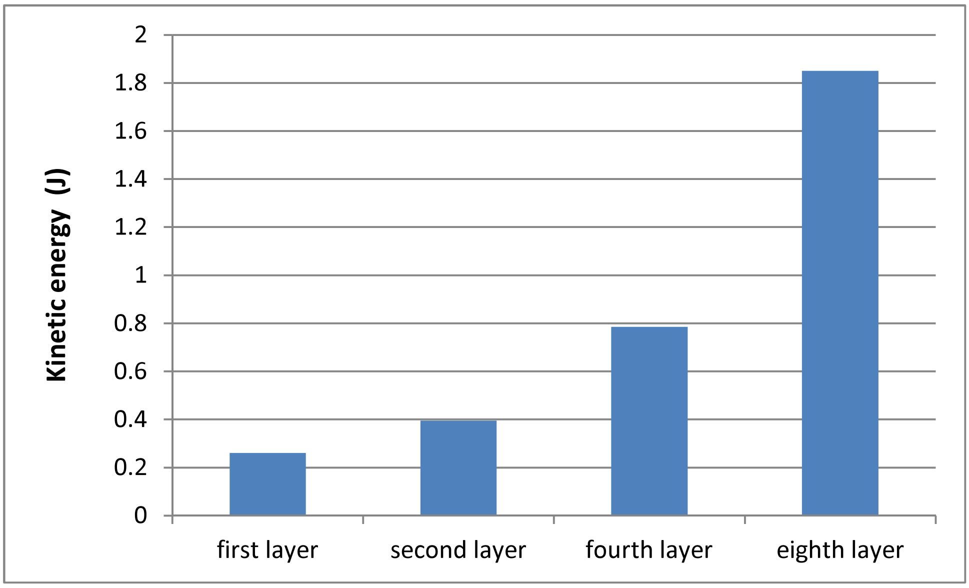

Figure 7-8 Kinetic energy of each layer at break

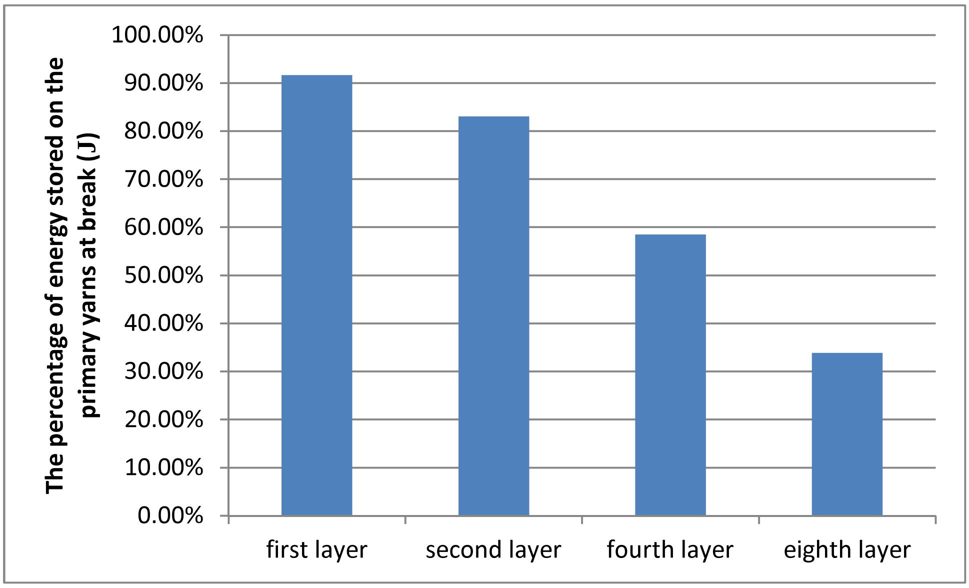

Figure 7-9 Percentage of strain and kinetic energy stored in the primary yarns at break

7.2.2 Strain analysis of the failure mode of different layers

As it has been established that the breaking time is closely associated with the performance and energy absorption of different layers of fabric in a panel，it is necessary to study the failure mode in a fabric system so that the a good understanding of the underlying factors influencing the breaking time could be developed. In FE simulation, failure occurs when the stress induced strain reaches material breaking strain. It has been mentioned in Chapter 3 that two failure criteria were set to define material failure in the FE model, namely tensile and shear failure criteria. The values were determined to be 0.02 and 0.04 respectively. In this research, failed elements will be selected from the first, second, fourth and eighth layer and the magnitude of strain will be used as an indicator for the damage analysis on the fabric. Three strain components associated with ballistic impact will be considered, where ε_{11} is the strain in vertical direction, ε_{22} is the tensile strain in horizontal direction and ε_{12} is the shear strain in vertical direction.

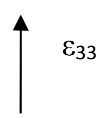

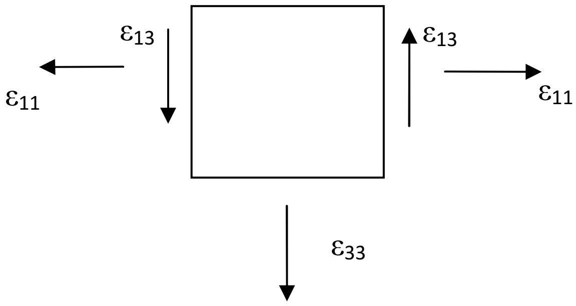

Figure 7-10 Stress components on an element

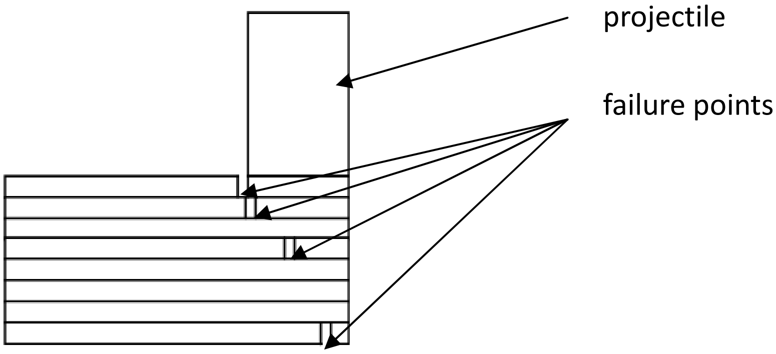

Figure 7-11 Schematic diagram of the failure point for each layer

It is observed in the FE model that for fabrics near the impact face, such as the first layer, failure tends to occur in the vicinity of the projectile edge. For the fabrics near the back face, however, failure is more likely to occur near the impact point, which is shown in Figure 7-11. This is because stress is more quickly concentrated on the front layers of fabric due to the reinforcement of their subsequent layers, causing the materials to be cut by the sharp edge of a projectile. Strain at the front layers of fabric tends to exceed the shear failure strain. As the projectile is not in direct contact with the rear layers of fabric, stress is transferred through the fabrics. This causes the material to be less likely to be subjected to shear failure. As a result, more stress is concentrated on the impact point, leading fabrics to fail in tension.

7.2.2.1 Strain analysis of the failed elements

The failed elements were extracted from the model for strain analysis, the results of which are shown in Figure 7-12. As can be seen, for the first and second layers, ε_{13} and ε_{33} give extremely high negative values at break. This indicates that fabrics near the impact face are subjected to high shear and compressive stress, which play a dominant role in failure in a ballistic event. For middle layer fabrics, such as layer 4, and fabrics near the back face, such as layer 8, the shear and compressive strain peaks yield much lower value at break. Nevertheless, tensile strain ε_{11} is found to be higher for layer 4 and layer 8 than for layer 1 and layer 2 at break, which shows that failure is mainly caused by tensile stress along the yarn path.

Figure 7-13 reveals the broken fibre ends taken from the penetrated fabric samples observed on a SEM. It was found that fibres taken from the front layers exhibited heat-induced melt due to the low melting temperature of polyethylene, the shear failure mode was not detectable. The tensile failure mode, however, was observed from the fibre taken from the rear layers of fabric. The results collaborate those of Chen *et al* [72], who observed the failure mode of broken Kevlar fibres taken from fabrics near and away from the impact face respectively. The failure ends of Kevlar fibre are shown in Figure 7-13. The shear-induced failure is more noticeable on Kevlar fibres than that on Dyneema fibres for front layers of fabric. In addition, fibrillation is observed in Figure 7-14 (b), indicating that Kevlar fibres fail in tension on the rear layers.

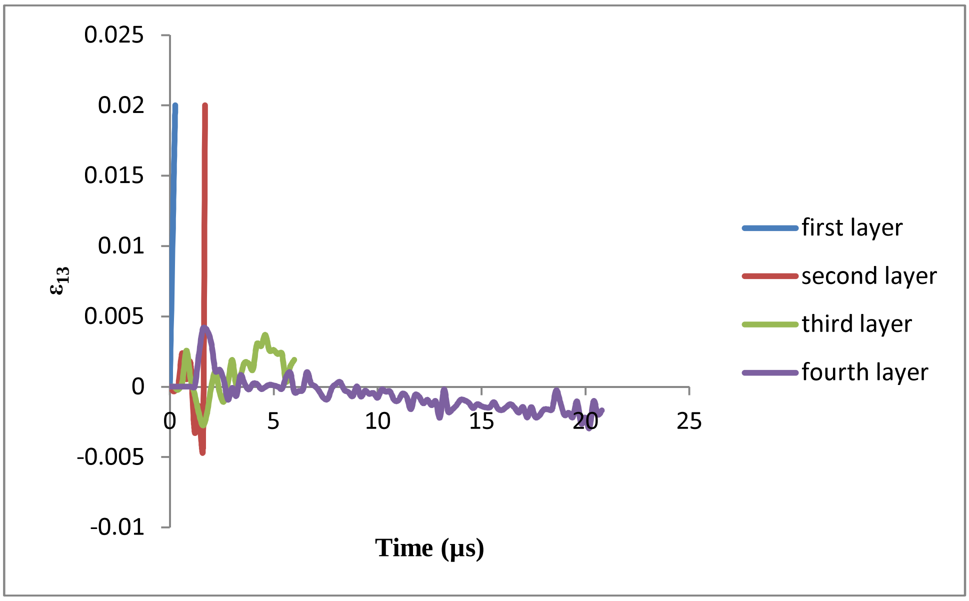

(a) ε_{13}

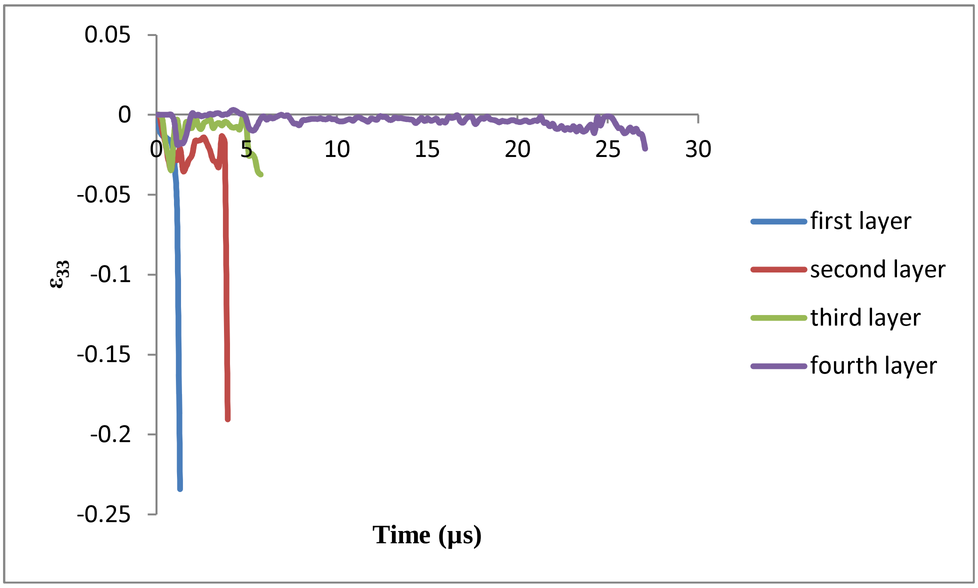

(b) ε_{33}

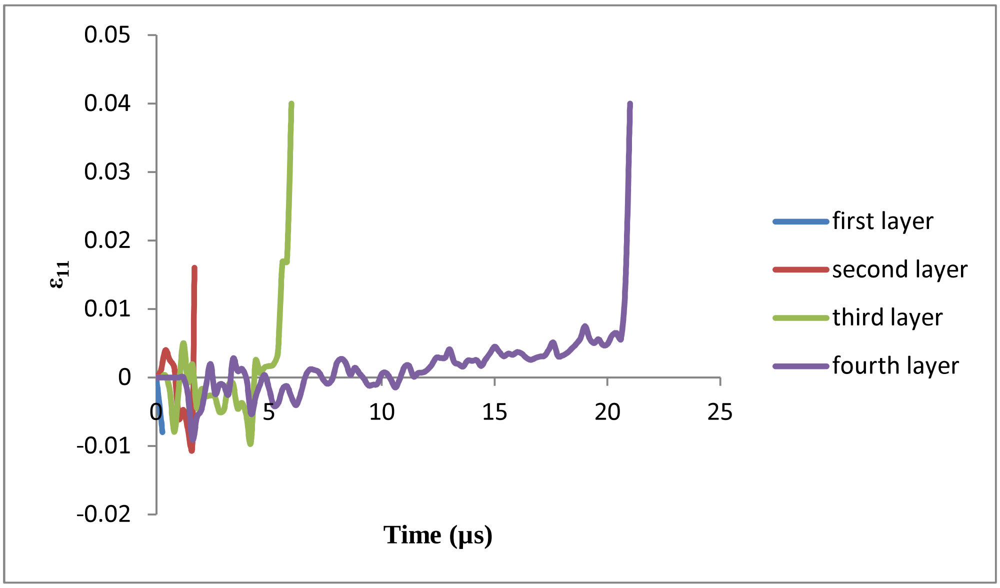

(c) ε_{11}

Figure 7-12 Strain components of failed elements for each layer

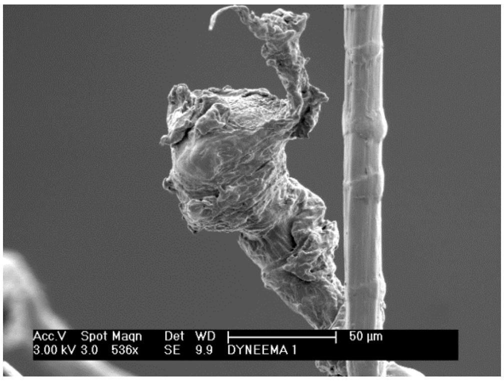

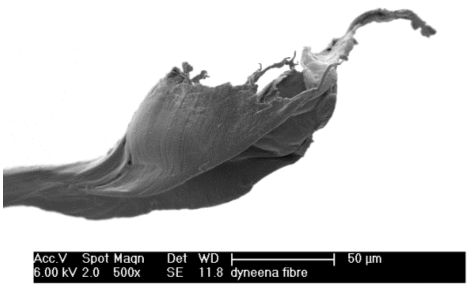

(a) fibre from the front layer **(b) fibre from the rear layer**

Figure 7-13 Broken Dyneema fibre ends taken from the ballistic panel

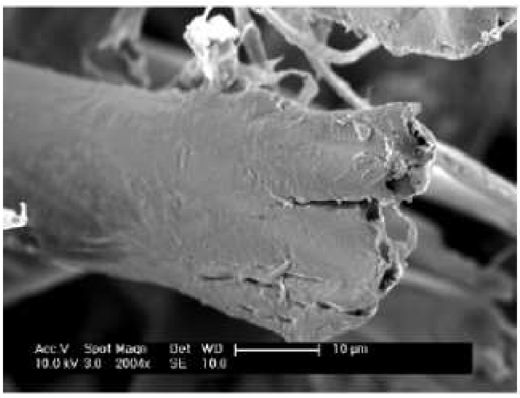

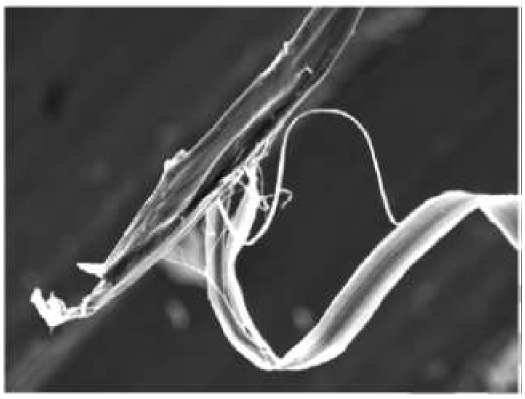

(a) Fibre from the front layer **(b) fibre from the rear layer**

Figure 7-14 Broken Kevlar fibres taken from front and rear layers of fabric [72]

7.3 Fabric Analysis and Evaluation

Since the predictions indicate that the front layers of fabric are more likely to be sheared to failure, and the rear layers tend to be stretched to failure, it follows that shear resistant materials would be desirable for the front layers and tensile resistant materials for the rear layers. This combination of the two types of materials could hopefully improve the ballistic performance of a fabric panel of a reduced weight.

A considerable amount of literature has been reported on the tensile properties of ballistic materials, such as para-aramid and high-performance polyethylene fibres. However, it is difficult to measure directly the fabric shear properties. Finlayson [135] set up a shear test apparatus and made a measurement for a series of fibres. He found that the shear strength is far less than the tensile strength. For ballistic fabrics, there is limited work on their shear strength. Instead of focusing on the fibres, this work aims to investigate the shear and tensile properties of different fabric structures. As has been mentioned in the introduction, the two main types of structure used for soft body armour are woven and UD. Consequently, these fabrics are characterized for the hybrid panel design.

7.3.1 Fabric structure characterisation

7.3.1.1 Plain woven fabric

In a plain woven fabric, yarns in the warp direction are interlaced with yarns in the weft direction. A Schematic diagram of plain woven fabric is shown in Figure 7-15. One of the characteristics of plain woven fabric is the existence of crimp, which is believed to reduce the tensile strength of the ballistic fabrics. The elongation at break and tenacity are lower in a fabric formation than in a single yarn [101]. As has been mentioned in the previous chapter, the plain woven fabric in use is made of Dyneema SK 75, with a yarn linear density of 174 Tex and a weave density of 6.75 yarns /cm.

Figure 7-15 Schematic diagram of plain woven fabric

7.3.1.2 Unidirectional fabric

A unidirectional fabric made of Dyneema® SB 21 was used in this study. The fabric was provided by DSM and is made of ultra-high molecular weight polyethylene fibres. In an unidirectional fabric, UHMWPE filaments are coated with resin and aligned in a [0/90/0/90] stack. The stack is then laminated by two films and is hot-pressed. The bonding of filament layers is achieved by the melting of resin applied before. The resultant UD fabric has a thickness of 0.18 mm and an area density of 145 g/m^2, which can be referred to Figure 2-8.

7.3.2 Fabric properties analysis and evaluation

7.3.2.1 The response of fabrics to out-of-plane shearing

There is a large volume of published studies describing the shear behaviour of woven fabrics in warp and weft directions, as it is important for garment design and new fabric development. However, little attention has been paid to the fabric out-of-plane shear properties, which are of vital importance in this study. The aim of this section is to analyse and evaluate the resistance of UHMWPE woven and UD fabric when subjected to transverse shear force.

The fundamental difference between the two types of fabric is the degree of freedom of fabric-forming-yarns/fibres. In a woven fabric, yarns are allowed to displace either laterally or transversely when subjected to an imposed force. In a UD fabric, fibres are stuck together and are not allowed to move due to the binding of the resin. As it is difficult to directly test the transverse shear properties of a fabric, the parallel work regarding fabric tearing properties could be used as a reference. In the tongue-tear test, a fabric sample is cut in middle, forming two "legs". The legs are laid parallel to each other and are clamped one in each jaw in a tensile test machine. Load is applied to one of the jaws to tear the fabric. Schematic diagram of Tongue-tear test is shown in Figure 7-16.

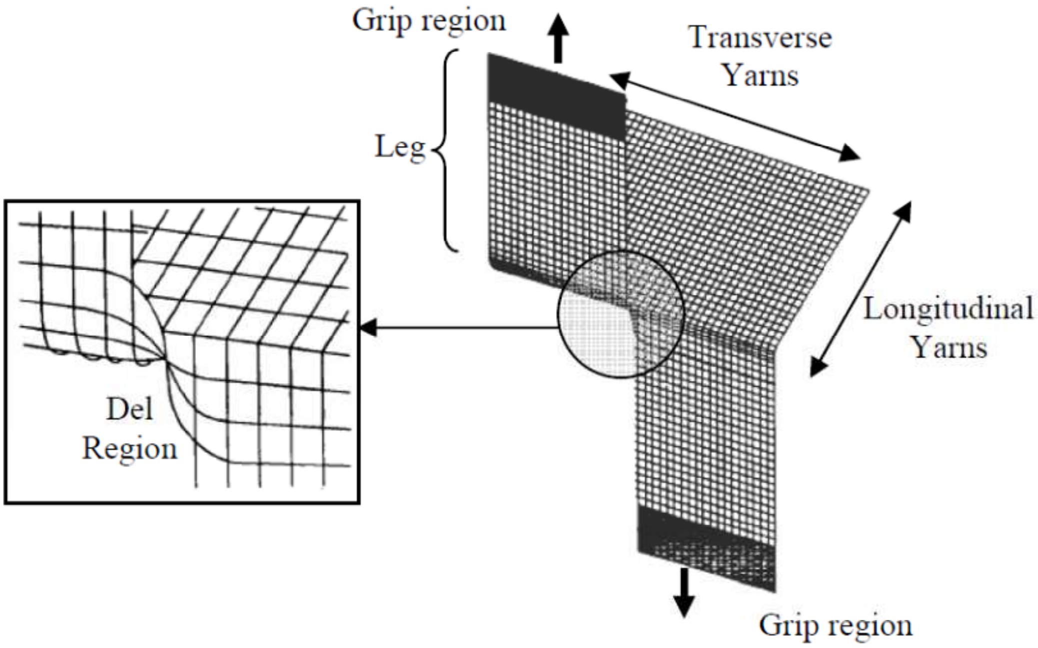

Figure 7-16 Schematic diagrams of tongue-tear test [145]

Theoretically, the fabric sample is subjected to shear stress perpendicular to the transverse yarn. However, due to the fabric deviation and yarn slippage, a Δ-shaped region is formed in the opening, leading the transverse yarns to fail in tension rather than in shearing [146]. Abbott *et al* [147] have performed a series of tests to study the tearing strength of coated and uncoated woven fabrics. He found that coating resulted in loss of tearing strength on all woven fabrics, among which basket weaves exhibits the highest strength reduction. This is probably because coating increases inter-yarn friction and reduces yarn movement, which consequently enables the fabrics to have a smaller Δ zone. This smaller Δ zone contains fewer transverse yarns to take the load and therefore the fabric tearing strength goes down. If the fabric-forming yarns are entirely constrained by the coating material and no slippage takes place, there are possibilities for the transverse yarns to be sheared to failure by the transverse load on the two fabric "legs".

This phenomenon is considered to be similar to the case of a ballistic event. When a fabric is impacted by a cylindrical-shaped projectile, the sharp edge tends to shear cut the material. For UHMWPE woven fabric, yarns subjected to impact are more likely to have lateral movement such as yarn pulled out due to its low inter-yarn friction and comparatively loose structure, which is noticeable in Figure 7-17 (a). The initial shearing effect on the material may well turn into a tensile one. When the ballistic impact takes place on the UD fabric, the binding resin restricts yarn movement and therefore the filaments which are in direct contact with the projectile tend to fail in shearing.

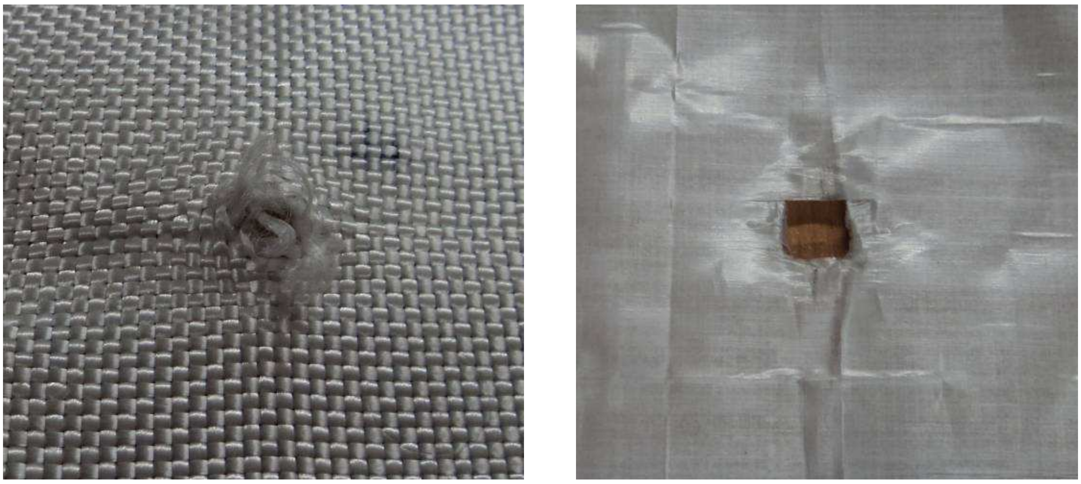

(a) Perforated plain woven fabric **(b) Perforated UD fabric**

Figure 7-17 Fabric morphology

Figure 7-18 shows the energy absorption capability of single-layer UHMWPE woven and UD fabrics. As the impact velocity varies over quite a wide range, it is not appropriate to compare their average energy absorption with 95% confidence intervals or error bars. The equations of the regression lines are therefore used to calculate their respective residual velocities at an arbitrarily chosen impact velocity (500 m/s), from which the corresponding energy absorptions are calculated. Given that the areal densities of the two types of fabric are different, the data are normalised by dividing the energy absorption of each fabric by their areal densities. The results show that the single-layer woven fabric (0.053J/ $g.m^{-2}$) absorbs around 12.76% more energy than the single-layer UD fabric (0.047J/ $g.m^{-2}$). This could be explained by the fact that the tensile failure mode enables fabrics to have a higher energy absorption than the shear failure mode.

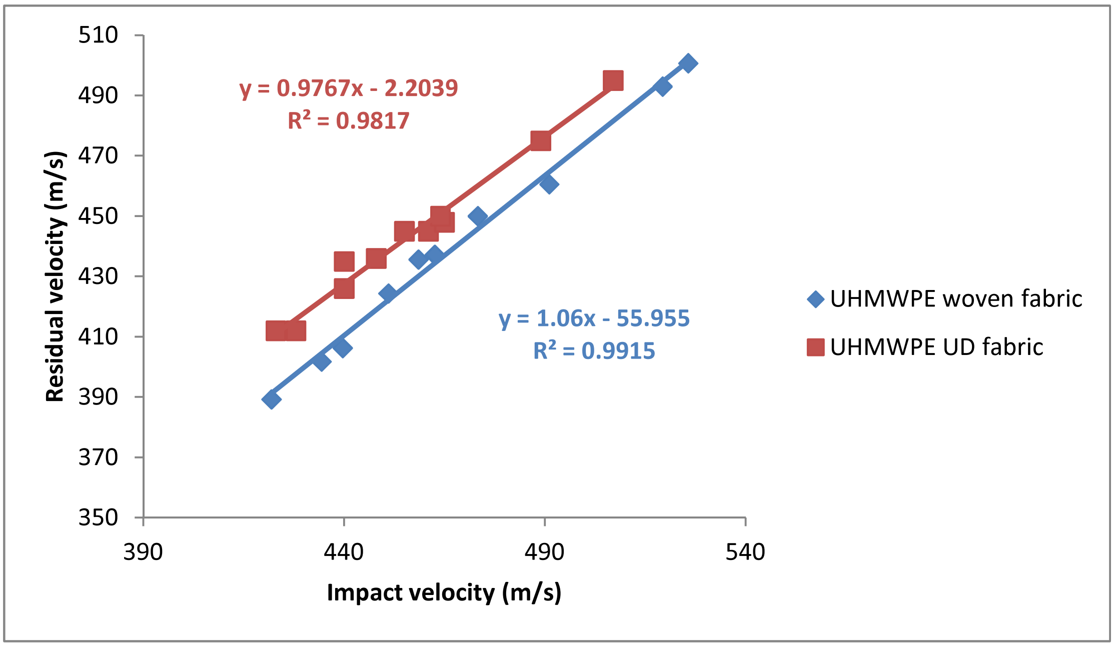

Figure 7-18 Ballistic protection of single-layer UHMWPE woven and UD fabrics

7.3.2.2 The response of fabrics to tensile load

When a woven fabric is in tension, its stress-strain curve exhibits an initial low slope region due to the de-crimping and crimp-interchange process, which is followed by a high slope region until its breaking strain is reached. This curve is shown in Figure 7-19. For this reason, the high modulus of UHMWPE fibre is not fully translated into the woven fabric upon impact. As a result, the initial low modulus of the woven fabric greatly influences the dissipation of energy and leads the impact to be concentrated in the local area. As is shown in Figure 7-20, the filaments are neatly oriented in the UD fabric. Due to the fact that there is no "de-crimping or crimp-interchange" process in this formation, its stress-strain curve shows no low-modulus region as does the woven fabric. For this reason, the high modulus of UHMWPE fibre could be fully exhibited in the fabric, which helps to globally dissipate the impact.

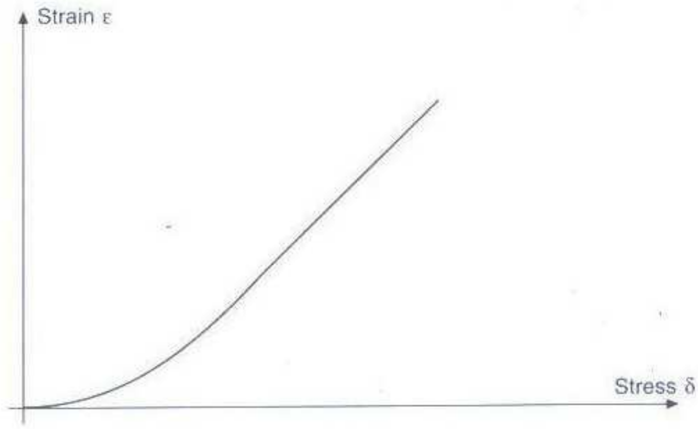

Figure 7-19 Typical tensile stress-strain curve for a woven fabric [148]

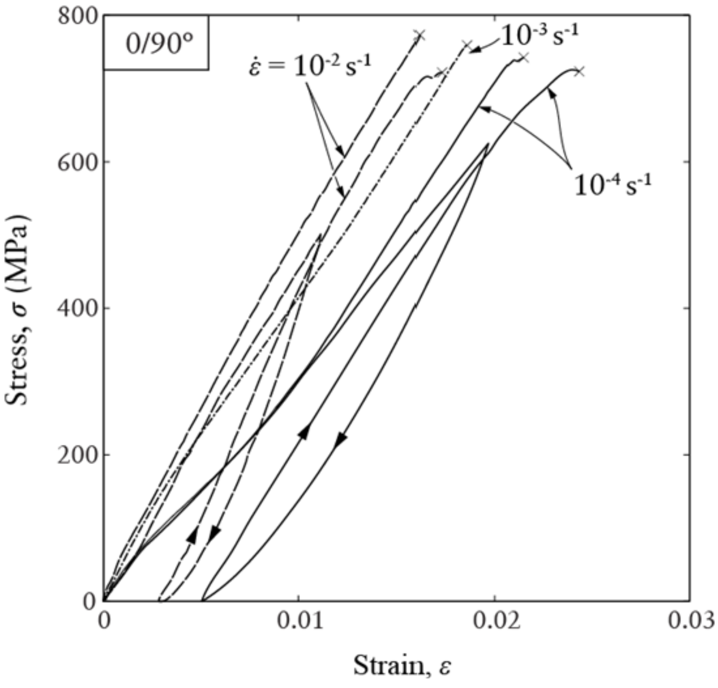

Figure 7-20 Stress-strain response of 0 UHMWPE laminate [149]

As it has been established in the previous part that materials tend to fail in tension in fabrics near the back face and the UD fabric shows higher tensile modulus than the woven fabric when subjected to tensile stretching, it is considered that the UD fabric is more energy absorbent when placed in the rear layers of a ballistic structure. Figure 7-21 compares the ballistic performance of the woven and UD fabric assemblies. Due to the limitation of the clamp, the maximum number of fabric layers that could be fixed is either 8 layers of woven fabric or 13 layers of UD fabric. It is apparent from this figure that, at low areal density, Dyneema woven fabric assemblies demonstrates superior energy absorption capability over Dyneema UD fabric assemblies. The two curves meet at the areal density of around 1200 g/m^2 and the UD fabric assemblies begins to absorb more energy with the increase of areal density. This is probably because, at high areal density, the tight structure of UD fabric enables the rear layers to sustain more tensile load, which gives the panel higher energy absorption. However, due to the comparatively loose structure, the woven fabric tends to cause yarn pull-out when the projectile is unable to break the fibre, the phenomenon which was also observed by Bazhenov [16] and Starratt *et al* [32], resulting in a more localised strain. This will lead to lower energy absorption. The results obtained are consistent with the data displayed by Lee *et al* [21], who compared Spectra fabric reinforced composite and angle-plied fibre laminate and found that the latter proved to offer better ballistic protection at high areal density.

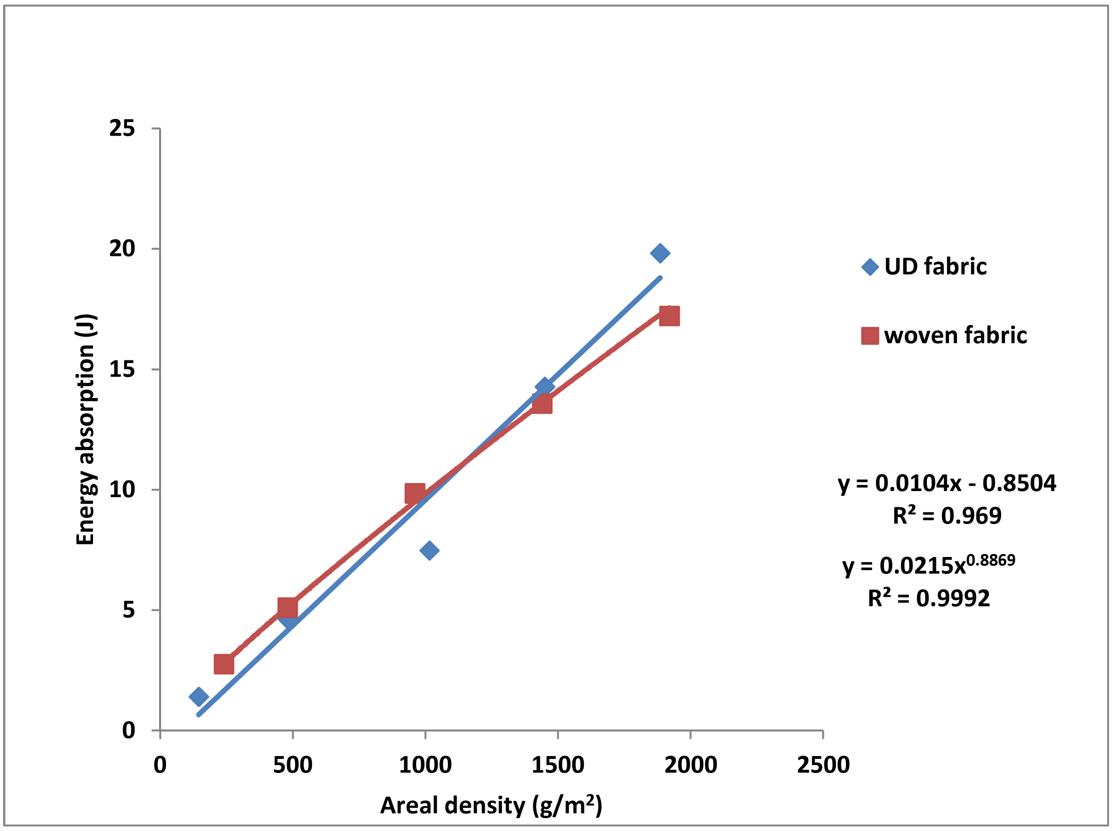

Figure 7-21 Comparison of energy absorption between woven and UD fabric

assemblies

It is considered that the decreased fabric tensile modulus not only affects the propagation of longitudinal waves [43], but in addition also lowers the fabric transverse wave velocity. For multi-layer fabric impact, an eight-layer FE woven fabric model and a thirteen-layer FE UD fabric model (of similar areal density) are compared. The width of transverse deflection is found to be higher in the UD fabric assembly (18.9mm) than in the woven fabric assembly (16.8mm), which is shown in Figure 7-22. This enables a larger area of fabric to become engaged in energy dissipation, and consequently leads to higher ballistic performance in the UD fabric assembly (17.4 J) than in the woven assembly (16.5J).

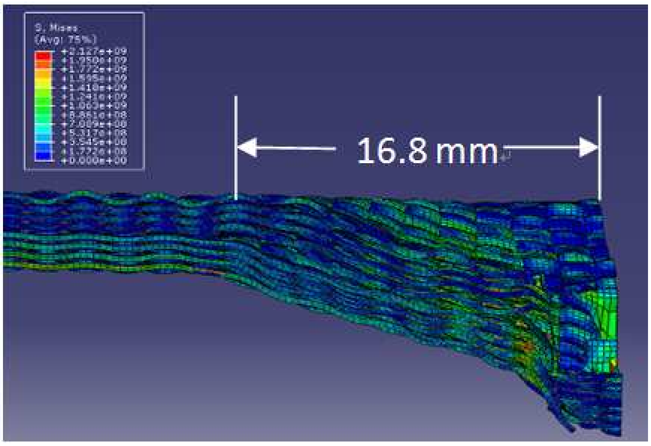

(a) 8-layer woven fabric assembly

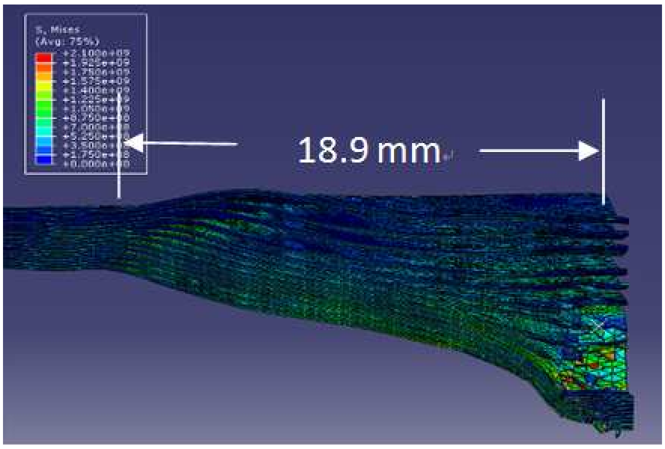

(b) 13-layer UD fabric assembly

Figure 7-22 Transverse deflection for different panels at 20 μs

7.4 Summary

This chapter aims to investigate the response of different layers in a panel upon impact so as to effectively combine different materials to improve the performance of the ballistic panel. In order to facilitate the theoretical analysis of the impact event on multilayer fabrics, the FE model created in Chapter 3 is simplified to reduce computing costs. For this reason, two approaches, model size reduction and mesh modification, were introduced and the results showed that simplifying the model mesh provides a more satisfactory accuracy than the model size reduction.

The FE simulation indicated that fabrics near the impact face tend to fail earlier than those near the back face, which enables rear layers of fabric to have longer engagement time and wider transverse deflection. This being so, a larger area of fabric gets strained and more energy is accumulated in the rear layers. It has also been established that energy is chiefly concentrated in the primary yarns in the front layers and is more equally distributed over the whole fabric in the rear layers. In addition, a strain analysis on the failed element was carried out to investigate the failure mode of different layers in the panel model. It has been found that the front layers of fabric are more likely to be broken in shear, and the rear layers of fabric tend to fail in tension. This suggested that using shear resistant materials for the front layers and tensile resistant materials for the rear layer may improve the ballistic performance of fabric panels.

Two types of structure, Ultra-High-Molecular-Weight Polyethylene (UHMWPE) woven and unidirectional (UD) fabrics, were analysed for their failure mode and response upon ballistic impact by using both FE and experimental methods. It was found that woven structures exhibit better resistance to shear failure and UD structures gives better resistance to tensile failure and wider transverse deflection upon ballistic impact. This indicates that combining the two types of material in a panel may possibly improve its ballistic performance. Hybrid panel engineering and testing will be presented in the next chapter, in detail.

Chapter 8 Engineering Design of Hybrid Ballistic Panels

It has been shown in Chapter 7 that UHMWPE woven fabric is more resistant to shear failure while UD fabric gives higher resistance to tensile failure and modulus. Consequently, it is of importance to further explore the possibility of judiciously combining these fabrics in a panel to improve panel performance. As has been established previously, in a panel under ballistic impact, the front layers of fabric tend to display a shear failure mode, suggesting woven fabric should be placed close to the impact face. Conversely, for the rear layers of fabric, tensile properties and transverse deflection play a more important role in energy absorption. Mixing the two types of fabric in an appropriate sequence is expected to improve the ballistic performance of a panel. The current chapter describes the design and testing of ballistic hybrid panels using UHMWPE woven and UD fabrics. The ballistic range mentioned in Chapter 5 was developed to allow non-penetration tests on fabric panels. An FE model was also employed to provide theoretical predictions for better understanding of the behaviour of hybrid panels upon ballistic impact.

8.1 Hybrid Panel Design

According to the guidance developed in Chapter 7, hybrid panels were designed using UHMWPE woven and UD fabrics. Two factors were taken into consideration in panel design: the packing sequence and the weight fraction of the two types of fabric. In addition, in order to better compare the panel performance, the areal densities of different panels were kept as similar as possible. As has been shown in Table 8-1, woven fabrics were placed in front of the UD fabrics in Type A panel. Type B panels were the reverse. Different weight ratio were also shown in the tables. For instance, '6 layers of woven fabric + 30 layers of UD fabric' indicates that woven fabric accounts for 25% of the panel mass, and UD fabrics 75%, and so forth. Panel details are given in Table 8-1 and Table 8-2. For non-penetration tests, fabric panels, which are made from a sufficient number of layers to stop the projectile, are mounted unclamped against a back face deformation indicating clay block. The clay in use is Roma Plastilina® No.1. In most cases, the panels are not fully perforated, and the ballistic performance of the panels is assessed by the number of fabric layers fractured and the shape and depth of the back face signature.

Table 8-1 Type A panels

Type A panel	**Panel model**	**Areal density(g/m^2)**
40 layers of UD fabric		5,800
6 layers of woven fabric + 30 layers of UD fabric		5,790
12 layers of woven fabric + 20 layers of UD fabric	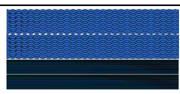	5,780
18 layers of woven fabric + 10 layers of UD fabric	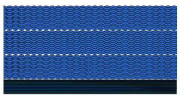	5,770
24 layers of woven fabric	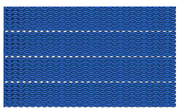	5,760

Table 8-2 Type B panels

Type B panel	**Panel model**	**Areal density(g/m^2)**
24 layers of woven fabric	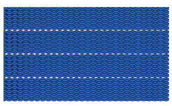	5,760

10 layers of UD fabric + 18 layers of woven fabric		5,770
20 layers of UD fabric + 12 layers of woven fabric		5,780
30 layers of UD fabric + 6 layers of woven fabric		5,790
40 layers of UD fabric		5,800

8.2 Results and Discussion

It can be seen in Figure 8-1 that the combination of 6 layers of woven fabric and 30 layers of UD fabric exhibits the lowest value (6 mm), which indicates its superior performance over other panels. It is found that, beyond this proportion, an increase in the proportion of Dyneema® woven fabrics in the panel leads to an increase in back face signature value. 40 layers of UD fabric panel and the combination of 12 layers of woven and 20 layers of UD fabrics give similar depth (around 8.5mm). The combination of 24 layers of woven fabric gives the worst performance. Figure 8-2 compares the ballistic performance of Type A panels and Type B panels. As can be seen, the results of all the combinations indicate that placing the woven fabrics near the impact face yields better performance than the reverse sequence, which verifies the guidelines developed previously.

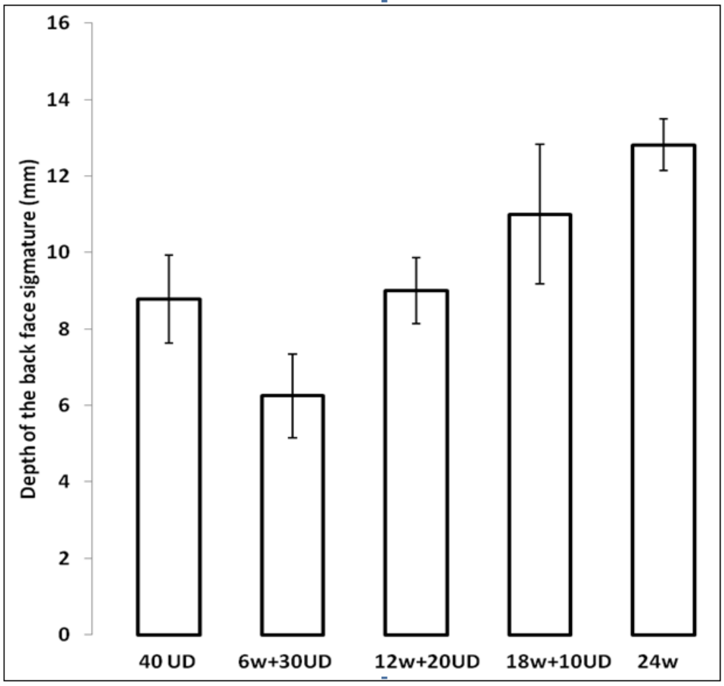

Figure 8-1 Depth of the back face signature for Type A panels

It has been revealed from Figure 8-3 that FE results share a similar trend with those in the ballistic test. One thing worth noting is that the values obtained from simulation are far lower than those from the experiments. This is probably caused by the different boundary conditions, backing material and sample size. In a real test, fabric panels were not fixed on a clamp, but backed by Roma Plastilina®No.1. In simulation, the boundaries were constrained and the backing materials were not simulated. Also, due to the computer power, the sample size in the FE simulation was limited to 5×5 cm. Table 8-3 reveals the depth of back face signature of other combinations in the FE model. It can be seen that the values lie in the vicinity of 3 mm and all the panels prove to have poorer performance than 6 layers of woven fabrics + 30 layers of UD fabrics.

The results shown above reinforce the guidelines developed from the FE model and also the analysis regarding the mechanical properties of woven and UD structures. That is, in panel design, it is desirable to have materials with better resistance to shear damage placed in the front layers and those with better resistance to tensile damage placed in the rear layers. If by special technique it were possible to measure the out-of-plane shear properties of different materials and fabric structures, more combinations in hybrid panel design could be achieved and an improvement in ballistic performance could be expected.

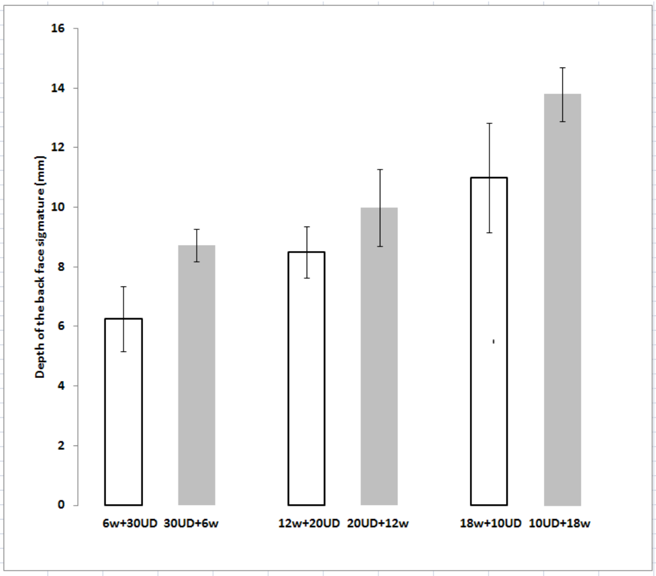

Figure 8-2 Comparison of Type A panels and Type B panels

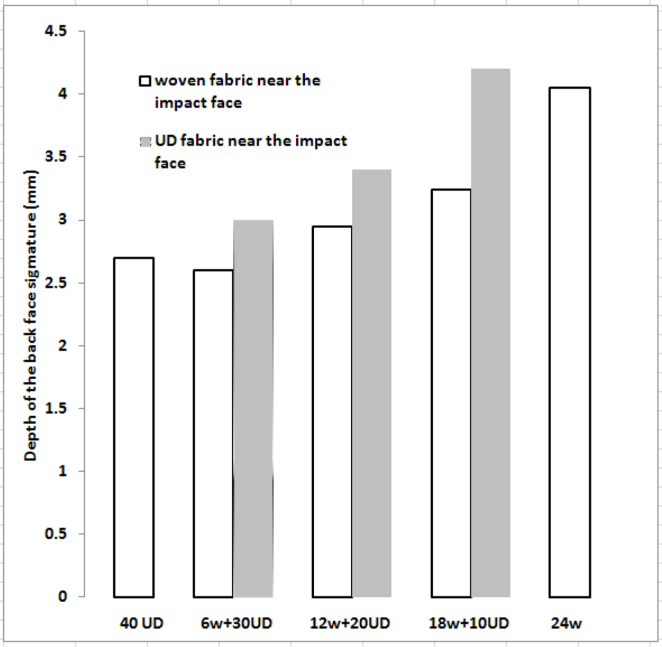

Figure 8-3 Finite element results for Type A panels and Type B panels

Table 8-3 Depth of back face signature of other combinations in simulation

Combinations	Depth (mm)
10UD+6woven+20UD	3.09
20UD+6woven+10 UD	3.1
10UD+12woven+10 UD	3.08
6woven+20UD+6woven	3.2
10UD+6woven+10UD+6woven	2.98
6woven+10UD+6woven+10UD	2.9
12woven+10UD+6woven	3.08
6woven+10UD+12woven	3.125

8.3 Summary

This chapter describes the design and testing process of ballistic hybrid panels. Two types of hybrid ballistic panels were created from the fabrics. The experimental results obtained from non-penetration tests showed that placing woven fabrics close to the impact face and using UD material as the rear layers led to better ballistic performance than the panel constructed in the reverse sequence. It has also been found that the optimum ratio of woven to UD materials in the hybrid ballistic panel was 1:3. The improvement in ballistic protection of the hybrid fabric panels allows less material to be used, leading to lighter weight body armour.

Chapter 9 Conclusions and Future Work

9.1 Conclusions

The aim of this research was to improve the ballistic performance of soft body armour at a reduced weight by using UHMWPE woven fabrics. In order to solve the problem of its low inter-yarn friction and explore its use in ballistic applications, two routes were followed: namely the development of woven fabrics with improved yarn-yarn friction and the engineering of hybrid panels.

Objectives set out for completing this PhD research include: (1) creation of a stable FE model for ballistic impact investigation; (2) a comprehensive investigation of the influence of inter-yarn friction on fabric ballistic performance (3) the development of weaving techniques to achieve an increase in yarn gripping in UHMWPE woven fabrics; (4) a study of the failure mode of different layers of fabric in a panel system; (5) the development of a design guidance for ballistic hybrid panels; (6) conduction of ballistic penetration and non-penetration tests to evaluate the performance of different fabrics and panels.

This research has led to the following conclusions:

(a) Characterisation of the energy dissipation mechanisms on inter-yarn friction increased fabrics:

It has been established from the FE model that the increase in inter-yarn frictional coefficient from $\mu=0$ to $\mu=0.4$ has an effect of increasing fabric energy absorption (from 2.5J to 3.5J). Further increase may restrict yarn movement, which would consequently decrease fabric performance. The mechanisms of inter-yarn friction could be concluded as follows

(1) The lack of inter-yarn friction in a fabric tends to cause slippage between the primary and the secondary yarns, leading the principal yarns to sustain most of the load. This causes the early failure and lower energy absorption of fabrics with low inter-yarn friction.

(2) The existence of friction influences the propagation of longitudinal wave along the primary yarns, causing the stress to be concentrated in the vicinity of the impact point. This explains the fact that excessive increase in inter-yarn friction leads the fabric to fail at an early stage.

(3) Inter-yarn friction enables stress to be distributed to the secondary yarns, which consequently facilitates distributing projectile impact energy to a larger area.

(4) A longer engagement time enables fabric with moderate inter-yarn coefficient of friction to absorb more strain energy in both the primary and secondary yarns.

(5) Energy dissipated by friction is another energy absorption sink for woven fabric. Increasing inter-yarn friction enables more energy to be absorbed through this mechanism. Too much friction may create a resistance to the relative movement between yarns and limit the amount of energy dissipated.

(b) Design and testing of the ballistic performance of structure modified woven fabrics

In the present work new weaving techniques have been employed to modify the structure of plain woven fabric based on the capstan equation. This enables the increase in yarn gripping by changing the crimp of weft and warp yarns in a designated area without affecting the yarn path of the rest of the fabric. Another achievement is that mass-production of gripping fabric on power looms becomes available, which possibly reduces manufacturing time and cost when compared to chemical treatment based techniques. The increase in yarn gripping in UHMWPE woven fabric is verified by yarn pull-out testing. For instance, the insertion of leno structure gives a peak load force of 2.99N for the PWL02, which is 0.75N higher than that of the PW. Although the increase in energy absorption is not as noticeable as for Kevlar woven fabrics, this approach has been proved to have better potential for the performance improvement of soft body armour.

(c) Identification of the failure mode of different layers in a ballistic panel

It has been determined in the FE model that fabrics near the impact face tend to fail earlier than those near the back face. The longer engaging time enables rear layers of fabric to have wider transverse deflection and to have larger areas of fabric become stressed due to the ballistic event which increases fabric energy absorption. Also, that energy is more locally concentrated in the primary yarns in the front layers of fabric. For the rear layers of fabric energy is more equally distributed on the whole fabric. By defining both tensile and shear failure criteria for the material, FE models show that the front layers of fabric are more likely to be broken in shear, and the rear layers of fabric tend to fail in tension.

(d) Development and verification of panel design guidance

The FE result suggested that using shear resistant materials for the front layer and tensile resistant materials for the rear layer may improve the ballistic performance of fabric panels. Two types of structure, UHMWPE woven and UD fabrics, were analysed for their failure mode and response upon ballistic impact by using both FE and experimental methods. It was found that the woven fabric gives better resistance to shear failure and the UD fabric shows better resistance to tensile failure. Hybrid panels consisting of the two types of fabric were designed and both FE and experimental results showed that placing woven fabrics close to the impact face and UD material as the rear layers led to better ballistic performance than the panel constructed in the reverse sequence. It has also been found that the optimum ratio of woven to UD materials in the hybrid ballistic panel was 1:3. The improvement in ballistic protection of the hybrid fabric panels allows less material to be used, leading to lighter weight body armour.

9.2 Recommendations for Future Research Work

A number of future recommendations could be set as continuations to the current work.

It has been established that the less noticeable improvement in the performance of UHMWPE woven fabric could be attributed to the low increase in yarn gripping, which is probably caused by its low inter-yarn friction and high bending stiffness. It is possible to further increase the influence of leno insertion by increasing leno yarn tension or using yarns with higher friction such as Kevlar. Another solution is to apply quilting to the fabric so that weft and warp yarns are completely locked by the stitch. One of the advantages of this approach over structure modification is that it eliminates the lines of weakness, which significantly improves the usefulness of gripping fabrics.

The ballistic range should be improved for its accuracy. Projectile tumbling and the variation of impact velocity are major problems which lead to data randomness when performing penetration test. It is suggested to use spherical projectile and stabilize the impact velocity of a projectile. In addition, testing should be extended to comparatively low velocities impact. This would allow a more comprehensive investigation of fabric performance at different impact velocities.

One of the recommendations for the investigation of gripping fabrics is to characterize the geometry of leno weave in woven fabrics and to enable it to be more precisely presented and incorporated in FE models.

In order to perfect the design guidance, it is desirable to combine other types of fabric in a ballistic panel. FE simulation and non-penetration tests could be employed to undertake this parametric and practical study on the ballistic performance of hybrid panels. It is also recommended to develop a testing rig and procedure to directly evaluate the materials resistance to shear failure, which will facilitate the characterisation of fabric properties and panel design.

References

1. Olive-Drab. *Body Armor (Flak Jackets) Post WW II*. Available at: http://olive-drab.com/od_soldiers_gear_body_armor_korea.php [cited 2012].
2. Yang, H.H., *Kevlar Aramid Fiber*. 1992, New York: John Wiley &Sons Ltd.
3. Farjo., L.A. and Miclau, T., *Ballistics and Mechanisms of Tissue Wounding* Injury, 1997. **28**: p. 12-17.
4. Roberts, J.C., Biermann, P.J., O'Connor, J.V., Ward, E.E., Cain, R.P., Carkhuff, B.G. and Merkle, A.C., *Modeling Nonpenetration Ballistic Impact on a Human Torso.* Johns Hopkins APL Technical Digest, 2005. **26**.
5. Mabry, R.L., Holcomb, J.B., Baker, A.M., Cloonan, C.C., Uhorchak, J.M., Perkins, D.E., Canfield, A.J. and Hagmann, J.H., *United States Army Rangers in Somalia: An Analysis of Combat Casualties on an Urban Battlefield.* The Journal of Trauma At Injury, Infection, and Critical Care, 2000. **49**.
6. Peleg, K., Rivkind, A. and Aharonson-Dame, L., *Does Body Armor Protect From Firearm Injuries?* J. Am. Coll. Surg, 2006. **202**: p. 643-648.
7. Brown, D., *War in Iraq Showed Body Armour*, in *Washington Post*. 2003: Washington. p. 28.
8. Latourrette, T., *The Life-Saving Effectiveness of Body Armor for Police Officers.*

Journal of Occupational and Environment Hygiene, 2010,. **7**: p. 557-562.

9. visiongain, *The Military Body Armour & Personal Protective Gear Market 2012-2022*. 2012: New York

10. Husaybah, *Marines Reject Overweight Body Armour*, in *the Age*. 2006.

11. Walsh, P.J., Hu, X., Cunniff, P. and Lesser, A.J., *Environmental Effects on Poly-p-phenylenebenzobisoxazole Fibers. I. Mechanisms of Degradation.* Journal of Applied Polymer Science, 2006. **102**: p. 3517-3525.

12. Liu, X. and Yu, W., *Degradation of PBO Fiber by Heat and Light.* Research Journal of Textile and Apparel, 2006. **10**: p. 26-32.

13. Cunniff, P.M. and Auerbach, M.A., *High Performance "M5" Fiber For Ballistic /Structure Composite* 2012.

14. Drury, I., *Bullet-Proof Custard: British Soldiers Could be Wearing Revolutionary New Liquid Body Armour Within Two Years*, in *Daily Mail*. 2011: London.

15. Dingenen, J.L.V., *Gel-Spun High Performance Polyethylene Fibres* in *High Performance Fibres*, H. J.W.S, Editor. 2001, Woodhead publishing and Maney Publishing limited: Cambrige. p. 70.

16. Bazhenov, S., *Dissipation of Energy by Bulletproof Aramid Fabric.* Journal of Material Science, 1997. **32**: p. 4167-4173.

17. Briscoe, B.J. and Motamedi, F., *The Ballistic Impact Characters of Aramid Fabrics: The Influence of Interface Friction.* Text Res J, 1992. **158**: p. 229-247.

18. Duan, Y., Keefe, M., Bogetti, T.A., Cheeseman, B.A. and Powers, B, *A Numerical Investigation of Influence of Friction on Energy Absorption by A High-Strength Fabric Subjected to Ballistic Impact.* International Journal of Impact Engineering, 2006. **32**(8): p. 1299-1312.

19. Zeng, X.S., Tan, V.B.C and Shim, V.P.W., *Modelling Inter-Yarn Friction in Woven Fabric Armour.* International Journal of Impact Engineering, 2006. **66**(8): p. 1309-1330.

20. Sun, D. and Chen, X., *Development of Improved Body Armour: MoD Progress*

Report. 2010: Manchester.

21. Lee, B.L., Song, J.W. and Ward, J.E., *Failure of Spectra Polyrthylene Fibre-Reinforced Composites Under Ballistic Impact Loading.* Journal of Composite Materials, 1994. **28**: p. 1202-1225.

22. Scott, B.R. *The Penetration of Compliant Laminates by Compact Projectiles*. in *Proceedings of the 18th international symposium on ballistics* 1999. San Antonio, Texas, U.S.A.

23. Gu, B., *Analytical Modeling for The Ballistic Perforation of Planar Plain-Woven Fabric Target by Projectile.* Compos Pt B, 2003. **34**: p. 361-371.

24. Roylance, D., Wilde, A and Tocci, G., *Ballistic Impact of Textile Structures.* Textile Research Journal, 1973. **43**: p. 34-41.

25. Ursenbach, D.O., *Penetration of CFRP Laminates by Cyclindrical Indenters*. 1995, the University of British Columbia.

26. Cantwell, W.J. and Morton, J., *Comparison of The Low And High Velocity Impact Response of CFRP.* Composite, 1989. **20**(6): p. 545-551.

27. Cantwell, W.J. and Morton, J., *Impact Perforation of Carbon Fibre Reinforced Plastic.* Composite, 1990. **38**(2): p. 119-141.

28. Carr, D.J., *Failure Mechanisms of Yarns Subjected to Ballistic Impact.* Mater Sci J, 1995. **18**: p. 585-588.

29. Roylance, D., *Stress Wave Propagation In Fibres: Effect of Crossoves.* Fibre science and technology 1980. **13**: p. 385-395.

30. Freeston, W.D., *Strain wave reflections during ballistic impact of fabric panels.* Text Res J, 1973. **43**: p. 348-351.

31. Tan, V.B.C., Lim, C.T. and Cheong, C.H., *Perforation of High-Strength Fabric by Projectiles of Different Geometry.* International Journal of Impact Engineering, 2003. **28**: p. 207-222.

32. Starratt, D., Pageau, G., Vaziri, R and Pourartip A. *An Instrumented Experimental Study of the Ballistic Impact Response of Kevlar Fabric*. in *Proc. 18th*

international symposium on ballistics. 1999.

33. Kirkwood, K.M., Wetzel, E.D. and Kirkwood, J.E., *Yarn Pull-Out as A Mechanism for Dissipating Ballistic Impact Energy in Kevlar KM-2 Fabric, Part 1: Quasi-Static Characterization of Yarn Pull-Out.* Textile Research Journal, 2004. **74**: p. 920-928.

34. Kirkwood, K.M., Wetzel, E.D. and Kirkwood, J.E., *Yarn Pull-Out as A Mechanism for Dissipating Ballistic Impact Energy in Kevlar KM-2 Fabric, Part 2: prediction of ballistic performance.* Text Res J, 2004. **74**: p. 939-948.

35. Shim, V.P.W., Tan, V.B.C. and Tay, T.E., *Modelling Deformation and Damage Characteristics of Woven Fabric Under Small Projectile Impact.* International Journal of Impact Energy, 1995. **6**: p. 605.

36. Lim, C.T., Tan, V.B.C. and Cheong, C.H., *Perforation of High-Strength Double-Ply Fabric System by Varying Shape Projectiles.* Journal of Impact Science, 1989. **28**: p. 160-172

37. Cheeseman, B.A. and Boggeti, T.A., *Ballistic Impact Into Fabric and Compliant Composite Laminates.* Composite Structure, 2003. **61**: p. 161-173.

38. Tabiei, A., *Ballistic Impact of Dry Woven Fabric Composites: A Review.* Applied Mechinics, 2008. **61**.

39. Shahkarami, A., Cepus, E., Vaziri, R. and Poursartip, A., *Material Responses To Ballistic Impact*, in *Lightweight Ballistic Composite*, A. Bhatnagar, Editor. 2006, Woodhead Publishing Limited and CRC Press LLC: Cambridge. p. 82-95.

40. Prosser, R.A., Cohen, S.H. and Segars, R.A., *Heat as A Factor in the Penetration of Cloth Ballistic Panels by 0.22 Caliber Projectiles.* Textile Research Journal, 2000. **70**(8): p. 709-722

41. Roylance, D., *Influencee of Fibre Propeerties On Ballistic Penetration of Textile Panels* Fibre science and technology, 1981. **14**: p. 183-190.

42. Lee, B.L., Walsh, T.F., Won, S.T., Patt, H.M., Song, J.W and Mayer A.H., *Penetration Failure Mechanisms of Armour-Grade Fibre Composite Under Impact.*

Journal of Composite Material 2001. **35**: p. 1605-1633.

43. Smith, J.C., McCrackin, F.L. and Schniefer, H.F, *Stress-Strain Relationships in Yarns Subjected to Rapid Impact Loading (Part 5: Wave Propagation in Long Textile Yarns Impacted Transversely).* Textile Research Journal, 1956. **28**(4): p. 288-302.

44. Field, J.E. and Sun, Q. *A High Speed Photographic Study of Impact On Fibres and Woven Fabrics*. in *proceedings of the 19th international congress on high speed photography and photonics*. 1990.

45. Roylance, D., *Ballistic of Transversely Impacted Fibres.* Textile Research Journal, 1977. **47**: p. 697.

46. Cunniff, P.M. *Dimensionless Parameters for Optimization of Textile Based Body Armour Systems*. in *Proceedings of the 18th International Symposium on Ballistics*. 1999. San Antonio, Texas.

47. Sierakowski, R.L. and Chaturvedi, S.K., *Dynamic Loading and Characterization of Fiber Reinforced Composites*. 1997, NY: John Wiley & Sons, Inc. 17.

48. Wang, Y. and Xia, Y., *Experimental and theoretical study on the strain rate and temperature dependence of mechanical behaviour of Kevlar fibre.* Compos Pt A, 1999. **30**: p. 1251-1257.

49. Wang, Y. and Xia, Y., *The Effect of Strain Rate On The Memechanical Behaviour of Kevlar Fibre Bundles: An Experimental And Theoretical Study.* Compos Pt A, 1998. **29A**: p. 1411-1415.

50. Lim, J., Chen, W. and Zheng, J., *Dynamic small strain measurements of Kevlar 129 fingle fibers with a miniaturized tension Kolsky bar.* Polymer Testing, 2010. **29**: p. 701-705.

51. Kinari, T., Hojo, A. and Chatani, A. *An Impact Testing Apparatus for Yarn And Mechanical Properties of Aramid Fibre Yarn at High Strain Rates* in *Proceedings of the 33rd Japan congress on Materials Research, p. 87-91*. 1990.

52. Cunniff, P.M., *An Analysis of The System Effects of Woven Fabrics Under Ballistic*

Impact. Textile Research Journal, 1992: p. 495-509.

53. Rao, Y. and Farris, R., *A Modeling and Experimental Study of the Influence of Twist on and Mechanical Properties of High-Performance Fibre Yarns.* Journal of Applied Polymer Science, 2000. **77**: p. 1938-1949.
54. Song, W.J., *Fabrics and Composites for the Ballistic Protection of Personnel*, in *Lightweight Ballistic Composite*, A. Bhatnagar, Editor. 2006, Woodhead publishing and Maney publishing limited.
55. Yang, D., *Design, Performance And Fit of Fabric For Female Body Armour* in *School of materials*. 2010, university of manchester: manchester.
56. Shi, W., Hu,H., Sun,B. and Gu, B., *Energy Absorption of 3D Orthogonal Woven Fabric Under Ballistic Penetration of Hemispherical-Cylindrical Projectile.* The journal of textile institute, 2011. **102**: p. 875-889.
57. Shockey, D.A., Erlich, D.C. and Simons, J.W., *Improved Barriers to Turbine Engine Fragments, Interm Report Ⅲ.* 2001.
58. Chitrangad(Midlothian, V., *Hybrid Ballistic Fabric* 1993, E. I. du Pont de Nemours and Company (Wilmington, DE)
59. Hu, J., *Structure And Mechanics of Woven Fabics*. 2004, Cambridge: Woodhead Publishing Ltd and CRC Press LLC. P. 92.
60. Tan, V.B.C., Shim, V.P.W and Zeng, X., *Modelling Crimp in Woven Fabrics Subjected to Ballistic Impact.* International Journal of Impact Engineering, 2005. **32**(561-574).
61. Hearle, J.W.S., Leech,C.M., Adeyefa,A., and Cork, C.R., *Ballistic Impact Resistance of Multi-Layer Textile Fabrics* 1981, University of manchester institute of science and technology: Manchester. p. 33.
62. Scott, B.R., in *Lightweight Ballistic Composite*, A. Bhatnagar, Editor. 2006, Woodhead publishing and Maney publishing limited, Cambrige, .
63. Scott, B.R., *New ballistic products and technologies*, in *Lightweight Ballistic Composites*, A. B, Editor. 2006, Woodhead publishing and Maney publishing

limited and CRC Press LLC: Cambridge. p. 348.

64. Karahan, M., *Comparison of Ballistic Performance and Energy Absorption Capabilities of Woven and Unidirectional Aramid Fabrics.* Text Res J, 2008. **78**(8): p. 718–730.

65. Hearle, J.W.S., *Research on A Basic Study of The High Speed Penetration Dynamics of Textile Materials*. 1974, University of Manchester Institute of Science and Technology: Manchester. p. 51.

66. Thomas, H.L., *Needle-Punched Non-Woven Fabric for Fragmentation Protection.* PASS, 2004.

67. Shockey, D.A., Erlich, D.C. and Simons, J.W., *Improved Barriers to Turbine Engine Fragments: Interim Report Ⅳ.* 2002.

68. Porwal, P.K. and Phoenix, S.L., *Effect of Layer Stacking Order on the V50 Velocity of a Two-Layered Hybrid Armour System* Journal of Mechanics of Materials and Structures, 2008. **3**: p. 627-639.

69. Cunniff, P.M. and Ting, J. *Decoupled Response of Textile Body Armour*. in *Proceedings of the 18th international symposium of ballistics, p. 814-821*. 1999.

70. Novotny, W.R., Cepus,E., Shahkarami, A., Vaziri, R. and Poursartip, A., *Numerical Investigation of The Ballistic Efficiency of Multi-Ply Fabric Armours During The Early Stages of Impact.* International Journal of Impact Engineering, 2007. **34**: p. 71-88.

71. Nader, J. and Dagher, H., *3D Hybrid Ballistic Fabric Testing Using A 3D Dgital Image* Experimental Techniques, 2011: p. 55-60.

72. Chen, X., Zhu, F. and Wells, G., *An Analytical Model for Ballistic Impact on Textile Based Body Armour.* Composites part b:engineering, 2012.

73. Thomas, G.A., *Non-Woven Fabrics for Military Applications*, in *Military Textiles*, W. E, Editor. 2008, Woodhead publishing and Maney Publishing limited: Cambrige. p. 47-48.

74. Karahan, M., Kus, A., Eren, R. and Karahan, N, *Investigation of Ballistic*

Properties of Woven-unidirectional Hybrid Panels according to Energy Absorption Capabilities, in *SAMPE’07 Conference*. 2007: Baltimore, MD, USA.

75. Price, A.L., Sun, R. and Young, S.A., *Ballistic Vest*. 1999, Safariland Ltd., Inc. (Ontario, CA)

76. Shahkarami, A., Cepus, E., Vaziri, R. and Poursartip, A., *Material Responses To Ballistic Impact*, in *Lightweight Ballistic Composite*, A. Bhatnagar, Editor. 2006, Woodhead Publishing Limited and CRC Press LLC: Cambridge. p. 77.

77. Tan, V.B.C., Tay, T.E.and Teo, W.K. , *Strengthening Fabric Armour With Silica Colloidal Suspensions.* International Journal of Solids and Structures, 2005. **52**: p. 1561–1576.

78. Lee, B.W., Kim, I.J. and Kim*, C.G. , *The Influence of the Particle Size of Silica on the Ballistic Performance of Fabrics Impregnated with Silica Colloidal Suspension.* Journal of Composite Materials, 2009. **43**: p. 2679-2698.

79. Young, S.L., Wagner, N.J and Wetzel, E.D., *The Ballistic Impact Characteristics of Kevlar Woven Fabrics Impregnated With A Colloidal Shear Thickening Fluid.* JOURNAL OF MATERIALS SCIENCE, 2003. **38**: p. 2825 – 2833.

80. Barnes, H.A., *Shear-Thickening ("Dilatancy") in Suspensions of Nonaggregating Solid Particles Dispersed in Newtonian Liquids.* Journal of Rheology, 1989. **33**: p. 329-366.

81. Chitrangad (Midlothian, V. and Rodriguez-parada., J., M (Wilmington, DE) *Fluorinated Finishes for Aramids* in *United State Patent*. 1993, E. I. du Pont de Nemours and Company (Wilmington, DE): U.S.

82. Dischler, L., (Spartanburg, SC) *Bullet Resistant Fabric and Method of Manufacture* 2001, Milliken & Company (Spartanburg, SC)

83. Hogenboom, E.H.M. and Bruinink, P., *Combinations of Polymer Filaments or Yarns Having A Low Coefficient of Friction and Filaments or Yarns Having A Hight Coefficient of Friction, and Use Therefore*, U.S. Patent, Editor. 1991, Stamicarbon, B.V., Geleen, Netherland: United States. p. 3.

84. Shockey, D.A., Erlich, D.C and Simons, J.W., *Improved Barriers to Turbine Engine Fragments: Interim Report Ⅱ*. 1999.

85. Talebi, H., Wong, S.V., and Hamouda, A.M.S., *Finite Element Evaluation of Projectile Nose Angle Effects in Ballistic Perforation of hHigh Strength Fabric.* Composite Structures, 2009. **87**: p. 314-320.

86. Cunniff, P.M. *The V50 Performancee of Body Armour Under Oblique Impact*. in *proceedings of the 18th international symposium on ballistics*. 1999. San Antonio: TX, pp 814-821.

87. Montgomery, T.G., Grady, P.L. and Tomasin, C., *The Effect of Projectile Geometry on the Perfoemance of Ballistic Fabrics.* Textile Research Journal, 1982. **52**: p. 442-450.

88. Shockey, D.A., Erlich, D.C. and Simons, J.W., *Improved Barriers to Turbine Engine Fragments, Interm Report Ⅰ*. 2001.

89. Chitrangad, M., *Ballistic Structure*, in *United States Patent*. 1994, E.I.Du pont de Nemours and Company, Wilmington, Del U.S.

90. Zeng, X.S., Shim,V.W., and Tan, V.B.C., *Influence of Boundary Conditions On The Ballistic Performance Of High-Strength Fabric Targets.* International Journal of Impact Engineering, 2005. **32**: p. 631-642.

91. Susich, G., Dogliotti, L. M. and Wrigley, A.S., *Microscopical Study of a Multilayer Nylon Body Armor Panel After Impact.* Textile Research Journal, 1958. **28**: p. 361-377.

92. Wilde, A.F., Roylance, D.K., and Rogers, J.M., *Photographic Investigation of High Speed Missile Impact upon Nylon Fabric Part 1: Energy Absorption and Cone Radial Velocity in Fabric.* Text Res J, 1973. **43**: p. 753-761.

93. Schmidt, T., Tyson, J. and Galanulis, K., *Full-Field Dynamic Deformation And Strain Measurement Using High-Speed Photography And Photonics*, in *26th international congress on high-speed photography and photonics*. 2005.

94. Nurick, G.N., *A New Technique to Measure The Deflection-Time History of A*

Structure Subjected to High Strain Rates. international journal of impact Engineering, 1985. **3**: p. 17-26.

95. Ramesh, K.T. and Kelkar, N., *Technique for The Continuous Measurement of Projectile Velocities In Plate Impact Experiments.* Review of science instrument, 1995. **66**(4): p. 3034-3036.

96. Kocer, H., B, *Laminated and Hybrid Soft Armour System for Ballistic Application*. 2007, Auburn University: Auburn,Turkey.

97. Shim, V.P.W., Lim, C.T. and Foo, K.J., *Dynamic Mechanical Properties of Fabric Armour.* International Journal of Impact Engineering, 2001. **25**: p. 1-15.

98. Prosser, R.A., *Penetration of Nylon Ballistic Panels by Fragment Simulation Projectiles, Part 2: Mechanism of Penetration.* Textile Research Journal, 1988. **58**: p. 616-165.

99. Wilde, A.F., *Photographic Investigation of High Speed Missile Impact upon Nylon Fabric Part 2: Retarded Force on Missile and Transeverse Critical Velocity.* Text Res J, 1974. **44**: p. 772-778.

100. Bhatnagar, A., *Standard and Specification for Lightweight Ballistic Materials* in *Lightweight Ballistic Composite*, B. Ashock, Editor. 2006, Woodhead publishing and Maney Publishing limited: Cambrige. p. 129.

101. Abiru, S. and Lizuka, K., *Bulletproof Fabric and Process for Its Production*, in *U.S Patent*. 1999, Toyo Boseki Kabushiki Kaisha U.S. p. 1.

102. Price, A.L., (Rising Sun, MD) and Young, S.A., (Richmond, VA) *Ballistic Vest*. 1999, Safariland Ltd., Inc. (Ontario, CA)

103. Figucia, F. *Energy Absorption of Kevlar Fabrics Under Ballistic Impact*. in *Proceedings for Army Science Conference, p.29-41*. 1982.

104. NIJ. *Ballistic Resistance of Body Armour NIJ Standard-0101.06*. Available at: https://www.ncjrs.gov/pdffiles1/nij/223054.pdf [cited 2013].

105. Croft, J. and Longhurst, D., *Home Office Scientific Development Branch (HOSDB) Body Armour Standards for UK Police (2007) Part 2: Ballistic Resistance*. 2007: p.

11-12.

106. Lomakin, E.V., Mossakovsky, P.A., Bragov, A. M., Lomunov, A.K., Konstantinov, A.Y., Kolotnikov, M.E., Antonov, A.K., Vakshtein, M.S *Investigation of Impact Resistance of Multilayered Woven Composite Barrier Impregnated With the Shear Thickening Fluid.* 2011.

107. Bilisik, K. and Korkmaz, M., *Multilayered and Multidirectionally-Stitched aramid Woven Fabric Structures: Experimental Characterization of Ballistic Performance by Considering the Yanr Pull-Out Test.* Text Res J, 2010. **80**: p. 1697-1720.

108. Lee, Y.S., Wetzel, E.D. and Wagner, N.J., *The Ballistic Impact Performance of Kevlar Woven Fabric Impregnated with A Colloidal Shear Thickening Fluid.* Journal of Materials, 2003. **38**: p. 2825-2833.

109. Chocron-Benloulo, I.S., Rodriguez, J. and V, S.-G., *A Simple Analytical Model To Simulate Textile Fabric Ballistic Behavior.* Text Res J, 1997. **67**(7): p. 520-528.

110. Parga-Landa, B. and Hernandez-Olivares, F., *An Analytical Model to Predict Impact Behaviour of Soft Armors.* international Journal of Impact Engineering, 1995. **16**(3): p. 455-466.

111. Porwal, P.K. and Phoenix, S.L., *Modeling System Effects in Ballistic Impact Into Multi-Layered Fbrous Materials for Soft Body Armour.* International Journal of Fracture, 2005. **135**: p. 217-249.

112. Roylance, D. and Wang, S.S., *Penetration Mechanism of Textile Structure.* Ballistic Material and Penetration Mechanics, 1980: p. 272-294.

113. Billon, H.H. and Robinson, D.J., *Models for The Ballistic Impact of Fabric Armour.* international Journal of Impact Engineering, 2001. **25**: p. 411-422.

114. Gu, B., *Ballistic Penetration of Conically Cylindrical Steel Projectile into Plain-Woven Fabric Target - A Finite Element Simulation.* Journal of composite Materials, 2004. **38**: p. 2094-2074.

115. Zhang, G.M., Batra, R.C. and Zheng, J., *Effect of Frame Size Frame Type and Clamping Pressure on the Ballistic Performance of Soft Body Armour.* Compos Pt

B.

116. Duan, Y., Keefe, M., Boggitti, T.A. and Cheeseman, B.A., *Modelling Friction Effects on the Ballistic Impact Behaviour of A Single-Ply High-Strength Fabric.* International Journal of Impact Engineering, 2004. **31**: p. 996-1012.

117. Duan, Y., Keefe, M., Boggeti, T.A. and Powers, B., *Finite Element Modeling of Transverse Impact on A Ballistic Fabric.* International Journal of Mechanical Science, 2006. **48**: p. 33-43.

118. Rao, M.P., Duan, Y., Keefe, M., Powers, B.M. and T.A, B., *Modelling The Effects of Yarn Material Properties And Friction On The Ballistic Impact of A Plain-Weave Fabric.* Composite Structures, 2009. **89**: p. 556-566.

119. Jin, L., Sun,B. and Gu, B., *Finite Element Simulation of Three-Dimensional Angle-Interlock Woven Fabric Undergoing Ballistic Impact.* The journal of textile institute, 2011: p. 1-12.

120. Shahkarami, A. and Vaziri, R., *A Continuum Shell Finite Element Model For Impact Simulation of Woven Fabrics.* International Journal of Impact Engineering, 2007. **34**: p. 104-119.

121. Kawabata, S., Niwa,M., and Kawai, H., *The Finite-Deformation Theory of Plain-Weave Fabrics Part 1: The Biaxial-Deformation Theory* Journal of the Textile Institute 1973. **64**(1): p. 21-46.

122. Grujicic a, M., Bell,W.C., Arakere, G., Hea,T., and Cheeseman, B.A., *A meso-scale unit-cell based material model for the single-ply flexible-fabric armor.* Materials and Design 2009. **30**: p. 3690-3704.

123. ABAQUS.Inc. *ABAQUS Documentation*. Availalbe at: http://abaqus.ethz.ch:2080/v6.11/books/gsa/default.htm [cited 2013].

124. Peirce, F.T., *The Geometry of Cloth Structure.* The journal of textile institute, 1937. **28**(3): p. 45-96.

125. Kemp, A., Textile Research Journal, 1958. **49**.

126. Shanahan, W.J. and Hearle, J.W.S., *An Energy Method for Calculations in Fabric*

Mechanics, Part 2: Examples of The Application of The Methods to Woven Fabrics. Textile Research Journal, 1978. **69**: p. 92-100.

127. Hearle, J.W.S., Potluri, P. and Thammandra, V.S., *Modelling Fabric Mechanics.* Textile Research Journal, 2001: p. 53-69.

128. ASTM. *Standard Test Method for Coefficient of Friction, Yarn to Yarn. ASTM D3412*. Avaialble at: http://www.spsp.gov.cn/Page/AS/2001/ASTM%20D3412-2001.shtml [cited 2013].

129. Grujicic, M., Arakere, G., Cheeseman, B.A., He1, T. and Gogulapati, M., *A Numerical Investigation of The Influence of Yarn-Level Finite-Element Model on Energy Absorption by A Flexible-Fabric Armour During Ballistic Impact,.* Materials: Design and Applications, 2008. **222**: p. 259-276.

130. DSM, *DSM Dyneema high-strength, high-modulus polyethylene fiber fact sheet* 2008.

131. Sherburn, M., *Geometric And Mechanical Modeling of Fabric Compression*. 2007, Nottingham University: Nottingham. p. 146.

132. Lin, H., Sherburn, M., Crookston, J., Long, A.C., Clifford, M.J. and Jones, I.A., *Finite Element Modelling of Fabric Compression.* Mater.Sci.Eng, 2008. **16**: p. 1-16.

133. Kawabata, S., *Measurement of the Transverse Mechanical Properties of High-performance Fibres.* Journal of Textile Institute 1990. **81**(4): p. 432-447.

134. Sadykova, F.K., *The Poisson ratio of Textile Fibres And Yarns.* Fibre Chem, 1972. **3**: p. 345-345.

135. Finlayson, D., *The Shear Strength of Filaments And Fibres.* journal of Textile Institute, 1947. **38**: p. 51-53.

136. Boedeker. *Polyethylene Specifications*. Avaialble at: http://www.boedeker.com/polye_p.htm [cited 2010].

137. Bunsell, A.R., *Chapter 10. Compressive Strength*, in *Composite material series-2.*

1988: Amsterdam.

138. Sebastian, S., Bailey, A.I., Briscoe, B.J and Tabor, D., *Extensions, Displacements and Forces Associated with Pulling A Single Yarn From A Fabric.* Journal of Physics, 1987: p. 130-139

139. Ahmed, A.Y., *Physical Properties of Leno Fabrics*, in *Institute of Science and Technology*. 1972, Victoria University of Manchester: Manchester.

140. Cork, C.R. and Foster, P.W., *The Ballistic Performance of Narrow Fabrics.* International Journal of Impact Engineering, 2007. **34**: p. 495-508.

141. Sun, D., Mrango,M and Chen, X., *Investigating Ballistic Impact On Fabric Targets With Gripping Yarns.* Fibres and Polymers, 2013. **14**(7): p. 1184-1189.

142. Sun, D., Chen,X. and Wells, G., *Engineering And Analysis of Gripping Fabrics For Improved Ballistic Performance.* Journal of Composite Materials, 2013: p. 1-10.

143. GoodFellow. *Polyethylene -UHMWPE Material Information* Availabe at: http://www.goodfellow.com/E/Polyethylene-UHMW.html [cited 2011].

144. Morton, W.E. and Hearle, J.W.S., *The Physical Properties of Textile Fibres*. 1993, Manchester: The Textile Institute. 401.

145. Arshad, H., Ramgulam,R. and Potluri, P., *Mechanics of Flexible Textile Composites*, in *17th International Conference on Composite Materials*. 2011: Edingburgh.

146. Krook, C.M. and Fox, K.R., *Study of The Tongue-Tear Test.* Textile Research Journal, 1945. **15**.

147. Abbott, N.J., Lannefeld, T.E., Barish, L. and Brysson, R.J., Journal Coated Fibrous Materials, 1971. **1**: p. 4-16.

148. Hu, J., *Structure And Mechanics of Woven Fabics*. 2004, Cambridge: Woodhead Publishing Ltd and CRC Press LLC. P. 91.

149. Russell, B.P., Kandan,K., Deshpande,V.S., and Fleck, N.A. *The High Strain Rate Response of UHMWPE:From Fibre to Laminate*. Available at:

http://www-mech.eng.cam.ac.uk/profiles/fleck/papers/294.pdf [cited 2012].

Appendix

Table 1 Thickness of UHMWPE woven fabric

Sample number	**Thickness of UHMWPE woven fabric (mm)**
1	0.398
2	0.381
3	0.366
4	0.374
5	0.383
Mean	0.380
Std.dev	0.0118
CV%	3.1

Table 2 Coefficient of friction between a metal pin and UHMWPE woven fabric

Sample number	**Coefficient of friction between a projectile and UHMWPE woven fabric**
1	0.196
2	0.16
3	0.16
4	0.18
5	0.173
Mean	0.174
Std.dev	0.0151
CV%	8.6

Table 3 Results of yarn pull-out tests for method A and Method B on plain woven fabrics in the weft direction

Sample number	Peak load force for method A (N)	Peak load force for method B (N)
1	3.839	2.282
2	4.16	2.322
3	2.996	2.2
4	3.611	2.188
5	3.168	2.389
6	3	2.282
7	3.396	2.054
8	3.624	2.282
Mean	3.47	2.249
Std.dev	0.417	0.10
CV%	12	4.5

Table 4 Results of yarn pull-out tests for UHMWPE woven fabrics in the weft direction

Sample number	Peak load force for PWL02 (N)	Peak load force for PWL03 (N)
1	3.047	2.56
2	2.819	2.35
3	2.26	2.64
4	3.168	2.66
5	2.899	2.4
6	2.889	2.54
7	2.94	2.56
8	2.953	2.54
Mean	2.99	2.531
Std.dev	0.15	0.107
CV%	5.01	4.22

Table 5 Results of yarn pull-out tests for UHMWPE woven fabrics in the warp direction

Sample number	Peak load force for PW (N)	Peak load force for PWL03DW (N)	Peak load force for PWL02WC (N)
1	2.564	2.886	3.248
2	2.537	3.02	3.195
3	2.55	3.047	2.966
4	2.557	3.02	3.168
5	2.416	3.047	3.181
6	2.644	2.993	3.128
7	2.497	3.168	2.996
8	2.711	3.065	2.913
Mean	2.599	3.03	3.095
Std.dev	0.08	0.07	0.12
CV%	3.07	2.3	3.8

Table 6 Ballistic test results for PW

Sample number	Impact velocity (m/s)	Residual velocity (m/s)	Projectile kinetic energy loss (J)
1	525.7271	500.6916	12.84846
2	519.337	495.212	12.23799
3	491.1181	460.5598	14.54082
4	462.5984	437.1981	11.42758
5	458.5366	435.6197	10.24562
6	451.0557	424.3845	11.67449
7	439.6632	406.2851	14.1181
8	434.3808	401.7758	13.63143
9	421.9031	389.2473	13.24436
10	473.3132	453.0663	9.37
Mean	467.7467	440	12.33
Std.dev	37.01316	39.6	1.67
CV%	7.9	9.02	13.56

Table 7 Ballistic test results for PWL02

Sample number	Impact velocity (m/s)	Residual velocity (m/s)	Projectile kinetic energy loss (J)
1	502.1368	473.2026	14.1103
2	497.8814	469.5201	13.71836
3	488.5655	468.3053	9.693189
4	485.0361	459.9746	11.84171
5	480.5726	453.0663	12.84046
6	478.6151	447.466	14.42328
7	472.3618	451.9351	9.440181
8	460.333	430.9524	13.09326
9	414.4621	380.2521	13.59358
10	489	463.5	12.14438
11	474.7	445.2	13.568
12	467	437	13.56
13	462	437	11.24
Mean	474.8203	447.4	11.69
Std.dev	22.18186	24.25	1.62
CV%	4.67	5.4	13.8

Table 8 Ballistic test results for PWL03

Sample number	Impact velocity (m/s)	Residual velocity (m/s)	Projectile kinetic energy loss (J)
1	507.0119	483.9572	11.42322
2	504.2918	476.9433	13.41765
3	497.3545	473.822	11.42711
4	495.7806	470.1299	12.38815
5	494.2166	465.8945	13.5962
6	490.0938	462.3244	13.22407
7	476.1905	443.6275	14.97603
Mean	494.9914	468.09	12.9
Std.dev	10.12	12.9	1.27
CV%	2.4	2.7	9.8

Table 9 Ballistic test results for PWL02WC

Sample number	Impact velocity (m/s)	Residual velocity (m/s)	Projectile kinetic energy loss (J)
1	513.6612	486.5591	13.55402
2	500	472.5849	13.33178
3	497.3545	465.2956	15.43074
4	496.3041	475.0656	10.31522
5	493.6975	465.8945	13.33977
6	486.5424	458.8086	13.1091
7	478.6151	447.466	14.42328
Mean	495.15	467.382	13.35
Std.dev	10.9	12.4	1.57
CV%	2.2	2.65	11.7

Table 10 Ballistic test results for PW03DW

Sample number	Impact velocity (m/s)	Residual velocity (m/s)	Projectile kinetic energy loss (J)
1	524.5536	502.7778	11.18548
2	509.7614	482.024	13.75478
3	497.3545	467.7003	14.30898
4	491.6318	470.7412	10.05226
5	486.5424	455.3459	14.69182
6	480.0817	449.6894	14.12893
7	480.0817	454.7739	11.82959
8	476.6734	446.3625	13.98903
9	465.8077	442.5428	10.56636
10	476	450	12.038
11	468	436	14.464
12	462	427	15.5575
13	457	432	11.1125
14	449.7	418.4	13.58577
Mean	480.37	452	12.94
Std.dev	20.55	22.5	1.75
CV%	4.26	4.97	13.5

Table 11 Results of yarn frictional test

Sample number	Dyneema-Dyneema	Kevlar-Kevlar	Dyneema-Kevlar	Kevlar-Dyneema
1	0.12	0.193	0.143	0.148
2	0.12	0.1925	0.138	0.143
3	0.123	0.191	0.135	0.139
4	0.115	0.1929	0.133	0.141
5	0.118	0.189	0.130	0.138
Mean	0.1192	0.1916	0.136	0.1418
Std.dev	0.00295	0.00169	0.00497	0.0039
CV%	2.47	0.88	3.6	2.7

Table 12 Bending rigidity of Dyneema and Kevlar yarns

Sample number	Bending rigidity of Kevlar yarn (g.cm^2/yarn)	Bending rigidity of Dyneema yarn (g.cm^2/yarn)
1	0.0732	0.1025
2	0.0976	0.1318
3	0.083	0.122
4	0.0927	0.1318
5	0.0781	0.161
Mean	0.0849	0.129
Std.dev	0.01	0.0211
CV%	11.7	15.5

Table 13 Ballistic test results for PW using spherical projectile

Sample number	Impact velocity (m/s)	Residual velocity (m/s)	Projectile kinetic energy loss (J)
1	528.0899	510.5783	6.184175
2	481.0645	464.1026	5.450828
3	492.6625	477.5726	4.97786
4	523.9688	507.7139	5.701765
5	470	451.3716	5.83566
6	476.1905	461.7347	4.60987
7	505.9203	490.5149	5.219178
8	520.4873	504.8815	5.440583
9	496.3041	480.1061	5.377409
Mean	499.4	483.175	5.42
Std.dev	21.52	21.66	0.46
CV%	4.2	4.3	8.4